Optimization Based Approaches for Score and Rank Level Fusion of Multimodal Biometrics

A thesis submitted to University of Hyderabad in partial fulfilment for the degree of

Doctor of Philosophy

by

Shadab Ahmad

Reg. No. 17MCPC11



SCHOOL OF COMPUTER AND INFORMATION SCIENCES UNIVERSITY OF HYDERABAD HYDERABAD -500046

Telangana

India

August, 2022



CERTIFICATE

This is to certify that the thesis entitled "Optimization Based Approaches for Score and Rank Level Fusion of Multimodal Biometrics" submitted by Shadab Ahmad bearing Reg. No. 17MCPC11 in partial fulfilment of the requirements for the award of Doctor of Philosophy in Computer Science is a bonafide work carried out by him under our supervision and guidance. This thesis is free from plagiarism and has not been submitted previously in part or in full to this or any other University or Institution for award of any degree or diploma. Parts of this thesis have been published online in the following publica-

- 1 Multimedia Tools and Applications, Springer, May-2022 (Chapter 3)
- 2 Proceedings of SIRS-2019, Springer, HITM Kerala (Chapter 3)
- 3 Proceedings of PReMI-2021, Springer, ISI Kolkata (Chapter 3)
- 4 Proceedings of CEC-2021, IEEE, Karkow, Poland (Chapter 4)

Further, the student has passed the following courses towards fulfilment of coursework requirement for Ph.D:

	Course Code	Name	Credits	Pass/Fail
1	CS801	Data structure and Programming Lab	2	Pass
2	CS802	Algorithms	4	Pass
3	CS803	Research Methods in Computer Science	4	Pass
4	CS808	Image Processing	3	Pass

Supervisor

Dr. Avatharam Ganivada

SCIS, UoH

Dr. Rajarshi Pal

Prof. Chakravarthy Bhagvati

IDRBT

SCIS, UoH

Hyderabad-500 057, India Hyderabad-500 046, India

hool of CIS

Hyderabad-500 046, Indiano Road. Central University Campus PO Gachibowli, Hyderabad-46. (India)

Assistant Professor School of CIS Prof. C.R. Rao Road, Central University Hyderabad-An (In tie)

DECLARATION

I, Shadab Ahmad, hereby declare that this thesis entitled "Optimization Based Approaches for Score and Rank Level Fusion of Multimodal Biometrics" submitted by me under the supervision of Dr. Avatharam Ganivada and Dr. Rajarshi Pal, is a bonafide research work and is free from plagiarism. I also declare that it has not been submitted previously in part or in full to this University or any other University or Institution for the award of any degree or diploma. I hereby agree that my thesis can be deposited in Shodganga/INFLIBNET.

A report on plagiarism statistics from the University Librarian is enclosed.

Date: 04 08 2022

Signature of the Student

(Shadab Ahmad)

Reg. No.: 17MCPC11

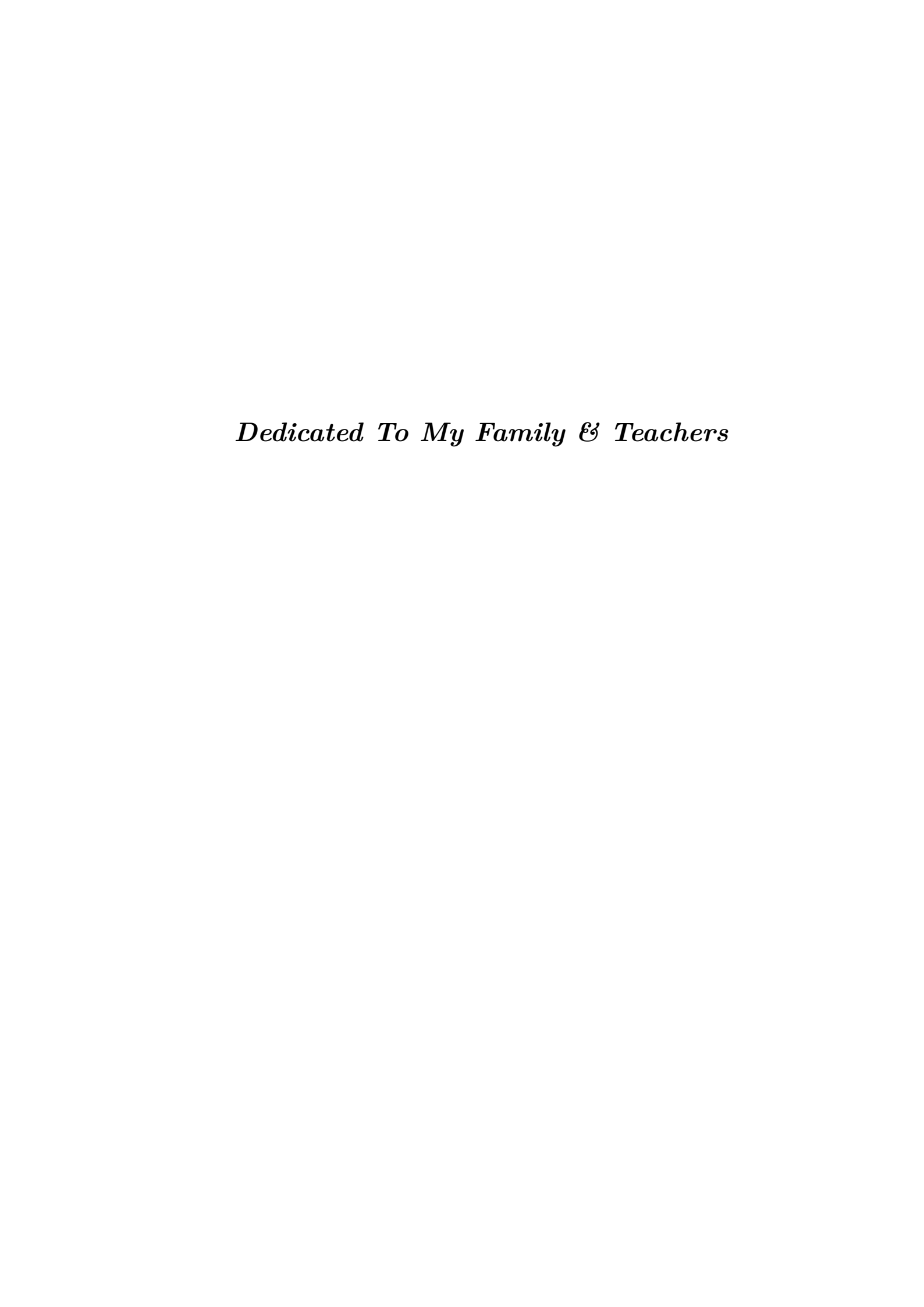
//Countersigned//

Signature of the Supervisors

FAvetharanou-08-22

(Dr. Avatharam Ganivada)

Rajashi Pal 5/8/22 (Dr. Rajarshi Pal)



Acknowledgements

I am deeply indebted to **Dr. Rajarshi Pal** and **Dr. Avatharam Ganivada**, my thesis supervisors for their guidance, wisdom and support during the course of my Ph.D. at Institute for Development and Research in Banking Technology in collaboration with University of Hyderabad. Their consistent encouragement and positive reinforcement have made it a gratifying experience. I have learned from them the virtues of rigour and professionalism. I am grateful to them for keeping me focused at the times when it mattered a lot. I express deep respect and gratitude to my supervisors for astute guidance and constant inspiration, without which this work would have never been possible.

I thank my doctoral review committee members, Prof. B. M. Mehtre and Prof. Chakravarthy Bhagvati for their encouragement, insightful comments and hard questions which strengthened my knowledge.

It is my privilege to thank **Prof. D. Janakiram**, Director, IDRBT for his considerate support and encouragement throughout the tenure of my research work and for extending the facilities to pursue my research. I thank **Prof. Chakravarthy Bhagvati**, Dean, School of Computer and Information Sciences (SCIS), University of Hyderabad, Hyderabad, for his academic support during my research work.

I express my sincere gratitude to every member of IDRBT family for providing a smooth and enriching environment so that I enjoyed the tenure at the institute. I thank every member at my lab for providing a lovely experience to me.

I, specially, thank my family members and friends for their support and inspiration during the Ph.D work. At the end, I am grateful to Institute for Development and Research in Banking Technology (IDRBT) and University of Hyderabad (UoH), for making it a memorable experience.

Abstract

Unimodal biometric systems have several limitations, like inter-class similarity, non-universality, and susceptibility to circumvention. Multiple biometric modalities are fused to overcome these issues. Here, the fusion is mainly applied to the information from multiple biometric modalities. Fusion in multimodal biometrics is performed at various levels, such as sensor level, feature level, score level, rank level and decision level. The score and rank level fusion are the two widely applied fusion techniques for multimodal biometrics. In the context of an identification task, these methods fuse matching score lists or rank lists from different biometric modalities into a single score or rank list, respectively.

In this thesis, rank and score level fusion problems are formulated as optimization problems. Here, the objective is to find a fused list (for either rank or score). The fused list minimizes a weighted summation of distances of the fused list with the input lists derived from individual biometric modalities. The stated distance between a pair of input lists is computed using the weighted Spearman footrule distance metric. Genetic algorithm based and particle swarm optimization based fusion approaches (at rank level and at score level) are proposed in this thesis to solve the stated optimization problems. For initial work, each modality is assigned equal significance (weight). Furthermore, the quality-based weight estimation approach is presented in this work to enhance the performance of proposed optimization based fusion approaches. The quality-incorporated optimization based fusion approaches perform better than the equal weight based optimization approaches.

The adopted optimization based fusion approaches (genetic algorithm and particle swarm optimization) are meta-heuristic algorithms. These algorithms iteratively search for the optimal solution in a large

search space. Therefore, these approaches take immense number of iterations to reach to the optimal solution. An approach to reduce the dimension of the search space is presented in this thesis for faster convergence of the proposed optimization based fusion approaches (at rank and at score levels). The proposed search space-reduction approaches aid in achieving faster convergence of proposed optimization based approaches without any degradation in performance.

Usefulness of the proposed search space-reduced quality-incorporated particle swarm optimization based score level fusion approach is evaluated on the problem of person identification in the era of Covid19. Here, fusion of masked face and iris is performed at score level to identify a person wearing face mask. Superiority of the proposed work is experimentally established with comparison to several other state-of-the-art score level and rank level fusion approaches.

Contents

A	cknov	wledgr	nents		V
A	bstra	ct			vi
$\mathbf{L}_{\mathbf{i}}$	ist of	Figur	es		xv
\mathbf{L}^{i}	ist of	Table	\mathbf{s}		xx
1	Intr	oduct	ion		1
	1.1	Introd	luction to	Biometric System	2
		1.1.1	Modules	s of Biometric System	2
		1.1.2	Metrics	for Evaluating a Biometric System	4
		1.1.3	Real Lif	e Applications of Biometrics	5
		1.1.4	Limitati	ions of Unimodal Biometrics	7
			1.1.4.1	Noisy Data	7
			1.1.4.2	Inter-class Similarity	8
			1.1.4.3	Intra-class Variation	8
			1.1.4.4	Non-universality	8
			1.1.4.5	Easy to Spoof	9
			1.1.4.6	Other Challenges	9
	1.2	Introd	luction to	Multibiometrics	9
		1.2.1	Levels o	f Multimodal Biometric Fusion	12
			1.2.1.1	Sensor Level Fusion	12
			1.2.1.2	Feature Level Fusion	13
			1.2.1.3	Score Level Fusion	14
			1.2.1.4	Rank Level Fusion	15
			1.2.1.5	Decision Level Fusion	15
		1.2.2	Real Lif	e Applications of Multimodal Biometrics	16

	1.3 1.4 1.5	Contr	ibution of	tive	16 18 20
2	$\operatorname{Lit}_{oldsymbol{\epsilon}}$	erature	e Survey	on Score and Rank Level Fusion Approaches	
	for	Multir	nodal B	iometrics	22
	2.1	Score	Level Fus	ion Approaches	22
		2.1.1	Rule-Ba	sed Methods	22
		2.1.2	Likeliho	od Ratio Based Score Level Fusion Approaches	30
		2.1.3	Classific	ation Based Approaches	31
		2.1.4	Optimiz	ation Based Approaches	31
	2.2	Rank	Level Fus	ion Approaches	32
		2.2.1	Borda C	Count Approach	32
		2.2.2		d Borda Count Approach	32
		2.2.3	Highest	Rank Approach	33
		2.2.4	Non-line	ear Weighted Approaches	33
		2.2.5		Chain Based Approach	34
		2.2.6		ank Based Approach	35
	2.3	Weigh		sion Approaches	35
		2.3.1		or Classifier Performance-Based Approaches	35
		2.3.2	_	ation-Based Approaches	36
		2.3.3	-	Based Approaches	36
	2.4	Summ	nary		38
3	Rar	ık Leve	el Fusion	of Multimodal Biometrics Using Optimization	
			proaches		39
	3.1	-	_	ion as an Optimization Problem	40
	3.2			tic Algorithm Based Approach	43
		3.2.1		Domain Specific Design of Genetic Algorithm	43
			3.2.1.1	Representation of a Chromosome	44
			3.2.1.2	Fitness of a Chromosome	44
			3.2.1.3	Initialization of Population	44
			3.2.1.4	Selection	45
			3.2.1.5	Crossover	46
			3.2.1.6	Mutation	47
			3.2.1.7	Stopping Criteria	49
		322	Perform	ance Evaluation and Discussion	49

		3.2.2.1	State-of-the-Art Approaches for Performance	
			Comparison	50
		3.2.2.2	Fusion of Multimodal Biometrics Involving Face	
			and Fingerprint (NIST BSSR1 Multimodal	
			Dataset (Set 1)) $\dots \dots \dots \dots \dots \dots$	51
		3.2.2.3	Fusion of Multimodal Biometrics for Multiple	
			Gait Feature Representations (OU-ISIR BSS4	
			Multi-Algorithm Dataset)	55
	3.2.3	Conclusi	ion	60
3.3	Propo	sed Partic	ele Swarm Optimization Based Approach	60
	3.3.1	Problem	Domain Specific Design of Particle Swarm Opti-	
		mization	Based Approach	61
		3.3.1.1	Representation of a Candidate Rank List as a Par-	
			ticle Position	61
		3.3.1.2	Fitness of a Candidate Rank List	61
		3.3.1.3	Initialization of Population of Candidate Rank Lists	61
		3.3.1.4	Exploring Other Candidate Rank Lists	62
		3.3.1.5	Stopping Criteria	64
	3.3.2	Perform	ance Evaluation and Discussion	64
		3.3.2.1	Fusion of Multimodal Biometrics Involving Face	
			and Fingerprint (NIST BSSR1 Multimodal	
			Dataset (Set 1))	64
		3.3.2.2	Fusion of Multimodal Biometrics for Multiple	
			Gait Feature Representations (OU-ISIR BSS4	
			Multi-Algorithm Dataset)	69
	3.3.3	Conclusi	ion	70
3.4	Analy	sis of Con	vergence Rate Between GA Based and PSO Based	
	Rank	Level Fus	ion Approaches	73
	3.4.1	Results	of Two-Sample K-S Test on Multimodal Biomet-	
		ric Data	set Involving Face and Fingerprint (NIST BSSR1	
		Multimo	odal Dataset (Set 1))	75
	3.4.2		of Two-Sample K-S Test on Multimodal Biometric	
			for Multiple Gait Feature Representations (OU-	
		ISIR BS	S4 Multi-Algorithm Dataset)	76
2.5	Summ		-	77

4	Sco	re Lev	el Fusion	of Multimodal Biometrics Using Optimization	n
	Bas	ed Ap	proaches		7 9
	4.1	Score	Level Fus	ion as an Optimization Problem	80
	4.2	Propo	sed Genet	cic Algorithm Based Score Level Fusion Approach .	83
		4.2.1	Problem	Domain Specific Design of Genetic Algorithm	84
			4.2.1.1	Representation of a Chromosome	84
			4.2.1.2	Fitness of a Chromosome	84
			4.2.1.3	Initialization of Population	85
			4.2.1.4	Selection	85
			4.2.1.5	Crossover	86
			4.2.1.6	Mutation	87
			4.2.1.7	Stopping Criteria	87
		4.2.2	Performa	ance Evaluation and Discussion	88
			4.2.2.1	Fusion of Multimodal Biometrics Involving Face	
				and Fingerprint (NIST BSSR1 Multimodal	
				Dataset (Set 1)	89
			4.2.2.2	Fusion of Multimodal Biometrics for Multiple	
				Gait Feature Representations (OU-ISIR BSS4	
				Multi-Algorithm Gait Dataset)	94
		4.2.3	Conclusi	on	95
	4.3	Propo	sed Partic	ele Swarm Optimization Based Score Level Fusion	
		Appro	oach		98
		4.3.1	Problem	Domain Specific Design of Particle Swarm Opti-	
			mization	Approach	98
			4.3.1.1	Representation of a Candidate Score List as a Par-	
				ticle Position	99
			4.3.1.2	Fitness of a Candidate Score List	99
			4.3.1.3	Initialization of Population of Candidate Score List	s 99
			4.3.1.4	Exploring Other Candidate Score Lists	100
			4.3.1.5	Stopping Criteria	101
		4.3.2	Performa	ance Evaluation and Discussion	102
			4.3.2.1	Fusion of Multimodal Biometrics Involving Face	
				and Fingerprint (NIST BSSR1 Multimodal	
				Dataset (Set 1))	102
			4.3.2.2	Fusion of Multimodal Biometrics for Multiple	
				Gait Feature Representations (OU-ISIR BSS4	
				Multi-Algorithm Gait Dataset)	106

		4.3.3 Conclusion	. 111
	4.4	Analysis of Convergence Rate Between Proposed Optimization	1
		Based Score and Rank Level Fusion Approaches	. 111
		4.4.1 Results of Two-Sample K-S Test Using Multimodal Bio-	-
		metrics Involving Face and Fingerprint (NIST BSSR1 Mul-	-
		timodal Dataset (Set 1))	. 112
		4.4.2 Results of Two-Sample K-S Test Using Multimodal Biometer	-
		rics for Multiple Gait Feature Representations (OU-ISIF	2
		BSS4 Multi-Algorithm Dataset)	. 116
	4.5	Summary	. 117
5	Inco	orporating Quality in Optimization Based Fusion Approach	nes
		Rank and Score Levels	119
	5.1	Multimodal Fusion as an Optimization Problem	
		5.1.1 Rank Level Fusion as an Optimization Problem	
		5.1.2 Score Level Fusion as an Optimization Problem	
	5.2	Proposed Approach for Estimating Quality of Biometric Informa-	
		tion in a Probe Signal	
	5.3	Proposed Quality-Incorporated Particle Swarm Optimization	
		Based Fusion Approaches	
		5.3.1 Proposed Quality-Incorporated Particle Swarm Optimiza	-
		tion Based Rank Level Fusion Approach	. 125
		5.3.2 Proposed Quality-Incorporated Particle Swarm Optimization	-
		tion Based Score Level Fusion Approach	. 126
	5.4	Performance Evaluation and Discussion	. 127
		5.4.1 Fusion of Multimodal Biometrics Involving Face and Iris	3
		(Virtual Multimodal Dataset FaceIris-V1)	. 127
		5.4.2 Fusion of Multimodal Biometrics Involving Face and Iris	3
		(Virtual Multimodal Dataset FaceIris-V2)	. 133
		5.4.3 Fusion of Multimodal Biometrics Involving Face and Fin-	-
		gerprint (NIST BSSR1 Multimodal Dataset (Set 1))	. 138
		5.4.4 Fusion of Multimodal Biometrics for Multiple Gait Fea	-
		ture Representations (OU-ISIR BSS4 Multi-Algorithm Gair	t
		Dataset)	. 141
	5.5	Summary	1/15

6	Rec	luction	of Search Space Dimension for Optimization Based
	Fus	ion Ap	oproaches at Rank and Score Levels 148
	6.1	Multin	modal Fusion as an Optimization Problem
		6.1.1	Rank Level Fusion as an Optimization Problem 149
		6.1.2	Score Level Fusion as an Optimization Problem 150
		6.1.3	Challenges in Above Optimization Based Approaches 151
	6.2	Propo	sed Approaches for Search Space Reduction 152
		6.2.1	Search Space Reduction for Rank Level Fusion 152
		6.2.2	Search Space Reduction for Score Level Fusion 155
	6.3	Propo	sed Search Space-Reduced Quality-Incorporated Particle
		Swarn	n Optimization Based Fusion Approaches
		6.3.1	Proposed Search Space-Reduced Quality-Incorporated Par-
			ticle Swarm Optimization Based Rank Level Fusion Approach 158
		6.3.2	Proposed Search Space-Reduced Quality-Incorporated Par-
			ticle Swarm Optimization Based Score Level Fusion Approach 159
	6.4	Perfor	mance Evaluation and Discussion
		6.4.1	Fusion of Multimodal Biometrics Involving Face and Iris
			(Virtual Multimodal Biometric Dataset FaceIris-V1) 160
		6.4.2	Fusion of Multimodal Biometrics Involving Face and Iris
			(Virtual Multimodal Dataset FaceIris-V2) 165
		6.4.3	Fusion of Multimodal Biometrics Involving Face and Fin-
			gerprint (NIST BSSR1 Multimodal Dataset (Set 1)) 171
		6.4.4	Fusion of Multimodal Biometrics for Multiple Gait Fea-
			ture Representations (OU-ISIR BSS4 Multi-Algorithm Gait
		~	Dataset)
	6.5	Summ	ary
7	Idei	ntifvin	g a Person in Mask: Fusion of Masked Face and Iris
•			a Identification in Post-Covid19 Era 182
	7.1		ance of the Proposed Fusion Task
	7.2		iew of Person Identification in Masked Face 185
	7.3		ing Score Generation for Face Modality
		7.3.1	GAN based Unmasking Approach
		7.3.2	Generating Matching Scores
	7.4	Match	ning Score Generation for Iris Modality
	7.5		Level Fusion
	7.6	Perfor	mance Evaluation and Discussion

CONTENTS

		7.6.1	Experim	ental Set	up								189
			7.6.1.1	Generat	ing Mas	sked I	Face	Dat	aset				190
			7.6.1.2	Division	of Data	aset .							190
		7.6.2	Experim	ental Res	sults								190
	7.7	Summ	ary										193
8	Con	clusio	n and Fu	ıture Wo	ork								195
	8.1	Summ	ary of Co	ntributio	ns								195
	8.2	Future	e Research	n Directio	ons								198
Re	efere	nces											202

List of Figures

1.1	Examples of physiological and behavioural biometric characteris-
	tics (modalities)
1.2	Pipeline of biometric recognition system
1.3	Limitations of unimodal biometrics
1.4	An example of multi-sensor biometric system
1.5	An example of multi-sample biometric system
1.6	An example of multi-instance biometric system
1.7	An example of multi-algorithm biometric system
1.8	An example of multi-trait biometric system
1.9	Sensor level fusion
1.10	Feature level fusion
1.11	Score level fusion
1.12	Rank level fusion
1.13	Decision level fusion
2.1	Genuine and impostor scores with their overlapping region (for
	similarity scores)
3.1	Fusion of multimodal biometrics at rank level
3.2	Weighted Spearman footrule distance computation
3.3	An illustration of crossover operation
3.4	An illustration of mutation operation
3.5	CMC plots for existing rank level fusion approaches being com-
	pared with that of the proposed GA based rank level fusion ap-
	proach for NIST BSSR1 Dataset (set 1)
3.6	CMC plots for existing score level fusion approaches being com-
	pared with that of the proposed GA based rank level fusion ap-
	proach for NIST BSSR1 Dataset (set 1)

3.7	CMC plots for existing rank level fusion approaches being com-	
	pared with that of the proposed GA based rank level fusion ap-	
	proach for OU-ISIR BSS4 multi-algorithm Dataset	59
3.8	CMC plots for existing score level fusion approaches being com-	
	pared with that of the proposed GA based rank level fusion ap-	
	proach for OU-ISIR BSS4 multi-algorithm dataset	59
3.9	CMC plots for existing rank level fusion approaches being com-	
	pared with those of the GA based and the proposed PSO based	
	rank level fusion approaches for NIST BSSR1 multimodal dataset	
	$(\text{set }1) \ldots \ldots$	68
3.10	CMC plots for existing score level fusion approaches being com-	
	pared with that of the proposed PSO based rank level fusion ap-	
	proach for NIST BSSR1 multimodal dataset (set 1)	68
3.11	CMC plots for existing rank level fusion approaches being com-	
	pared with those of the GA based and the proposed PSO based	
	rank level fusion approaches for OU-ISIR BSS4 multi-algorithm	
	dataset	72
3.12	CMC plots for existing score level fusion approaches being com-	
	pared with that of the proposed PSO based rank level fusion ap-	
	proach for OU-ISIR BSS4 multi-algorithm dataset	72
3.13	CDFs of the GA and PSO based rank level fusion approaches on	
	NIST BSSR1 multimodal dataset (set 1)	74
3.14	CDFs of the GA and PSO based rank level fusion approaches on	
	OU-ISIR BSS4 multi-algorithm gait dataset	74
11	Their of multipedal bismethics at some level	01
4.1	Fusion of multimodal biometrics at score level	81
4.2	Fitness evaluation of candidate score list δ through illustration	83 86
4.3	Illustration of crossover operation	
4.4	Illustration of mutation operation	88
4.5	CMC plots for existing rank level fusion approaches being com-	
	pared with that of the proposed GA based score level fusion approach for NIST PSSP1 detects (set 1)	റാ
1 E	proach for NIST BSSR1 dataset (set 1)	93
4.6	CMC plots for existing score level fusion approaches being com-	
	pared with that of the proposed GA based score level fusion ap-	00
	proach for NIST BSSR1 dataset (set 1)	93

4.7	CMC plots for existing rank level fusion approaches being com-	
	pared with that of the proposed GA based score level fusion ap-	
	proach for OU-ISIR BSS4 multi-algorithm dataset	97
4.8	CMC plots for existing score level fusion approaches being com-	
	pared with that of the proposed GA based score level fusion ap-	
	proach for OU-ISIR BSS4 multi-algorithm dataset	97
4.9	CMC plots for existing rank level fusion approaches being com-	
	pared with that of the proposed PSO based score level fusion ap-	
	proach for NIST BSSR1 multimodal dataset (set 1)	107
4.10	CMC plots for existing score level fusion approaches being com-	
	pared with those of the GA based and the proposed PSO based	
	score level fusion approaches for NIST BSSR1 multimodal dataset	
	$(\text{set }1) \ldots \ldots \ldots \ldots \ldots \ldots \ldots \ldots \ldots$	107
4.11	CMC plots for existing rank level fusion approaches being com-	
	pared with that of the proposed PSO based score level fusion ap-	
	proach for OU-ISIR BSS4 multi-algorithm dataset	110
4.12	CMC plots for existing score level fusion approaches being com-	
	pared with those of the GA based and proposed PSO based score	
	level fusion approaches for OU-ISIR BSS4 multi-algorithm dataset	110
4.13	CDFs on number of iterations for PSO based (Section 4.3) and	
	GA based (Section 4.2) score level approaches on NIST BSSR1	
	multimodal dataset (set 1)	113
4.14	CDFs on number of iterations for PSO based score level fusion	
	approach (Section 4.3) and PSO based rank level fusion approach	
	(Section 3.3) on NIST BSSR1 multimodal dataset (set 1)	113
4.15	CDFs on number of iterations for PSO based (Section 4.3) and GA	
	based (Section 4.2) score level fusion approaches on OU-ISIR BSS4	
	multi-algorithm dataset	114
4.16	CDFs on number of iterations for PSO based score level fusion	
	approach (Section 4.3) and PSO based rank level fusion approach	
	(Section 3.3) on OU-ISIR BSS4 multi-algorithm dataset	114
5.1	Quality-incorporated fusion of multimodal biometrics at rank level	125
5.2	Quality-incorporated fusion of multimodal biometrics at score level	
5.3	CMC plots for existing rank level fusion approaches being com-	
	pared with that of the proposed Q-PSO based fusion approaches	
	for first virtual multimodal biometric dataset FaceIris-V1	132

5.4	CMC plots for existing score level fusion approaches being com-	
	pared with that of the proposed Q-PSO based fusion approaches	
	for first virtual multimodal biometric dataset FaceIris-V1	133
5.5	CMC plots for existing rank level fusion approaches being com-	
	pared with that of the proposed Q-PSO based fusion approaches	
	for second virtual multimodal biometric dataset FaceIris-V2 $$	137
5.6	CMC plots for existing score level fusion approaches being com-	
	pared with that of the proposed Q-PSO based fusion approaches	
	for second virtual multimodal biometric dataset FaceIris-V2 $$	138
5.7	CMC plots for existing rank level fusion approaches being com-	
	pared with that of the proposed Q-PSO based fusion approaches	
	for NIST BSSR1 multimodal dataset (set 1)	142
5.8	CMC plots for existing score level fusion approaches being com-	
	pared with that of the proposed Q-PSO based fusion approaches	
	for NIST BSSR1 multimodal dataset (set 1)	142
5.9	CMC plots for existing rank level fusion approaches being com-	
	pared with that of the proposed Q-PSO based fusion approaches	
	for OU-ISIR BSS4 multi-algorithm dataset	146
5.10	CMC plots for existing score level fusion approaches being com-	
	pared with that of the proposed Q-PSO based fusion approaches	
	for OU-ISIR BSS4 multi-algorithm dataset	146
6.1	An illustration of search space-reduction for rank level fusion	153
6.2	An illustration of search space-reduction for score level fusion	156
6.3	CMC plots for existing rank level fusion approaches being com-	
	pared with that of the proposed RQ-PSO based fusion approaches	
	for first virtual multimodal biometric dataset FaceIris-V1	163
6.4	CMC plots for existing score level fusion approaches being com-	
	pared with that of the proposed RQ-PSO based fusion approaches	
	for first virtual multimodal biometric dataset FaceIris-V1	164
6.5	CMC plots for existing rank level fusion approaches being com-	
	pared with that of the proposed RQ-PSO based fusion approaches	
	for second virtual multimodal biometric dataset Face Iris-V2 $$	169
6.6	CMC plots for existing score level fusion approaches being com-	
	pared with that of the proposed RQ-PSO based fusion approaches	
	for second virtual multimodal biometric dataset FaceIris-V2 $$	169

LIST OF FIGURES

6.7	CMC plots for existing rank level fusion approaches being com-	
	pared with that of the proposed RQ-PSO based fusion approaches	
	for NIST BSSR1 multimodal dataset (set 1)	174
6.8	CMC plots for existing score level fusion approaches being com-	
	pared with that of the proposed RQ-PSO based fusion approaches	
	for NIST BSSR1 multimodal dataset (set 1)	174
6.9	CMC plots for existing rank level fusion approaches being com-	
	pared with that of the proposed RQ-PSO based fusion approaches	
	for OU-ISIR BSS4 multi-algorithm dataset	179
6.10	CMC plots for existing score level fusion approaches being com-	
	pared with that of the proposed RQ-PSO based fusion approaches	
	for OU-ISIR BSS4 multi-algorithm dataset	179
7.1	Stages of proposed masked face and iris fusion approach	186
7.2	Similarity scores between masked face images (probe) and corre-	
	sponding gallery images	190
7.3		
	ing gallery images	191

List of Tables

3.1	Performance comparison of the proposed GA based rank level fusion approach with unimodal matchers on NIST BSSR1 multimodal dataset (set 1)
3.2	Performance of the comparing fusion methods on NIST BSSR1 multimodal dataset (set 1) using cumulative recognition accuracies in %
3.3	Ranks at each modality for ideally correct subject and the top three identified subjects according to the fused list (for probe subject ID 81)
3.4	Ranks at each modality for ideally correct subject and the top three identified subjects according to the fused list (for probe subject ID 224)
3.5	Ranks at each modality for ideally correct subject and the top three identified subjects according to the fused list (for probe subject ID 419)
3.6	Performance comparison of the proposed GA based rank level fusion approach with unimodal matchers on OU-ISIR BSS4 multialgorithm dataset
3.7	Performance of the comparing fusion methods on OU-ISIR BSS4 multi-algorithm dataset using cumulative recognition accuracies in %
3.8	Performance comparison of the proposed PSO based rank level fusion approach with unimodal matchers on NIST BSSR1 multimodal dataset (set 1)
3.9	Performance of the comparing fusion approaches on NIST BSSR1 multimodal dataset (set 1) using cumulative recognition accuracies in %

3.10	Ranks at each modality for ideally correct subject and the top three identified subjects according to the fused list (for probe subject ID	
	81)	69
3.11	Ranks at each modality for ideally correct subject and the top three	
	identified subjects according to the fused list (for probe subject ID	
	$224) \dots \dots$	69
3.12	Ranks at each modality for ideally correct subject and the top three	
	identified subjects according to the fused list (for probe subject ID	
	419)	70
3.13	Performance comparison (using cumulative recognition accuracies	
	in %) of the proposed PSO based rank level fusion approach with	
	unimodal matchers on OU-ISIR BSS4 multi-algorithm dataset $$	70
3.14	Performance of the comparing fusion approaches on OU-ISIR BSS4	
	multi-algorithm dataset using cumulative recognition accuracies in	
	%	71
4.1	Performance comparison of the proposed GA based score level	
4.1	fusion approach with unimodal matchers on NIST BSSR1 mul-	
	timodal dataset (set 1)	90
4.2	Performance of the comparing fusion methods on NIST BSSR1	90
4.2	multimodal dataset (set 1) using cumulative recognition accuracies	
	in %	91
19		91
4.3	Normalized scores (and their ranks) at each modality for ideally	
	correct subject and the top three identified subjects according to	92
1 1	the fused list (for probe subject ID 81)	92
4.4	Normalized scores (and their ranks) at each modality for ideally	
	correct subject and the top three identified subjects according to	00
4 5	the fused list (for probe subject ID 224)	92
4.5	Normalized scores (and their ranks) at each modality for ideally	
	correct subject and the top three identified subjects according to	0.4
1 C	the fused list (for probe subject ID 419)	94
4.6	Performance comparison of the proposed GA based score level fu-	
	sion approach with unimodal matchers on OU-ISIR BSS4 multi-	0.5
4 7	algorithm dataset	95
4.7	Performance of the comparing fusion methods on OU-ISIR BSS4	
	multi-algorithm dataset using cumulative recognition accuracies in	0.0
	%	96

4.8	Performance comparison of the proposed PSO based score level	
	fusion approach with unimodal matchers on NIST BSSR1 multi-	
	modal dataset (set 1)	103
4.9	Performance of the comparing fusion approaches on NIST BSSR1	
	multimodal dataset (set 1) using cumulative recognition accuracies	
	in $\%$	104
4.10	Normalized scores (and their ranks) at each modality for ideally	
	correct subject and the top three identified subjects according to	
	the fused list (for probe subject ID 81)	105
4.11	Normalized scores (and their ranks) at each modality for ideally	
	correct subject and the top three identified subjects according to	
	the fused list (for probe subject ID 224)	105
4.12	Normalized scores (and their ranks) at each modality for ideally	
	correct subject and the top three identified subjects according to	
	the fused list (for probe subject ID 419)	106
4.13	Performance comparison (using cumulative recognition accuracies	
	in %) of the proposed PSO based score level fusion approach with	
	unimodal matchers on OU-ISIR BSS4 multi-algorithm dataset	108
4.14	Performance of the comparing fusion approaches on OU-ISIR BSS4	
	multi-algorithm dataset using cumulative recognition accuracies in	
	%	109
5.1	Performance on FaceIris-V1 dataset: Recognition accuracies (in %)	
0.1	for comparing weighted score and rank level fusion approaches us-	
	ing the proposed quality-derived weight estimation approach with	
	different values of h (in Eq. 5.3)	130
5.2	Performance comparison of existing weight estimation approaches	
		131
5.3	Performance comparison of the existing non-weighted rank and	
	score level fusion approaches with the proposed Q-PSO based fu-	
	sion approaches on virtual multimodal dataset FaceIris-V1	132
5.4	Performance on FaceIris-V2 dataset: Recognition accuracies (in %)	
	for comparing weighted score and rank level fusion approaches us-	
	ing the proposed quality-derived weight estimation approach with	
	different values of h	135
5.5	Performance comparison of existing weight estimation approaches	
	for weighted score and rank level fusion approaches on FaceIris-V2	136

5.6	Performance comparison of existing non-weighted rank and score	
	level fusion approaches with the proposed Q-PSO based fusion ap-	
	proaches on virtual multimodal biometric dataset FaceIris-V2	137
5.7	Performance on NIST BSSR1 multimodal dataset (set 1): Recog-	
	nition accuracies (in %) for comparing weighted score and rank	
	level fusion approaches using the proposed quality-derived weight	
	estimation approach with different values of h (in Eq. 5.3)	139
5.8	Performance comparison of existing weight estimation approaches	
	for weighted score and rank level fusion approaches on NIST	
	BSSR1 multimodal dataset (set 1)	140
5.9	Performance comparison of existing non-weighted rank and score	
	level fusion approaches with the proposed Q-PSO based fusion ap-	
	proaches on NIST BSSR1 multimodal dataset (set 1)	141
5.10	Performance on OU-ISIR BSS4 multi-algorithm dataset: Recog-	
	nition accuracies (in %) for comparing weighted score and rank	
	level fusion approaches using the proposed quality-derived weight	
	estimation approach with different values of h (in Eq. 5.3)	143
5.11	Performance comparison of existing weight estimation approaches	
	for weighted score and rank level fusion approaches on OU-ISIR	
	BSS4 multi-algorithm dataset	144
5.12	Performance comparison of existing non-weighted rank and score	
	level fusion approaches with the proposed Q-PSO based fusion ap-	
	proaches on OU-ISIR BSS4 multi-algorithm dataset using cumula-	
	tive recognition accuracies in $\%$	145
C 1	D	
6.1	Recognition accuracies (in %) of the proposed search space-reduced	
	quality-incorporated PSO based fusion approaches with respect	
	to those of unimodal matchers on virtual multimodal biometric	101
6.0	dataset FaceIris-V1	161
6.2	Performance comparison of the existing rank and score level fusion	
	approaches with the proposed RQ-PSO based fusion approaches	
	on virtual multimodal dataset FaceIris-V1 using cumulative recog-	1.00
	nition accuracies in $\%$	162

6.3	Performance comparison of PSO based rank (Section 3.3) and PSO	
	based score (Section 4.3) level fusion approaches with the proposed	
	RQ-PSO based fusion approaches on virtual multimodal dataset	
	FaceIris-V1 using average number of iterations, average execution	
	time and average dimension of search space	165
6.4	Recognition accuracies (in %) of the proposed search space-reduced	
	quality-incorporated PSO based fusion approaches with respect	
	to those of unimodal matchers on virtual multimodal biometric	
	dataset FaceIris-V2	167
6.5	Performance comparison of the existing rank and score level fusion	
	approaches with the proposed RQ-PSO based fusion approaches on	
	virtual multimodal biometric dataset FaceIris-V2 using cumulative	
	recognition accuracies in $\%$	168
6.6	Performance comparison of PSO based rank (Section 3.3) and PSO	
	based score (Section 4.3) level fusion approaches with the proposed	
	RQ-PSO based fusion approaches on virtual multimodal dataset	
	FaceIris-V2 using average number of iterations, average execution	
	time and average dimension of search space	170
6.7	Recognition accuracies (in $\%$) of the proposed search space-reduced	
	quality-incorporated PSO based fusion approaches with respect to	
	those of unimodal matchers on NIST BSSR1 multimodal dataset	
	$(\text{set }1) \ldots \ldots$	171
6.8	Performance comparison of the existing rank and score level fusion	
	approaches with the proposed RQ-PSO based fusion approaches on	
	NIST BSSR1 multimodal dataset (set 1) using cumulative recog-	
	nition accuracies in $\%$	172
6.9	Performance comparison of PSO based rank (Section 3.3) and PSO	
	based score (Section 4.3) level fusion approaches with the pro-	
	posed RQ-PSO based fusion approaches on NIST BSSR1 multi-	
	modal dataset (set 1) using average number of iterations, average	
	execution time and average dimension of search space	175
6.10	Recognition accuracies (in %) of the proposed search space-reduced	
	quality-incorporated PSO based fusion approaches with respect	
	to those of unimodal matchers on OU-ISIR BSS4 multi-algorithm	
	dataset	177

6.11	Performance comparison of the existing rank and score level fusion	
	approaches with the proposed RQ-PSO based fusion approaches on	
	OU-ISIR BSS4 multi-algorithm dataset using cumulative recogni-	
	tion accuracies in $\%$	178
6.12	Performance comparison of PSO based rank (Section 3.3) and PSO	
	based score (Section 4.3) level fusion approaches with the pro-	
	posed RQ-PSO based fusion approaches on OU-ISIR BSS4 multi-	
	algorithm gait dataset using average number of iterations, average	
	execution time and average dimension of search space	180
7 1	D (
7.1	Performance comparison (recognition accuracies in %) of the	
	adopted RQ-PSO based score level fusion approach and state-of-	
	the-art score and rank level fusion approaches in the context of	
	masked face and unmasked face and iris	192

Chapter 1

Introduction

Identity of a person plays an important role in society. A person is allowed to access certain facilities depending on his/her identity. Examples include distribution of government-sponsored welfare schemes, entry in a secure facility (such as data centers, defence establishments, nuclear plants and offices), crossing an international border and performing banking transactions. A wrong identification can cause a major security breach in such cases. Therefore, a reliable and secure identity establishment mechanism is need of the society.

Identity of a person can be determined based on: (i) what he knows, (ii) what he possesses and (iii) who he is [1]. Identity can be established based on a person's knowledge about password, personal identification number or answers to certain questions. A person can possess a government issued identification card (e.g., passport, driving licence, voter card etc.), a digital token, smart card, or a key to establish his identity. The third way to identify a person is based on his physical or behavioural characteristics such as face, signature etc. The person identification based on "who he is" (physical or behavioural characteristics) is known as biometric based identity management system.

This chapter is organized into the following sections: A brief introduction to biometric system is presented in Section 1.1. In Section 1.2, an introduction to multibiometric system is presented. The main research objectives of the thesis are highlighted in Section 1.3. Contributions of the thesis are presented in Section 1.4. Finally, the organization of the remaining chapters of this thesis is presented in Section 1.5.

1.1 Introduction to Biometric System

Biometrics is a burgeoning technology that captures and evaluates a person's physiological (iris, face, etc.) and behavioural (gait, keystrokes, etc.) characteristics for verification and identification of a person. Commonly used physiological and behavioural biometric characteristics (modalities) are shown in Fig. 1.1. Traditionally, a biometric system uses unimodal (single) biometric modality for identity management system.

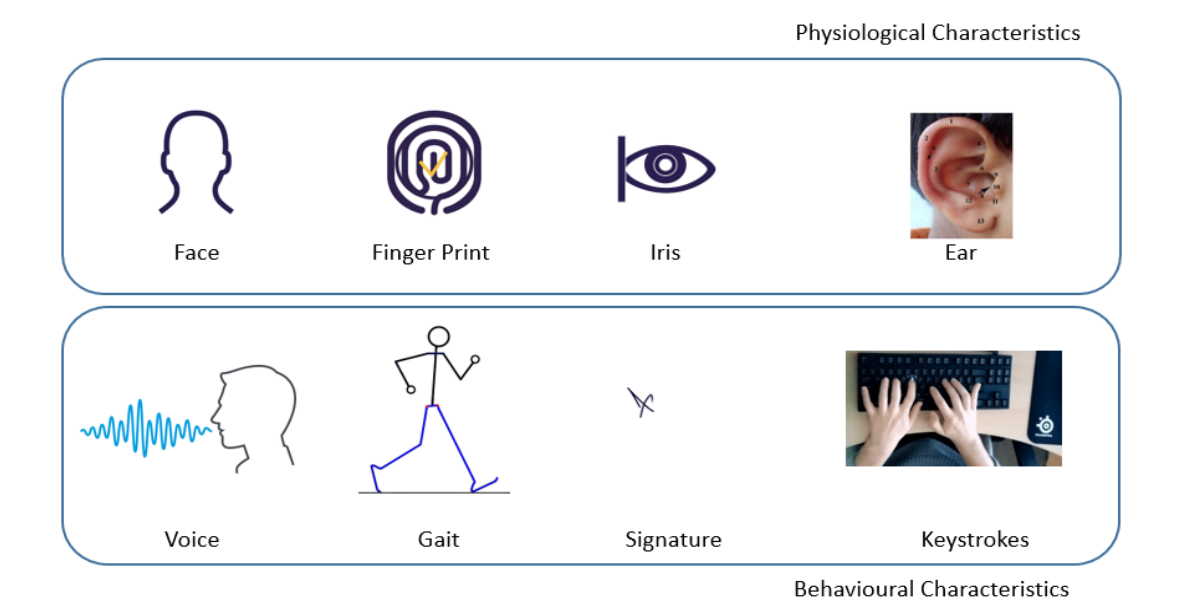


Figure 1.1: Examples of physiological and behavioural biometric characteristics (modalities)

1.1.1 Modules of Biometric System

A biometric system works in two phases: (i) enrolment phase and (ii) recognition phase. During the enrolment phase, the biometric information for a modality is acquired from each participating user in the biometric system. The acquired biometric information is stored in a database. In recognition phase, the biometric information of the user to be identified (probe user) is re-acquired. This reacquired biometric information is compared with the stored biometric information of the same user for verification. Similarly, the re-acquired biometric information

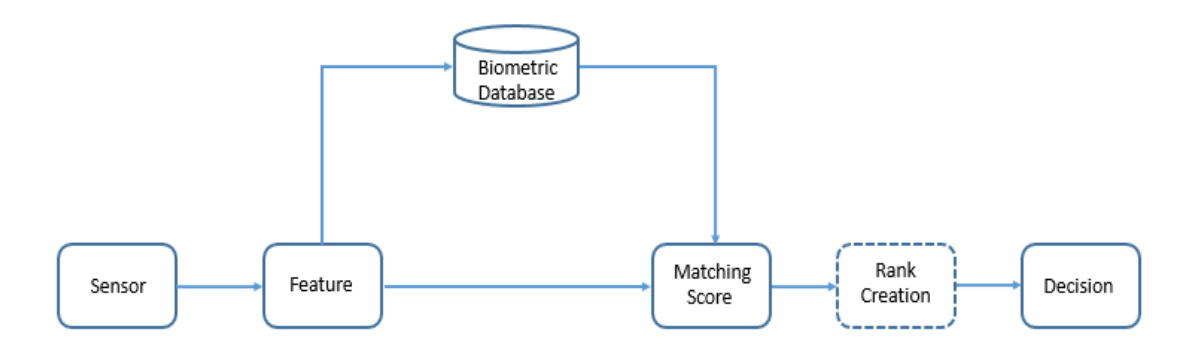


Figure 1.2: Pipeline of biometric recognition system

is compared with the biometric information of all the enrolled users for identification. Various modules of a biometric recognition system are presented in Fig. 1.2. These modules are discussed below:

- 1. **Sensor Module:** In the sensor module, the biometric information is acquired using a modality-specific sensor or device. For example, the finger-print of a user is captured using a fingerprint scanner. Similarly, the facial information for face biometrics is captured using a still camera or a video camera in the form of an image. The voice biometric information can be recorded using a voice recorder in the form of a signal.
- 2. Feature Extraction Module: In this module, the key features from the acquired image or signal are extracted. These extracted features are the digital representations of the biometric modality. These are also known as templates. These templates contain discriminative information to identify a person uniquely. For example, gait energy image (GEI) [2] is a key feature for the gait modality.
- 3. **Database Module:** After extracting the features (templates) from the raw biometric image or signal at the enrolment phase, the templates are stored in a database. This database is a repository of templates for all the enrolled users.
- 4. **Matching Module:** The matching module is a part of the recognition phase of a biometric system. The probe template is matched with the stored

template of the claimed user (verification) or with all the stored templates (identification) in the database to produce a matching score (similarity or dissimilarity score).

- 5. Rank Creation Module: The rank creation module is only used for identification task. In this module, the matching scores (similarity or dissimilarity scores) of all the enrolled users are sorted to rank each user. These ordered ranks produce a rank list. This rank list is used to identify the probe user.
- 6. **Decision Module:** The decision module is the last module of the biometric system. Based on the outcome of the matching module or the rank creation module, the decision module takes a final decision. This module is used to verify the claimed user or to identify a user.

1.1.2 Metrics for Evaluating a Biometric System

In order to evaluate the performance of a biometric system, the following metrics can be used:

1. False Acceptance Rate (FAR): The false acceptance rate (FAR) is also known as a false match rate (FMR). The false acceptance rate (FAR) refers to the rate by which an imposter is accepted as genuine user by the biometric system [1]. The FAR is measured as ratio of the total number of falsely identified genuine users (i.e., but actually impostors - false positive (FP)) by the biometric system to the total number of impostors in the biometric system. The total number of impostors in the biometric system is the summation of false positive (FP) and true negative (TN). Here, true negative (TN) refers to the total number of correctly identified impostors by the biometric system. The equation for FAR is presented in Eq. 1.1.

$$FAR = \frac{FP}{FP + TN} \tag{1.1}$$

2. False Rejection Rate (FRR): The false rejection rate (FRR) is also known as the false non-match rate (FNMR). The false rejection rate (FRR) refers to the rate by which a genuine user is rejected by the biometric system [1]. The FRR is measured as ratio of the total number of falsely identified impostors (i.e., actually genuine users- cases of false negative (FN)) by the

biometric system to the total number of genuine users in the biometric system. The total number of genuine users in the biometric system is the summation of false negative (FN) and true positive (TP). Here, true positive (TP) refers to the total number of correctly identified genuine users by the biometric system (Eq. (1.2)).

$$FRR = \frac{FN}{FN + TP} \tag{1.2}$$

- 3. Equal Error Rate (EER): The equal error rate (EER) is a measure of accuracy of a biometric system when the false rejection rate (FRR) and false acceptance rate (FAR) are equal. Lower value of EER implies higher accuracy of a biometric system.
- 4. Genuine Acceptance Rate (GAR): Another approach to measure the accuracy of a biometric system is genuine acceptance rate (GAR). The genuine acceptance rate (GAR) measures the rate by which the biometric system correctly accepts the genuine users. GAR is measured as following:

$$GAR = 1 - FRR \tag{1.3}$$

5. Recognition Accuracy: The performance measures FAR, FRR, EER and GAR are used to evaluate the performance of a biometric system in the context of a verification task. Similarly, recognition accuracy is used to evaluate the performance of the biometric system in the context of an identification task. The recognition accuracy (in %) measures the ratio of the number of correctly identified probes to the total number of probes in the biometric system. The recognition accuracy a_r (in %) is defined as:

$$a_r = \frac{n_c}{n_p} \times 100 \tag{1.4}$$

Here, n_c and n_p denote the number of correctly matched probes and the total number of probes, respectively.

1.1.3 Real Life Applications of Biometrics

A biometric system is used for two modes of identity establishment mechanism: (i) verification and (ii) identification. Verification refers to establishment of the claimed identity of a user as genuine or impostor. In verification mode, the template of a probe user is matched with only the template of a user for whom the identity is claimed by the probe user (one-to-one matching). Here, the biometric system answers the question: "are you who you claim to be?". In identification mode, the biometric system answers the question: "who are you?". The template of a probe user is matched with the templates of all the enrolled users (one-to-many matching). The probe user is identified as one of the known users of the system based on the matching scores. In the above case, it is a closed set identification task. In closed set identification, the probe user must be one of the enrolled users. On the contrary, in the case of open set identification, the probe user may not be an enrolled user too.

A biometric system has applications in diverse environments. Biometric systems are widely used in applications related to the government sector, financial sector and forensic applications. The government of India has initiated a large scale biometric based unique identification system (Aadhaar) [3] to assign a unique identity to all of its citizens. Over the past few years, the Aadhaar based welfare-disbursement programs are initiated by the Indian government [3]. Similarly, the Philippines government has introduced a biometric based identification system (PhilSys) [4]. This system aids in unique identification of its citizens and also provides an environment for secure banking transaction.

Border control and airport security are other applications of the biometric system. The United Kingdom (UK) iris recognition immigration system (IRIS) project [5], the United State (US) visitor and immigration status indicator technology (VISIT) [6] and the United Arab Emirates (UAE) iris-based airport security system [7] are few examples of biometric based border control and airport security systems.

Biometrics is also being used in the financial sector, such as for providing secure banking transactions [8], for the know-your-customer (KYC) [9, 10] process and for opening new bank account [11]. National Payments Corporation of India (NPCI) has recently introduced aadhaar enabled payment system (AePS) [12] to enable bank customers to avail banking services (e.g., cash deposit, cash withdrawal, aadhaar to aadhaar fund transfer and other banking transactions) over biometric based micro-ATM. Similarly, NPCI has also introduced bharat interface for money (BHIM) aadhaar pay system [13] to enable biometric based payment system for merchants.

Biometrics also plays an important part in law enforcement related applications. For decades, biometrics has been used as an investigative tool to find a suspect. It is also used as forensic evidence. The International Criminal Police Organization (Interpol) has initiated a biometric based law enforcement approach to counter terrorist activities. This initiative is named Facial, Imaging, Recognition, Searching and Tracking (FIRST) [14]. National Institute of Standards and Technology (NIST) has defined a standard for using biometrics for law enforcement [15]. Law enforcement agencies across the globe follow this standard for their investigations.

1.1.4 Limitations of Unimodal Biometrics

Apart from having various advantages of using biometrics for the identity management system, these systems suffer form various challenges due to increase in the number of users and use of only a single modality (unimodal) for identification and verification. Some of the challenges (Fig. 1.3) are discussed in this section.

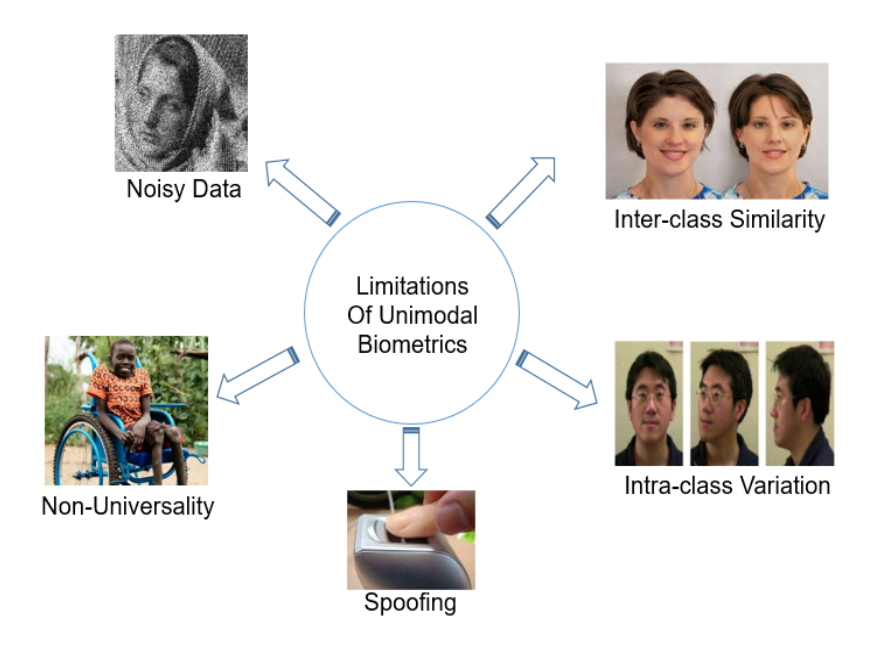


Figure 1.3: Limitations of unimodal biometrics

1.1.4.1 Noisy Data

A biometric image or signal can become noisy due to poor quality of the presented biometric information (e.g., cut or scar on fingerprint, change in voice due to

illness), faulty sensors (e.g., dust or scratches on fingerprint sensor, defocused face images) or uncontrolled acquisition approaches (e.g., poor illumination conditions for face image). A noisy biometric image or signal may decrease the recognition performance of the biometric system.

1.1.4.2 Inter-class Similarity

Inter-class similarity is defined as the similarity between two biometric templates belonging to different classes (i.e., users). Ideally, biometric templates of two different classes should be discriminative enough to differentiate between two users. This condition may be violated in some circumstances. Thus, it increases the chance of identifying an impostor as a genuine user. Inter-class similarity increases the false acceptance rate (FAR). Facial images of twins (Fig. 1.3) cause high inter-class similarity [16].

1.1.4.3 Intra-class Variation

Contrary to inter-class similarity, intra-class variation is defined as the variation among the biometric templates of the same user (same class). This can be due to the pose variation (facial pose) or due to the ageing effect on the biometric modality. Fingerprint and face biometrics change over the age [17]. Therefore, these biometrics can increase the intra-class variation. High intra-class variation increases the rejection of genuine users (i.e., increase in false rejection rate (FRR)) by the biometric system.

1.1.4.4 Non-universality

The considered biometric modality in a biometric system must be universal in nature. Every user in the biometric system must possess the biometric modality in consideration. Unfortunately, biometric modalities are not universal in nature. For example, the fingerprint modality does not work for the users who do not have fingerprints due to injury or any other reason. Similarly, gait based biometric system does not work for persons with disability to walk. Voice biometrics can not be captured for speech-impaired persons.

1.1.4.5 Easy to Spoof

Some of the biometric modalities such as fingerprints [18, 19] and face [20, 21], can easily be spoofed. A synthetically created fingerprint [19] or a spoofed face [20] can easily fool a biometric system. Therefore, spoofing is a major challenge for any biometric system.

1.1.4.6 Other Challenges

Captured biometric information may vary across sensors for the same biometric modality. Therefore, the biometric system faces interoperability issues. The biometric system may fail to correctly identify a genuine user if the sensor used for the enrolment phase is changed at the recognition phase [1]. Similarly, a biometric system is also vulnerable to a variety of attacks such as template alteration, reply attack, etc. [1].

1.2 Introduction to Multibiometrics

A unimodal biometric system faces various limitations as above (Section 1.1.4). Recognition accuracy of a unimodal biometric system decreases due to these limitations. Use of multiple biometric modalities increases the recognition accuracy and overcomes the limitations of a unimodal biometric system. By combining biometric information from multiple biometric modalities in a structured manner, a multibiometric system can overcome some of the constraints of a unimodal biometric system. This superiority of multibiometrics over unimodal biometrics is established through few of the initial experiments [22, 23]. In the literature, the word 'multibiometrics' widely refers to fusion of different biometric information from same biometric modality [1, 24, 25, 26] or fusion of multiple biometric modalities [27, 28, 29, 30] to verify or identify a probe user. Multibiometrics can be broadly classified as:

1. **Multi-sensor:** In a multi-sensor biometric system, multiple sensors are used to capture the biometric information from the same biometric modality. For example, face biometrics may be captured using a specially designed face recognition device, a digital camera and a surveillance camera (Fig. 1.4).

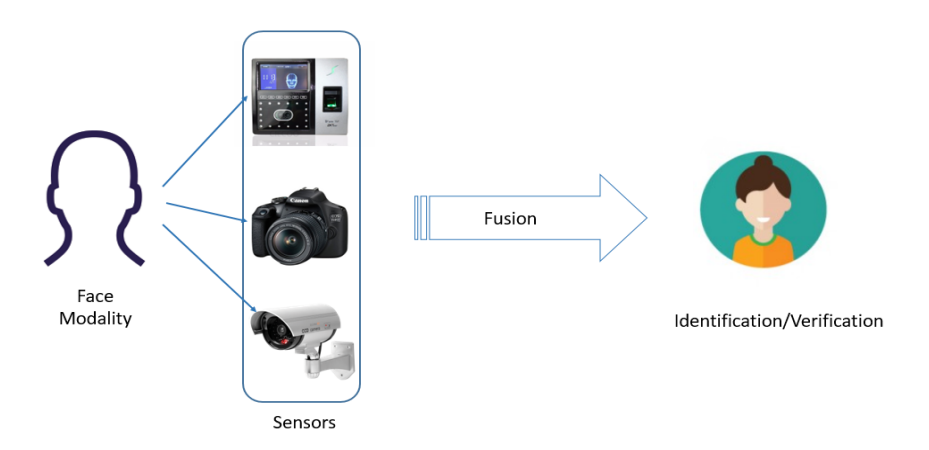


Figure 1.4: An example of multi-sensor biometric system

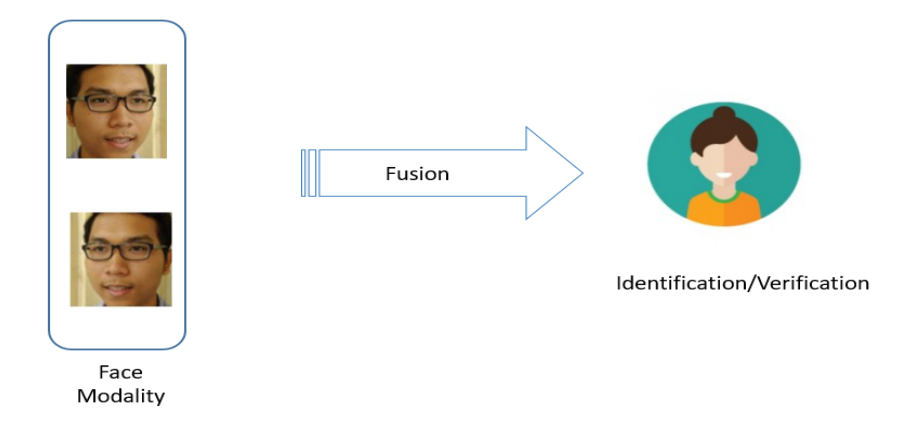


Figure 1.5: An example of multi-sample biometric system

- 2. **Multi-sample:** A multi-sample biometrics fuses multiple samples of the same biometric modality. Fusion of frontal face along with left and right profiles of face [31] (Fig. 1.5) is an example of multi-sample biometrics.
- 3. **Multi-instance:** A multi-instance biometrics fuses multiple instances of similar biometric modality. Example can be a fusion of fingerprint biometrics from different fingers (left and right index fingers) [32] (Fig. 1.6).
- 4. **Multi-algorithm:** In a multi-algorithm biometric system, multiple feature extraction algorithms are used to extract the features of the same biometric modality. These features are then fused together. One example is the

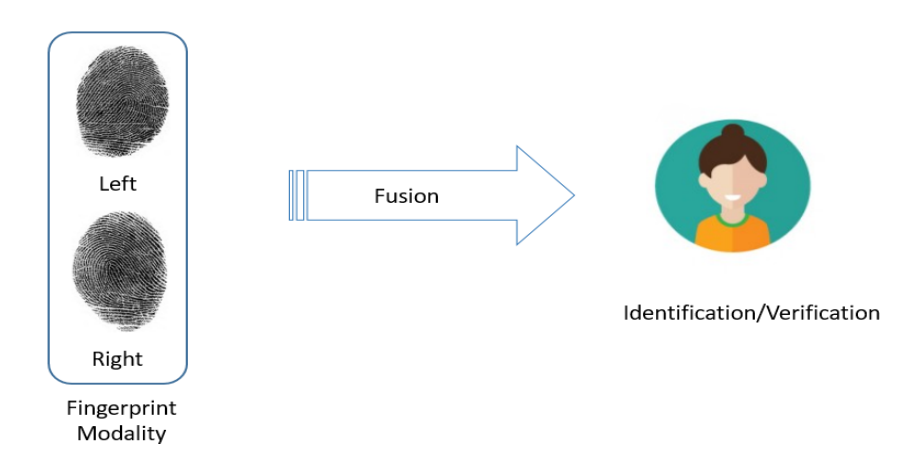


Figure 1.6: An example of multi-instance biometric system

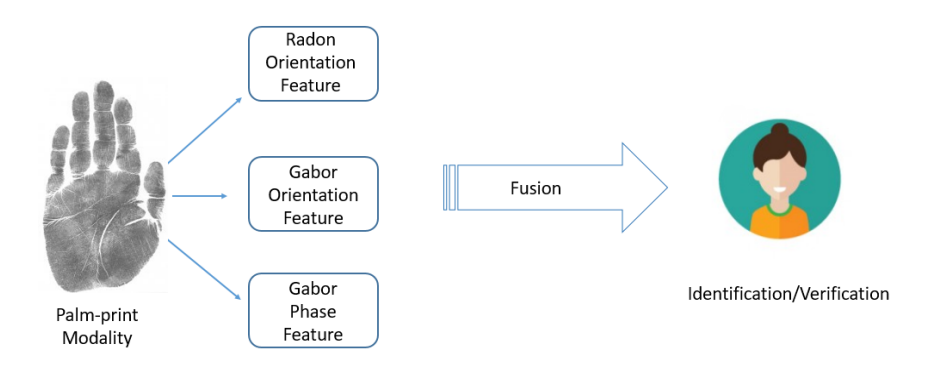


Figure 1.7: An example of multi-algorithm biometric system

extraction of features of palm-print by using Radon orientation, Gabor orientation and Gabor phase feature extraction methods [33] (Fig. 1.7). Similarly, several features of gait modality are extracted using several feature extraction methods [2].

5. **Multi-trait:** A multi-trait biometric system fuses multiple biometric traits together. Few examples include fusion of face and gait [34] and face and palm-print [35] (Fig. 1.8).

To build a multimodal biometric system, one needs to examine three questions: (i) what to fuse, (ii) when to fuse, and (iii) how to fuse. 'What to fuse' deals

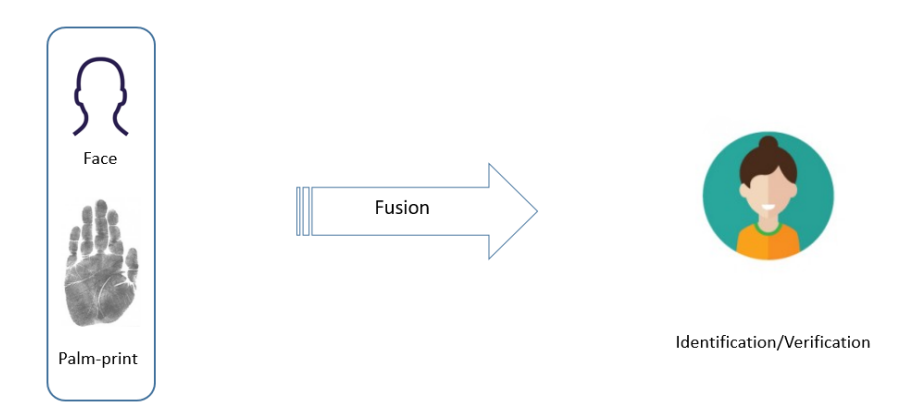


Figure 1.8: An example of multi-trait biometric system

with the biometric traits which have to be fused. 'When to fuse' answers the question regarding the stage in the biometric recognition pipeline where the given biometric information has to be fused. Various stages in the biometric recognition pipeline are presented in Fig. 1.2. At last, 'how to fuse' highlights the required approach to fuse the given biometric information at a given stage in the biometric recognition pipeline.

1.2.1 Levels of Multimodal Biometric Fusion

Fusion of multimodal biometrics can be performed at one or more of the following levels in all of the aforementioned categories: fusion before matching (sensor level [36, 37, 38], feature level [38, 39, 40, 41, 42, 43, 44, 45, 46, 47, 48]), and fusion after matching (score level [38, 41, 45, 49, 50, 51, 52, 53, 54, 55, 56, 57], rank level [34, 58], and decision level [38, 59, 60, 61]).

1.2.1.1 Sensor Level Fusion

Sensor level fusion falls under the category of 'fusion before matching' scheme. As the name suggests, the fusion of biometric information is performed at the sensor level. Acquired raw biometric images or signals from several sensors are fused at this level (Fig. 1.9). This level is also known as image-level or pixel-level fusion [1] as the raw images are directly fused at this level without undergoing the feature extraction stage. At this fusion level, the amount of biometric information is very high. At the same time, the size of a biometric image or signal may vary due to

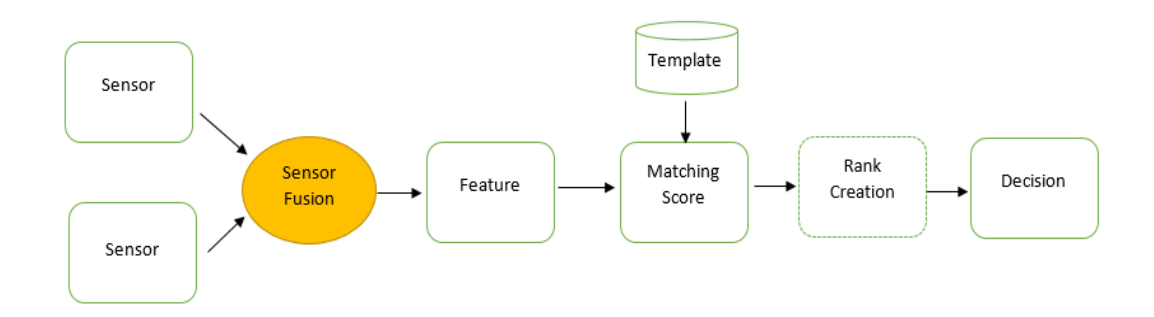


Figure 1.9: Sensor level fusion

change in biometric modalities. It poses a challenge for the fusion at this level. As a result, the use of sensor level fusion is limited to the fusion of the same kind of modality.

1.2.1.2 Feature Level Fusion

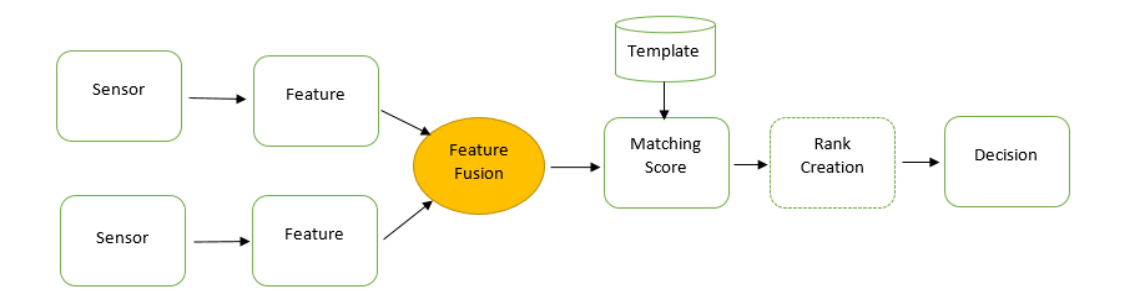


Figure 1.10: Feature level fusion

Feature level fusion is another fusion in the category of 'fusion before matching'. The features from the same or different modalities are extracted using modality-dependent feature extractor approaches in feature level fusion. These features are then fused to recognize a user. A schematic diagram of feature level

fusion is shown in Fig. 1.10. The extracted features from same modality using different feature extraction approaches or the extracted features from different modalities may vary in their dimensions. Therefore, the features are brought into a common dimension before fusing features at this level.

1.2.1.3 Score Level Fusion

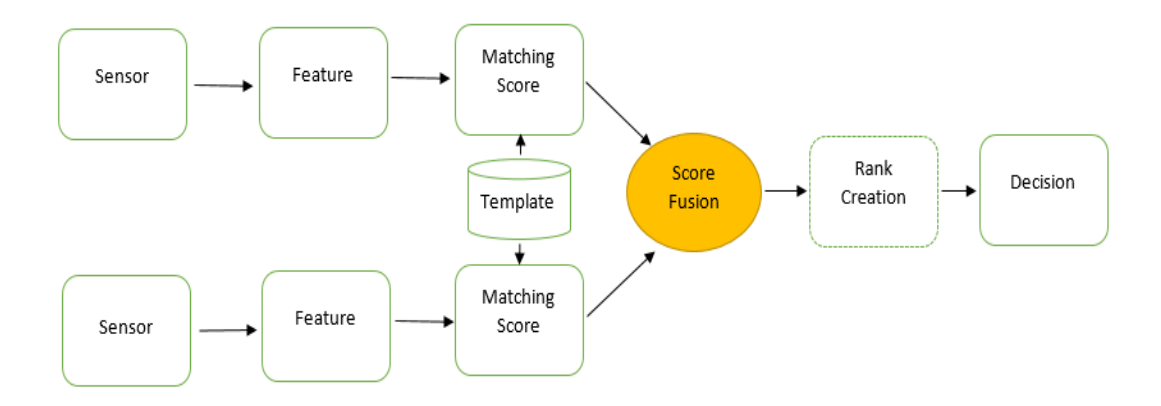


Figure 1.11: Score level fusion

The score level fusion is the first fusion level under the category of 'fusion after matching. The score level fusion is used for both user verification and user identification tasks. In the context of user verification task, the extracted feature (template) of a probe user is matched with the corresponding stored template (claimed identity by the probe user) to produce a match score (similarity or dissimilarity). A user is recognized as a genuine user or an impostor based on the match score. In the context of user identification task, the template of a probe user is compared with the templates of all the enrolled users to generate a score list. The score level fusion fuses such score lists to find a fused score list. This fused list is then used to establish the identity of the probe user. A schematic diagram of score level fusion is shown in Fig. 1.11. Furthermore, the score level fusion scheme can be used for any combination of modalities as the matching scores (similarity or dissimilarity) are used for fusion. Therefore, the score level fusion schemes are modality independent. Hence, these schemes are widely used for the fusion of multimodal biometrics. The major drawback of score level fusion is the varying range of scores across different modalities. The matching scores for

different modalities may have different ranges. Hence, all scores are normalized [49, 62, 63] into a common range before performing the fusion at score level.

1.2.1.4 Rank Level Fusion

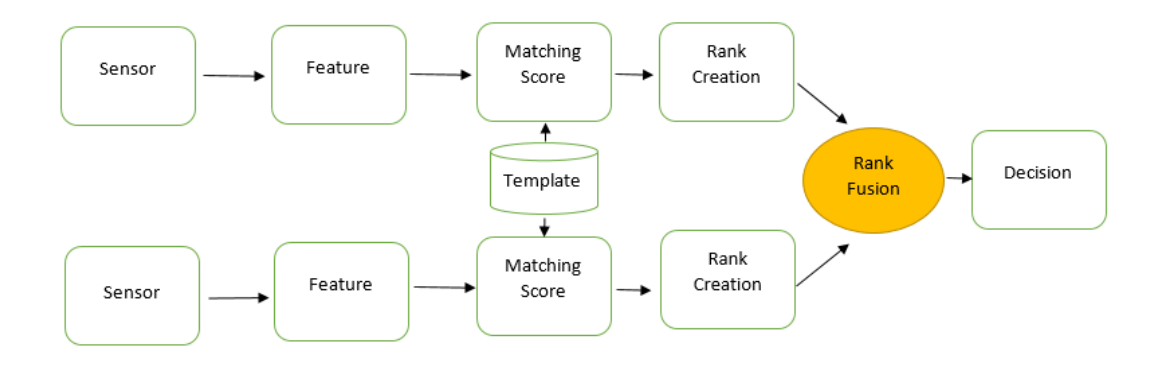


Figure 1.12: Rank level fusion

The computed matching scores at the score level are used to rank the users. Thus, a rank list is created. The rank lists for multiple modalities are fused using rank level fusion schemes to produce an aggregated rank list. The highest-ranked user (rank 1 being the best) is the matched user with the probe. Matching scores (similarity or dissimilarity) are directly used to generate the rank list. Therefore, score normalization is not required in rank level fusion. A schematic diagram of rank level fusion is shown in Fig. 1.12.

1.2.1.5 Decision Level Fusion

Decision level fusion is a more abstract level of fusion. At this fusion level, the least amount of biometric information is present. Only the final decisions of individual biometric modalities are available at decision level fusion. These decisions are fused to form the final decision about the genuineness of the probe user. A schematic diagram of decision level fusion is shown in Fig. 1.13.

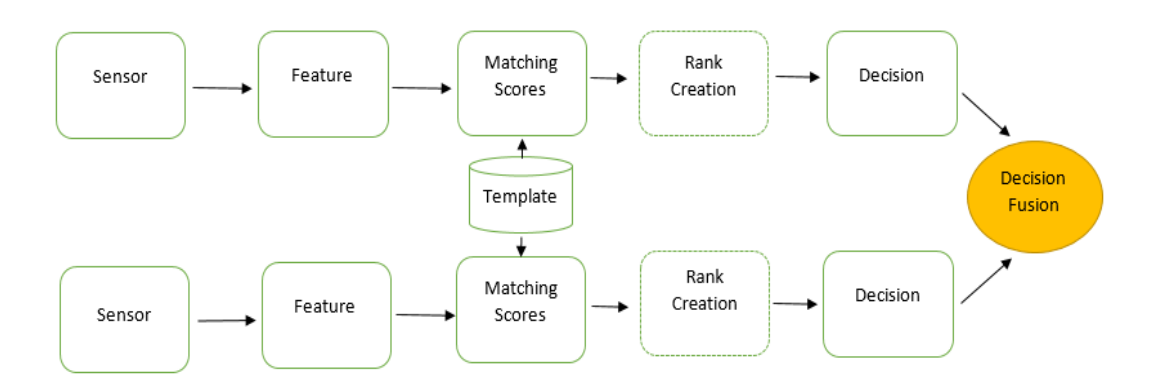


Figure 1.13: Decision level fusion

1.2.2 Real Life Applications of Multimodal Biometrics

In multimodal biometrics, the fused biometric information is likely to be more distinctive to an individual than the information in a single biometric modality. Multiple modalities often result in increased recognition performance and system reliability. As a result, multimodal biometrics is increasingly being employed as an authentication method. For example, the Emirates airline has developed a face and iris biometric-based check-in and boarding system at Dubai airport [64]. Similarly, Singapore has developed an immigration clearance system based on multimodal biometrics (MMBS) to enhance the security at immigration and checkpoints authority (ICA) [65]. Philippines has introduced the face, iris, and fingerprint-based identification system (PhilSys) [4]. This system aids the unique identification of its citizens and provides an environment for secure banking transactions. The future of identity in the financial sector is likewise being shaped by multimodal biometrics [66].

1.3 Research Objective

Traditional biometric systems (unimodal) suffer from various challenges such as noisy data, intra-class variation, inter-class similarity, non-universality and easiness to spoof. Therefore, research has been progressed in the direction of combining multiple biometric modalities. The combination of biometric information

from multiple modalities is called a multibiometrics or multimodal biometrics [1, 24]. Various types of multibiometric systems are listed in Section 1.2.

In a multimodal biometric system, fusion of biometric information from various modalities can be performed at five different levels: sensor, feature, score, rank and decision level. These levels of fusion are stated in Section 1.2.1. The sensor level and feature level fusion approaches fall in the category of 'fusion before matching' schemes. At sensor level fusion, the acquired biometric images or signals may vary in size across different biometric modalities. Therefore, it is difficult to combine images or signals at the sensor level unless they are captured using the similar sensors. Similarly, dimensions of the extracted features from these images or signals also vary for different modalities. Hence, all the feature vectors need to be in a common dimension to fuse biometric information at the feature level [1]. Therefore, these fusion schemes can only be used if either all of the modalities are of the same type of biometrics or all the feature vectors are normalized to the same dimension.

On the contrary, the 'fusion after matching' schemes (score, rank and decision level fusion) are not dependent on the nature of the captured images or signals and the extracted features. In all these schemes, fusion is performed only after obtaining scores from individual modalities. According to the score level fusion, similarity or dissimilarity scores are computed by comparing a probe subject's biometric information (template) with the enrolled biometric information (template) for each biometric modality. In rank level fusion, ranks are derived from the matching scores. These ranks represent the possible set of matching identities in decreasing order of confidence. Decision level fusion only requires the decisions from considered biometric modalities and combines them to generate the final decision. Therefore, very less information is available during decision level fusion. Hence, score and rank level fusion schemes have the maximum information available during fusion in comparison to decision level fusion schemes. Hence, score level fusion [49, 50, 51, 52, 53, 62, 67, 68, 69, 70, 71, 72, 73, 74, 75, 76] and rank level fusion [34, 58, 77, 78, 79, 80, 81] are mostly accepted levels of fusion for multimodal biometrics. Therefore, the scope of the research work in this thesis is also centred around the score and rank level fusion.

A good fusion strategy at the score and the rank level can enhance the performance of a multimodal biometric system. Moreover, these levels of fusions are modality independent. Hence, developed approaches for these levels of fusion can be applied to any modality. Therefore, as reported in this thesis, the objective of the research is to develop novel modality-independent score and rank level

fusion schemes to enhance the performance of the multimodal biometric system for identification task. The problem of score and rank level fusion is conceptualized as an optimization problem in this research. Novel modality-independent optimization based fusion approaches have been proposed in the context of score and rank level fusion. Furthermore, the quality of biometric modality is also considered to enhance the performance of proposed approaches at score and rank level fusion. The optimization based fusion approaches have slow convergence rate (i.e., take large amount of time to reach to optimal solution). Therefore, an approach to reduce the search space is also proposed in this research to achieve a fast convergence rate for proposed optimization based fusion approaches. Finally, the proposed fusion approaches are applied to the task of person identification in the era of covid-19 pandemic or similar situations where persons are using face masks. The key objective of the reported research in this thesis are as following:

- Proposing novel modality-independent optimization based fusion approaches for score and rank level fusion for multimodal biometric fusion.
- Incorporating the quality of biometric modality to enhance the performance of the proposed optimization based fusion schemes.
- Reducing the search space for achieving fast convergence rate of the proposed optimization based fusion approaches.
- Applying the proposed approaches on a task of person identification in the era of covid-19 pandemic or similar situation when face masks are used.

1.4 Contribution of the Thesis

Major contributions of the thesis are highlighted in this section. Contributions of this thesis are stated as proposing novel modality independent optimization based score and rank level fusion strategies as following:

1. Optimization Based Rank Level Fusion of Multimodal Biometrics: In the context of multimodal biometric fusion, rank level fusion is one of the widely used fusion level. In rank level fusion, the obtained rank lists from the matching scores of the considered modalities are fused to produce a final rank list. The fused list should be as close as possible with all the rank lists of considered modalities. Therefore, the rank level fusion problem is

conceptualized as an optimization problem to obtain the optimal fused rank list. Here, the objective is to find a fused rank list with a minimum weighted summation of distances from the rank lists of considered modalities. Here, weighted Spearman footrule distance measure is used to find the stated distance. A novel rank level fusion approach based on a genetic algorithm (GA) is proposed in this research to solve the stated optimization problem. Furthermore, a novel rank level fusion approach based on particle swarm optimization (PSO) is also proposed in this research.

- 2. Optimization Based Score Level Fusion of Multimodal Biometrics: Inspired by the performance of above optimization based rank level fusion approaches, a similar fusion strategy is investigated for score level fusion. Here, the optimization based score level fusion approach is proposed to enhance the performance of the multimodal biometric system. The score lists from different modalities are fused together to obtain the final fused score list in score level fusion. Similar to the optimization based rank level fusion approach, the score level fusion problem is conceptualized as an optimization problem. Furthermore, this research proposes two novel score level fusion approaches based on genetic algorithm and particle swarm optimization to solve this problem.
- 3. Quality Driven Optimization Based Multimodal Biometric Fusion: After investigating the optimization based approaches for rank and score level fusion of multimodal biometrics. The quality derived optimization based rank and sore level fusion approaches are proposed in this research. The quality of biometric modality can significantly increase or decrease the performance of the multimodal biometric system. Therefore, the quality of each biometric modality is estimated, this quality is used as a weight for the considered modality. The estimated weights are incorporated into the optimization based score and rank level fusion approach to further enhance the performance of multimodal biometric system.
- 4. Reduced Search Space Driven Optimization Based Multimodal Biometric Fusion: The acceptability of multimodal biometric fusion schemes depends on the recognition accuracy (finding an optimal solution) of the proposed approach and how quickly the approach finds the optimal solution (convergence time). The above optimization based multimodal fusion

approaches are slow in finding the optimal solution. A particle swarm optimization (PSO) is a population-based search algorithm. The PSO searches for an optimal solution in a large search space containing all possible candidate solutions. As a result, the PSO based fusion approaches take a considerable amount of time to reach at the optimal solution. Therefore, novel approaches to reduce the search space of particle swarm optimization based rank and score level fusion are proposed in this research to reduce the amount of time (convergence time) to reach at the optimal solutions. The same discussion is applied for the genetic algorithm (GA) based approached too. But PSO based approaches converge faster than GA based approaches. Hence, in this work, only PSO based approaches have been taken up for further reduction of their convergence time.

5. Person Identification in the Era of Covid-19 Pandemic Using Proposed Optimization Based Multimodal Biometric Fusion Approach: Finally, proposed quality and reduced search space driven particle swarm optimization based score level fusion approach is applied to a person identification task in the era of covid-19 pandemic. Performances of the designed system are evaluated in the context of multimodal fusion of masked face and iris biometrics at score level. Here, the masked face biometric information is fused with the iris biometric information to improve the recognition accuracy of the multimodal biometric system in the era of covid-19 pandemic or similar situation.

1.5 Organization of the Thesis

Rest of the thesis is organized as following:

- A literature survey of existing score and rank level fusion approaches for multimodal biometrics is presented in **Chapter** 2.
- In **Chapter** 3, novel modality-independent optimization based rank level fusion approaches for multimodal biometrics are proposed.
- In **Chapter** 4, novel modality-independent optimization based score level fusion approaches for multimodal biometrics are proposed.

- In **Chapter** 5, novel modality-independent quality driven optimization based score and rank level fusion approaches for multimodal biometrics are proposed.
- In **Chapter** 6, novel reduced search space driven optimization based score and rank level fusion approaches for multimodal biometrics are proposed.
- Application of proposed optimization based multimodal fusion approach in the era of covid-19 pandemic is reported in **Chapter** 7.
- Conclusive remarks of this thesis are drawn in **Chapter** 8. Additionally, future research directions are highlighted in this chapter.

Chapter 2

Literature Survey on Score and Rank Level Fusion Approaches for Multimodal Biometrics

A literature survey of existing score and rank level fusion approaches for multimodal biometrics is presented in this chapter. This chapter is organized into the following sections: A literature survey of existing score level fusion approaches is presented in Section 2.1. In Section 2.2, a literature survey of existing rank level fusion approaches is presented. In Section 2.3, various weight estimation approaches for score and rank level fusion are presented.

2.1 Score Level Fusion Approaches

Score level fusion approaches can be broadly categorised as: (i) rule-based, (ii) likelihood ratio-based, (iii) classification-based and (iv) optimization based approaches. A brief literature review of each one of these categories is presented in this section.

2.1.1 Rule-Based Methods

In rule-based methods, simple mathematical operations (e.g., summation, product, minimum and maximum) are performed on the matching scores from multiple biometric modalities to generate an aggregated score. Prior to carrying out these mathematical operations, obtained scores from individual modalities are normalized into a common range of values. Various normalization methods exist in literature. Examples include min-max [49, 62, 63], z-score [1, 63], tanh [1, 63], generalized extreme value distribution-based [50] and anchored score normalization [67, 82].

1. **Min-Max Normalization:** The min-max normalization [49, 62, 63] is one of the widely used score normalization approach. In this normalization, the scores are normalized in the range of [0,1]. The minimum and the maximum scores after normalization are set to 0 and 1, respectively. All other scores are set to real values in the range of [0,1]. The normalized score using min-max normalization is computed as following:

$$\hat{s}_{ij} = \frac{s_{ij} - min(S_i)}{max(S_i) - min(S_i)}$$

$$(2.1)$$

Here, s_{ij} represents a matching score of the probe with the j^{th} enrolled subject for a biometric modality i. A list S_i contains such matching scores of the probe subject with all the enrolled subjects for the biometric modality i. The terms $min(S_i)$ and $max(S_i)$ represent the minimum and the maximum scores, respectively, for the score list S_i . Normalized score of an enrolled subject j for an input biometric modality i is represented as $\hat{s_{ij}}$. A list of these scores $\hat{s_{ij}}$ of all subjects for biometric modality i represents a normalized score list $\hat{S_i}$.

2. **z-score Normalization:** The z-score normalization [1, 63] uses mean μ_{S_i} and standard deviation σ_{S_i} of a score list S_i to compute the normalized score \hat{s}_{ij} of an enrolled subject j for biometric modality i. The function to compute normalized score using z-score normalization is as following:

$$\hat{s}_{ij} = \frac{s_{ij} - \mu_{S_i}}{\sigma_{S_i}} \tag{2.2}$$

The z-sore normalization approach is sensitive to outliers as both mean and standard deviation are sensitive to outliers [1, 63]. The z-score $\hat{s_{ij}}$ is equal to 0 if the matching score s_{ij} is equal to the mean. The rest of the scores are either negative or positive. A matching score s_{ij} below the mean μ_{S_i} produces a negative z-score. On the other side, a matching score s_{ij} above the mean μ_{S_i} produces a positive z-score. These normalized scores are not in common range for each modality. The z-score normalization is useful in the presence of outliers in a score list [1, 63].

3. **tanh Normalization:** The hyperbolic tangent (tanh) normalization [1, 63] is genuine score distribution based normalization approach. A genuine score is the matching score between two biometric templates of the same user. The normalized score using tanh normalization is computed as following:

$$\hat{s_{ij}} = \frac{1}{2} \left\{ tanh\left(0.01 \times \left(\frac{s_{ij} - \mu_{G_i}}{\sigma_{G_i}}\right)\right) + 1 \right\}$$
 (2.3)

Here, μ_{G_i} and σ_{G_i} represent mean and standard deviation, respectively, of the genuine score distribution G_i . The hyperbolic tangent (tanh) function returns a value in the range of [-1,1]. Therefore, the normalized scores using tanh normalization are in the range of [0,1] due to Eq. 2.3.

4. Generalized Extreme Value (GEV) Distribution Based Normalization: This approach [50] is based on the extreme value theory [83]. The genuine scores are present at the extreme (tail) of the entire score distribution containing genuine and impostor scores. Therefore, the generalized extreme value (GEV) distribution considers only the genuine scores. The mean (μ), scale (σ) and shape (k) parameters of the GEV distribution are estimated using the maximum likelihood estimation. The normalized score using GEV distribution based normalization approach is computed as following:

$$\hat{s}_{ij} = \begin{cases} exp\left(-\left(1 + k \times \left(\frac{s_{ij} - \mu}{\sigma}\right)^{-(1/k)}\right)\right), & \text{if } k \neq 0\\ exp\left(-exp\left(-\left(\frac{s_{ij} - \mu}{\sigma}\right)\right)\right), & \text{if } k = 0 \end{cases}$$

$$(2.4)$$

The above Eq. 2.4 resembles the cumulative distribution function of GEV distribution.

5. Anchored Score Normalization: In anchor value based score normalization approach [67, 82], an anchor value is computed using the overlapping region between the distributions of genuine score G_i and impostor score I_i for biometric modality i. The computed anchor value generates the normalized score $\hat{s_{ij}}$. Figure 2.1 illustrates the overlapping region of genuine and impostor scores. In this figure, the blue box represents the impostor scores. Similarly, the green box represents the genuine scores. The red rectangle highlights the overlapping region of genuine and impostor scores. In [67, 82], following three approaches are presented to compute the anchor value:

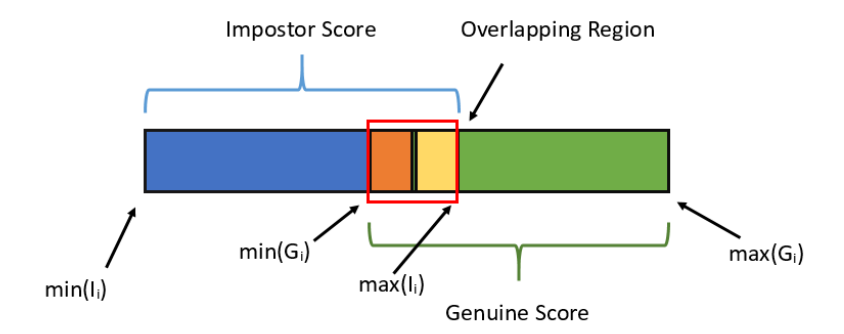


Figure 2.1: Genuine and impostor scores with their overlapping region (for similarity scores)

• Overlap extrema-based anchor (OEBA): The anchor value for biometric modality *i* is computed as:

$$A(i) = max(I_i) - min(G_i)$$
(2.5)

Here, $max(I_i)$ and $min(G_i)$ represent the maximum value of impostor scores (I_i) and the minimum value of genuine scores (G_i) , respectively.

• Mean-to-overlap extrema-based anchor (MOEBA): The anchor value for biometric modality i is computed as:

$$A(i) = \{ max(I_i) - \mu(I_i) \} + \{ \mu(G_i) - min(G_i) \}$$
 (2.6)

Here, $\mu(I_i)$ and $\mu(G_i)$ represent the mean values of impostor scores (I_i) and genuine scores (G_i) , respectively.

• Overlap extrema-variation-based anchor (OEVBA): The anchor value for biometric modality i is computed as:

$$A(i) = \frac{max(I_i) - min(G_i)}{std(I_i) - std(G_i)}$$
(2.7)

Here, $std(I_i)$ and $std(G_i)$ represent the standard deviations of impostor scores (I_i) and genuine scores (G_i) , respectively.

These computed anchor values are applied on the genuine and impostor scores for a biometric modality i to compute the normalized score $\hat{s_{ij}}$ as:

$$\hat{s_{ij}} = \begin{cases} \frac{s_{ij} - \min(G_i, I_i)}{2(A(i) - \min(G_i, I_i)}, & \text{if } s_{ij} <= A(i) \\ 0.5 + \frac{s_{ij} - A(i)}{\max(G_i, I_i) - A(i)}, & \text{if } s_{ij} > A(i) \end{cases}$$

$$(2.8)$$

Here, $min(G_i, I_i)$ represents the minimum value among all genuine G_i and all impostor I_i scores. Similarly, $max(G_i, I_i)$ represents the maximum value among all genuine G_i and all impostor I_i scores.

The obtained normalized scores using either of the above mentioned normalization approaches are then fused using rule-based approaches. The rule-based score level fusion approaches are summarized here.

1. **Sum Rule:** One basic rule-based method for score level fusion is the sum rule method [1, 67, 70, 84, 85, 86, 87]. Here, the summation of the normalized scores for several biometric modalities is considered as an aggregated score. The fused score is computed as:

$$s_j' = \sum_{i=1}^{N} \hat{s_{ij}} \tag{2.9}$$

Here, the normalized and the fused scores for subject j are represented as \hat{s}_{ij} and s'_{j} , respectively. The number of biometric modalities is represented by N.

2. Weighted Sum Rule: In the weighted sum rule approach, a weighted summation of a subject's normalized scores for all modalities generates an aggregated score [49, 51, 57, 67, 68, 70, 71, 72, 82, 84, 88, 89, 90, 91, 92, 93, 94, 95, 96, 97, 98, 99, 100, 101, 102, 103, 104]. The fused score is computed as:

$$s_j' = \sum_{i=1}^{N} w_i \hat{s_{ij}} \tag{2.10}$$

Here, w_i represents the weight for i^{th} biometric modality. The weight for a biometric modality indicates the significance of i^{th} biometric modality (matcher) while fusing the corresponding scores. Several approaches for estimating weight for each biometric modality have been proposed in the literature: (i) matcher or classifier performance-based [49], (ii) optimization-based [105], and (iii) quality-based [54]. Various weight estimation approaches are discussed in Section 2.3.

3. **Product Rule:** In product rule based score level fusion approach [1, 84, 86], the normalized scores of the considered subject from multiple modalities are

combined using the product of these normalized scores. The computation is performed as:

$$s_j' = \prod_{i=1}^{N} \hat{s_{ij}} \tag{2.11}$$

4. Weighted Product Rule: Similarly, in weighted product rule based score level fusion approach [68], the normalized scores of the considered subject from different modalities are combined using weighted product of normalized scores from each biometric modality. The fused score is computed as:

$$s_j' = \prod_{i=1}^N (\hat{s}_{ij})^{w_i} \tag{2.12}$$

5. Min Rule: In min rule based score level fusion approach, the minimum among the subject's normalized scores from N different biometric modalities is considered as the fused score [1, 70].

$$s_j' = \min_{\forall i}(\hat{s_{ij}}) \tag{2.13}$$

6. Max Rule: In max rule based score level fusion approach, the maximum among the subject's normalized scores from N different biometric modalities is considered as the fused score [1, 70, 106].

$$s_j' = \max_{\forall i}(\hat{s_{ij}}) \tag{2.14}$$

7. **Triangular Norm Based:** The works in [55, 69, 86, 107] adopt triangular norm (t-norm) based techniques for score level fusion. In these works, Hamacher, Frank, Einstein product, Yager and Schweizer–Sklar t-norm approaches are used on a pair of normalized scores for fusion. The functions of Hamacher, Frank, Einstein product, Yager and Schweizer–Sklar t-norms to compute the fused score s'_i are defined in following equations:

$$s_{j}' = \frac{\hat{s}_{1j}\hat{s}_{2j}}{\hat{s}_{1j} + \hat{s}_{2j} - \hat{s}_{1j}\hat{s}_{2j}}$$
(2.15)

$$s'_{j} = \log_{p} \left(1 + \frac{(p^{\hat{s}_{1j}} - 1)(p^{\hat{s}_{2j}} - 1)}{p - 1} \right) \text{ for } p > 0$$
 (2.16)

$$s_{j}' = \frac{\hat{s}_{1j}\hat{s}_{2j}}{2 - (\hat{s}_{1j} + \hat{s}_{2j} - \hat{s}_{1j}\hat{s}_{2j})}$$
(2.17)

$$s_{j}' = \max(1 - ((1 - \hat{s}_{1j})^{p} + (1 - \hat{s}_{2j})^{p})^{1/p}, 0) \text{ for } p > 0$$
(2.18)

$$s'_{j} = ((\hat{s_{1j}})^{p} + (\hat{s_{2j}})^{p} - 1)^{1/p}, \text{ for } p < 0$$
 (2.19)

Here, \hat{s}_{1j} and \hat{s}_{2j} represent the normalized scores of a subject j for a pair of biometric modalities. In the case of fusion involving more than two modalities, the scores from remaining modalities are iteratively fused with the already fused score.

8. **Symmetric Summation Based:** A symmetric summation based approach is proposed for score level fusion in [108]. The symmetric summation function is defined as following:

$$s_{j}' = \frac{t(\hat{s}_{1j}, \hat{s}_{2j})}{t(\hat{s}_{1j}, \hat{s}_{2j}) + t(1 - \hat{s}_{1j}, 1 - \hat{s}_{2j})}$$
(2.20)

Here, t() is a t-norm function. In the case of fusion involving more than two modalities, the scores from remaining modalities are iteratively fused with the already fused score.

9. Weighted Quasi-Arithmetic Mean: In comparison to all of the above rule based techniques, score level fusion using weighted quasi-arithmetic mean (WQAM) [62] has recently proved to be more efficient. This approach fuses the normalized scores by using the weighted quasi-arithmetic mean. A weighted arithmetic mean (wam) is defined as:

$$wam(\hat{s_{1j}}, \dots, \hat{s_{Nj}}) = (\sum_{i=1}^{N} w_i \hat{s_{ij}}) / \sum_{i=1}^{N} w_i$$
 (2.21)

Similarly, for strictly monotonous continuous generating function g(), the quasi-arithmetic mean (qam) is defined as:

$$qam(\hat{s}_{1j}, \dots, \hat{s}_{Nj}) = g^{-1} \left(\frac{1}{N} \sum_{i=1}^{N} g(\hat{s}_{ij}) \right)$$
 (2.22)

The function $g^{-1}()$ is the inverse of the generating function g().

The weighted quasi-arithmetic mean approach ([62]) is combination of weighted arithmetic mean (Eq. 2.21) and weighted quasi-arithmetic mean (Eq. 2.22) approaches. It computes the fused scores as following:

$$s'_{j} = wqam(\hat{s}_{1j}, \dots, \hat{s}_{Nj}) = g^{-1}\left(\left(\sum_{i=1}^{N} w_{i}g(\hat{s}_{ij})\right) / \sum_{i=1}^{N} w_{i}\right)$$
 (2.23)

The WQAMs are estimated using various generating functions. Following generating functions are used in [62]:

$$g(\hat{s}_{ij}) = tan(\frac{\pi}{2}\hat{s}_{ij}) \tag{2.24}$$

$$g(\hat{s}_{ij}) = \sin(\frac{\pi}{2}\hat{s}_{ij}) \tag{2.25}$$

$$g(\hat{s}_{ij}) = \cos(\frac{\pi}{2}\hat{s}_{ij}) \tag{2.26}$$

$$g(\hat{s}_{ij}) = (\cos(\frac{\pi}{2}\hat{s}_{ij}))^r \tag{2.27}$$

$$g(\hat{s_{ij}}) = (\hat{s_{ij}})^r \tag{2.28}$$

$$g(\hat{s_{ij}}) = r^{\hat{s_{ij}}} \tag{2.29}$$

$$g(\hat{s_{ij}}) = r^{1/\hat{s_{ij}}} \tag{2.30}$$

$$g(\hat{s_{ij}}) = \exp^{-(r/\hat{s_{ij}})}$$
 (2.31)

2.1.2 Likelihood Ratio Based Score Level Fusion Approaches

The density distributions of genuine and imposter scores are considered in the likelihood ratio-based fusion approach [73, 74, 109, 110]. Let these two distributions of genuine and impostor scores for i^{th} biometric modality be represented as $l_{i,gen}(s_{ij})$ and $l_{i,imp}(s_{ij})$, respectively. The likelihood ratio test on the generalized density in [109] is computed using Eq. 2.32. Similarly, the likelihood ratio test on the joint density (incorporating quality of a probe) in [73, 74, 110] is computed using Eq. 2.33.

$$s_{j}' = \prod_{i=1}^{N} \frac{l_{i,gen}(s_{ij})}{l_{i,imp}(s_{ij})}$$
(2.32)

$$s_{j}' = \prod_{i=1}^{N} \frac{l_{i,gen}(s_{ij}, q_{i})}{l_{i,imp}(s_{ij}, q_{i})}$$
(2.33)

Here, q_i is a quality estimate of the input signal in i^{th} modality. Moreover, an actual matching score s_{ij} is used here instead of a normalized matching score $\hat{s_{ij}}$. If the fused score s'_j is greater than a threshold value, the probe is considered as a genuine user. Otherwise, it is considered as an impostor.

A non-parametric kernel density estimation technique with a Gaussian kernel is used in [109] to estimate the generalized densities of genuine and impostor scores. The work in [110] further improves the work in [109] by incorporating the quality score to estimate the joint density using copula model [110]. Similarly, a Gaussian mixture model (GMM) is used in [73, 74] to estimate the two score densities.

The work in [111] proposes two approaches to improve the performance of likelihood ratio based score level fusion approach. At first, the biometric modalities having poor quality images are excluded while estimating the densities. This process is named as voting likelihood ratio test. Furthermore, a sequential likelihood ratio test is also proposed to decide the genuineness of a user. This test is performed for those subjects for whom the decision can not be deduced with the initial observation using two threshold values. If the fused score lies in between these two thresholds, the decision is suspended. In this case, voting likelihood ratio test is applied to make the final decision. In [112], a naive based likelihood ratio approach is proposed for score level fusion. Here, the naive likelihood ratio is estimated by summation of log-likelihood ratios of several biometric modalities.

2.1.3 Classification Based Approaches

In classification based score level fusion approach, the problem of score fusion is converted as a binary class classification problem (genuine and impostor class). Support vector machine (SVM) based score level fusion approaches in [75, 76, 113, 114, 115, 116] are few such examples. In these approaches, scores of a subject from multiple modalities are represented as a score vector. This vector is passed through a SVM classifier to classify it as either of two classes: genuine user or impostor. Other classification based score level fusion approaches involve Dempster-Shafer (D-S) theory [117, 118, 119] and Dezert-Smarandache (DSmT) theory [50, 120].

The work in [121, 122] uses a sequential fusion approach to fuse several biometric modalities. Likelihood ratio and support vector machine (SVM) classifiers are sequentially used to decide wither a score vector belongs to genuine user or impostor.

2.1.4 Optimization Based Approaches

In optimization based score level fusion approaches, the problem of score fusion is converted as an optimization problem. In [123], a differential evolution based score level fusion method is proposed. In this work, scores from multiple biometric modalities are aggregated to minimize the overlapping area between genuine and impostor score distributions. This objective is achieved by a differential evolution based search of suitable parameters for the score aggregation function.

The work in [124] uses the grasshopper optimization algorithm [125] to find the best confidence factors for belief assignments in various modalities. Similarly, particle swarm optimization based [126] and backtracking search optimization algorithm based [127] approaches are proposed to determine the best confidence factors for belief assignments in various modalities.

In [128], a particle swarm optimization (PSO) based approach selects the best score level fusion rule and its parameters among several competing rule-based methods. Here, minimization of the weighted sum of the false rejection rate (FRR) and false acceptance rate (FAR) is the main objective. The cost of incorrectly admitting an impostor and the cost of incorrectly rejecting a legitimate user determine the weight. Similarly, PSO is applied in [129] to choose the best belief function for score level fusion among a set of competing belief functions. Here, the objective is to reduce the weighted equal error rate.

2.2 Rank Level Fusion Approaches

In this section, several existing rank level fusion approaches for multimodal biometrics fusion are briefly discussed.

2.2.1 Borda Count Approach

According to Borda count approach [34, 35, 130, 131, 132, 133, 134, 135, 136, 137, 138, 139], summation of ranks of a subject across several modalities provides an aggregated rank for the concerned subject. Mathematically, it can be expressed as:

$$r'_{j} = \sum_{i=1}^{N} r_{ij} \tag{2.34}$$

Here, N represents number of different biometric modalities and r_{ij} represents the rank of j^{th} subject for the i^{th} modality. At the end, the final aggregated rank of a subject is decided based on the ordering of r'_j values of all subjects. In [140], a modified Borda count approach is presented. A weak matcher is identified as having the worst rank for a subject j. Then, the effect of the weak matcher is reduced by eliminating (i.e., setting to 0) the assigned rank by the matcher for the subject j. Finally, the Borda count is used to fuse the ranks.

2.2.2 Weighted Borda Count Approach

This method [34, 132, 133, 134, 135, 138, 140, 141] is an extension of Borda count method. It is also known as logistic regression. In this approach, a weight is assigned to each biometric modality. Then, the final rank is calculated by weighted summation of ranks of a subject for each modality. Mathematical expression to find the rank of a subject using weighted Borda count method is defined as:

$$r'_{j} = \sum_{i=1}^{N} w_{i} r_{ij} \tag{2.35}$$

Here, N represents number of different biometric modalities. w_i is the weight given to i^{th} modality and r_{ij} represents the rank of j^{th} subject for the i^{th} modality. At the end, the final aggregated rank of a subject is decided based on the ordering of r'_j values of all subjects. Introduction of weight in this method is advantageous when biometric modalities have significant differences in their performances.

2.2.3 Highest Rank Approach

This ranking approach [35, 136, 138, 142, 143, 144] finds the highest rank of a subject among the ranks in various modalities as the final rank for that subject. For example, let a subject have 1^{st} rank and 3^{rd} rank in two different biometric modalities. The highest rank for the subject is 1 between the ranks in these two modalities. Therefore, final rank of the subject is 1. Expression to find the rank of a subject using the highest rank method is given below:

$$r_j' = \min_{i=1}^{N} (r_{ij}) \tag{2.36}$$

Here, N represents number of different biometric modalities, r_{ij} represents the rank of j^{th} subject for the i^{th} modality. It is to be noted that a lower rank value is better. Therefore, min() function is used in Eq. 2.36 to determine the highest rank.

As this method computes the highest rank for each subject, many subjects may have the same rank. These ties are randomly broken to get the final rank of a subject [32]. It can lead to decrease in identification accuracy.

2.2.4 Non-linear Weighted Approaches

Several non-linear weighted rank methods for rank level fusion are also present in literature. Exponential ranking method [33] is one of these methods. Mathematically, it can be expressed as:

$$r'_{j} = \sum_{i=1}^{N} exp(w_{i} \ r_{ij})$$
 (2.37)

A modified version of above exponential rank level fusion is also presented in [33]. It is known as weighted exponential rank fusion method. It can be mathematically defined as following:

$$r'_{j} = \sum_{i=1}^{N} w_{i} \ exp(r_{ij})$$
 (2.38)

A division exponential based non-linear rank level fusion method is proposed in [32]. It can be mathematically defined as following:

$$r'_{j} = \sum_{i=1}^{N} \frac{1}{1 + exp(w_{i} \ r_{ij})}$$
 (2.39)

A logarithm based non-linear rank level fusion is also presented in [32]. Metamerically, it can be expressed as following:

$$r'_{j} = \sum_{i=1}^{N} log(1 + w_{i} \ r_{ij})$$
(2.40)

A hyperbolic tangent (tanh) based non-linear rank level fusion is also presented in [32]. Metamerically, it can be expressed as following: Hyperbolic arc sinus,

$$r'_{j} = \sum_{i=1}^{N} tanh(w_{i} \ r_{ij})$$
 (2.41)

A hyperbolic arc sine (asinh) based non-linear rank level fusion is also presented in [32]. Metamerically, it can be expressed as following:

$$r'_{j} = \sum_{i=1}^{N} asinh(w_{i} \ r_{ij})$$
 (2.42)

Similarly, hyperbolic arc tangent (atanh) based non-linear rank level fusion is also presented in [32]. Metamerically, it can be expressed as following:

$$r'_{j} = \sum_{i=1}^{N} atanh(w_{i} \ r_{ij})$$

$$(2.43)$$

In above equations, N represents number of different biometric modalities. w_i is the assigned weight to i^{th} modality. The term r_{ij} represents the rank of j^{th} subject for the i^{th} modality. The final aggregated rank of a subject j is decided based on the ordering of r'_j values of all subjects.

2.2.5 Markov Chain Based Approach

Rank level fusion of multimodal biometrics is performed in [58, 139, 145] by using Markov chain [146]. In this method, a node in the Markov chain is associated with a subject. Transitions in this Markov chain represent an ordered relation among these enrolled subjects. Stationary distribution for each state (subject) is computed based on the number of pairwise contests (elections) which have been won by the subject considering all the rank lists. Stationary distribution of this Markov chain gives the final rank for each state (subject).

2.2.6 Fuzzy Rank Based Approach

A fuzzy rank level fusion method is proposed in [147]. A classifier generates a fuzzy rank and a confidence factor for each enrolled subject (class) in each biometric modality for a concerned probe subject. The rank sum for each class is computed as the summation of fuzzy ranks of the concerned classes across all modalities. The computed fuzzy rank sum is penalized if the class dose not belong to a few selected top ranks for a modality. Similarly, the complement of confidence factor sum is also penalized if the class dose not belong to a few selected top ranks for a modality. The final fused rank is generated by performing multiplication operation between rank sum and complement of confidence factor sum for each class.

2.3 Weight Estimation Approaches

The existing score (weighted sum rule [49], WQAM [62]) and rank (weighted Borda count [34], non-linear approaches [33]) level fusion approaches use weight for each modality. These weights indicate the significance of each modality. Several approaches for estimating weight for individual modalities have been proposed in the literature. These approaches are divided into three categories: (i) matcher or classifier performance-based, (ii) optimization-based, and (iii) quality-based weight estimation.

2.3.1 Matcher or Classifier Performance-Based Approaches

The weight w_i for i^{th} modality is obtained in [49] by taking reciprocal of its equal error rate (EER) value. Less value of EER indicates high significance of that modality. Therefore, high weight value is assigned to that modality. Similarly, low weight value is assigned to a modality having high value of EER. This weight assignment using EER is shown in following equation:

$$w_i = \frac{1}{EER_i} \tag{2.44}$$

Similarly, the weight for a biometric modality is also considered as inversely proportional to EER in [148]. This weight assignment using EER is shown in following equation:

$$w_i = \frac{\left(\frac{1}{\sum_{i=1}^{N} 1/EER_i}\right)}{EER_i} \tag{2.45}$$

Additionally, the weights are normalized in [148] to have a summation as 1, i.e., $\sum_{i=1}^{N} w_i = 1$.

2.3.2 Optimization-Based Approaches

An appropriate combination of weights for the biometric modalities can also be searched among all possible combinations of weights. In optimization-based schemes, the optimal weight for each modality is derived using meta-heuristic optimization algorithms. In [105, 128], the objective is to find a set of optimal weights that minimizes the summation of Bayesian costs for false acceptance and false rejection. The work in [149] selects the optimal weights for each modality by minimizing the weighted summation of equal error rate (EER) values across all modalities. In another approach [150], the weights are selected by maximizing the recognition accuracy. In all of the above approaches, particle swarm optimization (PSO) algorithm is used to find the optimal weights. Moreover, minimization of recognition error is considered as the objective function in [151]. A genetic algorithm (GA) based approach is used to find the optimal weights for each biometric modality in [151].

2.3.3 Quality-Based Approaches

The quality of a biometric signal has a substantial impact on the performance of a biometric recognition system [152, 153]. Hence, a subpar quality biometric signal negatively impacts the overall performance of the recognition system. The quality describes a biometric signal's potential to be used for recognition while providing consistent, accurate, and predictable results [153]. Therefore, it is essential to incorporate the quality of a biometric signal in multimodal biometric fusion [154, 155, 156, 157].

The works in [54, 73, 110] use quality-derived weights for fusion of multimodal biometrics. The quality of a biometric signal can be estimated by (i) assessment of biometric signal quality in terms of blurring, defocus, poor illumination, noise, and other artefacts [158, 159, 160] or (ii) analyzing the biometric information present in the acquired signal [153, 161].

The first category of approaches to assess the biometric signal quality is dependent on the characteristics of the signal. Several approaches of this category are discussed here. The universal quality index in [158] estimates illumination quality of a facial image in [159]. Here, the quality is assessed by combining three factors: loss of correlation, luminance distortion, and contrast distortion. Similarly, the sharpness and brightness of an image are used to estimate the quality of the face image in [160]. In [162], several factors are used to assess the quality of iris biometrics, such as interlacing, illumination, lighting, occlusion, pixel count, dilation, off-angle, and blur. A composite no-reference quality score is computed by combining blockiness and activity estimation in both vertical and horizontal directions in an image [163]. In [164], blurriness in an image due to defocus and motion is estimated as a quality metric. In [165], a convolutional neural network (CNN) based approach is used to estimate the quality of the face image. The CNN estimates face image quality by analyzing the blurriness in the face image due to its poor resolution. Few other no-reference image quality metrics exist in literature, such as blind image quality index (BIQI) [166], gradient-magnitude map Laplacian-of-Gaussian based blind image quality assessment (GM-LOG-BIQA) [166] and a blind/reference-less image spatial quality evaluator (BRISQUE) [54, 166].

Above mentioned quality estimation approaches focus on image quality. On the contrary, the amount of biometric information in an acquired image is equally important for biometric recognition [153, 161]. Several methods for estimating quality using biometric information exist in literature. For example, the quality of fingerprint biometrics is estimated using a wavelet-based quality assessment approach in [110]. In [167], the quality is estimated using another wavelet-based quality assessment approach. Similarly, redundant discrete wavelet transform (RDWT) is used to estimate the quality score of face [168], iris [168, 169] and fingerprint [170] images. In [171], image quality metric based on wave atom transform is presented for fingerprint biometrics. In [172], the quality of fingerprint image is estimated using the energy distribution in the power spectrum.

National Institute of Standards and Technology (NIST) fingerprint image quality (NFIQ) [173] is one of the primarily used quality estimation approaches for fingerprint biometrics. It consists of 11 quality features, including local orientation, contrast and other fingerprint-related features. Recently, NFIQ 2.0 [174] is introduced with additional features for fingerprint quality estimation. Similarly, in [175], various fingerprint features are used to estimate the quality of the fingerprint biometrics.

In [176], the quality of the entire eye image is estimated based on amount of occlusion. Furthermore, the quality of iris is estimated by correlation between the neighbouring features of iris. Additionally, dilation is also used to estimate the quality of iris. In [177], several statistical measures are used to estimate the quality of the iris.

A face quality estimation based on convolutional neural network (CNN) is presented in [178]. Here, a face quality network is trained on the ground truth quality score. In a completely different approach in [179], a face quality is estimated using a CNN-based face recognition model. In this approach, several instances of the trained face recognition model are considered by randomly selecting the dropout layers. An image is presented to every instance of this model. The quality is estimated by measuring variation among the generated embeddings across all instances of the model.

2.4 Summary

A detailed literature review on existing score and rank level fusion approaches is presented in this chapter. This review helps in developing a good understanding about these approaches. It can be observed from the presented literature that the rule based approaches are widely adopted for score (weighted sum rule [49, 51, 67]) and rank (weighted Borda count [34, 132, 133]) level fusion. However, these approaches do not guarantee the optimal performance of the multimodal biometric system. On the other hand, few optimization based approaches exist for multimodal biometrics. These approaches search for the optimal fusion technique [128], the optimal controlling parameters [123] or the optimal set of weights [105, 128]. This motivates to further explore optimization-based approaches for score and rank level fusion of multimodal biometrics. Hence, the subsequent chapters describe the proposed approaches in this direction.

Moreover, several score and rank level fusion approaches use weight for each modality. These weights indicate significance of the concerned modalities. These weights are estimated using matcher or classifier performance [49, 148], optimization techniques [105, 128], and quality assessment [54, 110].

Chapter 3

Rank Level Fusion of Multimodal Biometrics Using Optimization Based Approaches

In rank level fusion [34, 58, 77, 78, 79, 80, 81] approaches, rank lists are derived by considering relative ordering of the similarity or the dissimilarity scores between biometric traits of a probe and those of a set of enrolled subjects. Several such rank lists corresponding to various biometric modalities are combined to generate an aggregated or fused rank list. Several rank level fusion approaches can be found in literature (Section 2.2). Traditional rank level fusion approaches (e.g., Borda count [34], weighted Borda count [34], the highest rank [35], and non-linear weighted approaches [32, 33]) derive an aggregated rank list through simple mathematical calculations involving the input rank lists. As an example, Borda count [34] considers summation of ranks of a subject in the input rank lists. Similarly, non-linear weighted exponential approach [33] considers weighted summation of exponential values of ranks of a subject in the input lists. The works in [58, 139, 145] utilize Markov chain based models to find the aggregated rank list.

In a completely different approach, the work in this chapter perceives the rank level fusion of multimodal biometrics as an optimization problem. In this context, the objective is to minimize the weighted summation of distances between an aggregated rank list and the input rank lists. A widely used distance measure in the domain of rank aggregation problems - weighted Spearman footrule distance [180] - is considered in the proposed approach. In this chapter, genetic algorithm

based and particle swarm optimization based approaches are proposed to solve the above optimization problem in the context of multimodal biometric fusion.

The rest of this chapter is organized as following: A detailed formulation of rank level fusion of multimodal biometrics as an optimization problem is presented in Section 3.1. The proposed rank level fusion approach using genetic algorithm and experimental evaluation of the proposed work are presented in Section 3.2. In Section 3.3, the proposed rank level fusion approach using particle swarm optimization and experimental evaluation of the proposed work are presented. Comparison of convergence rate between genetic algorithm based and particle swarm optimization based rank level fusion approaches is presented in Section 3.4. Finally, the concluding remarks on the proposed rank level fusion approaches are drawn in Section 3.5.

3.1 Rank Level Fusion as an Optimization Problem

Let $B_1, B_2, ..., B_N$ be various biometric modalities to identify a person. Let the matching score s_{ij} be associated with each such biometric modality B_i for a j^{th} person (subject) for an input probe. A rank-ordered list L_i of those subjects can be generated from an ordering of these matching scores. Considering a high value of s_{ij} as good (for a similarity score), the following is true about the ordered list L_i : $s_{ij} > s_{ik}$ implies $r^{L_i}(j) < r^{L_i}(k)$. Here, $r^{L_i}(j)$ indicates the rank (i.e., position) of the j^{th} subject in the list L_i . On the contrary, considering a low value of s_{ij} as good (for a dissimilarity score), the following is true about the ordered list L_i : $s_{ij} < s_{ik}$ implies $r^{L_i}(j) < r^{L_i}(k)$.

Therefore, N ordered lists are created as $L_1, L_2, ..., L_N$ for biometric modalities $B_1, B_2, ..., B_N$, respectively. A combination of these N ordered lists generates an aggregated list δ^* as it is shown in Fig. 3.1.

$$\delta^* = aggregate(L_1, L_2, \dots, L_N) \tag{3.1}$$

Constructing a fused rank list δ^* with the minimum weighted summation of distances of the input lists $L_1, L_2, ..., L_N$ from the fused list is the objective here. As a result, the objective function for generating the aggregated list is:

$$minimize \ \phi(\delta) = \sum_{i=1}^{N} w_i \times d(\delta, L_i)$$
 (3.2)

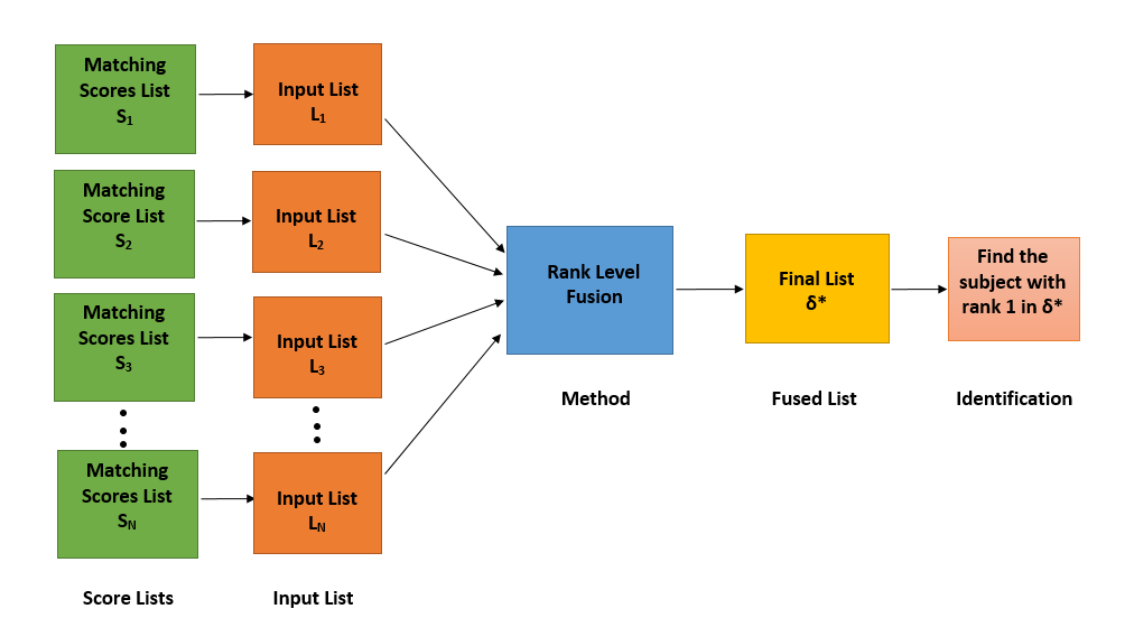


Figure 3.1: Fusion of multimodal biometrics at rank level

A candidate fused list is represented by δ . The fused list which minimizes the above objective function is denoted as δ^* . A weight w_i is associated with each of the N biometric modalities. Here, the weight represents the significance of the corresponding biometric modality. In this present work, the significance of each modality is considered as equal.

The function d() in Eq. 3.2 denotes a distance between a fused and an input rank list. In the current work, weighted Spearman footrule [180] metric is used for the distance measure $d(\delta, L_i)$ between a pair of lists δ and L_i . The stated distance metric estimates the weighted summation of absolute differences between the subjects ranks (pair-wise) in the input and the aggregated lists as following:

$$d(\delta, L_i) = \sum_{t \in L_i \cup \delta} I(t) * |r^{\delta}(t) - r^{L_i}(t)|$$
(3.3)

Here, $r^{\delta}(t)$ represents the rank (i.e, position) of subject t in the list δ . $r^{L_i}(t)$ represents the rank (i.e, position) of subject t in the input list L_i . An influence factor I(t) is associated with the rank difference for each subject t in Eq. 3.3. The motivation for considering these weights are mentioned as following: If rank (i.e., position) of the subject t is good (i.e., close to 1) in any one of the lists, then the subject will have more influence on the computed distance. Otherwise, the assigned influence factor I(t) is less to indicate lesser influence of the lower-ranked

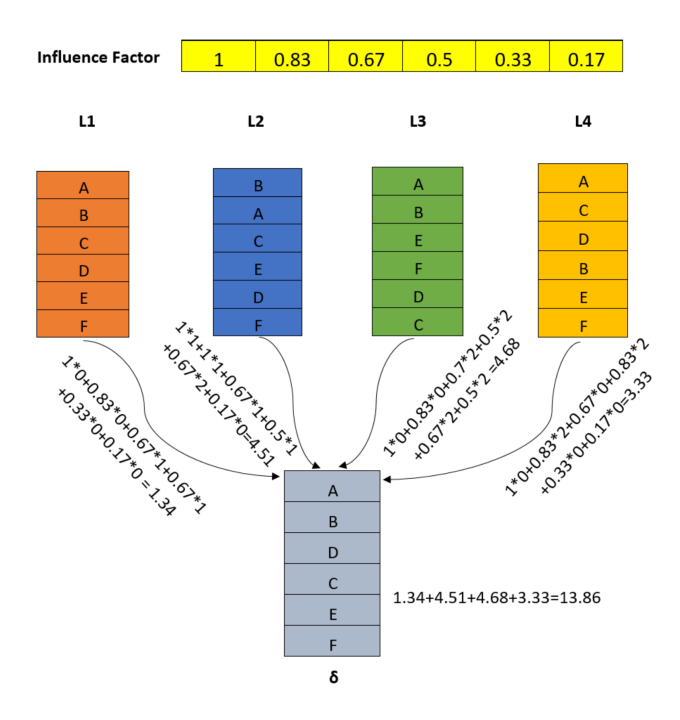


Figure 3.2: Weighted Spearman footrule distance computation

subject (in both lists) on the distance computation. Hence, the value of I(t) is decided by following Eq. 3.4.

$$I(t) = 1 - \frac{(\min(r^{\delta}(t), r^{L_i}(t)) - 1)}{n}$$
(3.4)

Here, n represents the number of enrolled subjects. If subject t is not present in one of the two lists (either δ or L_i), the rank of the subject $(r^{\delta}(t))$ or $r^{L_i}(t)$ in the list is considered as one more than the size of the list.

Figure 3.2 presents an example of applying weighted Spearman footrule distance for aggregating ranked lists of subjects. Let there be four input lists L_1, L_2, L_3 and L_4 . Each list contains six subjects (A, B, C, D, E and F). There is one candidate list δ . Weighted distance of this candidate list δ from each input list is computed using Eq. 3.3. For example, subjects A and B are at same position in the list L_1 and δ . Hence, rank difference is zero. Subject C is at third position in list L_1 and is present at fourth position in δ list. Hence, absolute difference of the two ranks of subject C is one. Minimum of these two ranks is three. Hence, influence factor I(t) is selected as 0.67 as it is at third position as shown in Fig. 3.2. Similarly, rank difference is calculated for each subject and a weighted summation is taken as shown in Fig. 3.2. Thus, it can be estimated that

weighted Spearman footrule distance between lists L_1 and δ is 1.34. Similarly, estimated weighted Spearman footrule distance of δ from the input lists L_2, L_3 and L_4 are 4.51, 4.68 and 3.33, respectively. Finally, distances of a candidate list from each of the input lists are added to generate the final fitness value $\phi(\delta)$ as 13.86.

3.2 Proposed Genetic Algorithm Based Approach

In this section, a genetic algorithm based approach is proposed to solve the above optimization problem (Eq. 3.2). Genetic algorithm is a widely accepted paradigm to solve this kind of optimization problem involving large search spaces [181, 182, 183, 184, 185, 186, 187]. This algorithm is based on the process of natural selection where the fit solutions (chromosomes) are selected from a population based on a fitness function. These selected chromosomes produce the off-springs having better chance of survival due to inheritance of the characteristics of these parent chromosomes. The proposed genetic algorithm based approach uses the elitism concept. In elitism based genetic algorithm, better solutions are memorised. If the newly produced offsprings do not have better fitness values than their parents, then the parents are retained in the new population. Otherwise, produced offsprings substitute their parents in the new population. This concept of elitism ensures that the best solution in an iteration does not deteriorate. The speed up of the performance of genetic algorithm due to this elitism is well documented in [188, 189].

The genetic algorithm based rank level fusion approach provides an aggregated rank list which has the minimum weighted summation of distances from all the input rank lists. A weighted Spearman footrule distance is used (Section 3.1) to prioritize the top-ranked subjects. Detail of the proposed genetic algorithm based approach is presented in this section.

3.2.1 Problem Domain Specific Design of Genetic Algorithm

The major contribution of this work is formulation of rank level fusion of multimodal biometrics as an optimization problem and adoption of genetic algorithm in this context. Representation of chromosomes and custom-designed operators to suite this problem domain are presented in this section.

3.2.1.1 Representation of a Chromosome

The objective of this proposed genetic algorithm based rank level fusion scheme for multimodal biometrics is to find an ordered list of subjects based on their ranks. Therefore, a chromosome in the proposed approach represents an ordered list of subjects. Two main characteristics of this representation of chromosome are stated as following:

- Unique position of a subject in a list indicates its rank. Hence, a subject appears in a list only once.
- Every subject is present in a list.

Based on the above facts about the design of a chromosome, it can be said that length of a chromosome is equal to the number of enrolled subjects. For example, an ordered list δ in Fig. 3.2 is represented by a chromosome (A,B,D,C,E,F). Here, subject A has rank one and subject B has rank two. Similar observations can be made for other subjects in the list too.

3.2.1.2 Fitness of a Chromosome

In order to solve the formulated optimization problem in Section 3.1, fitness of a chromosome (i.e., a candidate list) is measured as a weighted summation of distances of the candidate list from the input lists (Eq. 3.2). Weighted Spearman footrule distance (Eq. 3.3) is used as the distance measure between the candidate list and an input list. Here, the objective is to minimize the fitness value. Therefore, the fittest solution is having the lowest fitness value.

3.2.1.3 Initialization of Population

In traditional genetic algorithm, chromosomes in an initial population are generated randomly. On the contrary, domain knowledge is used to generate the chromosomes in initial population for achieving fast convergence [190, 191, 192]. Similarly, initialization of chromosomes in the proposed genetic algorithm is carried out using a mix of knowledge-based and random initialization. Let a population of fixed size M is considered. N out of these M chromosomes are initialized

to represent N input lists (i.e., solutions from each individual modality). Justification of initializing N chromosomes using input lists is that an input list represents a ranked list of subjects based on matching scores for the concerned biometric modality. Ideally, all biometric modalities should generate the same ranked order of the subjects. But practically, some deviations will be observed for each modality. Hence, the problem of list aggregation arises. Unless the quality of the acquired biometric signal is poor, consideration of the input lists in the initial population improves the convergence rate. Remaining (M-N) chromosomes are randomly generated (i.e., a random sequence of subjects are considered as chromosome). But two characteristics of a chromosome (Section 3.2.1.1) are maintained during this random initialization.

3.2.1.4 Selection

A roulette wheel based selection process is used in the proposed work. The chromosomes with better fitness values $\phi(\delta)$ (smaller distances) share the larger areas in roulette wheel. Let M chromosomes be $\delta_1, \delta_2, ..., \delta_M$. Corresponding fitness values of these chromosomes are $\phi(\delta_1), \phi(\delta_2), ..., \phi(\delta_M)$, respectively. As the objective is minimization of distances, each fitness value $\phi(\delta_m)$ is converted as:

$$\phi'(\delta_m) = \max(\phi(\delta_1), \phi(\delta_2), \dots, \phi(\delta_M)) / \phi(\delta_m)$$
(3.5)

Then, the proportion of area A_m in the roulette wheel for a chromosome is determined as following:

$$A_m = \frac{\phi'(\delta_m)}{\phi'(\delta_1) + \phi'(\delta_2) + \ldots + \phi'(\delta_M)}$$
(3.6)

Thus, a fitter chromosome having lower objective function value $\phi(\delta_m)$) gets a larger area on the roulette wheel. The roulette wheel is rotated M times to select M chromosomes for the new population. Every time, one chromosome is selected form M chromosomes in the current population. The chromosome, whose assigned area in the roulette wheel appears in front of a pivot, is selected each time. Larger the assigned area in the roulette wheel is, the probability of getting selected into the new population for the chromosome is higher.

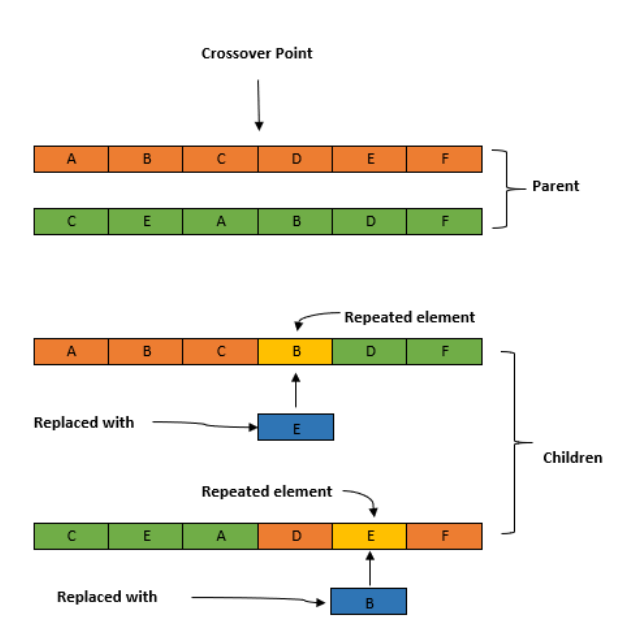


Figure 3.3: An illustration of crossover operation

3.2.1.5 Crossover

The newly generated population based on fitness values is then randomly divided into $\frac{M}{2}$ non-overlapping pairs. In the proposed work, population size M is considered as an even number. Crossover is performed between each pair of parent chromosomes. For each pair of chromosomes, a crossover point is decided randomly. In crossover operation, a pair of offspring chromosomes are generated by interchanging the parts of parent chromosomes around the crossover point. This operation can be understood using illustration in Fig. 3.3. A crossover point is marked for two parent chromosomes in Fig. 3.3. Every element of the first parent up to the crossover point (i.e, A, B and C) and every element of the second parent after the crossover point (i.e, B, D and F) are combined together to produce the first offspring. It has elements of both parents (i.e, A, B, C, B, D and F). Similarly, the second offspring is produced by combining elements of the second parent up to crossover point (i.e., C, E and A) and elements of the first parent after crossover point (i.e., D, E and F). The second offspring contains elements as C, E, A, D, E and F. After interchanging parts of the chromosomes, repetition of subjects is possible in a chromosome. As the length of the chromosome is fixed, it causes missing subjects in the chromosome. It is illustrated using an example in Fig. 3.3. It violates the designed characteristics of a chromosome in this context. In order to deal with this situation, the second occurrence of every repeated subject is replaced with a missing subject in that chromosome. This process is performed for every newly generated child chromosome. As it is shown in Fig. 3.3, there are six subjects (A to F) in each of the parent chromosomes. After crossover, two generated offsprings may contain repeated subjects. As an example in Fig. 3.3, subject B and subject E are repeated in the first and the second offsprings, respectively. In order to remove these repetitions, the second occurrence of each of the repeated subjects is replaced with a missing subject. As an example in Fig. 3.3, subject B is repeated and subject E is missing in the first offspring. Therefore, the second occurrence subject B is replaced by subject E. Similarly, subject E is repeated and subject B is missing in the second offspring. Therefore, the second occurrence of subject E is replaced by subject B. Moreover, an elitist genetic algorithm is adopted to speed up convergence. Therefore, all four chromosomes (both offsprings and both parents) are evaluated using the fitness function. The two fittest chromosomes (having the two least fitness values) are selected from the set of four chromosomes. These two selected chromosomes are retained in the population. It ensures retaining of better solutions in the population.

3.2.1.6 Mutation

The newly generated population after crossover further goes through the mutation process. The population of chromosomes can be represented using a matrix of size $M \times n$. Here, the number of chromosome in population is M. The total number of subjects (length of a chromosome) is n. Each row in this matrix refers to a chromosome in the population. Another matrix of size $M \times n$ is randomly generated. Each element in the randomly generated matrix has a value in the range [0,1]. The positions in this matrix having the values less than or equal to a small mutation probability p_{mut} are considered for mutation operation. Thus, all such genes are identified, which will go through a mutation process. Let k_m number of such candidate positions are identified for mutation in each chromosome m. Then, such candidate positions in each chromosome m are paired into $\left|\frac{k_n}{\alpha}\right|$ number of pairs. Here, $\left|\cdot\right|$ refers to the largest integer which is smaller than or equal to its argument. Here, the mutation operation is designed as pair-wise swapping of gene values in each $\lfloor \frac{k_m}{2} \rfloor$ position pairs for the m^{th} chromosome. As an example in Fig. 3.4, there are ten chromosomes from C1 to C10. Each chromosome contains six subjects. A random matrix of size 10×6 is generated. Elements

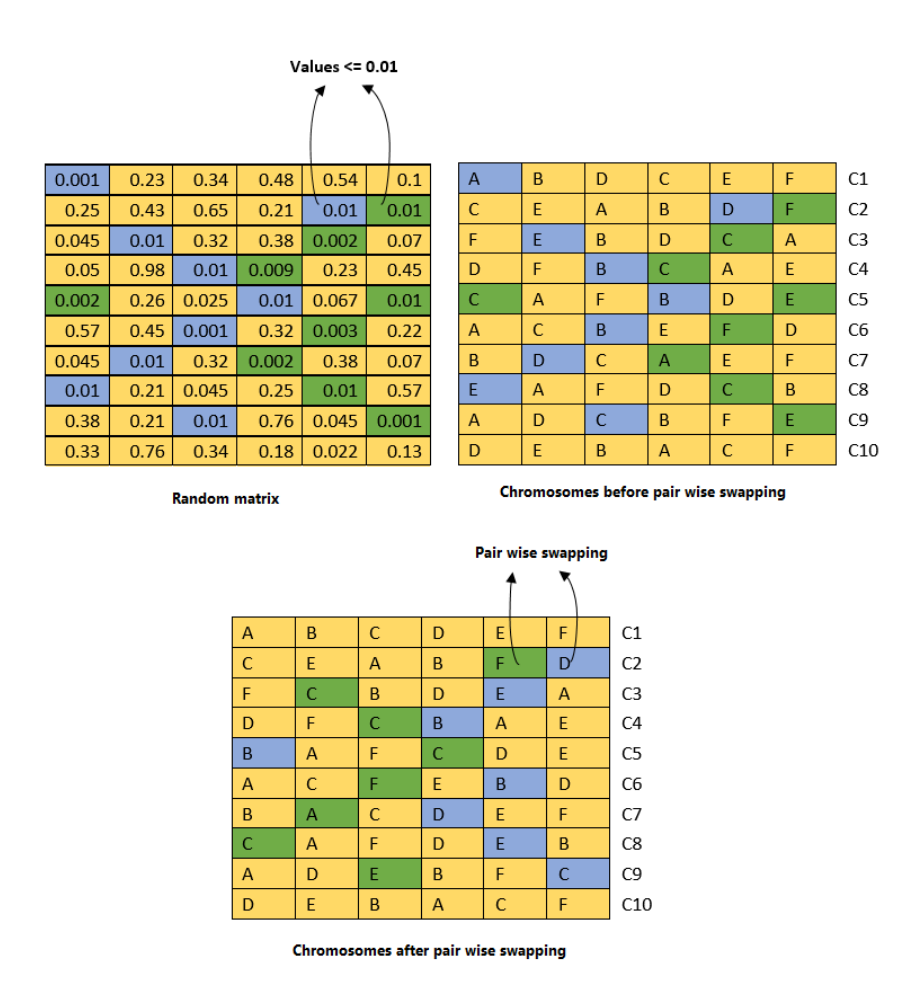


Figure 3.4: An illustration of mutation operation

of this matrix have randomly generated values in the range [0,1]. Each position in the matrix having value less than or equal to mutation probability as 0.01 is marked using either blue or green color. These elements are candidate positions for mutation. Pairs of such positions are selected in each chromosome. The genes in the selected pairs of positions are interchanged to generate new chromosome. The process also helps in avoiding the repetition of subjects in a chromosome. As an example in Fig. 3.4, a chromosome in the second row has two subjects (genes) D and F, whose positions are interchanged. Interestingly, chromosome C1 has only one candidate position. Another candidate position is not there for mutation in C1. Hence, the mutation does not take place for this chromosome. Similarly, chromosome C5 has three candidate positions for mutation with gene values C, B and E. Here, only first two genes (C and B) are interchanged. There

is no other position with which the gene E can be interchanged. After this step, each mutated chromosome is tested using the fitness function. If the fitness value of a new chromosome is better than the fitness value of its parent chromosome, then the new chromosome replaces the parent chromosome. Otherwise, the parent chromosome is retained in the new population. Thus, elitism is maintained for the proposed genetic algorithm. It is to be noted that swapping is always performed between genes of same chromosome. If genes of different chromosomes are swapped, then repetition of subjects may occur in chromosomes. Therefore, genes of the same chromosome are swapped to avoid this problem.

3.2.1.7 Stopping Criteria

Genetic algorithm is iterative in nature. Selection, crossover and mutation steps are repeated iteratively until a stopping criteria is satisfied. If the chromosomes in the population do not change due to either crossover or mutation over a number of iterations, the algorithm stops. The stated window size on the number of iterations is experimentally decided as 2000 for NIST BSSR1 multimodal biometric dataset (set 1) [193] and 3500 for OU-ISIR BSS4 multi-algorithm gait dataset [2, 194]. Then, the best chromosome in the final population is considered as the final ranked list of the subjects.

3.2.2 Performance Evaluation and Discussion

Detailed performance analysis is carried out for the proposed genetic algorithm based rank level fusion approach against several existing fusion approaches (both at rank level and at score level). The proposed approach is experimentally studied on two different multimodal biometric datasets: (i) NIST BSSR1 multimodal dataset [193] involving fingerprint and face modalities and (ii) OU-ISIR BSS4 multi-algorithm dataset [2, 194] involving multiple feature extraction methods of gait biometrics. It is experimentally established that the proposed genetic algorithm based rank level fusion approach performs better than several existing state-of-the-art rank and score level fusion approaches. These existing state-of-the-art approaches are mentioned in Section 3.2.2.1. The datasets along with the corresponding performance measures of all these comparing approaches are discussed in subsequent subsections.

3.2.2.1 State-of-the-Art Approaches for Performance Comparison

Performances of the existing state-of-the-art linear and non-linear rank level fusion approaches are compared with that of the proposed genetic algorithm based rank level fusion approach. Following rank level fusion approaches are used for experimental comparison: Borda count [34], weighted Borda count [34] and highest rank approach [35] belong to linear rank level fusion approach. Even in recent years, these three approaches are widely used in the context of rank level fusion [72, 138]. Exponential [33], weighted exponential [33], division exponential [32] and logarithm [32] are non-linear rank level fusion approaches. Performance of the proposed approach is also compared against those of few state-of-the-art score level fusion approaches, such as weighted sum-rule [51], product-rule [1], max-rule [1], min-rule [1], weighted quasi arithmetic mean (WQAM) [62], Frank t-norm [69] and Hammcher t-norm [69]. All these comparing approaches for score level fusion use min-max normalization technique (Eq. 2.1). The performance of the proposed approach is also compared with those of few recent sum-rule based approaches using overlap extrema-based anchor (OEBA) [67], mean-to-overlap extrema-based anchor (MOEBA) [67] and overlap extrema-variation-based anchored (OEVBA) normalization techniques [82].

Some of these existing rank level fusion approaches (weighted Borda count, exponential, weighted exponential, division exponential and logarithm) and existing score level fusion approaches (weighted sum and WQAM) need weights for different biometric modalities. These weights have a significant influence in the performance of these approaches. Hence, an optimal set of weights for various modalities are obtained to produce the best performance for these comparing approaches. Therefore, an elitist genetic algorithm is used to obtain the optimum set of weights for each of the comparing approaches. A chromosome contains weights in the range of [0,1], i.e, each gene in a chromosomes contains a weight value. Recognition accuracy (defined in Eq. 3.7) is considered as a fitness function. Here, r_a represents recognition accuracy, n_c is number of correctly matched probes and n_p is the total number of probes.

$$r_a = \frac{n_c}{n_p} \times 100 \tag{3.7}$$

Initial population is set to 10. Hence, fitness value is computed for each chromosome. Selection of these chromosomes for next generation is done using roulette wheel based method. For crossover, 5 random pairs of chromosomes are selected from the population. After generation of offsprings from a pair of parent

chromosomes, all four chromosomes (two parents and two offsprings) are tested for fitness value. Among these four chromosomes, the two chromosomes having higher fitness values are selected for next generation. Mutation is performed with the mutation probability of 0.1. In mutation, the selected gene values are subtracted from 1 to produce new gene values. Elitist approach is followed to retain better chromosomes. A new chromosome having higher fitness value replaces the old chromosome. Otherwise, the old chromosome is retained. The algorithm converges when the optimal weights are found.

The set of selected weights depends on the dataset on which the weights are trained. Hence, k-fold cross-validation (using k=5) is used to eliminate this dependency. The dataset is split into k parts. k-1 parts are considered for training. These k-1 parts learn the set of weights using the elitist genetic algorithm. The remaining one part is used as a test set to report the recognition accuracy. The whole training and testing steps are repeated k-times to get different sets of weights and corresponding accuracies on the test sets. Finally, average accuracy from k such test sets are presented in the result. This process of obtaining weights for each modality is followed for each of the two datasets being used for performance comparison. On contrary, proposed work assigns same weight to each individual modality (input list) to check the efficiency of the proposed work over state-of-the-art rank level fusion approaches.

3.2.2.2 Fusion of Multimodal Biometrics Involving Face and Fingerprint (NIST BSSR1 Multimodal Dataset (Set 1))

Description of the Dataset: In this work, NIST BSSR1 multimodal dataset (set 1) [193] is considered for performance comparison. This dataset is widely used to study the fusion of multimodal biometrics [33, 50, 52, 195]. This dataset contains information from two biometric modalities- fingerprint and face. Fingerprints of right index finger and left index finger are considered as part of this dataset. Two different face matching modules are used for face biometrics-termed as G and C in the dataset. Biometric information for the above biometric modalities were acquired during the enrolment phase form each of the 517 persons (subjects). In this dataset, similarity scores of each of these subjects as a probe with all 517 subjects are provided as per two different face matchers (termed as G and C) and fingerprint matchers for right and left index fingers. In the context of score level fusion, these similarity scores from various biometric modalities are fused using existing score level fusion approaches. In order to perform a rank

Table 3.1: Performance comparison of the proposed GA based rank level fusion approach with unimodal matchers on NIST BSSR1 multimodal dataset (set 1)

	Method	Top-1 Rank	Top-2 Ranks	Top-3 Rank
	Face Matcher G	83.37	86.28	88.40
Unimodal	Face Matcher C	88.78	90.52	91.50
Ummodai	Left Fingerprint	85.70	87.04	87.81
	Right Fingerprint	92.07	93.23	93.62
Proposed GA Rank Fusion		99.42	99.42	99.42

level fusion, rank lists are generated from the given similarity scores. These rank lists are fused using the proposed genetic algorithm based as well as the existing rank level fusion approaches.

Performance Analysis: The recognition accuracies (in %) as defined in Eq. 3.7 for the proposed approach along with each unimodal matcher are presented in Table 3.1 for the probe being found within top-1 (Rank 1), top-2 (Rank 2) and top-3 (Rank 3) ranks (cumulative) in the aggregated rank list. The usefulness of the proposed rank level fusion approach over each of the unimodal matchers is obvious from the reported results in Table 3.1.

The recognition accuracies of the comparing approaches within top-1 (Rank 1), top-2 (Rank 2) and top-3 (Rank 3) positions along with the proposed approach are also presented in Table 3.2. It can be seen from the reported recognition accuracies that the proposed genetic algorithm based rank level fusion approach performs better than the majority of existing state-of-the-art rank level and score level fusion approaches. Among these existing rank level fusion approaches, division exponential approach [32] exhibits equivalent performance to the proposed approach while top-2 (Rank 2) and top-3 (Rank 3) positions are considered. But performance of the the proposed approach is better than that of the division exponential approach if only top-1 position (Rank 1) is considered. Among the score level approaches, only the WQAM [62] based approaches exhibit equal performance as with the proposed approach. The reason for this superiority of the proposed approach is that the approach considers minimization of a weighted summation of the distances between aggregated and input rank lists.

It can be noted that 99.42% is the maximum achievable accuracy on NIST BSSR1 multimodal dataset (set 1) [193]. It is observed that 514 probes among

Table 3.2: Performance of the comparing fusion methods on NIST BSSR1 multimodal dataset (set 1) using cumulative recognition accuracies in %

Method		Top-1 Rank	Top-2 Ranks	Top-3 Ranks
	Weighted Sum [51]	98.65	98.84	99.03
	Max Rule [1]	79.90	94.00	98.45
	Min Rule [1]	94.80	95.40	95.60
	Product [1]	97.87	98.26	98.67
	Sum-OEBA [67]	99.03	99.03	99.26
	Sum-MOEBA [67]	98.45	98.84	98.84
	Sum-OEVBA [82]	98.70	99.03	99.26
	Hamacher t-norm [69]	97.29	97.68	97.68
Score Level	Frank t-norm [69]	98.07	98.65	98.84
	WQAM cos [62]	99.42	99.42	99.42
	WQAM cos^r [62]	98.65	99.03	99.03
	WQAM tan [62]	99.42	99.42	99.42
	WQAM sin [62]	98.65	98.84	98.84
	WQAM $r^{1/s}$ [62]	99.42	99.42	99.42
	WQAM r^s [62]	99.42	99.42	99.42
	WQAM s^r [62]	99.42	99.42	99.42
	WQAM log [62]	99.42	99.42	99.42
	WQAM exp [62]	99.42	99.42	99.42
	Borda Count [34]	92.07	93.04	94.00
	WBorda [34]	92.50	94.20	95.36
	Highest Rank [35]	79.70	94.81	98.26
Rank Level	Exp [33]	89.16	90.13	91.30
	WExp [33]	87.81	89.16	90.71
	DivExp [32]	99.23	99.42	99.42
	Log [32]	98.45	99.03	99.23
	Proposed GA Rank	99.42	99.42	99.42

a total of 517 probes (99.42%) appear at the Rank 1 (first position) in the fused list. The improvement in the recognition accuracy is not observed even if top-3 positions are considered in the fused list. This is because the dataset contains three probe subjects for whom all four biometric matchers fail to correctly identify the actual subject. These probe subject IDs are 81,224 and 419. The rank for the probe ID 81 in the aggregated list as well as in all the input rank lists are reported in Table 3.3. The rank of subject ID 81 (actual subject) is 143 in the fused list (Table 3.3). The identified subject at first position (ID 419) using the proposed GA based fusion approach has rank 1 in all the individual matcher lists. Therefore, the subject ID 419 has been identified at first position (rank 1) in the proposed GA based rank level fusion approach. Similarly, the identified subject at second position (ID 377) using the proposed GA based rank level fusion approach has ranks 155, 79, 109 and 2 in the left index finger, right index finger, face matcher C and face matcher G, respectively. As this subject has good ranks in two of the modalities (right index finger and face matcher G), this subject is identified as the second best subject (rank 2) in the fused list. The other two probes (ID 224 and 419) that are incorrectly identified suffer from the same problem as seen in Table 3.4 and Table 3.5. Because of this, even the best of the fusion techniques are unable to correctly identify these three probes (Table 3.2).

Table 3.3: Ranks at each modality for ideally correct subject and the top three identified subjects according to the fused list (for probe subject ID 81)

Modality	Ideally correct	1^{st} Identified	2^{nd} Identified	3^{rd} Identified
Wiodanity	subject (ID 81)	subject (ID 419)	subject (ID 377)	subject (ID 513)
Left index finger	480	1	155	3
Right index finger	353	1	79	46
Face matcher C	143	1	109	272
Face matcher G	12	1	2	37
GA Rank	143	1	2	3

The changes in recognition accuracies (in %) with the changes in cumulative ranks are represented using cumulative match characteristic (CMC) curves in Fig. 3.5 and Fig. 3.6 for rank level and score level approaches, respectively. The proposed method outperforms several existing rank and score level fusion approaches, as it can be observed in the CMC curves in Fig. 3.5 and Fig. 3.6. It is observed from Fig. 3.5 that the CMC curve for the division exponential approach [32] is overlapping with that of the proposed genetic algorithm based rank level fusion approach for cumulative rank beyond 2 and above.

Table 3.4: Ranks at each modality for ideally correct subject and the top three identified subjects according to the fused list (for probe subject ID 224)

Modality	Ideally correct	1^{st} Identified	2^{nd} Identified	3^{rd} Identified
Widdanty	subject (ID 224)	subject (ID 68)	subject (ID 66)	subject (ID 300)
Left index finger	59	1	123	204
Right index finger	51	1	241	72
Face matcher C	122	5	1	3
Face matcher G	11	29	9	26
GA Rank	12	1	2	3

Table 3.5: Ranks at each modality for ideally correct subject and the top three identified subjects according to the fused list (for probe subject ID 419)

Modality	Ideally correct	1^{st} Identified	2^{nd} Identified	3^{rd} Identified
Wiodanity	subject (ID 419)	subject (ID 81)	subject (ID 120)	subject (ID 356)
Left index finger	478	1	180	69
Right index finger	470	1	2	183
Face matcher C	282	1	5	16
Face matcher G	279	2	20	1
GA Rank	497	1	2	3

The recognition accuracies of several WQAM based approaches [62] are equal to those of the proposed genetic algorithm based rank level fusion approach. Therefore, the CMC curves of these approaches overlap with the CMC curve of the proposed genetic algorithm based rank level fusion approach in Fig. 3.6.

3.2.2.3 Fusion of Multimodal Biometrics for Multiple Gait Feature Representations (OU-ISIR BSS4 Multi-Algorithm Dataset)

Description of the Dataset: Additionally, the second dataset (BSS4) is form the Institute of Scientific and Industrial Research (ISIR), Osaka University (OU) [2, 194]. This dataset has also been used for fusion of multi-biometrics in [196]. In this dataset, an input image sequence from gait has been processed using five different feature extraction methods: (i) Gait energy image (GEI), (ii) Frequency-domain feature (FDF), (iii) Gait entropy image (GEnI), (iv) Chrono-gait image (CGI), (v) Gait flow image (GFI). The dataset is composed of dissimilarity scores of each of these 3249 subjects as probe with all 3249 subjects for above mentioned features. These dissimilarity scores from above gait features are fused using existing score level fusion approaches. Details of these gait feature extraction methods

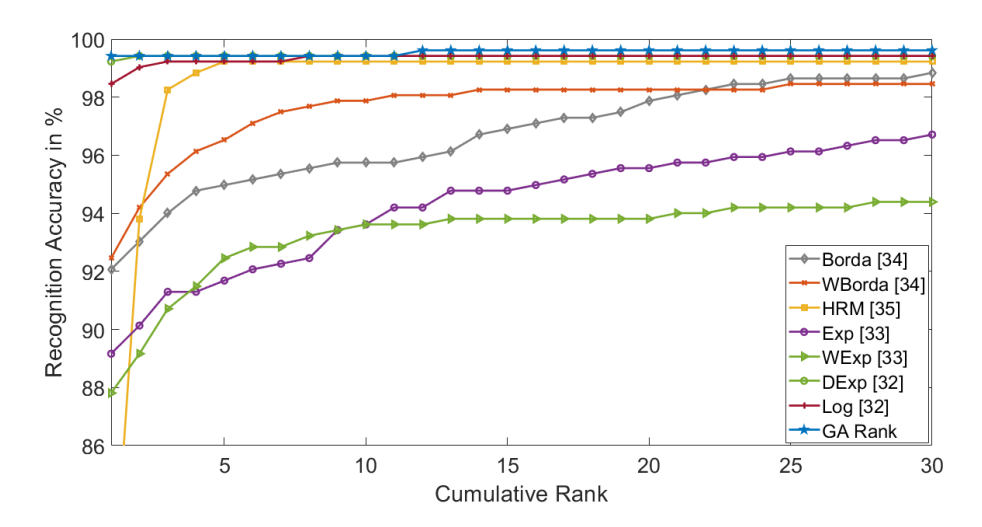


Figure 3.5: CMC plots for existing rank level fusion approaches being compared with that of the proposed GA based rank level fusion approach for NIST BSSR1

Dataset (set 1)

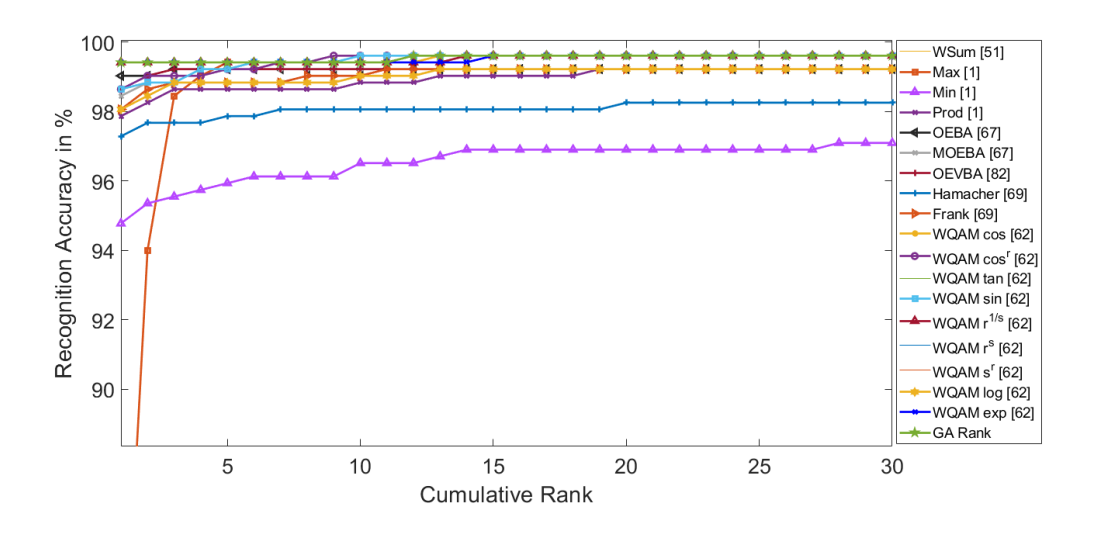


Figure 3.6: CMC plots for existing score level fusion approaches being compared with that of the proposed GA based rank level fusion approach for NIST BSSR1

Dataset (set 1)

Table 3.6: Performance comparison of the proposed GA based rank level fusion approach with unimodal matchers on OU-ISIR BSS4 multi-algorithm dataset

Me	ethod	Top-1 Rank	Top-2 Ranks	Top-3 Ranks
	CEnI	80.95	85.50	87.50
	CGI	83.35	87.44	89.04
Unimodal	FDF	85.90	89.87	91.23
	GEI	85.72	89.54	91.20
	GFI	74.92	79.93	82.12
Proposed GA Rank		86.49	90.98	92.24

can be found [2, 196].

Performance Analysis: Rank lists are generated based on the given dissimilarity scores. This provides five rank lists for each probe. These rank lists are combined using the proposed rank level fusion approach (Section 3.2.1) and other existing rank and score level fusion approaches as discussed in Section 3.2.2.1. The proposed method is compared with each unimodal biometric matcher. The recognition accuracies (in %) for the probe subjects within top-1 (Rank 1), top-2 (Rank 2) and top-3 (Rank 3) ranks (cumulative) are presented in the Table 3.6. It is worthy to note that the proposed method outperforms each unimodal matcher. It justifies the need for multi-biometric system.

Similarly, the recognition accuracies are presented in Table 3.7 for various approaches at score and at rank level fusion along with the proposed genetic algorithm based rank level fusion approach. These results in Table 3.7 clearly show that the proposed genetic algorithm based rank level fusion approach has superior performance over other existing approaches except score level fusion approach with weighted sum rule [51] for top-1 position (Rank 1). Performance of the proposed approach increases with top-2 (Rank 2) and top-3 (Rank 3) positions.

The changes in recognition accuracies (in %) with the changes in cumulative ranks are presented using cumulative match characteristic (CMC) curve in Fig. 3.7 and Fig. 3.8 for OU-ISIR BSS4 multi-algorithm dataset [2, 194]. The proposed method outperforms several existing rank and score level fusion approaches, as it can be observed in the CMC curve in Fig. 3.7 and Fig. 3.8.

Table 3.7: Performance of the comparing fusion methods on OU-ISIR BSS4 multialgorithm dataset using cumulative recognition accuracies in %

Method		Top-1 Rank	Top-2 Ranks	Top-3 Ranks
	Weighted Sum [51]	86.61	89.72	91.23
	Max Rule [1]	85.38	88.27	89.60
	Min Rule [1]	77.41	88.15	91.60
	Product [1]	77.41	88.21	91.60
	Sum-OEBA [67]	86.08	89.60	91.07
	Sum-MOEBA [67]	86.45	89.75	91.17
	Sum-OEVBA [82]	86.40	89.75	91.19
	Hamacher t-norm [69]	86.37	89.57	91.07
Score Level Fusion	Frank t-norm [69]	81.63	89.32	91.47
	WQAM cos [62]	86.43	89.50	91.23
	$WQAM cos^r [62]$	85.78	88.98	90.34
	WQAM tan [62]	86.43	89.50	91.19
	WQAM sin [62]	86.43	89.50	91.23
	WQAM $r^{1/s}$ [62]	85.29	88.15	89.38
	WQAM r^s [62]	86.43	89.54	91.07
	WQAM s^r [62]	85.35	88.89	90.43
	WQAM log [62]	86.43	89.50	91.17
	WQAM $\exp [62]$	85.29	88.15	89.44
	Borda Count [34]	83.63	87.47	88.77
	WBorda [34]	84.58	88.34	89.47
	Highest Rank [35]	77.41	88.15	91.54
Rank Level Fusion	Exp [33]	83.56	87.47	88.83
	WExp [33]	81.60	85.29	87.32
	DivExp [32]	86.40	89.94	91.51
	Log [32]	85.47	89.20	90.90
	Proposed GA Rank	86.49	90.98	92.24

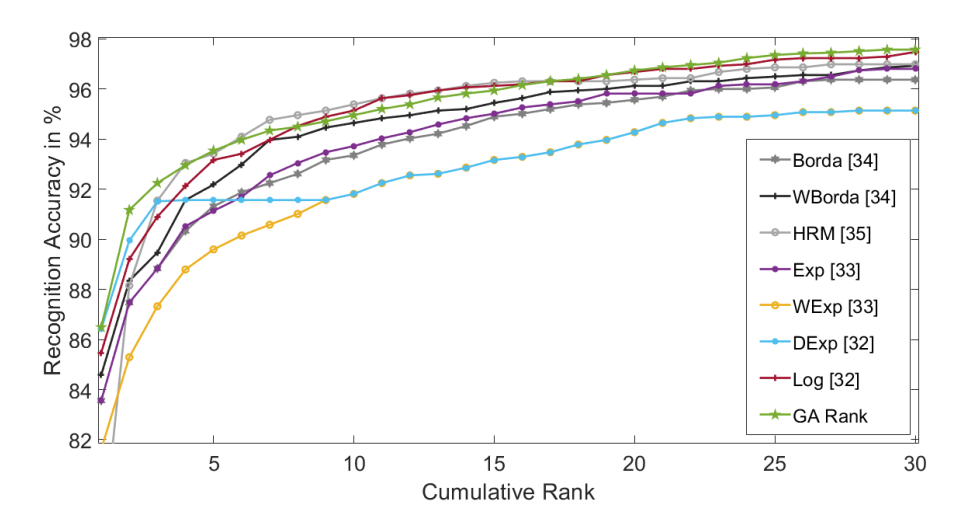


Figure 3.7: CMC plots for existing rank level fusion approaches being compared with that of the proposed GA based rank level fusion approach for OU-ISIR BSS4 multi-algorithm Dataset

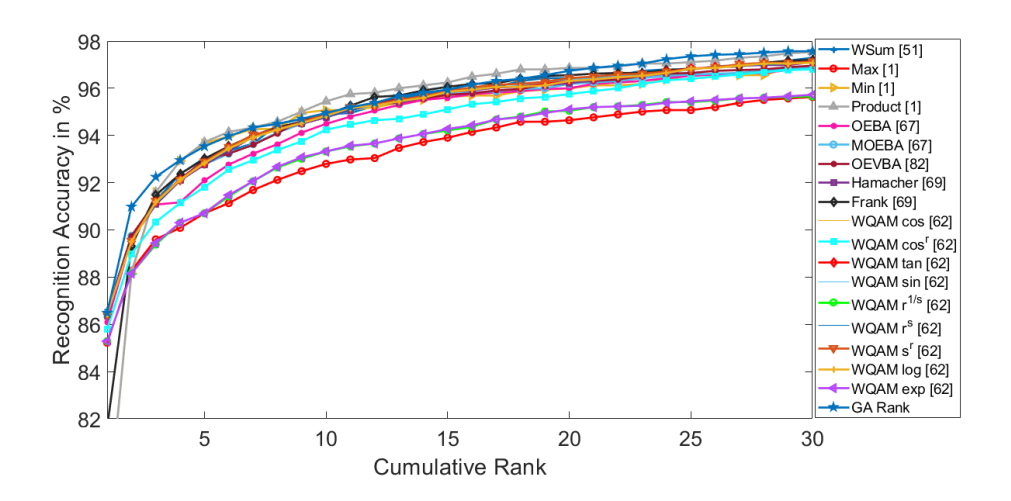


Figure 3.8: CMC plots for existing score level fusion approaches being compared with that of the proposed GA based rank level fusion approach for OU-ISIR BSS4 multi-algorithm dataset

3.2.3 Conclusion

The proposed genetic algorithm based rank level fusion approach exhibits better performance in identifying the subjects than majority of the existing approaches of fusion at rank and at score levels for multimodal biometric systems. Though few of the existing approaches exhibit equal performance as with the proposed approach. This justifies the introduction of a novel genetic algorithm based approach in this section. Experiments also justify the usefulness of multimodal biometric systems over the unimodal biometric systems. The reported results show significant improvement in performance inspite of considering the same weight to each input list. Moreover, initial success for the reported experiments is encouraging enough to try out other meta-heuristic search and optimization strategies (like particle swarm optimization) in the context of rank level fusion of multimodal biometrics.

3.3 Proposed Particle Swarm Optimization Based Approach

The success of genetic algorithm based rank level fusion approach (Section 3.2) has provided the motivation to attempt another similar evolutionary computing based optimization approach - namely, particle swarm optimization (PSO). It is another well-established paradigm to solve optimization problems involving large search spaces [197, 198, 199, 200]. Normally, particle swarm optimization achieves convergence faster than genetic algorithm [201]. Hence, the work in this section proposes a particle swarm optimization-based approach as a solution to the stated optimization problem (Eq. 3.2) of rank level fusion.

A weighted summation of distances of the input rank lists from a candidate aggregate rank list is minimized in this context. Here, the distance between two rank lists is computed using a weighted Spearman footrule distance (Eq. 3.3). Experimental study on the performance of the proposed approach is reported using two multimodal biometrics datasets: (i) NIST BSSR1 multimodal dataset (set 1) [193] involving face and fingerprint modalities and (ii) OU-ISIR BSS4 multi-algorithm dataset [2, 194] involving multiple feature extraction methods for gait biometrics. Supremacy of the proposed particle swarm optimization based rank level fusion approach with respect to existing fusion schemes at score and

at rank levels is experimentally exhibited. Detail of the proposed particle swarm optimization based rank level fusion approach is presented in this section.

3.3.1 Problem Domain Specific Design of Particle Swarm Optimization Based Approach

The major contribution of this work is adoption of particle swarm optimization to solve the formulated optimization problem for rank level fusion of multimodal biometrics (Section 3.1). Representation of particles and custom-designed operators to suite this problem domain are presented in this section.

3.3.1.1 Representation of a Candidate Rank List as a Particle Position

In the context of the stated problem, a position of a particle represents a candidate rank list of the enrolled subjects. These ranks of the subjects indicate relative closeness of the probe subject with the enrolled subjects. The position of a particle can be perceived as a point in n-dimensional discrete and finite space. Here, n represents number of enrolled subjects. As shown in Fig. 3.2, a particle position (A, B, D, C, E, F) represents a candidate rank list δ . It indicates the rank of enrolled subjects A, B, C, D, E, and F in comparison to the probe subject as 1, 2, 4, 3, 5, and 6, respectively.

3.3.1.2 Fitness of a Candidate Rank List

In particle swarm optimization, fitness of each candidate solution (i.e., particle position) is evaluated. In the context of the proposed rank level fusion method, a fitness value is calculated for a candidate rank list (i.e., position of a particle) as a weighted summation of the distances between the candidate rank list and each of the input rank lists (Eq. 3.2). All of these input rank lists (i.e., corresponding biometric modalities) are assigned equal weight in this work. Here, the goal is to minimize the fitness value. As a result, the solution with the lowest fitness value is considered as the fittest solution.

3.3.1.3 Initialization of Population of Candidate Rank Lists

A swarm of particles is used in particle swarm optimization by parallelly searching for the optimal solution in the solution space. The initialization of these positions of a population (or swarm) of particles (i.e., candidate solutions) is random. But incorporation of domain knowledge to initialize the particle positions can be found in [202, 203]. This domain knowledge-based initialization aids the particle swarm optimization algorithm to converge fast. Similarly, in the proposed particle swarm optimization based approach, a combination of random and knowledge-based initialization is used to initialize the particle positions. Let the swarm have M particles. For the experiments in this work, the value of M is considered as 10. The initial positions for N of these M particles are taken as N input rank lists. Here, N denotes the number of modalities. The input rank lists are assumed to be the closest candidates for becoming the aggregated rank list in this case. This is also the basis for the problem formulation (Eq. 3.2), which involves minimization of a weighted summation of distances of the fused rank list from the input rank lists. As a result, this form of initialization is justified in the current context. The positions of remaining (M-N) particles are randomly initialized. In order to do so, ranks are generated randomly in the range of [1,n] to determine their initial positions. Here, n represents total number of enrolled users.

3.3.1.4 Exploring Other Candidate Rank Lists

To evaluate the fitness of new candidate rank lists, these M rank lists (i.e., particle positions) in the population are iteratively updated. The position of the k^{th} particle (i.e., corresponding rank list) is updated as following:

$$x_k(t+1) = x_k(t) + v_k(t+1)$$
(3.8)

Here $v_k(t+1)$ relates to the amount of change in the position of the k^{th} particle from iteration t (i.e, $x_k(t)$) to its new position at iteration (t+1) (i.e, $x_k(t+1)$). The new velocity while going to the $(t+1)^{th}$ iteration is referred as $v_k(t+1)$. Each iteration affects the velocity of particles. The k^{th} particle's new velocity $v_k(t+1)$ is determined by three factors: (a) the particle's current velocity $v_k(t)$ at the t^{th} iteration, (b) the particle's propensity to move towards its personal best position $pbest_k(t)$, and (c) the particle's propensity to move towards its social best position gbest(t). The social best position in the adopted PSO refers to the global best position (gbest(t)) of the entire swarm of particles. As a result, considering the prior velocity of the particle, its personal best position $(pbest_k(t))$, and the global best position (gbest(t)) at the given iteration, the new velocity of the particle is computed using Eq. 3.9.

$$v_k(t+1) = \omega \times v_k(t) + c_1 \times r_{1k}(t) \times (pbest_k(t) - x_k(t)) + c_2 \times r_{2k}(t) \times (gbest(t) - x_k(t))$$

$$(3.9)$$

Here, inertia weight is represented as ω . The velocity of the particle k at iteration t is defined as $v_k(t)$. In the current work, initial particle velocity is set to 10% of the values at the elements in the initial position vector. If the velocity is initialized to zero, it indicates that all particles at initial stage are not moving and any direction. This can lead to the slow convergence of PSO algorithm [204]. Hence, in the proposed work, particle velocity is initialized as 10% of the values of its initial position vector. At iteration t, $x_k(t)$ represents the current position of the k^{th} particle (i.e., the current candidate rank list). The particle's personal best position $pbest_k(t)$ is the best among all the positions which it has visited till iteration t. It refers to the fittest candidate rank list as viewed by the k^{th} particle up to iteration t. The global best position till iteration t is gbest(t). It refers to the fittest candidate rank list which have been generated by the swarm of particles up to iteration t.

It should be observed that in Eq. 3.9, the addition and subtraction operations are carried out element-wise in the respective position vectors (i.e., rank lists). The two coefficients - the cognitive coefficient c_1 and the social coefficient c_2 - control the velocity updation stage. The cognitive coefficient c_1 assists the particle in exploring the search space towards its personal best position $pbest_k(t)$ by regulating the size of steps taken toward its personal best position. The social coefficient c_2 assists the particle in exploring the search space towards its global best position gbest(t) by adjusting the magnitude of steps taken towards the global best location. The values of c_1 and c_2 are set to be 0.5 for the reported experiments in this section. The randomness of PSO is maintained by introducing two random numbers $(r_{1k}(t))$ and $r_{2k}(t)$ at each iteration. These random numbers have values in the range [0,1].

The above updation of these M rank lists (i.e., new particle positions) may no longer yield a valid solution in the discrete and finite solution space. Due to the above computation, the coordinates in the new position $x_k(t+1)$ (i.e., the ranks) may not be an integer in the range [0,n]. Here, n is total number of enrolled subjects (i.e., the number of elements defining a position in the solution space). In order to get a valid solution in the discrete and finite solution space, newly computed values in $x_k(t+1)$ are sorted in ascending order and are re-ranked to get back the rank list in the given range (i.e., a legitimate solution in the discrete

and finite space). Thus, it is ensured that the rank lists will always have ranks for all the subjects as a sequence of integers in the range [1, n].

3.3.1.5 Stopping Criteria

In particle swarm optimization, the updation of a particle's velocity and position in the solution space is performed iteratively until a stopping criteria is met. When the personal best positions of all the particles do not change during a series of iteration, the proposed rank level fusion approach based on particle swarm optimization is considered to have converged. The stated window size on the number of iterations is experimentally decided as 2000 for NIST BSSR1 multimodal biometric dataset (set 1) [193] and 5000 for OU-ISIR BSS4 multialgorithm dataset [2, 194].

3.3.2 Performance Evaluation and Discussion

Performance of the proposed particle swarm optimization based rank level fusion approach for multimodal biometrics is experimentally evaluated with respect to the performances of several existing fusion approaches (at score and at rank levels). These existing approaches for performance comparison are discussed in Section 3.2.2.1. Two multimodal biometrics datasets, namely NIST BSSR1 multimodal dataset (set 1) [193] and OU-ISIR multi-algorithm dataset [2, 194], are used in these experiments to evaluate the performances of the proposed approach along with existing score and rank level fusion approaches. The weights for the comparing weighted score and rank level fusion approachers are obtained using a genetic algorithm based weight estimation approach. This approach for obtaining a suitable set of weights for the existing weighted fusion approaches is discussed in Section 3.2.2.1. This process of obtaining weights for the concerned modalities is followed for each of the above two datasets. On the contrary, proposed particle swarm optimization based rank level fusion approach assigns the same weight to each individual modality (input list) to check the efficacy of the proposed approach over state-of-the-art rank and score level fusion approaches.

3.3.2.1 Fusion of Multimodal Biometrics Involving Face and Fingerprint (NIST BSSR1 Multimodal Dataset (Set 1))

A brief description of NIST BSSR1 multimodal dataset (set 1) [193] can be found in Section 3.2.2.2. The recognition accuracies (in %) for the proposed approach

as well as each unimodal matcher are presented in Table 3.8 for NIST BSSR1 multimodal dataset (set 1) [193]. The recognition accuracies are estimated using Eq. 3.7. These recognition accuracies are reported for the probe being found within top-1 (Rank 1), top-2 (Rank 2) and top-3 (Rank 3) ranks (cumulative) in the aggregated rank list. The usefulness of the proposed rank level fusion method over each of the unimodal matchers is obvious from the reported results in Table 3.8.

The recognition accuracies of the comparing approaches within top-1 (Rank 1), top-2 (Rank 2) and top-3 (Rank 3) positions along with the proposed approach are presented in Table 3.9. It can be seen from the reported recognition accuracies that the proposed particle swarm optimization based rank level fusion approach performs better than the majority of existing state-of-the-art rank and score level fusion approaches. Among the rank level fusion approaches, genetic algorithm based rank level fusion approach (Section 3.2) exhibits identical recognition accuracies as compared with the proposed particle swarm optimization based approach for all the rank positions. Moreover, division exponential [32] approach demonstrate identical recognition accuracies as compared with the proposed approach while considering the top-2 (Rank 2) and top-3 (Rank 3) positions. However, when only the top-1 (Rank 1) position is considered, the proposed PSO based rank level fusion approach outperforms the division exponential approach. Among the score level fusion approaches, only the weighted quasi-arithmetic mean (WQAM) approaches [62] exhibit identical performance as with the proposed approach in this work. Similar to the genetic algorithm based approach (Section 3.2), this improved performance of the proposed PSO based approach can be attributed to minimization of a weighted summation of the distances between aggregated and input rank lists.

Similar to the genetic algorithm based score level fusion approach in Section 3.2, the maximum achievable recognition accuracy of the proposed PSO based approach on NIST BSSR1 multimodal dataset (set 1) [193] is 99.42%. Three out of 517 probes are not correctly identified. These probe subject IDs are 81,224 and 419. The ranks for the probe subject ID 81 in aggregated list as well as in all the input rank lists are reported in Table 3.10. The rank of subject ID 81 (actual subject) is 33 in the fused list (Table 3.10). The identified subject at the first position (ID 419) using the proposed PSO based fusion approach has rank 1 in all the individual matcher lists. Therefore, the subject ID 419 has been identified at the first position (rank 1) in the proposed PSO based rank level fusion approach. Similarly, the identified subject at the second position (ID 314)

Table 3.8: Performance comparison of the proposed PSO based rank level fusion approach with unimodal matchers on NIST BSSR1 multimodal dataset (set 1)

Method		Top-1 Rank	Top-2 Ranks	Top-3 Ranks
	Face Matcher G	83.37	86.28	88.40
Unimodal	Face Matcher C	88.78	90.52	91.50
Ullillodai	Left Fingerprint	85.70	87.04	87.81
	Right Fingerprint	92.07	93.23	93.62
Proposed PSO Rank Fusion		99.42	99.42	99.42

using the proposed PSO based rank level multimodal fusion approach has ranks 440, 321, 10 and 6 in the left index finger, right index finger, face matcher C and face matcher G, respectively. As this subject has good ranks in two of the modalities (face matcher C and face matcher G), this subject is identified as the second best subject (rank 2) in the fused list. The other two incorrectly identified probes (ID 224 and 419) suffer from the same problem as seen in Table 3.11 and Table 3.12. Because of this, even the best of the fusion techniques are unable to correctly identify these three subjects, i.e., maximum achievable recognition accuracy is 99.42% (Table 3.9).

The changes in recognition accuracies (in %) with the changes in cumulative ranks are represented using cumulative match characteristic (CMC) curves in Fig. 3.9 and Fig. 3.10 for rank level and score level approaches, respectively. The proposed method outperforms several existing rank and score level fusion approaches, as it can be observed in the CMC curves in Fig. 3.9 and Fig. 3.10. It is observed from Fig. 3.9 that CMC curves for the genetic algorithm based rank level fusion approach (Section 3.2) and division exponential approach [32] are overlapping with that of the particle swarm optimization based rank level fusion approach.

The recognition accuracies of several WQAM based score level fusion approaches [62] are equal to those of the proposed particle swarm optimization based rank level fusion approach. Therefore, the CMC curves of these approaches overlap with the CMC curve of the proposed particle swarm optimization based rank level fusion approach in Fig. 3.10.

Table 3.9: Performance of the comparing fusion approaches on NIST BSSR1 multimodal dataset (set 1) using cumulative recognition accuracies in %

Method		Top-1 Rank	Top-2 Ranks	Top-3 Ranks
	Weighted Sum [51]	98.65	98.84	99.03
	Max Rule [1]	79.90	94.00	98.45
	Min Rule [1]	94.80	95.40	95.60
	Product [1]	97.87	98.26	98.67
	Sum-OEBA [67]	99.03	99.03	99.26
	Sum-MOEBA [67]	98.45	98.84	98.84
	Sum-OEVBA [82]	98.70	99.03	99.26
	Hamacher t-norm [69]	97.29	97.68	97.68
Score Level	Frank t-norm [69]	98.07	98.65	98.84
	WQAM cos [62]	99.42	99.42	99.42
	$\overline{\text{WQAM } cos^r [62]}$	98.65	99.03	99.03
	WQAM tan [62]	99.42	99.42	99.42
	WQAM sin [62]	98.65	98.84	98.84
	$\overline{\text{WQAM } r^{1/s} \text{ [62]}}$	99.42	99.42	99.42
	WQAM r^s [62]	99.42	99.42	99.42
	WQAM s^r [62]	99.42	99.42	99.42
	WQAM log [62]	99.42	99.42	99.42
	WQAM exp [62]	99.42	99.42	99.42
	Borda Count [34]	92.07	93.04	94.00
	WBorda [34]	92.50	94.20	95.36
	Highest Rank [35]	79.70	94.81	98.26
Rank Level	Exp [33]	89.16	90.13	91.30
nank Lever	WExp [33]	87.81	89.16	90.71
	DivExp [32]	99.23	99.42	99.42
	Log [32]	98.45	99.03	99.23
	GA Rank (Section 3.2)	99.42	99.42	99.42
	Proposed PSO Rank	99.42	99.42	99.42

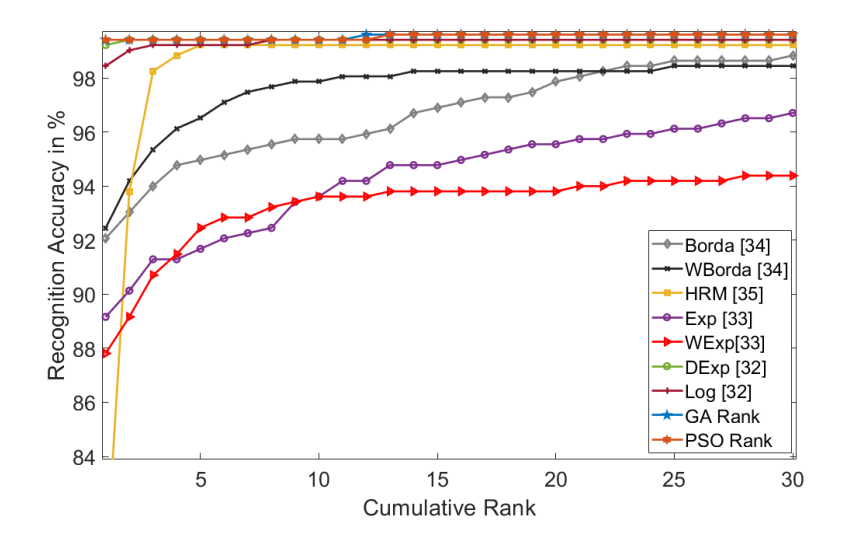


Figure 3.9: CMC plots for existing rank level fusion approaches being compared with those of the GA based and the proposed PSO based rank level fusion approaches for NIST BSSR1 multimodal dataset (set 1)

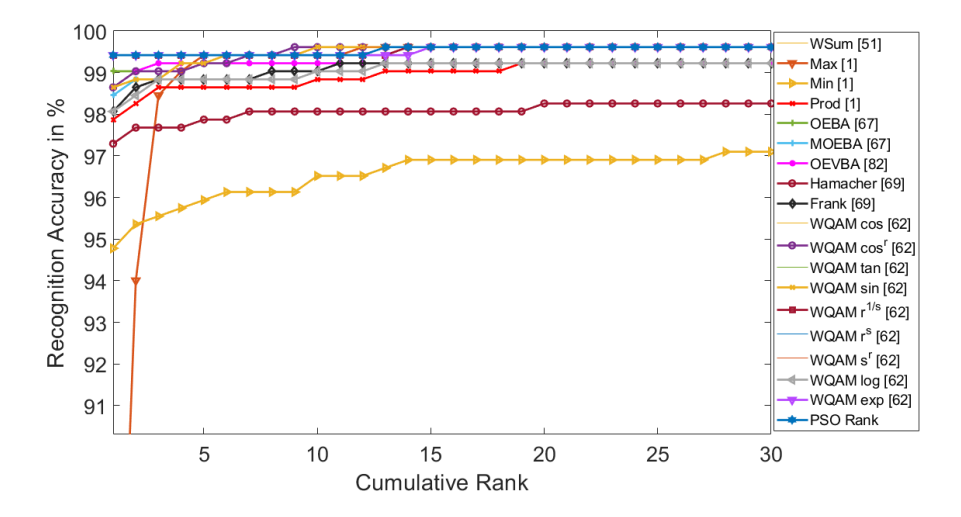


Figure 3.10: CMC plots for existing score level fusion approaches being compared with that of the proposed PSO based rank level fusion approach for NIST BSSR1 multimodal dataset (set 1)

Table 3.10: Ranks at each modality for ideally correct subject and the top three identified subjects according to the fused list (for probe subject ID 81)

Modality	Ideally correct	1^{st} Identified	2^{nd} Identified	3^{rd} Identified
Wiodanty	subject (ID 81)	subject (ID 419)	subject (ID 314)	subject (ID 105)
Left index finger	480	1	440	340
Right index finger	353	1	321	124
Face matcher C	143	1	10	13
Face matcher G	12	1	6	17
PSO Rank	33	1	2	3

Table 3.11: Ranks at each modality for ideally correct subject and the top three identified subjects according to the fused list (for probe subject ID 224)

Modality	Ideally correct	1^{st} Identified	2^{nd} Identified	3^{rd} Identified
Wiodanity	subject (ID 224)	subject (ID 68)	subject (ID 66)	subject (ID 300)
Left index finger	59	1	123	204
Right index finger	51	1	241	72
Face matcher C	122	5	1	3
Face matcher G	11	29	9	26
PSO Rank	13	1	2	3

3.3.2.2 Fusion of Multimodal Biometrics for Multiple Gait Feature Representations (OU-ISIR BSS4 Multi-Algorithm Dataset)

A brief description of OU-ISIR BSS4 multi-algorithm dataset [2, 194] can be found in Section 3.2.2.3. The proposed method is compared with each unimodal biometric matcher. The recognition accuracies (in %) for the probe subjects within top-1 (Rank 1), top-2 (Rank 2) and top-3 (Rank 3) ranks (cumulative) are presented in the Table 3.13. It is worthy to note that the proposed method outperforms each unimodal matcher. It justifies the need for multi-biometric system.

Similarly, the recognition accuracies are presented in Table 3.14 for various approaches at score and at rank level fusion along with the proposed particle swarm optimization based rank level fusion approach. It can be seen from these results in Table 3.14 that the proposed PSO based rank level fusion approach exhibits superior performance over other existing rank and score level fusion approaches for each one of the top-1 (Rank 1), top-2 (Rank 2) and top-3 (Rank 3) positions (cumulatively) in the aggregated list.

The changes in recognition accuracies (in %) with the changes in cumulative

Table 3.12: Ranks at each modality for ideally correct subject and the top three identified subjects according to the fused list (for probe subject ID 419)

Modality	Ideally correct	1^{st} Identified	2^{nd} Identified	3^{rd} Identified
wiodaniby	subject (ID 419)	subject (ID 81)	subject (ID 120)	subject (ID 492)
Left index finger	478	1	18	56
Right index finger	470	1	2	68
Face matcher C	282	1	5	10
Face matcher G	279	2	20	49
PSO Rank	468	1	2	3

Table 3.13: Performance comparison (using cumulative recognition accuracies in %) of the proposed PSO based rank level fusion approach with unimodal matchers on OU-ISIR BSS4 multi-algorithm dataset

Method		Top-1 Rank	Top-2 Ranks	Top-3 Ranks
	CEnI	80.95	85.50	87.50
	CGI	83.35	87.44	89.04
	FDF	85.90	89.87	91.23
	GEI	85.72	89.54	91.20
	GFI	74.92	79.93	82.12
Proposed PSO Rank Fusion		86.73	91.16	92.31

ranks are presented using cumulative match characteristic (CMC) curves in Fig. 3.11 and Fig. 3.12 for OU-ISIR BSS4 multi-algorithm dataset [2, 194]. It is observed from the CMC curves in Fig. 3.11 and Fig. 3.12 that the proposed method outperforms several existing rank and score level fusion approaches. It is also observed from Fig. 3.11 that the CMC curves of the genetic algorithm based (Section 3.2) and the proposed particle swarm optimization based rank level fusion approaches are overlapping.

3.3.3 Conclusion

The proposed particle swarm optimization (PSO) based rank level fusion approach exhibits better performance in identifying the subjects than majority of the existing approaches for fusion at rank and at score levels for multimodal biometrics using NIST BSSR1 multimodal dataset (set 1) [193]. Moreover, the

Table 3.14: Performance of the comparing fusion approaches on OU-ISIR BSS4 multi-algorithm dataset using cumulative recognition accuracies in %

Method		Top-1 Rank	Top-2 Ranks	Top-3 Ranks
	Weighted Sum [51]	86.61	89.72	91.23
	Max Rule [1]	85.38	88.27	89.60
	Min Rule [1]	77.41	88.15	91.60
	Product [1]	77.41	88.21	91.60
	Sum-OEBA [67]	86.08	89.60	91.07
	Sum-MOEBA [67]	86.45	89.75	91.17
	Sum-OEVBA [82]	86.40	89.75	91.19
	Hamacher t-norm [69]	86.37	89.57	91.07
Score Level Fusion	Frank t-norm [69]	81.63	89.32	91.47
	WQAM cos [62]	86.43	89.50	91.23
	$WQAM \ cos^r \ [62]$	85.78	88.98	90.34
	WQAM tan [62]	86.43	89.50	91.19
	WQAM sin [62]	86.43	89.50	91.23
	$\overline{\text{WQAM } r^{1/s} \text{ [62]}}$	85.29	88.15	89.38
	$\overline{\text{WQAM } r^s \text{ [62]}}$	86.43	89.54	91.07
	WQAM s^r [62]	85.35	88.89	90.43
	WQAM log [62]	86.43	89.50	91.17
	WQAM exp [62]	85.29	88.15	89.44
	Borda Count [34]	83.63	87.47	88.77
	WBorda [34]	84.58	88.34	89.47
	Highest Rank [35]	77.41	88.15	91.54
	Exp [33]	83.56	87.47	88.83
Rank Level Fusion	WExp [33]	81.60	85.29	87.32
	DivExp [32]	86.40	89.94	91.51
	Log [32]	85.47	89.20	90.90
	GA Rank (Section 3.2)	86.49	90.98	92.24
	Proposed PSO Rank	86.73	91.16	92.31

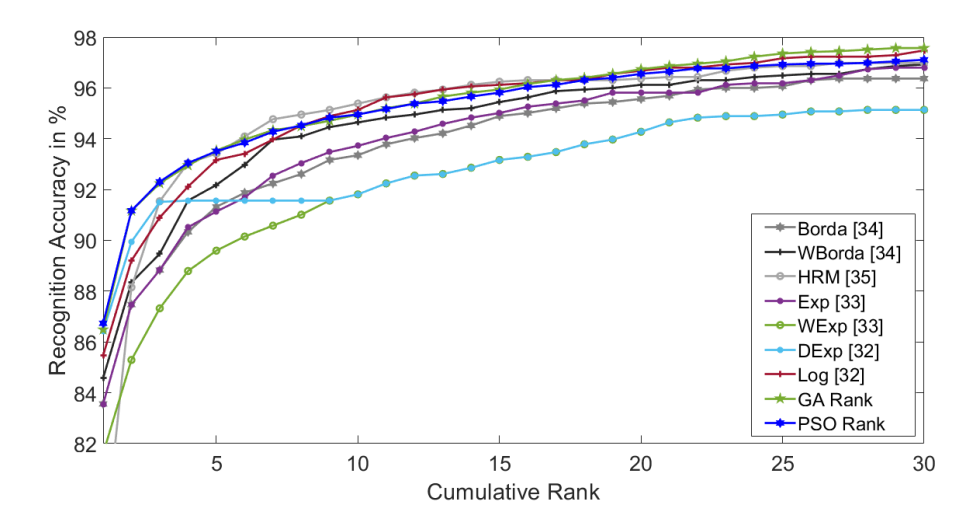


Figure 3.11: CMC plots for existing rank level fusion approaches being compared with those of the GA based and the proposed PSO based rank level fusion approaches for OU-ISIR BSS4 multi-algorithm dataset

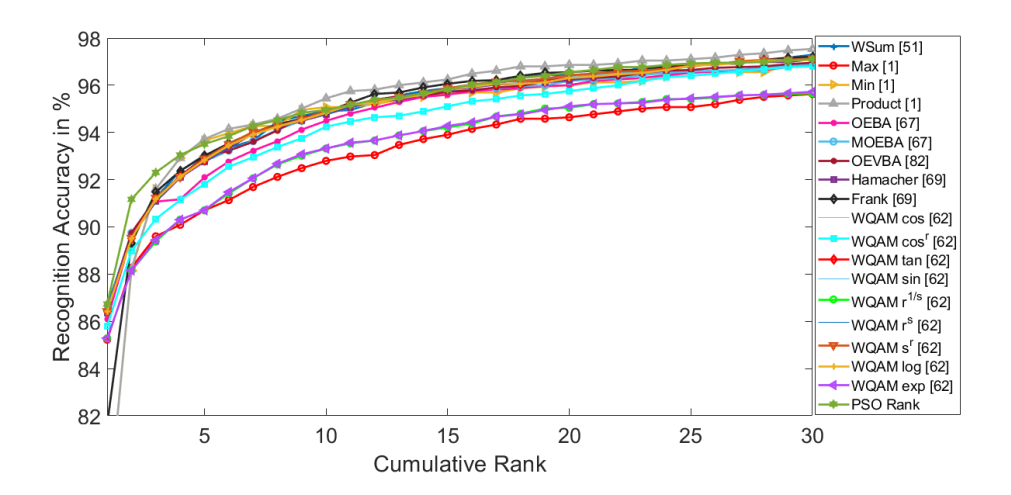


Figure 3.12: CMC plots for existing score level fusion approaches being compared with that of the proposed PSO based rank level fusion approach for OU-ISIR BSS4 multi-algorithm dataset

proposed PSO based rank level fusion approach performs better than all the existing rank and score level fusion approaches as well as the GA based rank level fusion approach (Section 3.2). This justifies the introduction of a novel particle swarm optimization based approach in this section. Experiments also justify the usefulness of multimodal biometric system over the unimodal biometric system. The reported results show significant improvement in performance inspite of considering same weight for each biometric modality in the proposed approach.

3.4 Analysis of Convergence Rate Between GA Based and PSO Based Rank Level Fusion Approaches

It is observed from the reported results in Section 3.3.2 that the performances of GA based and PSO based rank level fusion approaches are similar. Both the approaches are evolutionary computing-based approaches for solving the optimization problem in Section 3.1. Both of these evolutionary computing based approaches exhibit similar performances in terms of recognition accuracies. Therefore, comparison among these two approaches is carried out using the number of iterations being taken for convergence. Number of iterations for convergence of these two evolutionary computing-based approaches are observed for NIST BSSR1 multimodal (set 1) [193] and OU-ISIR BBS4 multi-algorithm [2, 194] datasets. The cumulative distribution functions (CDFs) on the number of iterations are plotted for these comparing evolutionary computing-based methods in Fig. 3.13 and Fig. 3.14 for NIST BSSR1 multimodal dataset (set 1) [193] and OU-ISIR BSS4 multi-algorithm [2, 194] dataset, respectively. It is observed from these plots that the rank level fusion approach based on particle swarm optimization converges faster (lesser number of iterations) than the rank level fusion approach based on genetic algorithm.

In order to statically conclude about the above-reported faster convergence of the PSO based rank level fusion approach over the GA based rank level fusion approach, a two-sample Kolmogorov-Smirnov (K-S) test is performed on the number of iterations for convergence between these two approaches. A two-sample K-S test is a statistical test for comparing the cumulative distributions of two samples. The following hypothesis are tested:

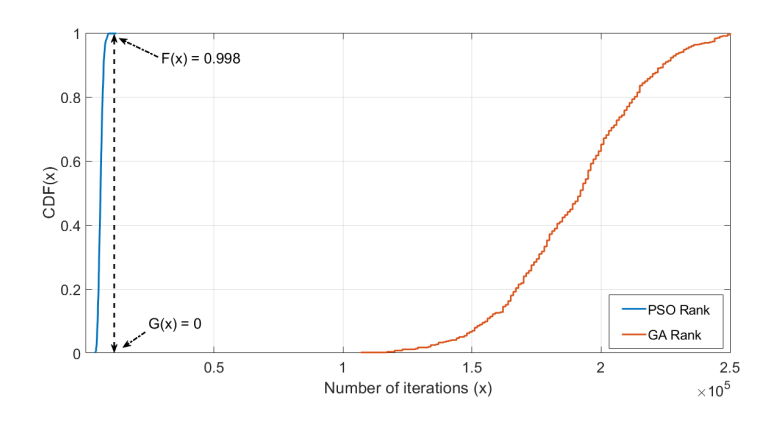


Figure 3.13: CDFs of the GA and PSO based rank level fusion approaches on NIST BSSR1 multimodal dataset (set 1)

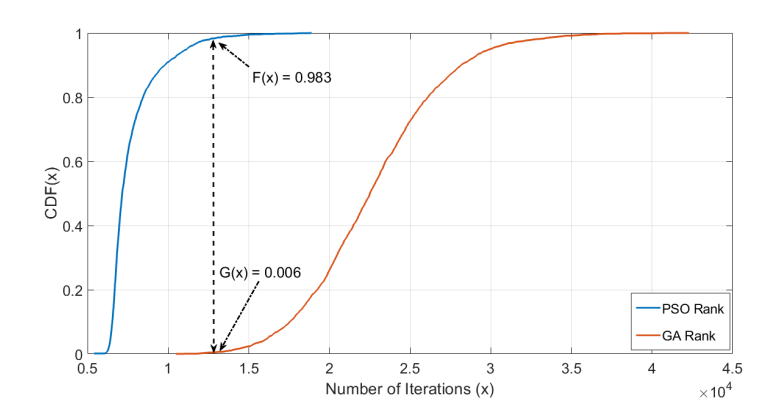


Figure 3.14: CDFs of the GA and PSO based rank level fusion approaches on OU-ISIR BSS4 multi-algorithm gait dataset

- Null Hypothesis H_0 : two samples follow same distribution.
- Alternate Hypothesis H_1 : two samples follow different distributions.

Let the two samples having sizes m and n are derived from two distributions. An observed cumulative distribution function of the first sample is represented as F(x) and the observed cumulative distribution function of the second sample is represented as G(x). The maximum difference between these two CDFs is computed using Eq. 3.10.

$$D_{m,n} = \max_{\forall x} |F(x) - G(x)| \tag{3.10}$$

The null hypothesis H_0 is rejected if the computed difference between CDFs $(D_{m,n})$ is greater than the critical value $D_{m,n,\alpha}$ for a significance level α . The critical value $D_{m,n,\alpha}$ is calculated using Eq. 3.11.

$$D_{m,n,\alpha} = c(\alpha) * \sqrt{\frac{m+n}{m*n}}$$
(3.11)

Here, $c(\alpha)$ is computed as:

$$c(\alpha) = \sqrt{-ln(\frac{\alpha}{2}) * 0.5} \tag{3.12}$$

3.4.1 Results of Two-Sample K-S Test on Multimodal Biometric Dataset Involving Face and Fingerprint (NIST BSSR1 Multimodal Dataset (Set 1))

Number of iterations for convergence is noted down for each probe during the executions of the above discussed GA and PSO based rank level fusion approaches on NIST BSSR1 multimodal dataset (set 1) [193]. Cumulative distribution function (CDF) F(x) on number of iterations for convergence is computed for the PSO based rank level fusion approach. Similarly, cumulative distribution function (CDF) G(x) on number of iterations for convergence is obtained for GA based rank level fusion approach. These two cumulative distribution functions are shown in Fig. 3.13. Then, the maximum difference between these two CDFs is computed using Eq. 3.10. It is noted from Fig. 3.13 that the maximum difference between the two CDFs $D_{m,n}$ is 0.998.

$$D_{m,n} = |0.998 - 0| = 0.998$$

The critical value is computed using Eq. 3.11 with 0.05 significance level (α) . Considering $\alpha = 0.05$, $c(\alpha)$ is calculated as 1.36 using Eq. 3.12. NIST BSSR1 multimodal dataset (set 1) [193] has 517 subjects. Hence, each of the comparing evolutionary computation based rank level fusion approaches are executed 517 times by considering each subject as probe. Hence, the value of m and n are 517 for Eq. 3.11. Thus, the value of $D_{m,n,\alpha}$ is computed as following:

$$D_{m,n,\alpha} = 1.36 * \sqrt{\frac{517 + 517}{517 * 517}} = 0.0846$$

Here, null hypothesis is rejected as the value of $D_{m,n}$ is greater than the value of $D_{m,n,\alpha}$. Hence, it is concluded that the two distributions are different.

3.4.2 Results of Two-Sample K-S Test on Multimodal Biometric Dataset for Multiple Gait Feature Representations (OU-ISIR BSS4 Multi-Algorithm Dataset)

Number of iterations for convergence is noted down for each probe during the executions of the above discussed GA and PSO based rank level fusion approaches on OU-ISIR BSS4 multi-algorithm gait dataset [2, 194]. Cumulative distribution function (CDF) F(x) on number of iterations for convergence is computed for the PSO based rank level fusion approach. Similarly, cumulative distribution function (CDF) G(x) on number of iterations for convergence is obtained for GA based rank level fusion approach. These two cumulative distribution functions are shown in Fig. 3.14. Then, the maximum difference between these two CDFs is computed using Eq. 3.10. It is noted from Fig. 3.14 that the maximum difference between these two CDFs $D_{m,n}$ is 0.977.

$$D_{m,n} = |0.983 - 0.006| = 0.977$$

The critical value is computed using Eq. 3.11 with 0.05 significance level (α). Considering $\alpha = 0.05$, $c(\alpha)$ is calculated as 1.36 using Eq. 3.12. OU-ISIR BSS4 multi-algorithm dataset [2, 194] has 3249 subjects. Hence, each of the comparing evolutionary computation based rank level fusion approaches are executed 3249 times by considering each subject as probe. Hence, the value of m and n are 3249 for Eq. 3.11. Thus, the value of $D_{m,n,\alpha}$ is computed as following:

$$D_{m,n,\alpha} = 1.36 * \sqrt{\frac{3249 + 3249}{3249 * 3249}} = 0.0337$$

Here, null hypothesis is rejected as the value of $D_{m,n}$ is greater than the value of $D_{m,n,\alpha}$. Hence, it is concluded that the two distributions are different.

3.5 Summary

In this chapter, rank level fusion is studied for multimodal biometrics. The manifold contributions of the works in this chapter are summarized in this section. The rank level fusion in multimodal biometrics is formulated as an optimization problem. The formulation of this optimization problem considers minimization of a weighted summation of distances between the aggregated rank list and the input rank lists. This problem formulation adds novelty to the proposed works in this chapter. The weighted Spearman footrule distance metric [180] is used to compute the distance between two rank lists. The weight in the weighted Spearman footrule distance is incorporated to ensure more influence of a better ranked subject than other subjects. A novel way to decide the weight of a subject is conceptualized in this context.

To solve the stated optimization problem in the context of rank level fusion of multimodal biometrics, two novel approaches are proposed using genetic algorithm (GA) and particle swarm optimization (PSO). Context-specific representation of a candidate solution and custom-designed operators are the highlights of the proposed GA and PSO based approaches.

The proposed approaches are tested using two different multi-biometric datasets, namely (i) NIST BSSR1 multimodal dataset (set 1) [193] involving fingerprint and face modalities and (ii) OU-ISIR BSS4 multi-algorithm gait dataset [2, 194] involving several gait feature extraction methods. These approaches exhibit better performance in identifying the subjects than majority of the existing approaches of fusion at rank and at score levels for multimodal biometrics.

It is experimentally observed that the proposed particle swarm optimization based approach achieves faster convergence than the proposed genetic algorithm based approach. This superiority of the proposed PSO based approach over the proposed GA based approach is established using two-sample Kolmogorov-Smirnov (K-S) test.

It is to be admitted that the execution time of the proposed approaches is longer than traditional score and rank level fusion approaches as these proposed approaches are based on evolutionary computation. But better performance in terms of recognition accuracies is achieved here. Though execution speed can be improved by using parallel implementations of these evolutionary-computing based approaches [205, 206, 207]. Moreover, the success of these optimization based rank level approaches are encouraging enough to try out optimization based

approaches in the context of score level fusion of multimodal biometrics. This direction in score level fusion of multimodal biometrics is discussed in next chapter.

Chapter 4

Score Level Fusion of Multimodal Biometrics Using Optimization Based Approaches

Comparison between the biometrics of a probe subject and an enrolled subject derives a matching score (either similarity or dissimilarity) for each modality. The matching scores across multiple modalities are fused in score level scheme for multimodal biometrics. Score level fusion has more information in comparison to rank and decision level fusion schemes. Hence, score level fusion is mostly accepted level of fusion for multimodal biometrics [49, 50, 51, 52, 53, 62, 67, 68, 69, 70, 71, 72, 73, 74, 75, 76].

Various score level fusion approaches for multimodal biometrics exist in literature (Section 2.1). These approaches include simple rule based approaches [1, 49, 62, 67, 68, 69, 70], likelihood ratio-based methods [73, 74, 109, 110], classification based methods [75, 76, 116] and optimization based methods [123, 124, 127]. In [123], the objective of the optimization based approach is to minimize the overlapping area between genuine and impostor score distributions. The objective of the optimization based approaches in [124, 127] is to find the best confidence factors for belief assignments in various modalities. On the similar direction, the proposed approaches in this chapter consider the score level fusion as an optimization problem. But contrary to previous optimization based score level fusion approaches [123, 124, 127], the approaches in this chapter minimize a weighted summation of distances between the aggregated score list and the score lists from individual modalities. The success of the earlier approaches in

Chapter 3 in the domain of rank level fusion has guided the optimization problem formulation in this chapter for score level fusion.

The rest of this chapter is organized as following: A detailed formulation of score level fusion of multimodal biometrics as an optimization problem is presented in Section 4.1. A novel score level fusion approach is proposed in Section 4.2 using genetic algorithm. Another novel approach is proposed in Section 4.3 for score level fusion of multimodal biometrics using particle swarm optimization. Comparative analysis of convergence rates among genetic algorithm based and particle swarm optimization based fusion approaches at rank level and at score level is presented in Section 4.4. Finally, the concluding remarks on the proposed score level fusion approaches are drawn in Section 4.5.

4.1 Score Level Fusion as an Optimization Problem

In the earlier work on optimization based rank level fusion for multimodal biometrics (Chapter 3), the rank level fusion has been conceptualized as an optimization problem. Being inspired by this earlier work, the current works in this chapter conceptualize the score level fusion as an optimization problem. Details of this problem formulation is presented in this section.

In order to identify a probe subject as one of the enrolled subjects, the biometric modalities of the probe subject are matched against the corresponding biometric modalities of each of the enrolled subjects. Let N biometric modalities be used for the identification task. For an input probe subject, let a matching score be defined as s_{ij} being a similarity between the probe and the j^{th} enrolled subject for the biometric modality i, where i = 1...N. A score list S_i of such matching scores of the probe subject with all the enrolled subjects is generated for each biometric modality. As a result, N score lists are generated as $S_1, S_2, ..., S_N$.

The ranges of these matching scores may vary across several modalities. Therefore, these matching scores are normalized to bring them into a common range. There exist several score normalization approaches in literature (Section 2.1.1). Examples include min-max [63], tanh [63], z-score [63] and anchored score normalization [67, 82]. One of the widely used score normalization approach is the min-max normalization [49, 62, 63]. Hence, min-max normalization approach is adopted in this work. It is defined in following equation:

$$\hat{s}_{ij} = \frac{s_{ij} - min(S_i)}{max(S_i) - min(S_i)} \tag{4.1}$$

The terms $min(S_i)$ and $max(S_i)$ represent the minimum and the maximum scores, respectively, for the list S_i . Normalized score of an enrolled subject j for an input biometric modality i is represented as $\hat{s_{ij}}$. The above discussion considers the matching score as a similarity score. If the matching score is a dissimilarity score, the above normalized score \hat{s}_{ij} is subtracted from 1 to convert it into a normalized similarity score. The subsequent discussion in this chapter assumes the term \hat{s}_{ij} as a normalized similarity score. A list of these normalized scores \hat{s}_{ij} of all the enrolled subjects for biometric modality i represents a normalized score list \hat{S}_i . As shown in Fig. 4.1, an aggregated (fused) list δ^* is created by combining these N normalized score lists \hat{S}_1 , \hat{S}_2 , ..., \hat{S}_N .

$$\delta^* = aggregate(\hat{S}_1, \hat{S}_2, \dots, \hat{S}_N) \tag{4.2}$$

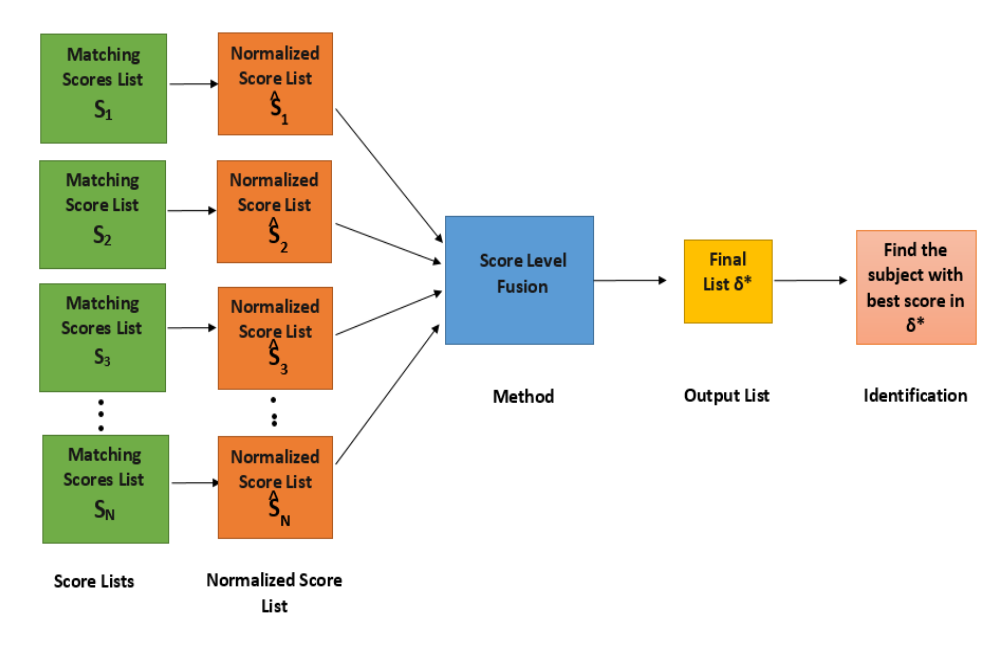


Figure 4.1: Fusion of multimodal biometrics at score level

Here, the objective is to derive a fused score list δ^* having the minimum weighted summation of distances of the normalized input score lists from the fused list. The objective function for generating the aggregated list is defined as

following:

$$minimize \ \phi(\delta) = \sum_{i=1}^{N} w_i \times d(\delta, \hat{S}_i)$$
 (4.3)

A candidate fused list is represented by δ in the above equation (Eq. 4.3). The fused list which minimizes the above objective function is denoted as δ^* . A weight w_i is associated with each of the N biometric modalities. Here, the weight represents the significance of the corresponding biometric modality. In this present work, the significance of each modality is considered as equal.

The function d() in Eq. 4.3 denotes a distance between a fused list and a normalized input score list. In the current work, weighted Spearman footrule [180] metric is used for the distance measure $d(\delta, \hat{S}_i)$ between a pair of lists δ and \hat{S}_i . The stated distance metric estimates the weighted summation of absolute differences between the normalized matching scores (pair-wise) of a subject in the input and the aggregated lists as following:

$$d(\delta, \hat{S}_i) = \sum_{j \in \hat{S}_i \cup \delta} I(j) * |\hat{s}_{\delta j} - \hat{s}_{ij}|$$

$$(4.4)$$

In Eq. 4.4, the absolute difference between the normalized scores of a subject j in the pair of lists is influenced by a factor I(j). This term I(j) is subsequently being referred as influence factor. The following is the justification for considering these influence factors as weights: A subject j having high normalized score in either of the lists must have substantial influence on the distance computation. It is because of the fact that the probe matches well with this subject in this scenario. Alternatively, a small value for I(j) indicates that the computed distance is less impacted by a low-scoring subject (in both lists). Therefore, the value of I(j) is computed as:

$$I(j) = \max(\hat{s}_{\delta j}, \hat{s}_{ij}) \tag{4.5}$$

One such illustration of computing the distance using the weighted Spearman footrule distance is shown in Fig. 4.2. This illustration shows four normalized score lists $\hat{S}_1, \hat{S}_2, \hat{S}_3$, and \hat{S}_4 . These lists contain matching scores of six subjects (A, B, C, D, E, and F). The score list δ represents one candidate solution. Weighted distance between a normalized input score list and the candidate list δ is estimated based on Eq. 4.4. As an illustration, the scores of subject A are 1 and 0.8 in the lists \hat{S}_1 and δ , respectively. Hence, influence factor I(j) is estimated as 1 (i.e., maximum of the two normalized scores). Absolute difference of scores

for subject A is 0.2. Likewise, the influence factor and the absolute difference of scores are computed for all other subjects. Therefore, the distance between δ and \hat{S}_1 lists is 0.62. Likewise, the distances between δ and each of the input lists \hat{S}_2, \hat{S}_3 , and \hat{S}_4 are estimated as 1.47, 1.08, and 0.65, respectively. The fitness value $\phi(\delta)$ of the candidate list δ is finally generated as 3.82 by summation of the above distances (considering equal weight as 1 for each input list). This fitness evaluation is illustrated in Fig. 4.2.

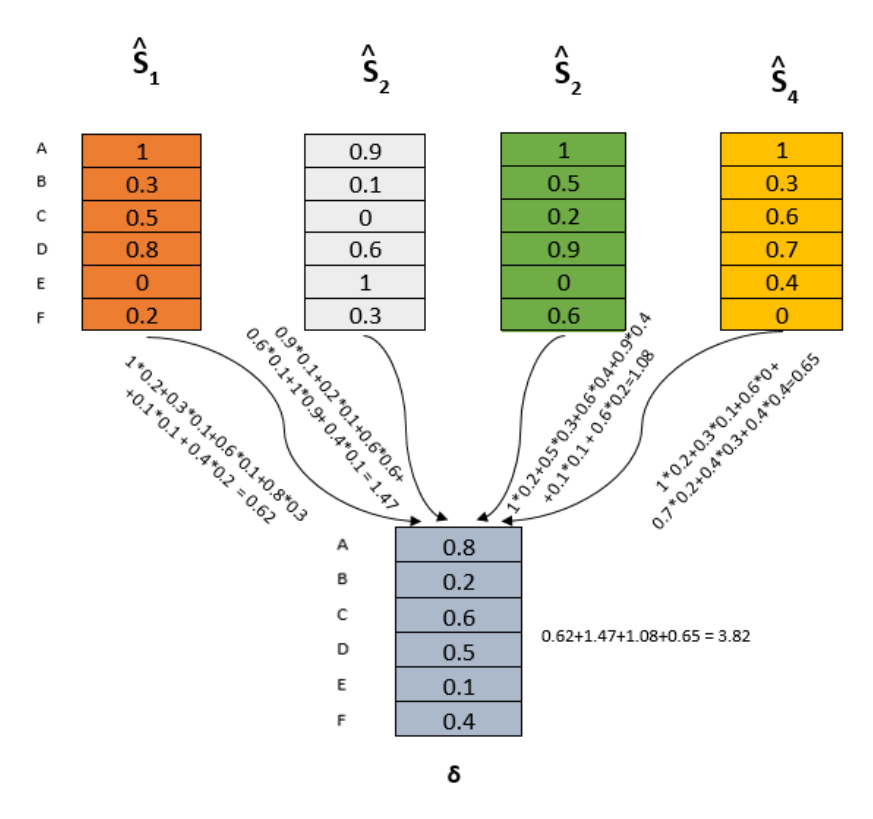


Figure 4.2: Fitness evaluation of candidate score list δ through illustration

4.2 Proposed Genetic Algorithm Based Score Level Fusion Approach

A genetic algorithm (GA) based approach is proposed in this section for score level fusion of multimodal biometrics for solving the stated optimization problem (Eq. 4.3). This algorithm is based on natural selection, where the fit solutions (chromosomes) are selected from a population based on a fitness function. These

4.2 Proposed Genetic Algorithm Based Score Level Fusion Approach

selected chromosomes produce the offsprings having better chances of survival as they inherit the characteristics of their parents. The proposed genetic algorithm-based approach uses the elitism concept. In an elitism-based genetic algorithm, better solutions are memorized across iterations. The speed up of the performance of genetic algorithm due to this elitism is well documented in literature [188, 189]. Detail of the proposed genetic algorithm based approach is presented in this section.

4.2.1 Problem Domain Specific Design of Genetic Algorithm

The major contribution of this work is formulation of score level fusion of multimodal biometrics as an optimization problem and adoption of genetic algorithm in this context. Representation of chromosomes and custom-designed operators to suite this problem domain are presented in this section.

4.2.1.1 Representation of a Chromosome

The objective of this proposed genetic algorithm-based score level fusion approach for multimodal biometrics is to find an aggregated score list. Therefore, a chromosome in the proposed approach represents a candidate score list having normalized scores of all the enrolled subjects. Hence, length of a chromosome is equal to the number of enrolled subjects. For example, the candidate normalized score list δ in Fig. 4.2 is represented by a chromosome (0.8, 0.2, 0.6, 0.5, 0.1, 0.4). Here, subject A has a score of 0.8 and subject B has a score of 0.2. Similar observations can be made for other subjects in this list too.

4.2.1.2 Fitness of a Chromosome

In order to solve the formulated optimization problem in Section 4.1, the fitness of a chromosome (i.e., a candidate list) is evaluated as weighted summation of distances of the candidate list from each normalized input score list (Eq. 4.3). Weighted Spearman footrule distance (Eq. 4.4) is used as the distance measure between the candidate list and a normalized input score list. Here, the objective is to minimize the fitness value. Therefore, the fittest solution has the lowest fitness value.

4.2.1.3 Initialization of Population

In a traditional genetic algorithm, chromosomes in an initial population are generated randomly. There also exist approaches where domain knowledge is used to generate the chromosomes in the initial population [190, 191, 192]. This knowledge-based initialization helps in fast convergence of the genetic algorithm. Similarly, chromosome initialization in the proposed genetic algorithm is carried out using a mix of knowledge-based and random initialization. Let a population of fixed size M chromosomes be considered. N out of these M chromosomes are initialized to represent N normalized input lists (i.e., solutions from each modality). Justification of initializing N chromosomes using the normalized input lists is that these lists represent normalized matching score lists of subjects for the concerned biometric modalities. Ideally, all biometric modalities should generate similar normalized scores for the same subject against the probe. But practically, some deviations will be observed for each modality. Hence, the problem of list aggregation arises. Unless the quality of the acquired biometric signal is poor, the normalized input lists will ideally be a close match to an optimally aggregated list. Hence, consideration of the input lists in the initial population improves the convergence rate. The remaining (M-N) chromosomes are randomly generated to represent lists of normalized scores. Each one of these scores is a random number in the range [0,1].

4.2.1.4 Selection

A roulette wheel based selection process is used in the proposed work. The chromosomes which are having better fitness values $\phi(\delta)$ (i.e., lower distances), share larger areas in the roulette wheel. Let M chromosomes be $\delta_1, \delta_2, \ldots, \delta_M$. Corresponding fitness values of these chromosomes are $\phi(\delta_1), \phi(\delta_2), \ldots, \phi(\delta_M)$, respectively. As the aim is minimization of the objective function, each fitness value $\phi(\delta_m)$ is converted as:

$$\phi'(\delta_m) = \max(\phi(\delta_1), \phi(\delta_2), \dots, \phi(\delta_M)) / \phi(\delta_m)$$
(4.6)

Then, the proportion of area A_m in the roulette wheel for a chromosome is determined as following:

$$A_m = \frac{\phi'(\delta_m)}{\phi'(\delta_1) + \phi'(\delta_2) + \ldots + \phi'(\delta_M)}$$

$$(4.7)$$

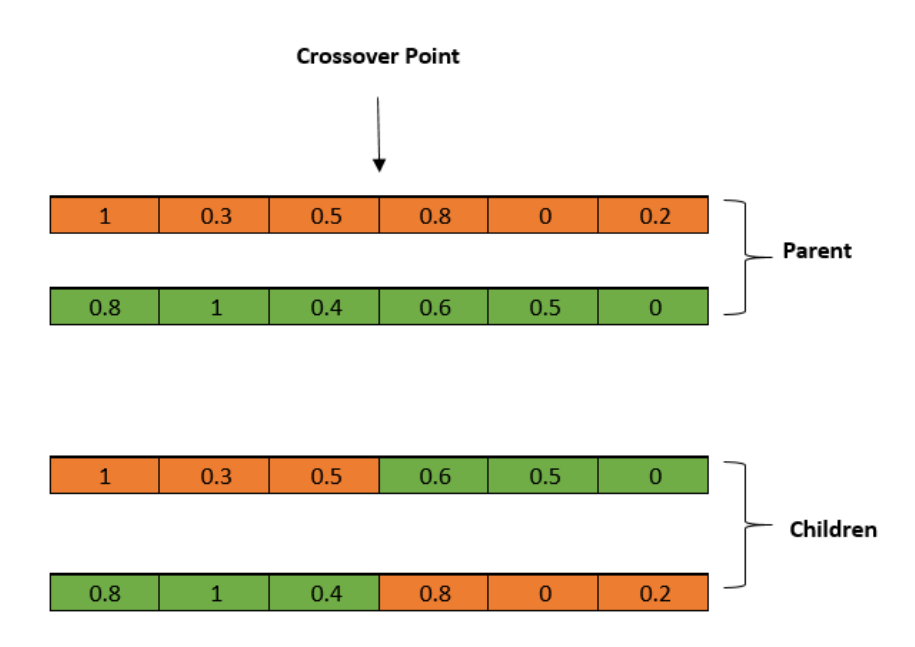


Figure 4.3: Illustration of crossover operation

Thus, a fitter chromosome (having lower objective function value $\phi(\delta_m)$ will get a larger area on the roulette wheel. The roulette wheel is rotated M times to select M chromosomes for the new population. Every time, one chromosome is selected from M chromosomes in the current population. The chromosome, whose assigned area in the roulette wheel appears in front of a pivot, is chosen each time. Bigger designated area in the roulette wheel increases the probability of getting selected into the new population for the chromosome.

4.2.1.5 Crossover

The newly generated population based on fitness values are then randomly divided into $\frac{M}{2}$ non-overlapping pairs. In the proposed work, population size M is considered as an even number. Crossover is performed between each pair of parent chromosomes. For each pair of chromosomes, a crossover point is selected randomly. In the crossover operation, a pair of offspring chromosomes are generated by interchanging parts of the parent chromosomes around the crossover point. Two parent chromosomes are presented in Fig. 4.3 to illustrate the crossover operation. A crossover point is also marked. Elements of the first parent up to the crossover point (i.e., 1, 0.3 and 0.5) and elements of the second parent after the

crossover point (i.e., 0.6, 0.5 and 0) are combined to produce the first offspring. It has elements of both parents (i.e, 1, 0.3, 0.5, 0.6, 0.5 and 0). Similarly, the second offspring is produced by combining elements of the second parent up to crossover point (i.e., 0.8, 1 and 0.4) and elements of the first parent after crossover point (i.e., 0.8, 0 and 0.2). The second offspring contains elements as 0.8, 1, 0.4, 0.8, 0 and 0.2. Moreover, an elitist genetic algorithm is adopted to speed up convergence. Therefore, all four chromosomes (both offsprings and both parents) are evaluated using the fitness function. The two fittest chromosomes (having the two least fitness values) are selected from these four chromosomes. These two chosen chromosomes are retained in the population. It ensures the retaining of better solutions in the population.

4.2.1.6 Mutation

The newly generated population after crossover further goes through the mutation process. For each gene value of a chromosome, a random value is generated in the range [0,1]. If this random value is less than a mutation probability p_m , the gene value is subtracted from 1 to generate a new gene value. The above mutation process is applied to each gene in all the chromosomes in the population. As an example in Fig. 4.4, there is a chromosome having gene values as (1,0.3,0.5,0.8,0) and (0.2). For each gene value a random value is generated (0.001, 0.23, 0.34, 0.48, 0.009 and 0.1) respectively. Random values for the first gene and the fifth gene from left hand side are less than mutation probability p_m (0.01 in this example). Hence, these gene values are subtracted from 1 to generate a new chromosome. The chromosome after mutation is (0,0.3,0.5,0.8,1) and (0.2). In this current work, an elitist genetic algorithm is adopted. Hence, after mutation of a chromosome, the fitness value for the mutated chromosome is computed. If the mutated chromosome has a lower fitness value than the chromosome before mutation, the mutated chromosome replaces the chromosome in the population (as it is a minimization problem). Otherwise, the chromosome before mutation is retained in the population.

4.2.1.7 Stopping Criteria

Genetic algorithm is an iterative algorithm. Hence, selection, crossover, and mutation steps are repeated iteratively until a stopping criterion is satisfied. If there is no change in any chromosome in the population due to crossover or mutation over several iterations, the algorithm is stopped. The stated window size on

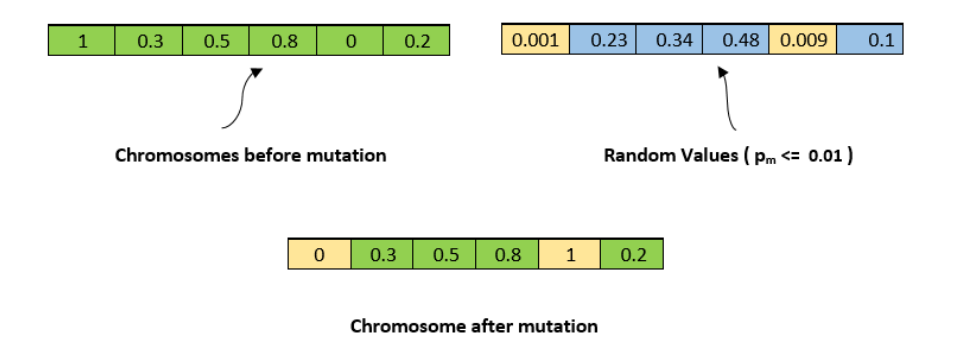


Figure 4.4: Illustration of mutation operation

the number of iterations is experimentally decided as 600 for NIST BSSR1 multimodal biometric dataset (set 1) [193] and 5000 for OU-ISIR BSS4 multi-algorithm dataset [2, 194]. The best chromosome in the final population is considered as the final aggregated score list of the subjects.

4.2.2 Performance Evaluation and Discussion

Detailed performance analysis is carried out for the proposed genetic algorithm based score level fusion approach against several existing fusion approaches (both at score level and at rank level). The existing approaches being used for performance comparison are mentioned in Section 3.2.2.1. The weights for the comparing weighted score and rank level fusion approachers are obtained using a genetic algorithm based weight estimation approach. This approach for obtaining the suitable set of weights for the existing weighted fusion approaches is discussed in Section 3.2.2.1. On the contrary, proposed genetic algorithm based score level fusion approach assigns the same weight to each individual modality (input list) to check the efficacy of the proposed approach over state-of-the-art rank and score level fusion approaches. The proposed approach is experimentally evaluated on two different multi-biometric datasets, namely: (i) NIST BSSR1 multimodal dataset (set 1) [193] involving face and fingerprint biometrics and (ii) OU-ISIR BSS4 multi-algorithm gait dataset [2, 194] involving different feature extraction methods for gait biometrics. The performance measures of all the comparing approaches on these two datasets are discussed in subsequent subsections.

4.2.2.1 Fusion of Multimodal Biometrics Involving Face and Fingerprint (NIST BSSR1 Multimodal Dataset (Set 1)

In this work, NIST BSSR1 multimodal dataset (set 1) [193] is considered for performance comparison. A brief description of this dataset can be found in Section 3.2.2.2. This dataset is widely used to study the fusion of multimodal biometrics [33, 50, 52, 195]. As it is discussed in Section 3.2.2.2, similarity scores of each of 517 subjects as a probe with all the enrolled subjects are provided in this dataset as per two different face matchers (termed as G and C) and fingerprint matchers for right and left index fingers.

Finally, the proposed genetic algorithm based score level fusion approach (Section 4.2.1) is used to combine the given four score lists. The recognition accuracies (in %), as defined in Eq. 3.7, for the proposed approach along with each unimodal matcher are presented in Table 4.1 for the probe being found within top-1 (Rank 1), top-2 (Rank 2) and top-3 (Rank 3) ranks (cumulative) in the aggregated score list. The usefulness of the proposed score level fusion approach over each of the unimodal matchers is obvious from the reported results in Table 4.1.

The recognition accuracies of the comparing approaches within top-1 (Rank 1), top-2 (Rank 2) and top-3 (Rank 3) positions along with proposed approach are also presented in Table 4.2. It can be seen from the reported recognition accuracies that the proposed genetic algorithm based score level fusion approach performs better than majority of existing state-of-the-art rank and score level fusion approaches. Among the rank level fusion approaches, genetic algorithm based (Section 3.2) and particle swarm optimization based (Section 3.3) rank level fusion approaches demonstrate identical recognition accuracies to the proposed GA based score level fusion approach for the top-1 (Rank 1), the top-2 (Rank 2) and top-3 (Rank 3) positions. Moreover, the division exponential approach [32] exhibits equivalent performance to the proposed approach while top-2 (Rank 2) and top-3 (Rank 3) positions are considered. But performance of the proposed approach is better than the division exponential approach if only top-1 position (Rank 1) is considered. Among the score level approaches, only the WQAM based approaches [62] exhibit equal performance as with the proposed approach. The reason for this superiority of the proposed GA based score level fusion approach as well as the GA based (Section 3.2) and PSO based (Section 3.3) rank level fusion approaches is that these approaches consider minimization of the weighted summation of the distances between the aggregated list and the input lists.

Table 4.1: Performance comparison of the proposed GA based score level fusion approach with unimodal matchers on NIST BSSR1 multimodal dataset (set 1)

	Method	Top-1 Rank	Top-2 Ranks	Top-3 Ranks
	Face Matcher G	83.37	86.28	88.40
Unimodal	Face Matcher C	88.78	90.52	91.50
Unimodal	Left Fingerprint	85.70	87.04	87.81
	Right Fingerprint	92.07	93.23	93.62
Proposed	d GA Score Fusion	99.42	99.42	99.42

It can be noted that 99.42% is the maximum achievable accuracy on NIST BSSR1 multimodal dataset (set 1) [193]. It is observed that 514 probes among 517 probes (99.42%) appear at the Rank 1 (first position) in the fused list. The improvement in the recognition accuracy is not observed even if the Rank 3 (top-3 positions) were considered in the fused list. This is because the dataset contains three probe subjects for whom all four biometric matchers fail to correctly identify the actual subject. These probe subject IDs are 81,224 and 419. The same observation was also reported in Section 3.2.2.2. The normalized score and associated rank for the probe ID 81 in the aggregated list as well as in all the input score lists are reported in Table 4.3. Similarly, the normalized scores and associated ranks for the wrongly identified subjects at first position, second position and third position are also shown in Table 4.3. The normalized score of subject ID 81 (actual subject) is 0.10 and is present at 43^{rd} position in the aggregated score list (Table 4.3). The identified subject at first position (ID 419) using the proposed GA based score level fusion approach has normalized score 1 and is present at first position in all the individual matcher lists. Therefore, the subject ID 419 has been identified at first position (rank 1) in the proposed GA based score level fusion approach. Similarly, the identified subject at second position (ID 276) using the proposed GA based score level fusion approach has normalized scores 0.05 (rank 238), 0.31 (rank 2), 0.29 (rank 380) and 0.84 (rank 3) in the left index finger, right index finger, face matcher C and face matcher G, respectively. As, this subject has good normalized scores in two of the modalities (right index finger and face matcher G), this subject is identified as the second best subject in the fused list. The other two incorrectly identified probes (ID 224 and 419) suffer from the same problem as seen in Table 4.4 and Table 4.5.

Table 4.2: Performance of the comparing fusion methods on NIST BSSR1 multimodal dataset (set 1) using cumulative recognition accuracies in %

Method		Top-1 Rank	Top-2 Ranks	Top-3 Ranks
	Weighted Sum [51]	98.65	98.84	99.03
	Max Rule [1]	79.90	94.00	98.45
	Min Rule [1]	94.80	95.40	95.60
	Product [1]	97.87	98.26	98.67
	Sum-OEBA [67]	99.03	99.03	99.26
	Sum-MOEBA [67]	98.45	98.84	98.84
	Sum-OEVBA [82]	98.70	99.03	99.26
	Hamacher t-norm [69]	97.29	97.68	97.68
Score Level	Frank t-norm [69]	98.07	98.65	98.84
	WQAM cos [62]	99.42	99.42	99.42
	$WQAM cos^r [62]$	98.65	99.03	99.03
	WQAM tan [62]	99.42	99.42	99.42
	WQAM sin [62]	98.65	98.84	98.84
	WQAM $r^{1/s}$ [62]	99.42	99.42	99.42
	WQAM r^s [62]	99.42	99.42	99.42
	WQAM s^r [62]	99.42	99.42	99.42
	WQAM log [62]	99.42	99.42	99.42
	WQAM exp [62]	99.42	99.42	99.42
	Proposed GA Score	99.42	99.42	99.42
	Borda Count [34]	92.07	93.04	94.00
	WBorda [34]	92.50	94.20	95.36
	Highest Rank [35]	79.70	94.81	98.26
D l- T l	Exp [33]	89.16	90.13	91.30
Rank Level	WExp [33]	87.81	89.16	90.71
	DivExp [32]	99.23	99.42	99.42
	Log [32]	98.45	99.03	99.23
	GA Rank (Section 3.2)	99.42	99.42	99.42
	PSO Rank (Section 3.3)	99.42	99.42	99.42

4.2 Proposed Genetic Algorithm Based Score Level Fusion Approach

Because of this, none of the fusion techniques are able to correctly identify these three probes (Table 4.2).

Table 4.3: Normalized scores (and their ranks) at each modality for ideally correct subject and the top three identified subjects according to the fused list (for probe subject ID 81)

Modality	Ideally correct	1^{st} Identified	2^{nd} Identified	3^{rd} Identified
Wiodanty	subject (ID 81)	subject (ID 419)	subject (ID 276)	subject (ID 13)
Left index finger	0.03 (480)	1 (1)	0.05 (238)	0.05 (238)
Right index finger	0.05 (353)	1 (1)	0.31 (2)	0.23 (3)
Face matcher C	0.43 (143)	1 (1)	0.29 (380)	0.50 (2)
Face matcher G	0.78 (12)	1 (1)	0.84 (3)	0.74 (39)
GA Score	0.10 (43)	1 (1)	0.28 (2)	0.19 (3)

Table 4.4: Normalized scores (and their ranks) at each modality for ideally correct subject and the top three identified subjects according to the fused list (for probe subject ID 224)

Modality	Ideally correct	1^{st} Identified	2^{nd} Identified	3^{rd} Identified
Wiodanity	subject (ID 224)	subject (ID 66)	subject (ID 184)	subject (ID 327)
Left index finger	0.39 (59)	1 (1)	0.22 (165)	0.87 (2)
Right index finger	0.09 (51)	1 (1)	0.09 (51)	0.06 (223)
Face matcher C	0.62 (122)	1 (1)	0.91 (3)	0.75 (31)
Face matcher G	0.97 (11)	0.98 (2)	0.92 (25)	0.37 (267)
GA Score	0.37 (185)	1 (1)	0.92 (2)	0.75 (3)

The changes in recognition accuracies (in %) with the changes in cumulative ranks are represented using cumulative match characteristic (CMC) curves in Fig. 4.5 and Fig. 4.6 for rank level and score level approaches, respectively. The proposed method outperforms several existing rank and score level fusion approaches, as it can be observed in the CMC curves in Fig. 4.5 and Fig. 4.6. It is observed from Fig. 4.5 that the CMC curves of GA based (Section 3.2) and PSO based (Section 3.3) rank level fusion approaches are overlapping with that of the proposed GA based score level fusion approach. Moreover, the CMC curve of the division exponential approach [32] is also overlapping with that of the proposed genetic algorithm based score level fusion approach when cumulative rank is beyond 2 and above.

The recognition accuracies of several WQAM based approaches [62] are equal to those of the proposed genetic algorithm based score level fusion approach.

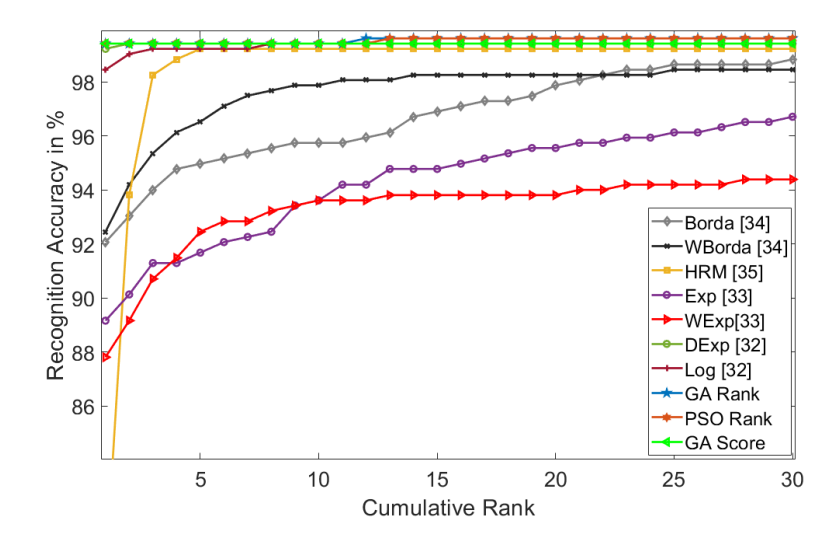


Figure 4.5: CMC plots for existing rank level fusion approaches being compared with that of the proposed GA based score level fusion approach for NIST BSSR1 dataset (set 1)

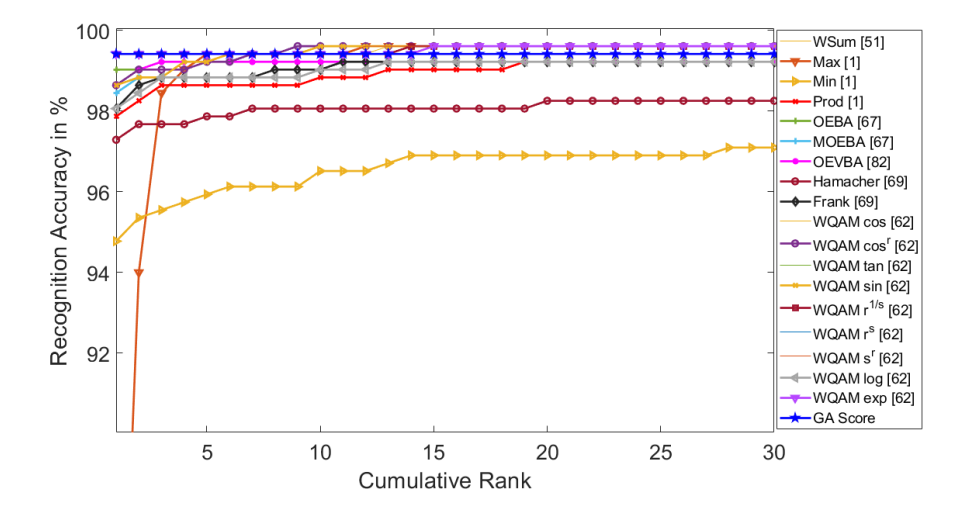


Figure 4.6: CMC plots for existing score level fusion approaches being compared with that of the proposed GA based score level fusion approach for NIST BSSR1 dataset (set 1)

4.2 Proposed Genetic Algorithm Based Score Level Fusion Approach

Table 4.5: Normalized scores (and their ranks) at each modality for ideally correct subject and the top three identified subjects according to the fused list (for probe subject ID 419)

Modality	Ideally correct	1^{st} Identified	2^{nd} Identified	3^{rd} Identified
Wiodanity	subject (ID 419)	subject (ID 81)	subject (ID 120)	subject (ID 273)
Left index finger	0.04 (478)	1 (1)	0.12 (216)	0.18 (83)
Right index finger	0.05 (470)	1 (1)	0.70 (9)	0.95 (2)
Face matcher C	0.35 (282)	1 (1)	0.64 (4)	0.63 (5)
Face matcher G	0.34 (279)	0.98 (2)	0.97 (3)	0.89 (17)
GA Score	0.08 (367)	1 (1)	0.64 (2)	0.63 (3)

Therefore, the CMC curves of these WQAM based approaches overlap with the CMC curve of the proposed genetic algorithm based score level fusion approach in Fig. 4.6.

4.2.2.2 Fusion of Multimodal Biometrics for Multiple Gait Feature Representations (OU-ISIR BSS4 Multi-Algorithm Gait Dataset)

The second dataset (OU-ISIR BSS4 multi-algorithm gait dataset [2, 194]) provides five score lists for each probe. These score lists are combined using the proposed genetic algorithm based score level fusion approach (Section 4.2.1) and other existing rank and score level fusion approaches as discussed in Section 3.2.2.1. The proposed method is compared with each unimodal biometric matcher. The recognition accuracies (in %) for the probe subjects within top-1 (Rank 1), top-2 (Rank 2) and top-3 (Rank 3) ranks (cumulative) are presented in the Table 4.6. It can be noted from Table 4.6 that the proposed method outperforms each unimodal matcher. It justifies the need for multi-biometric system. Similarly, Table 4.7 presents the recognition accuracies of various approaches at score and rank level fusion along with the proposed genetic algorithm based score level fusion approach.

It is evident from the presented results in Table 4.7 for OU-ISIR multialgorithm gait dataset [2, 194] that the proposed score level fusion approach using genetic algorithm exhibits superior performance over majority of rank level fusion approaches except PSO based rank level fusion approach in Section 3.3. Moreover, the proposed genetic algorithm based score level fusion approach exhibits superior performance over existing score level fusion approaches for each one of

Table 4.6: Performance comparison of the proposed GA based score level fusion approach with unimodal matchers on OU-ISIR BSS4 multi-algorithm dataset

Me	ethod	Top-1 Rank	Top-2 Ranks	Top-3 Ranks
	CEnI	80.95	85.50	87.50
	CGI	83.35	87.44	89.04
Unimodal	FDF	85.90	89.87	91.23
	GEI	85.72	89.54	91.20
	GFI	74.92	79.93	82.12
Proposed	d GA Score	86.62	91.07	92.24

the top-1 (Rank 1), top-2 (Rank 2) and top-3 (Rank 3) positions (cumulatively) in the aggregated list. Justification of this superiority is same as that for the experiments involving the previous dataset NIST BSSR1 multimodal dataset (set 1) [193] (Section 4.2.2.1).

The changes in recognition accuracies (in %) with the changes in cumulative ranks are presented using cumulative match characteristic (CMC) curves in Fig. 4.7 and Fig. 4.8.

4.2.3 Conclusion

The proposed genetic algorithm based score level fusion approach exhibits better performance in identifying the subjects than majority of the existing approaches of fusion at rank and score levels for multimodal biometric systems. Though the proposed approach is outperformed by particle swarm optimization based rank level fusion approach (Section 3.3) for OU-ISIR BSS4 multi-algorithm gait dataset [2, 194]. This justifies the introduction of a novel genetic algorithm based score level fusion approach in this section. Experiments also justify the usefulness of multimodal biometric systems over the unimodal biometric systems. The reported results show significant improvement in performance in spite of considering same weight for each input list. Moreover, the initial success for the reported experiments is encouraging enough to try out other meta-heuristic search and optimization strategies in the context of score level fusion for multimodal biometrics. Furthermore, the superior performance of the particle swarm optimization based rank level fusion approach (Section 3.3) leads the way to apply particle swarm

4.2 Proposed Genetic Algorithm Based Score Level Fusion Approach

Table 4.7: Performance of the comparing fusion methods on OU-ISIR BSS4 multialgorithm dataset using cumulative recognition accuracies in %

Method		Top-1 Rank	Top-2 Ranks	Top-3 Ranks
	Weighted Sum [51]	86.61	89.72	91.23
	Max Rule [1]	85.38	88.27	89.60
	Min Rule [1]	77.41	88.15	91.60
	Product [1]	77.41	88.21	91.60
	Sum-OEBA [67]	86.08	89.60	91.07
	Sum-MOEBA [67]	86.45	89.75	91.17
	Sum-OEVBA [82]	86.40	89.75	91.19
	Hamacher t-norm [69]	86.37	89.57	91.07
Score Level Fusion	Frank t-norm [69]	81.63	89.32	91.47
	WQAM cos [62]	86.43	89.50	91.23
	$\overline{\text{WQAM } cos^r [62]}$	85.78	88.98	90.34
	WQAM tan [62]	86.43	89.50	91.19
	WQAM sin [62]	86.43	89.50	91.23
	$\overline{\text{WQAM } r^{1/s} \text{ [62]}}$	85.29	88.15	89.38
	WQAM r^s [62]	86.43	89.54	91.07
	$\overline{\text{WQAM } s^r \text{ [62]}}$	85.35	88.89	90.43
	WQAM log [62]	86.43	89.50	91.17
	$WQAM \exp [62]$	85.29	88.15	89.44
	Proposed GA Score	86.62	91.07	92.24
	Borda Count [34]	83.63	87.47	88.77
	WBorda [34]	84.58	88.34	89.47
	Highest Rank [35]	77.41	88.15	91.54
	Exp [33]	83.56	87.47	88.83
Rank Level Fusion	WExp [33]	81.60	85.29	87.32
	DivExp [32]	86.40	89.94	91.51
	Log [32]	85.47	89.20	90.90
	GA Rank (Section 3.2)	86.49	90.98	92.24
	PSO Rank (Section 3.3)	86.73	91.16	92.31

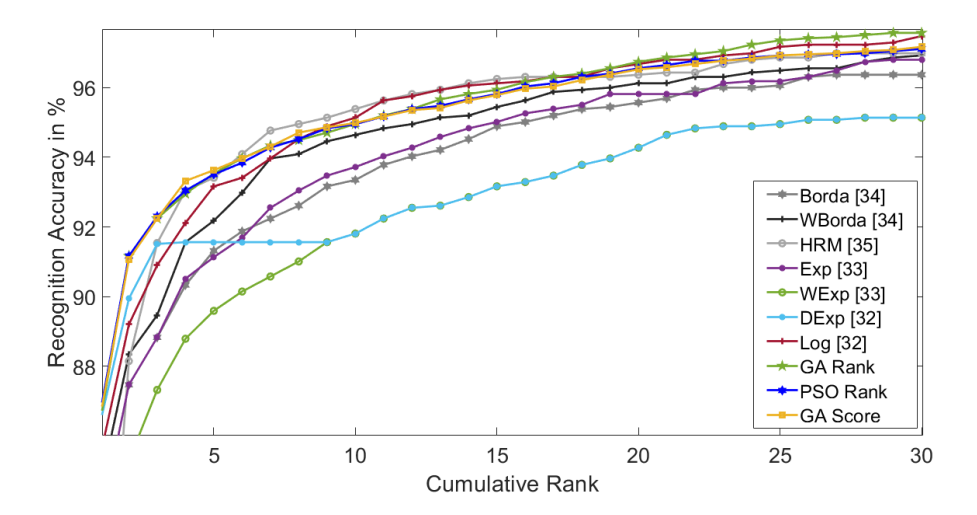


Figure 4.7: CMC plots for existing rank level fusion approaches being compared with that of the proposed GA based score level fusion approach for OU-ISIR BSS4 multi-algorithm dataset

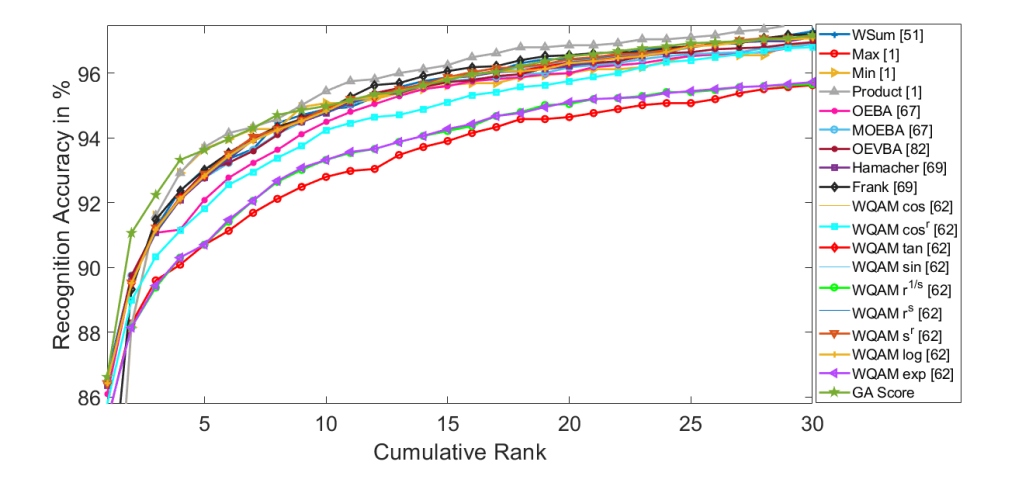


Figure 4.8: CMC plots for existing score level fusion approaches being compared with that of the proposed GA based score level fusion approach for OU-ISIR BSS4 multi-algorithm dataset

optimization based approach in the context of score level fusion of multimodal biometrics.

4.3 Proposed Particle Swarm Optimization Based Score Level Fusion Approach

One of the most well-regarded algorithms in the literature of meta-heuristic optimization is particle swarm optimization (PSO). The navigation and foraging behaviour of birds in nature is imitated by this algorithm. The particle swarm optimization is commonly used in various fields of study to solve the optimization problems [197, 198, 199, 200].

In this section, a particle swarm optimization based score level fusion approach is proposed for solving the optimization problem in Eq. 4.3. A weighted summation of distances of the normalized input score lists from a candidate aggregate score list is minimized in this context. Here, the distance between two score lists is computed using a weighted Spearman footrule distance in Eq. 4.4. Experimental study on the performance of the proposed PSO based score level fusion approach is reported using two multimodal biometric datasets: (i) NIST BSSR1 multimodal dataset (set 1) [193] involving face modalities and fingerprint and (ii) OU-ISIR BSS4 multi-algorithm gait dataset [2, 194] involving multiple feature extraction methods for gait biometrics. Supremacy of the proposed particle swarm optimization based score level fusion approach with respect to existing fusion schemes at score and rank levels is experimentally exhibited. Detail of the proposed particle swarm optimization based rank level fusion approach is presented in this section.

4.3.1 Problem Domain Specific Design of Particle Swarm Optimization Approach

The major contribution of this work is formulation of score level fusion of multimodal biometrics as an optimization problem and adoption of particle swarm optimization in this context. Representation of particle position and custom-designed operators to suite this problem domain are presented in this subsection.

4.3.1.1 Representation of a Candidate Score List as a Particle Position

In particle swarm optimization, position of a particle represents a candidate solution. In the context of the proposed score level fusion approach, the position of a particle represents a candidate fused list of similarity scores of a probe subject with each of the enrolled subjects. Let the number of enrolled subjects be n. Hence, position of a particle can be thought of as a point in a n-dimensional space. As shown in Fig. 4.2, a particle position $(0.8,0.2,0.6,\,0.5,0.1,0.4)$ represents a candidate similarity score list δ . It indicates the similarity scores of the probe with the enrolled subjects A,B,C,D,E, and F as 0.8,0.2,0.6,0.5,0.1, and 0.4, respectively.

4.3.1.2 Fitness of a Candidate Score List

In particle swarm optimization, fitness of each candidate solution (i.e., particle position) is evaluated. In the context of the proposed score level fusion method, a fitness value is calculated for a candidate score list (i.e., position of a particle) as a weighted summation of the distances between the candidate score list and each of the input score lists (Eq. 4.3). All of these input score lists (i.e., corresponding biometric modalities) are given equal weight in this work. The goal is to minimize the fitness. As a result, the solution with the lowest fitness value is considered as the fittest solution.

4.3.1.3 Initialization of Population of Candidate Score Lists

A swarm of particles is used in particle swarm optimization to parallelly search for the optimal solution in the solution space. The initialization of these positions of a population (or swarm) of particles (i.e., candidate solutions) is random. But incorporation of domain knowledge to initialize the particle positions can be found in [202, 203]. This domain knowledge-based initialization aids the particle swarm optimization algorithm to converge fast. Similarly, in the proposed particle swarm optimization approach, a combination of random and knowledge-based initialization is used to initialize the particle positions. Let the swarm have M particles. For the experiments in this paper, the value of M is considered as 10. The initial positions for N of these M particles are taken as N normalized input score lists. The input score lists are assumed to be close candidates for becoming the aggregated score list in this case. This is also the basis for the problem formulation (Eq. 4.3), which involves minimization of a weighted summation of distances

of the fused list from the input lists. As a result, this form of initialization is justified in the current context. The positions of remaining (M-N) particles are randomly initialized. In order to do so, scores are generated randomly in the range of [0,1] to determine their initial positions.

4.3.1.4 Exploring Other Candidate Score Lists

To evaluate the fitness of new candidate score lists, these M score lists (i.e., particle positions) in the population are iteratively updated. The position of the k^{th} particle (i.e., corresponding score list) is updated as following:

$$x_k(t+1) = x_k(t) + v_k(t+1)$$
(4.8)

Here, $v_k(t+1)$ relates to the amount of change from the position of the k^{th} particle at iteration t (i.e, $x_k(t)$) to its new position at iteration (t+1) (i.e, $x_k(t+1)$). The new velocity while going to the $(t+1)^{th}$ iteration is referred as $v_k(t+1)$. The velocity of a particle is changed with each iteration. The k^{th} particle's new velocity $v_k(t+1)$ is determined by three factors: (a) the particle's current velocity $v_k(t)$ at the t^{th} iteration, (b) the particle's propensity to move towards its personal best position $pbest_k(t)$, and (c) the particle's propensity to move towards its social best position gbest(t). The social best position in the PSO refers to the global best position (gbest(t)) of the entire swarm of particles. As a result, considering the prior velocity of the particle, its personal best position $(pbest_k(t))$, and the global best position (gbest(t)) at the given iteration, the new velocity of the particle is computed using Eq. 4.9.

$$v_k(t+1) = \omega \times v_k(t) + c_1 \times r_{1k}(t) \times (pbest_k(t) - x_k(t)) + c_2 \times r_{2k}(t) \times (gbest(t) - x_k(t))$$

$$(4.9)$$

Here, inertia weight is represented as ω . The velocity of the particle k at iteration t is defined as $v_k(t)$. Initial particle velocity is set to 10% of the values at the elements in the initial position vector in the current work. If the velocity is initialized to zero, it indicates that all particles at initial stage are not moving and any direction. This can lead to the slow convergence of PSO algorithm [204]. Hence, particle velocity is initialized in the proposed work as 10% of the values of its initial position vector. At iteration t, $x_k(t)$ represents the current position of the k^{th} particle (i.e., the current candidate score list). The particle's personal best position $pbest_k(t)$ is the best among all the positions which it has visited till iteration t. It refers to the fittest candidate score list as viewed by the k^{th} particle

up to iteration t. The global best position till iteration t is gbest(t). It refers to the fittest candidate score list among the lists which have been generated by the swarm of particles up to iteration t.

It should be observed that in Eq. 4.9, the addition and subtraction operations are carried out element-by-element in the respective position vectors (i.e., score lists). The two coefficients - the cognitive coefficient c_1 and the social coefficient c_2 - control the velocity updation stage. By regulating the step size by the particle toward its personal best position $pbest_k(t)$, the cognitive coefficient c_1 assists the particle in exploring the search space toward its personal best position. By adjusting the magnitude of steps by the particle toward the global best location (gbest(t)), the social coefficient c_2 assists the particle in exploring the search space toward its global best position. For the reported experiments, the value of c_1 and c_2 are set to be 0.5. The randomness of PSO is maintained by introducing two random numbers, $r_{1k}(t)$ and $r_{2k}(t)$ at each iteration. These random numbers have values in the range [0,1].

The above updation of these M score lists (i.e., new particle positions) may no longer represent a valid solution in the solution space consisting normalized scores. Due to the above computation, the coordinates in the new position $x_k(t+1)$ (i.e., the normalized scores) may not remain in the range [0,1]. To solve this issue, newly computed values in $x_k(t+1)$ are clamped in the range [0,1] by replacing values less than zero with zero and values larger than one with one. As a result, scores will remain in the range [0,1].

4.3.1.5 Stopping Criteria

In particle swarm optimization, the updation of a particle's velocity and position in the solution space is performed iteratively until a stopping criteria is met. When the personal best positions of all the particles do not change during a series of iterations, the proposed score level fusion approach based on particle swarm optimization is considered to have converged. The stated window size on the number of iterations is experimentally decided as 600 for NIST BSSR1 multimodal biometric dataset (set 1) [193] and 5000 for OU-ISIR BSS4 multialgorithm dataset [2, 194].

4.3.2 Performance Evaluation and Discussion

Performance of the proposed particle swarm optimization based score level fusion approach for multimodal biometrics is experimentally evaluated with respect to the performances of several existing fusion approaches (score and rank levels). The comparing approaches are mentioned in Section 3.2.2.1. Two multimodal biometric datasets, namely NIST BSSR1 multimodal dataset (set 1) [193] and OU-ISIR multi-algorithm gait dataset [2, 194], are used in these experiments to evaluate the performances of the proposed approach along with existing score and rank level fusion approaches. The weights for the comparing weighted score and rank level fusion approachers are obtained using a genetic algorithm based weight estimation approach. This approach for obtaining a suitable set of weights for the existing weighted fusion approaches is discussed in Section 3.2.2.1. This process of obtaining weights for the concerned modalities is followed for each of the above two datasets. On the contrary, proposed particle swarm optimization based score level fusion approach assigns the same weight to each individual modality (input list).

4.3.2.1 Fusion of Multimodal Biometrics Involving Face and Fingerprint (NIST BSSR1 Multimodal Dataset (Set 1))

A brief description of NIST BSSR1 multimodal dataset (set 1) [193] can be found in Section 3.2.2.2. The recognition accuracies (in %) on NIST BSSR1 multimodal dataset (set 1) [193] for the proposed PSO based score level fusion approach along with each unimodal matcher are presented in Table 4.8 for the probe being found within top-1 (Rank 1), top-2 (Rank 2) and top-3 (Rank 3) ranks (cumulative) in the aggregated score list. Recognition accuracies are estimated using Eq. 3.7. The usefulness of the proposed PSO based score level fusion approach over each of the unimodal matchers is obvious from the reported results in Table 4.8.

The recognition accuracies of the comparing approaches within top-1 (Rank 1), top-2 (Rank 2) and top-3 (Rank 3) positions (cumulative) along with those of the proposed PSO based score level fusion approach are also presented in Table 4.9. It can be seen from the reported recognition accuracies that the proposed particle swarm optimization based score level fusion approach performs better than the majority of existing state-of-the-art rank and score level fusion approaches. Among the rank level fusion approaches, genetic algorithm based (Section 3.2) and particle swarm optimization based (Section 3.3) rank level fusion approaches demonstrate identical recognition accuracies as compared with the proposed PSO

Table 4.8: Performance comparison of the proposed PSO based score level fusion approach with unimodal matchers on NIST BSSR1 multimodal dataset (set 1)

	Method	Top-1 Ranks	Top-2 Ranks	Top-3 Ranks
	Face Matcher G	83.37	86.28	88.40
Unimadal	Face Matcher C	88.78	90.52	91.50
Ummodai	Left Fingerprint	85.70	87.04	87.81
	Right Fingerprint	92.07	93.23	93.62
Proposed	d PSO Score Fusion	99.42	99.42	99.42

based score level fusion approach for the top-1 (Rank 1), the top-2 (Rank 2) and top-3 (Rank 3) positions. Moreover, the division exponential approach [32] exhibits equivalent performance to the proposed approach while top-2 (Rank 2) and top-3 (Rank 3) positions are considered. However, when only the top-1 (Rank 1) position is considered, the proposed score level fusion approach using PSO outperforms the division exponential approach [32]. Additionally, among the score level fusion approaches, the weighted quasi-arithmetic mean (WQAM) based approaches [62] and GA based (Section 4.2) approach exhibit identical performance as with the proposed PSO based score level fusion approach in this work. This improved performance of the proposed approach can be attributed to minimization of the weighted summation of distances of the fused list from the input lists.

Similar to the genetic algorithm based score level fusion approach in Section 4.2, the maximum achievable recognition accuracy of the proposed PSO based approach on NIST BSSR1 multimodal dataset (set 1) [193] is 99.42%. Three out of 517 probes are not correctly identified. These probe subject IDs are 81,224 and 419. The normalized score and associated rank for the probe subject ID 81 in aggregated list as well as in all the normalized input score lists are reported in Table 4.10. The normalized score of subject ID 81 (actual subject) is 0.07 and it is present at 56th position in the fused list (Table 4.10). The identified subject at the first position (ID 419) using the proposed PSO based score level fusion approach has normalized score 1 and is present at first position (rank 1) in all the individual matcher lists. Therefore, the subject ID 419 has been identified at the first position (rank 1) in the proposed PSO based score level fusion approach. Similarly, the identified subject at the second position (ID 427) using the proposed PSO based score level fusion approach has normalized scores 0.03 (rank 391), 0.15 (rank 9), 0.41 (rank 180) and 0.82 (rank 4) in the left index finger, right index

Table 4.9: Performance of the comparing fusion approaches on NIST BSSR1 multimodal dataset (set 1) using cumulative recognition accuracies in %

Method		Top-1 Rank	Top-2 Ranks	Top-3 Ranks
	Weighted Sum [51]	98.65	98.84	99.03
	Max Rule [1]	79.90	94.00	98.45
	Min Rule [1]	94.80	95.40	95.60
	Product [1]	97.87	98.26	98.67
	Sum-OEBA [67]	99.03	99.03	99.26
	Sum-MOEBA [67]	98.45	98.84	98.84
	Sum-OEVBA [82]	98.70	99.03	99.26
	Hamacher t-norm [69]	97.29	97.68	97.68
Score Level	Frank t-norm [69]	98.07	98.65	98.84
	WQAM cos [62]	99.42	99.42	99.42
	$\overline{\text{WQAM } \cos^r [62]}$	98.65	99.03	99.03
	WQAM tan [62]	99.42	99.42	99.42
	WQAM sin [62]	98.65	98.84	98.84
	$\overline{\text{WQAM } r^{1/s} \text{ [62]}}$	99.42	99.42	99.42
	WQAM r^s [62]	99.42	99.42	99.42
	$\overline{\text{WQAM } s^r \text{ [62]}}$	99.42	99.42	99.42
	WQAM log [62]	99.42	99.42	99.42
	WQAM exp [62]	99.42	99.42	99.42
	GA Score (Section 4.2)	99.42	99.42	99.42
	Proposed PSO Score	99.42	99.42	99.42
	Borda Count [34]	92.07	93.04	94.00
	WBorda [34]	92.50	94.20	95.36
	Highest Rank [35]	79.70	94.81	98.26
Rank Level	Exp [33]	89.16	90.13	91.30
nank Lever	WExp [33]	87.81	89.16	90.71
	DivExp [32]	99.23	99.42	99.42
	Log [32]	98.45	99.03	99.23
	GA Rank (Section 3.2)	99.42	99.42	99.42
	PSO Rank (Section 3.3)	99.42	99.42	99.42

4.3 Proposed Particle Swarm Optimization Based Score Level Fusion Approach

finger, face matcher C and face matcher G, respectively. As this subject has better scores and their associated ranks than those of the ideally correct subject in two of the modalities (right index finger and face matcher G), this subject is identified as the second best subject in the fused list. The other two incorrectly identified probes (ID 224 and 419) suffer from the same problem as seen in Table 4.11 and Table 4.12. Because of this, none of the fusion techniques are able to correctly identify these three probes (Table 4.9).

Table 4.10: Normalized scores (and their ranks) at each modality for ideally correct subject and the top three identified subjects according to the fused list (for probe subject ID 81)

Modality	Ideally correct	1^{st} Identified	2^{nd} Identified	3^{rd} Identified
Wiodanty	subject (ID 81)	subject (ID 419)	subject (ID 427)	subject (ID 371)
Left index finger	0.03 (480)	1 (1)	0.03 (391)	0.02 (513)
Right index finger	0.05 (353)	1 (1)	0.15 (9)	0.10 (59)
Face matcher C	0.43 (143)	1 (1)	0.41 (180)	0.57 (26)
Face matcher G	0.78 (12)	1 (1)	0.82 (4)	0.80 (9)
PSO Score	0.07 (56)	1 (1)	0.41 (2)	0.40 (3)

Table 4.11: Normalized scores (and their ranks) at each modality for ideally correct subject and the top three identified subjects according to the fused list (for probe subject ID 224)

Modality	Ideally correct	1^{st} Identified	2^{nd} Identified	3^{rd} Identified
Wiodanity	subject (ID 224)	subject (ID 68)	subject (ID 66)	subject (ID 300)
Left index finger	0.39 (59)	1 (1)	0.26 (123)	0.22 (204)
Right index finger	0.09 (51)	1 (1)	0.06 (241)	0.09 (72)
Face matcher C	0.62 (122)	0.93 (5)	1 (1)	0.91 (3)
Face matcher G	0.97 (11)	0.84 (29)	0.98 (9)	0.92 (26)
PSO Score	0.22 (11)	1 (1)	0.59 (2)	0.57 (3)

The changes in recognition accuracies (in %) with the changes in cumulative ranks are represented using cumulative match characteristic (CMC) curves in Fig. 4.9 and Fig. 4.10 for rank level and score level approaches, respectively. The proposed method outperforms several existing rank and score level fusion approaches, as it can be observed in the CMC curves in Fig. 4.9 and Fig. 4.10. It is observed from Fig. 4.9 that the CMC curves of the genetic algorithm based (Section 3.2) and particle swarm optimization based (Section 3.3) rank level fusion approaches

Table 4.12: Normalized scores (and their ranks) at each modality for ideally correct subject and the top three identified subjects according to the fused list (for probe subject ID 419)

Modality	Ideally correct	1^{st} Identified	2^{nd} Identified	3^{rd} Identified
Wiodanity	subject (ID 419)	subject (ID 81)	subject (ID 120)	subject (ID 273)
Left index finger	0.04 (478)	1 (1)	0.12 (180)	0.04 (443)
Right index finger	0.05 (470)	1 (1)	0.95 (2)	0.70 (14)
Face matcher C	0.35 (282)	1 (1)	0.63 (5)	0.64 (4)
Face matcher G	0.34 (279)	0.98 (2)	0.88 (20)	0.97 (4)
PSO Score	0.23 (466)	1 (1)	0.74 (2)	0.64 (3)

overlap with that of the proposed PSO based score level fusion approach. Moreover, the CMC curve of division exponential approach [32] overleaps with CMC curves of the GA based rank level (Section 3.2), PSO based rank level (Section 3.3) and the proposed PSO based score level fusion approaches, when cumulative rank is beyond 2 and above.

The recognition accuracies of several WQAM based approaches [62] and GA based score level fusion approach (Section 4.2) are equal to the proposed particle swarm optimization based score level fusion approach. Therefore, the CMC curves of these approaches overlap with that of the proposed PSO based score level fusion approach as shown in the Fig. 4.10.

4.3.2.2 Fusion of Multimodal Biometrics for Multiple Gait Feature Representations (OU-ISIR BSS4 Multi-Algorithm Gait Dataset)

The second dataset (OU-ISIR BSS4 multi-algorithm gait dataset [2, 194]) provides five score lists for each probe. These score lists are combined using the proposed particle swarm optimization based score level fusion approach (Section 4.3.1) and other existing rank and score level fusion approaches as discussed in Section 3.2.2.1. The proposed PSO based score level fusion approach is compared with each unimodal biometric matcher. The recognition accuracies (in %) for the probe subjects within top-1 (Rank 1), top-2 (Rank 2) and top-3 (Rank 3) ranks (cumulative) are presented in the Table 4.13. It is to be noted that the proposed PSO based score level fusion approach outperforms each unimodal matcher. It justifies the need for multi-biometric system.

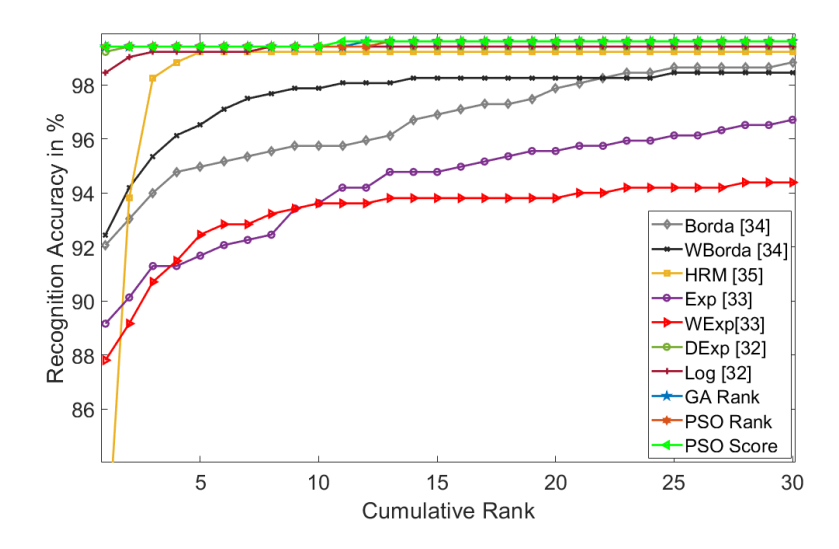


Figure 4.9: CMC plots for existing rank level fusion approaches being compared with that of the proposed PSO based score level fusion approach for NIST BSSR1 multimodal dataset (set 1)

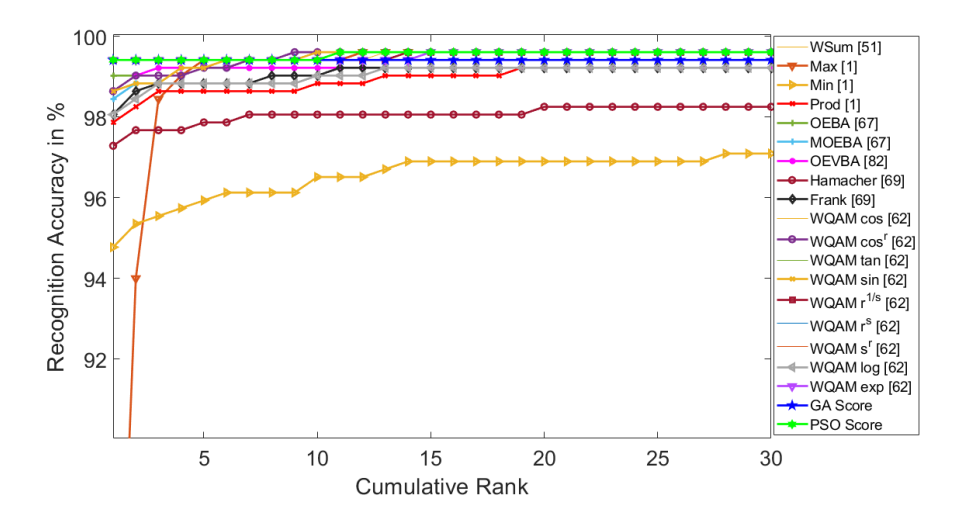


Figure 4.10: CMC plots for existing score level fusion approaches being compared with those of the GA based and the proposed PSO based score level fusion approaches for NIST BSSR1 multimodal dataset (set 1)

Table 4.13: Performance comparison (using cumulative recognition accuracies in %) of the proposed PSO based score level fusion approach with unimodal matchers on OU-ISIR BSS4 multi-algorithm dataset

Method		Top-1 Rank	Top-2 Ranks	Top-3 Ranks
Unimodal	CEnI	80.95	85.50	87.50
	CGI	83.35	87.44	89.04
	FDF	85.90	89.87	91.23
	GEI	85.72	89.54	91.20
	GFI	74.92	79.93	82.12
Proposed PSO Score		86.95	91.16	92.31

Similarly, Table 4.14 presents the recognition accuracies of various approaches at score and rank level fusion along with the proposed particle swarm optimization based score level fusion approach. It is evident from the results presented in Table 4.14 that the proposed PSO based score level fusion approach exhibits superior performance over other rank and score level fusion approaches for each one of the top-1 (Rank 1), top-2 (Rank 2) and top-3 (Rank 3) positions (cumulatively) in the aggregated list. Only PSO based rank level fusion approach (Section 3.3) exhibits equal performance as the proposed PSO based score level fusion approach (in terms of recognition accuracy) when top-2 (Rank 2) and top-3 (Rank 3) positions are considered. The performance of the proposed PSO based score level fusion approach is better than the PSO based rank level fusion approach when top-1 position (Rank 1) is considered.

Table 4.14 presents cumulative recognition accuracies of the comparing approaches only up to rank 3. In order to further understand the results, the changes in recognition accuracies (in %) with the changes in cumulative ranks for these comparing approaches are presented using cumulative match characteristic (CMC) curves in Fig. 4.11 and Fig. 4.12. These plots reveal the performances of the comparing approaches at least up to rank 30. The proposed approach outperforms majority of the rank and score level fusion approaches, as it can be observed in the CMC curves in Fig. 4.11 and Fig. 4.12. It is observed from Fig. 4.11 that the CMC curves of the proposed particle swarm optimization based score level fusion approach and particle swarm optimization based rank level fusion approach (Section 3.3) overlap when the cumulative rank is beyond 1.

4.3 Proposed Particle Swarm Optimization Based Score Level Fusion Approach

Table 4.14: Performance of the comparing fusion approaches on OU-ISIR BSS4 multi-algorithm dataset using cumulative recognition accuracies in %

Method		Top-1 Rank	Top-2 Ranks	Top-3 Ranks
	Weighted Sum [51]	86.61	89.72	91.23
	Max Rule [1]	85.38	88.27	89.60
	Min Rule [1]	77.41	88.15	91.60
	Product [1]	77.41	88.21	91.60
	Sum-OEBA [67]	86.08	89.60	91.07
	Sum-MOEBA [67]	86.45	89.75	91.17
	Sum-OEVBA [82]	86.40	89.75	91.19
	Hamacher t-norm [69]	86.37	89.57	91.07
Score Level Fusion	Frank t-norm [69]	81.63	89.32	91.47
	WQAM cos [62]	86.43	89.50	91.23
	$\overline{\text{WQAM } cos^r [62]}$	85.78	88.98	90.34
	WQAM tan [62]	86.43	89.50	91.19
	WQAM sin [62]	86.43	89.50	91.23
	WQAM $r^{1/s}$ [62]	85.29	88.15	89.38
	WQAM r^s [62]	86.43	89.54	91.07
	WQAM s^r [62]	85.35	88.89	90.43
	WQAM log [62]	86.43	89.50	91.17
	$WQAM \exp [62]$	85.29	88.15	89.44
	GA Score (Section 4.2)	86.62	91.07	92.24
	Proposed PSO Score	86.95	91.16	92.31
	Borda Count [34]	83.63	87.47	88.77
	WBorda [34]	84.58	88.34	89.47
	Highest Rank [35]	77.41	88.15	91.54
	Exp [33]	83.56	87.47	88.83
Rank Level Fusion	WExp [33]	81.60	85.29	87.32
	DivExp [32]	86.40	89.94	91.51
	Log [32]	85.47	89.20	90.90
	GA Rank (Section 3.2)	86.49	90.98	92.24
	PSO Rank (Section 3.3)	86.73	91.16	92.31

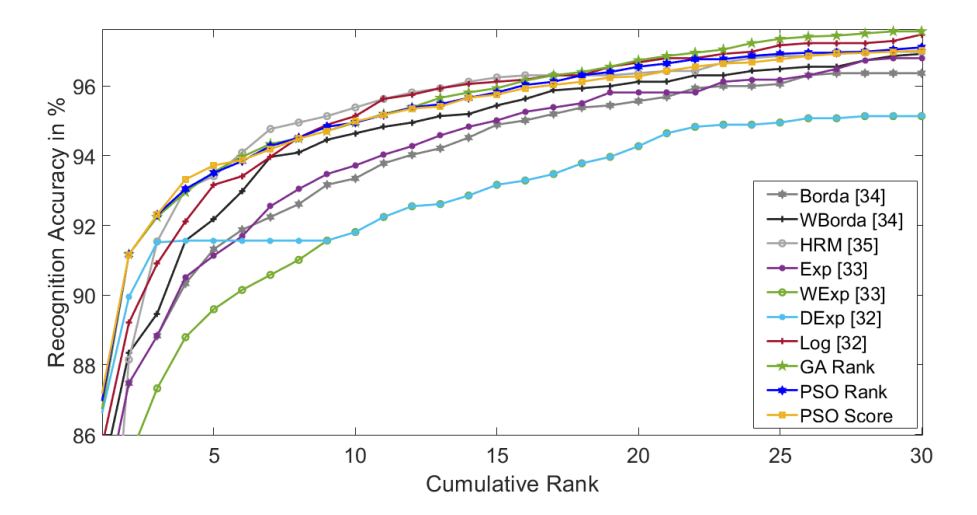


Figure 4.11: CMC plots for existing rank level fusion approaches being compared with that of the proposed PSO based score level fusion approach for OU-ISIR BSS4 multi-algorithm dataset

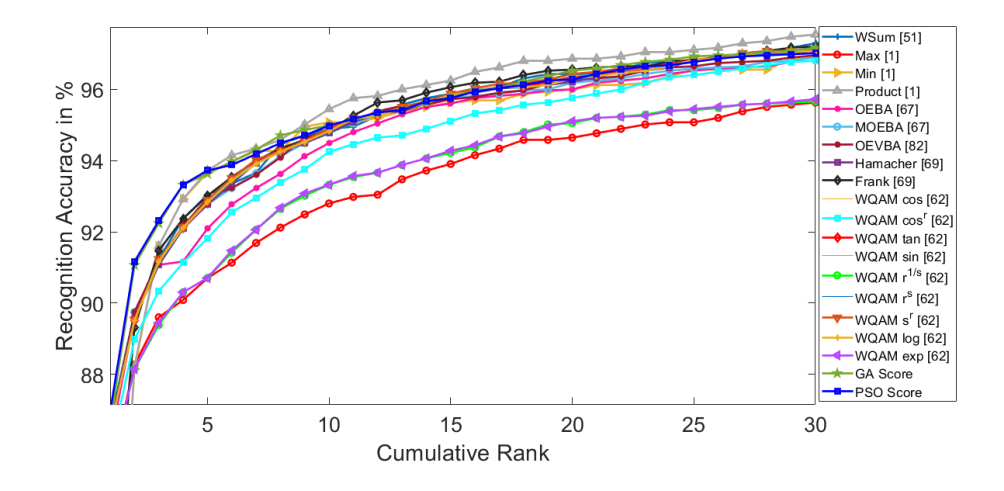


Figure 4.12: CMC plots for existing score level fusion approaches being compared with those of the GA based and proposed PSO based score level fusion approaches for OU-ISIR BSS4 multi-algorithm dataset

4.3.3 Conclusion

The proposed particle swarm optimization based score level fusion approach exhibits better performance in identifying the subjects than the state-of-the-art approaches of fusion at rank and at score levels for multimodal biometrics using both the datasets. This justifies the introduction of a novel particle swarm optimization based approach in this section. Experiments also justify the usefulness of multimodal biometric system over the unimodal biometric system. The reported results show significant improvement in performance in spite of considering same weight for each biometric modality in the proposed approach.

4.4 Analysis of Convergence Rate Between Proposed Optimization Based Score and Rank Level Fusion Approaches

Four novel optimization based approaches are presented in Chapter 3 and Chapter 4. These are listed below:

- 1. Genetic algorithm (GA) based rank level fusion approach (Section 3.2)
- 2. Particle swarm optimization (PSO) based rank level fusion approach (Section 3.3)
- 3. Genetic algorithm (GA) based score level fusion approach (Section 4.2)
- 4. Particle swarm optimization (PSO) based score level fusion approach (Section 4.3)

It is observed from the reported results in Section 4.3.2 that the performances (in terms of cumulative recognition accuracies) of these optimization based approaches are comparable to each other. All the methods are evolutionary computing based approaches for solving the optimization problem either in the context of rank level fusion (Section 3.1) or in the context of score level fusion (Section 4.1). As all these evolutionary computing based approaches exhibit equivalent performance in terms of recognition accuracies, comparison among these approaches are carried out using the number of iterations being taken for convergence.

Number of iterations for convergence of these four evolutionary computing based approaches are observed for NIST BSSR1 multimodal dataset (set 1) [193]

4.4 Analysis of Convergence Rate Between Proposed Optimization Based Score and Rank Level Fusion Approaches

and OU-ISIR BSS4 multi-algorithm dataset [2, 194]. Faster convergence of the PSO based rank level fusion approach (Section 3.3) in comparison to GA based rank level fusion approach (Section 3.2) is already established through the analysis in Section 3.4. Therefore, the comparison (in terms of convergence rate) is presented in this section among GA based score level fusion (Section 4.2), PSO based score level fusion (Section 4.3) and PSO based rank level fusion (Section 3.3) approaches.

The cumulative distribution functions (CDFs) on the number of iterations are plotted for these comparing evolutionary computing based approaches in Fig. 4.13 and Fig. 4.14 for NIST BSSR1 multimodal dataset (set 1) [193]. Similar plots are presented in Fig. 4.15 and Fig. 4.16 for OU-ISIR BSS4 multi-algorithm dataset [2, 194]. It is observed from these plots that PSO based score level fusion approach (Section 4.3) converges faster (lesser number of iterations) than other two comparing approaches.

In order to prove the above reported faster convergence of the PSO based score level fusion approach (Section 4.3) than other two approaches, a two-sample Kolmogorov-Smirnov (K-S) test is performed on the number of iterations for convergence between a pair of methods. A two-sample K-S test is a statistical test for comparing the CDFs of two samples. The following hypothesis are tested:

- Null Hypothesis H_0 : two samples follow same distribution.
- Alternate Hypothesis H_1 : two samples follow different distributions.

The detail of this test has already been defined in Section 3.4. Hence, the results of this test are directly presented in following subsections.

4.4.1 Results of Two-Sample K-S Test Using Multimodal Biometrics Involving Face and Fingerprint (NIST BSSR1 Multimodal Dataset (Set 1))

Number of iterations for convergence is noted down for each probe during the executions of the above discussed optimization based rank and score level fusion approaches on NIST BSSR1 multimodal dataset (set 1) [193]. Cumulative distribution functions for PSO based score level fusion approach (Section 4.3) (F(x)) and GA based score level fusion approach (Section 4.2) (G(x)) are computed using number of iterations for convergence in both approaches, as shown in Fig.

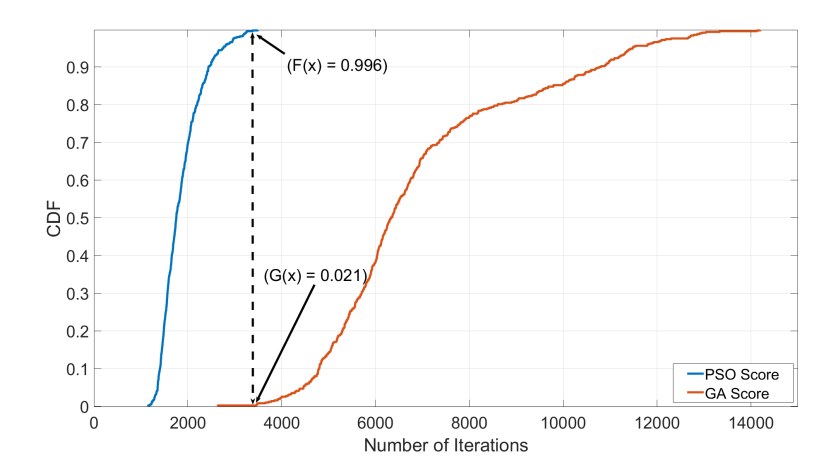


Figure 4.13: CDFs on number of iterations for PSO based (Section 4.3) and GA based (Section 4.2) score level approaches on NIST BSSR1 multimodal dataset (set 1)

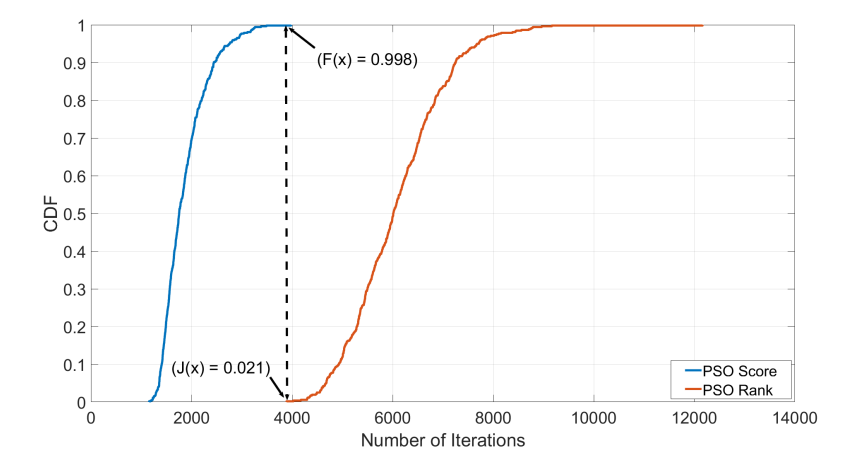


Figure 4.14: CDFs on number of iterations for PSO based score level fusion approach (Section 4.3) and PSO based rank level fusion approach (Section 3.3) on NIST BSSR1 multimodal dataset (set 1)

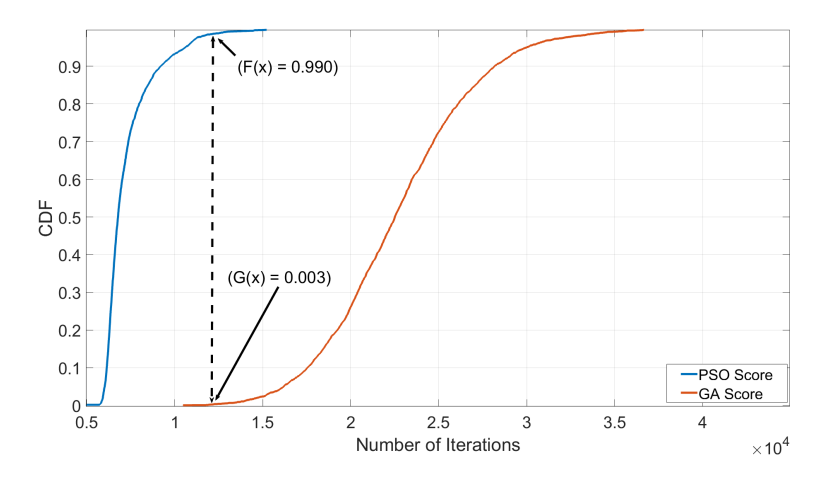


Figure 4.15: CDFs on number of iterations for PSO based (Section 4.3) and GA based (Section 4.2) score level fusion approaches on OU-ISIR BSS4 multi-algorithm dataset

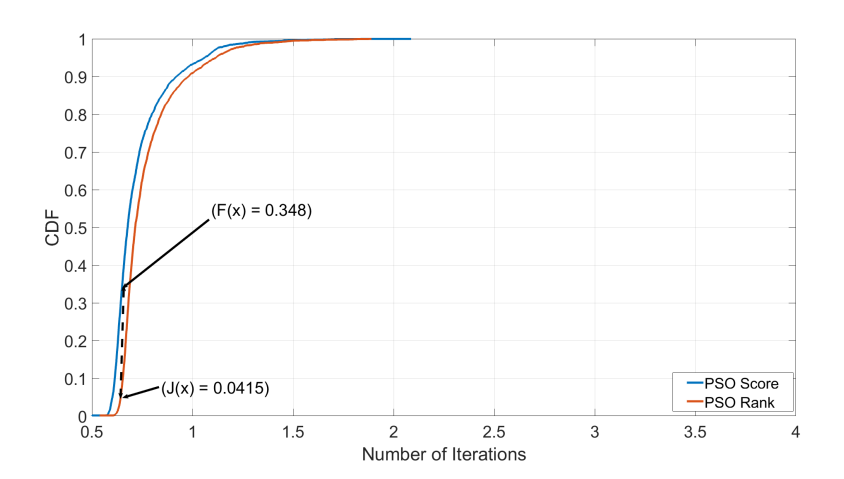


Figure 4.16: CDFs on number of iterations for PSO based score level fusion approach (Section 4.3) and PSO based rank level fusion approach (Section 3.3) on OU-ISIR BSS4 multi-algorithm dataset

4.4 Analysis of Convergence Rate Between Proposed Optimization Based Score and Rank Level Fusion Approaches

4.13. Then, the maximum difference between the two CDFs is computed using Eq. 3.10. From Fig. 4.13, it is noted that the maximum difference between the two CDFs is 0.975.

$$D_{m,n} = |0.996 - 0.021| = 0.975$$

The critical value is computed using Eq. 3.11 with 0.05 significance level (α). Considering $\alpha = 0.05$, $c(\alpha)$ is calculated as 1.36 using Eq. 3.12. NIST BSSR1 multimodal dataset (set 1) [193] has 517 subjects. Hence, considering each subject as probe, the comparing multimodal biometric fusion algorithms are executed 517 times. Hence, the value of m and n are 517 for Eq. 3.11. Thus, the value of $D_{m,n,\alpha}$ is computed as following:

$$D_{m,n,\alpha} = 1.36 * \sqrt{\frac{517 + 517}{517 * 517}} = 0.0846$$

Here, null hypothesis is rejected as the value of $D_{m,n}$ is greater than the value of $D_{m,n,\alpha}$. Hence, it is concluded that number of iterations to converge for PSO based score level fusion (Section 4.3) and GA based score level fusion (Section 4.2) approaches follow two separate distributions. It establishes that PSO based score level fusion approach (Section 4.3) converges faster than GA based score level fusion approach (Section 4.2).

Similarly, to compare the performance of PSO based score level fusion approach (Section 4.3) against the PSO based rank level fusion approach (Section 3.3), the two CDFs F(x) and J(x) for the above approaches are computed as shown in Fig. 4.14. The maximum difference between the CDF of PSO based score level fusion approach (Section 4.3) (F(x)) and the CDF of PSO based rank level fusion approach (Section 3.3) (J(x)) is computed using Eq. 3.10. From Fig. 4.14, it is observed that the maximum difference $D_{m,n}$ between F(x) and J(x) is (0.998-0.021)=0.977. Thus, the statistical test rejects the null hypothesis as the value of $D_{m,n}$ (0.977) is greater than the value of $D_{m,n,\alpha}$ (0.0846). Hence, it shows that number of iterations to converge for PSO based score level fusion (Section 4.3) and PSO based rank level fusion (Section 3.3) approaches follow two separate distributions. It establishes that PSO based score level fusion approach (Section 4.3) converges faster than PSO based rank level fusion approach (Section 4.2).

4.4.2 Results of Two-Sample K-S Test Using Multimodal Biometrics for Multiple Gait Feature Representations (OU-ISIR BSS4 Multi-Algorithm Dataset)

Number of iterations for convergence is noted down for each probe during the executions of the above discussed optimization based rank and score level fusion approaches on OU-ISIR BSS4 multi-algorithm gait dataset [2, 194]. Cumulative distribution functions for PSO based score level fusion approach (Section 4.3) (F(x)) and GA based score level fusion approach (Section 4.2) (G(x)) are computed using number of iterations for convergence in both methods as shown in Fig. 4.15. Then, the maximum difference between the two CDFs is computed using Eq. 3.10. From Fig. 4.15, it is noted that the maximum difference $D_{m,n}$ between the two CDFs is 0.987.

$$D_{m,n} = |0.990 - 0.003| = 0.987$$

The critical value is computed using Eq. 3.11 with 0.05 significance level (α) . Considering $\alpha = 0.05$, $c(\alpha)$ is calculated as 1.36 using Eq. 3.12. OU-ISIR BSS4 dataset [2, 194] has 3249 subjects. Hence, considering each subject as probe, the comparing multimodal biometric fusion algorithms are executed 3249 times. Hence, the value of m and n are 3249 for Eq. 3.11. Thus, the value of $D_{m,n,\alpha}$ is computed as following:

$$D_{m,n,\alpha} = 1.36 * \sqrt{\frac{3249 + 3249}{3249 * 3249}} = 0.0337$$

Here, null hypothesis is rejected as the value of $D_{m,n}$ (0.987) is greater than the value of $D_{m,n,\alpha}$ (0.0337). Hence it proves the difference between the distributions on number of iterations to converge for PSO based score level fusion approach (Section 4.3) and GA based score level fusion approach (Section 4.2).

Similarly, to compare the convergence rate of PSO based score level fusion approach (Section 4.3) against PSO based rank level fusion approach (Section 3.3), the two CDFs F(x) and J(x) are computed as shown in Fig. 4.16. The maximum difference between the CDF of PSO based score level fusion approach (Section 4.3) (F(x)) and the CDF of PSO based rank level fusion approach (Section 3.3) (J(x)) is computed using Eq. 3.10. From Fig. 4.16, it is observed that

the maximum difference $D_{m,n}$ between these two distributions F(x) and J(x) is (0.348-0.0415)=0.3065. Thus, the statistical test rejects the null hypothesis as the value of $D_{m,n}$ (0.3065) is greater than the value of $D_{m,n,\alpha}$ (0.0337). Therefore, faster convergence of PSO based score level fusion approach (Section 4.3) is established over the convergence of PSO based rank level fusion approach (Section 3.3).

Thus, superiority (in terms of convergence rate) of PSO based score level fusion approach (Section 4.3) over other proposed approaches in Chapter 3 and Chapter 4 is established for both datasets - NIST BSSR1 multimodal dataset (set 1) [193] and OU-ISIR BSS4 multi-algorithm dataset [2, 194].

4.5 Summary

Score level fusion for multimodal biometrics is studied in this chapter. The manifold contributions of the works in this chapter are highlighted here: The score level fusion in multimodal biometrics is formulated as an optimization problem. The formulation of this optimization problem considers minimization of a weighted summation of distances between the aggregated score list and the normalized input score lists. This problem formulation adds novelty to the proposed works in this chapter. The weighted Spearman footrule distance metric [180] is used to compute the distance between two score lists. The weight in the weighted Spearman footrule distance is incorporated to ensure more influence of a high scoring subject than other subjects. A novel way to decide the weight of a subject is conceptualized in this context.

To solve the stated optimization problem, two novel score level fusion approaches based on (i) genetic algorithm (GA) and (ii) particle swarm optimization (PSO) are proposed in Section 4.2 and Section 4.3, respectively. Context-specific representation of a candidate solution and custom-designed operators are the highlights of the proposed GA and PSO based score level fusion approaches.

The performances of these proposed score level fusion approaches are experimentally evaluated on two different multimodal biometric datasets, namely (i) NIST BSSR1 multimodal dataset (set 1) [193] and (ii) OU-ISIR BSS4 multialgorithm gait dataset [2, 194]. The proposed approaches exhibit better performance in identifying the subjects than majority of the existing approaches of fusion at rank and score levels for multimodal biometrics. The reported experimental results in Section 4.3.2 also show that the proposed particle swarm based

fusion approaches at both rank (Section 3.3) and score (Section 4.3) levels of fusion perform better than the proposed genetic algorithm based fusion approaches (score and rank level) in terms of recognition accuracy.

Moreover, it is experimentally observed that the particle swarm optimization based fusion approaches (at rank (Section 3.3) and at score (Section 4.3) levels) achieve faster convergence than the GA based fusion approaches (at rank (Section 3.2) and at score (Section 4.2) levels). This superiority of the PSO based fusion approaches over the GA based fusion approaches are established using two-sample Kolmogorov-Smirnov (K-S) test. Therefore, particle swarm optimization based score and rank level fusion approaches are adopted in all the subsequent chapters. It is additionally to be noted that particle swarm optimization based score level fusion approach (Section 4.3) converges faster than particle swarm optimization based rank level fusion approach (Section 3.3).

The reported results also show significant improvement in performances of the proposed optimization based fusion approaches (score and rank level) in spite of considering same weight to each input list. The performances of the proposed optimization based approaches at both rank (Chapter 3) and score (Chapter 4) levels of fusion can further be enhanced by incorporating the quality-derived weight for each modality. The initial success for the reported experiments is encouraging enough to try out quality-derived weights for particle swarm optimization based fusion approaches (score and rank level) in the context of multimodal biometrics. This direction of using quality-derived weights for the particle swarm optimization based fusion approaches (score and rank level) is explored in next chapter.

Chapter 5

Incorporating Quality in Optimization Based Fusion Approaches at Rank and Score Levels

Performance of a multimodal biometric system depends on the individual biometric modalities involved in fusion [1]. Performances of these biometric modalities may vary due to their intrinsic nature and the quality of acquired signal. For example, identification of a person in wild scenario may be a challenge [208, 209]. Hence, multimodal biometrics enhances the performance of a biometric system. It is to be noted that every biometric modality has been assigned an equal weight in the proposed works in Chapter 3 and Chapter 4. But ideally, a challenging biometric modality may not be assigned the same weight as of a good quality biometric modality. It is essential to estimate the significance of the considered biometric modality before performing the fusion. Higher significance of an individual biometric modality relates to better performance of that modality. Therefore, several researches [49, 54, 73, 110, 148] estimate this significance of each biometric modality and assign a weight for each of them. A high weight is assigned to a more significant biometric modality. Hence, the influence of more significant modality will be high on the multimodal biometric system.

Several approaches of weight estimation for a biometric modality are present in the literature [49, 54, 73, 105, 110, 128, 148]. These approaches for weight estimation are broadly classified into three categories: (i) matcher or classifier

performance-based [49, 148], (ii) optimization-based [105, 128], and (iii) quality-based [54, 73, 110]. A detailed review of existing weight estimation approaches is presented in Section 2.3. Matcher performance-based weight estimation approaches [49, 148] decide a weight of a modality based on its performance (in terms of equal error rate, i.e., EER). Optimization-based approaches [105, 128] use meta-heuristic optimization techniques to select the optimal set of weights for the concerned modalities. Assignment of a weight to a modality is a major characteristic of matcher performance-based and optimization-based weight estimation techniques. On the contrary, the quality-based weight estimation approaches assign weight to a modality depending on the quality of the presented signal. A poor signal quality for a modality will lead to a less weight for it. Therefore, weight for a modality will vary across probe users depending on their signal quality.

The quality estimation approaches are based on either the presented signal quality (e.g., illumination, lighting, occlusion, pixel count, dilation, off-angle, and blur) or the quality of biometric information (i.e., individuality) in the given signal. These quality estimation approaches are discussed in Section 2.3.3. An image can be of good quality but it may not contain the required biometric information to uniquely identify a person [1]. Therefore, the quality estimation approach based on biometric information is widely used [172, 173, 176]. The main drawback of these approaches is that these approaches are modality-dependent. For example, a quality estimation approach for fingerprint modality [173] can not be used to estimate the quality of any other biometric modality. Therefore, a modality-independent approach to estimate the quality of biometric information is required.

The proposed optimization based rank level and score level fusion approaches in Chapter 3 and Chapter 4 give equal importance (equal weight) to each modality. These optimization based approaches show superior performance than state-of-the-art rank level and score level fusion approaches. The success of these works encourages to improve the performance of optimization based rank level and score level fusion approaches by incorporating quality-derived weight for each biometric modality. In this work, unlike the existing weight estimation approaches for rank level and score level fusion, each biometric modality of a probe user is assigned a weight based on a modality-independent estimation of the quality of biometric information. Here, individuality of a probe user in terms of the acquired signal in a modality is estimated to assign weight for the modality. Therefore, weight for a modality may vary across the probe users. In this work, the quality is

estimated by assessing the ability to distinguish the best matching score of a probe with respect to a few next best matching scores. The estimated quality derives weight in the formulation of the optimization problems. Then, particle swarm optimization based rank level and score level fusion approaches are applied to solve the stated optimization problems.

The remainder of this chapter is organized as following: The formulation of each of the rank level and the score level fusion of multimodal biometrics as an optimization problem is revisited in Section 5.1. The proposed approach for biometric quality-derived weight estimation is presented in Section 5.2. The quality-incorporated particle swarm optimization based rank level and score level fusion approaches are presented in Section 5.3. Performance of the proposed quality-incorporated rank level and score level fusion approaches are discussed in Section 5.4. Finally, the concluding remarks are drawn in Section 5.5.

5.1 Multimodal Fusion as an Optimization Problem

In the earlier works on rank level and score level fusion (Chapter 3 and Chapter 4, respectively), the fusions of multimodal biometrics at rank and at score levels have been conceptualized as optimization problems. The problem formulations for rank level fusion (Chapter 3) and score level fusion (Chapter 4) are briefly revisited in the following subsections.

5.1.1 Rank Level Fusion as an Optimization Problem

Let $L_1, L_2, ..., L_N$ be rank-ordered lists of subjects corresponding to N number of biometric modalities for identifying a person. In Section 3.1, the problem of obtaining an aggregated rank-ordered list of subjects has been formulated as an optimization problem. The objective function for this optimization problem minimizes a weighted summation of distances of the input lists $L_1, L_2, ..., L_N$ from the aggregated list. The objective function (which has been stated earlier in Eq. 3.2) is repeated here for the sake of completeness of this chapter:

$$minimize \ \phi(\delta) = \sum_{i=1}^{N} w_i \times d(\delta, L_i)$$
 (5.1)

Here, a candidate fused list is represented by δ . A weight w_i is associated with each of the N biometric modalities. Here, the weight represents the significance of the corresponding biometric modality. In the earlier approaches of rank level fusion (Chapter 3), the significance of each modality is considered as equal. The distance $d(\delta, L_i)$ is a distance between a candidate fused list δ and input list L_i . The weighted Spearman footrule distance [180] is used to estimate the distance between these two lists. The estimation of the said distance for two such lists is given in Eq. 3.3. The influence factor as weight in the weighted Spearman footrule distance is estimated using Eq. 3.4.

Here, it should be noted that the weight being used for weighted Spearman footrule distance metric [180] is different from the weight w_i being used in Eq. 5.1. The weight in the weighted Spearman footrule distance metric is used for the purpose of considering more influence of subjects at better positions in the rank list (Eq. 3.3). It is emphasised that w_i is the weight (significance) for the i^{th} biometric modality for a probe user.

5.1.2 Score Level Fusion as an Optimization Problem

Similarly, let \hat{S}_1 , \hat{S}_2 , ..., \hat{S}_N be normalized score lists corresponding to N number of biometric modalities for identifying a person. Min-max normalization (Eq. 2.1) of the matching scores are used for score normalization throughout this thesis. Fusion of these normalized score lists has been formulated as an optimization problem in Section 4.1. The objective of this optimization problem is to obtain a fused score list having minimum weighted summation of distances of the input normalized score lists \hat{S}_1 , \hat{S}_2 , ..., \hat{S}_N from the fused list. As a result, the objective function for generating the aggregated score list is:

minimize
$$\phi(\delta) = \sum_{i=1}^{N} w_i \times d(\delta, \hat{S}_i)$$
 (5.2)

Here, a candidate fused score list is represented by δ . A weight w_i is associated with each of the N biometric modalities. Here, the weight represents the significance of the corresponding biometric modality. In PSO based score level fusion approach (Chapter 4), the significance of each modality is considered as equal. The function $d(\delta, \hat{S}_i)$ denotes distance between a candidate fused score list δ and a normalized input score list \hat{S}_i . A weighted Spearman footrule distance [180] is used to measure the above said distance. The estimation of the weighted Spearman footrule distance is presented in Eq. 4.4. The influence factor of an enrolled

subject as a weight in the estimation of weighted Spearman footrule distance is determined using Eq. 4.5.

Here, it should be noted that the weight being used for weighted Spearman footrule distance metric [180] is different from the weight w_i being used in Eq. 5.2. The weight in the weighted Spearman footrule distance metric is used for the purpose of considering more influence of subjects having better matching scores in the score list (Eq. 4.4). It is emphasised that w_i is the weight (significance) for the i^{th} biometric modality for a probe user.

It can be seen in Eq. 5.1 and Eq. 5.2 that a weight w_i is associated with each biometric modality. The weight w_i represents the significance of the corresponding modality. In the earlier works in Chapter 3 and Chapter 4, the same weight value 1 is assigned to every modality. These methods will deliver good results if the captured biometric signals are of equally good quality across all the modalities. In contrast to assigning equal weight to each modality, the work in this chapter estimates the weight for each modality of a probe user based on a novel approach of estimating the quality of biometric information (individuality) in the probe signal. The weights in Eq. 5.1 and Eq. 5.2 are derived from the estimated qualities. The proposed approach for estimating the quality of biometric information (individuality) is presented in next section.

5.2 Proposed Approach for Estimating Quality of Biometric Information in a Probe Signal

In this section, a novel approach is proposed for estimating the quality of biometric information in a probe signal. At first, the philosophy behind the proposed approach is discussed as following: A good quality probe signal distinguishes between the highest matching score and the average of next few matching scores in the sorted order. This difference is used to estimate the quality of biometric information (individuality) in a probe signal. However, this difference between the highest matching score and the average of the next few matching scores in the sorted order is small for a poor quality probe signal. In this case, no subject stands out distinctly based on the matching scores.

The estimated quality q_i of biometric information (individuality) in a probe signal is used to derive the weight w_i in Eq. 5.1 and Eq. 5.2. Here, the quality q_i of biometric information in the probe signal for each modality i is estimated

using the normalized similarity scores between probe and gallery. Max-min normalization (Eq. 2.1) is used in this work for score normalization. The quality q_i of biometric information for a biometric modality i is estimated by taking the difference between the maximum normalized similarity score $max_1(\hat{S}_i)$ and the average of the next h normalized similarity scores in sorted order. Here, it is assumed that the value of h is very less than n-1, i.e., h < n-1. The number of enrolled users is denoted by n. The above difference is, then, normalized by the difference between the maximum normalized similarity score $max_1(\hat{S}_i)$ and the average of all other normalized similarity scores in the list \hat{S}_i (excluding the maximum normalized similarity score $max_1(\hat{S}_i)$). Therefore, the proposed quality of biometric information (individuality) in the probe signal of i^{th} modality is estimated using Eq. 5.3.

$$q_{i} = \frac{\max_{1}(\hat{S}_{i}) - \frac{1}{h} \sum_{l=2}^{h+1} \max_{l}(\hat{S}_{i})}{\max_{1}(\hat{S}_{i}) - \frac{1}{n-1} \sum_{l=2}^{n} \max_{l}(\hat{S}_{i})}$$
(5.3)

Here, the maximum normalized similarity score in the normalized score list \hat{S}_i for i^{th} modality is represented as $max_1(\hat{S}_i)$. The l^{th} maximum normalized similarity score in sorted order at the normalized score list \hat{S}_i for the i^{th} modality is denoted as $max_l(\hat{S}_i)$.

The proposed estimation of biometric quality (Eq. 5.3) considers a list of normalized similarity scores. If the biometric matcher generates dissimilarity scores, then these normalized dissimilarity scores are subtracted from 1 to convert them into normalized similarity scores.

Finally, the weight w_i for each biometric modality is decided using the estimated qualities as following:

$$w_i = \frac{q_i}{\sum_{i=1}^{N} q_i} \tag{5.4}$$

This ensures that the summation of weights across modalities is 1. N indicates number of biometric modalities in Eq. 5.4.

It is to be noted that the proposed estimation of quality of biometric information (individuality) in a probe signal uses the normalized matching scores. Unlike [172, 173, 176], the proposed approach dose not depend on any modality. Hence, it is a modality-independent approach for quality estimation.

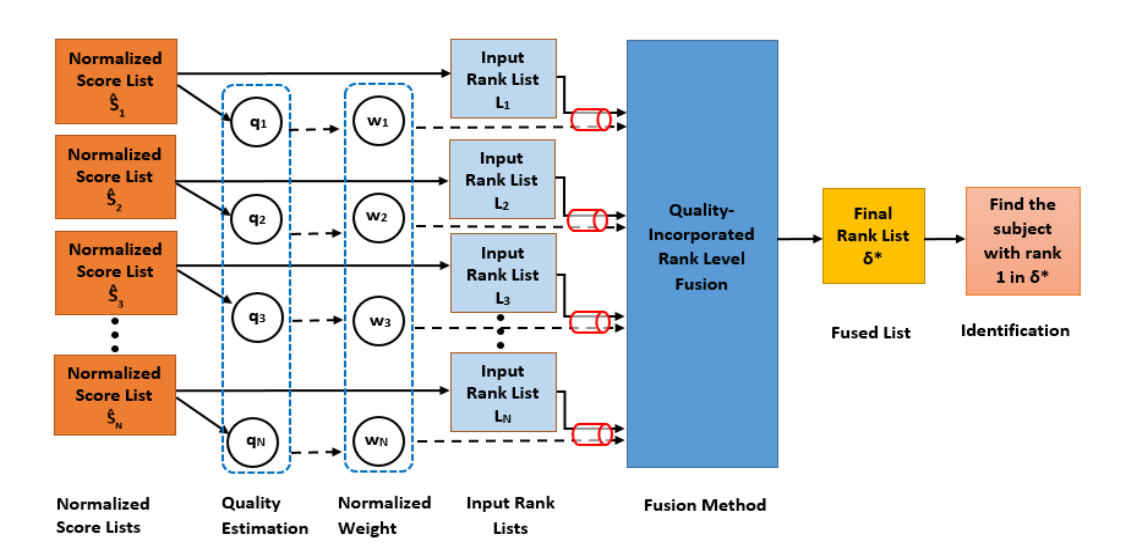


Figure 5.1: Quality-incorporated fusion of multimodal biometrics at rank level

5.3 Proposed Quality-Incorporated Particle Swarm Optimization Based Fusion Approaches

The previous work on particle swarm optimization based fusion approaches for rank level (Section 3.3) and score level (Section 4.3) have considered equal weight (significance) for each biometric modality. On the contrary, novel quality-incorporated particle swarm optimization based fusion approaches are presented in this section as solution to the stated optimization problems (Eq. 5.1 and Eq. 5.2) of rank level and score level fusion.

5.3.1 Proposed Quality-Incorporated Particle Swarm Optimization Based Rank Level Fusion Approach

In this work, a quality-derived weight is adopted to assign significance to each biometric modality of a probe user. A schematic diagram of the quality-incorporated optimization based rank level fusion is given in Fig. 5.1. The rest of the proposed approach is same as the PSO based rank level fusion approach in Section 3.3. Representation of a particle position, initialization of a population, exploration of other candidate solutions and stopping criteria in the proposed quality-

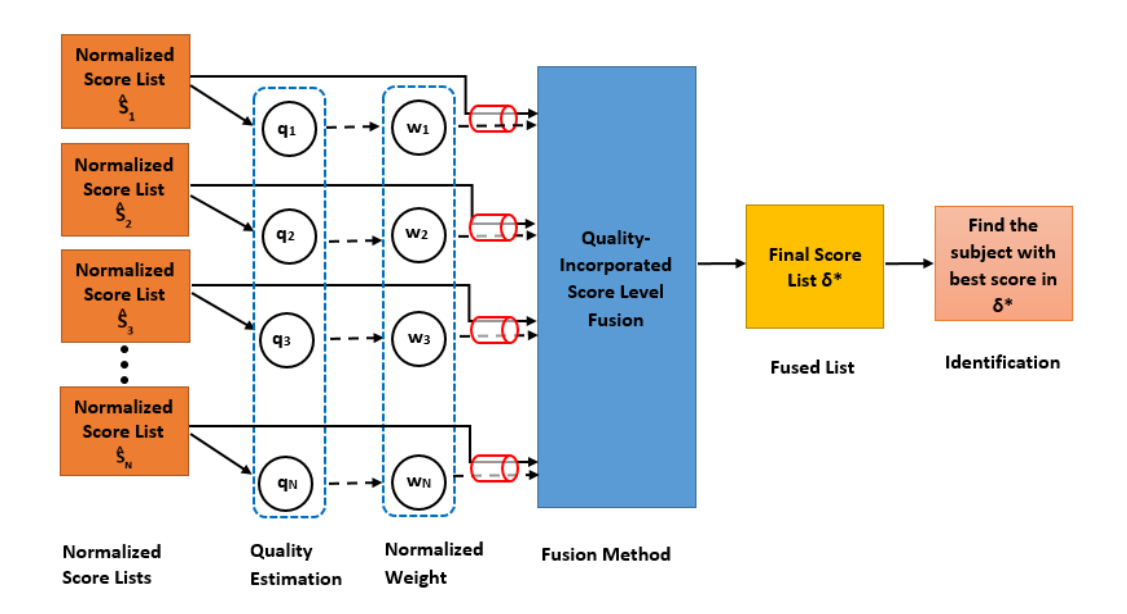


Figure 5.2: Quality-incorporated fusion of multimodal biometrics at score level

incorporated PSO based approach are maintained as exactly same as the previous PSO based rank level fusion approach in Section 3.3.

5.3.2 Proposed Quality-Incorporated Particle Swarm Optimization Based Score Level Fusion Approach

Similar to rank level fusion, in score level fusion too, a quality-derived weight is adopted to assign significance to each biometric modality of a probe user. A schematic diagram of the quality-incorporated optimization based score level fusion is given in Fig. 5.2. The rest of the proposed approach is same as the PSO based score level fusion approach in Section 4.3. Representation of a particle position, initialization of a population, exploration of other candidate solutions and stopping criteria in the proposed quality-incorporated PSO based approach are maintained as exactly same as the previous PSO based score level fusion approach in Section 4.3.

5.4 Performance Evaluation and Discussion

Detailed performance analysis is carried out for the proposed quality-incorporated particle swarm optimization based approaches for rank level and for score level fusion of multimodal biometrics. Experimental studies on the performances of the proposed approaches are reported using four multimodal biometric datasets. The first two datasets are virtually created multimodal biometric datasets involving face and iris biometrics. In the first virtual dataset, the cross-age LFW (CALFW) database [210] and IIT Delhi iris database (version 1.0) [211] are combined to create a multimodal biometric dataset. This dataset is referred as FaceIris-V1 in subsequent portions of the thesis. Similarly, in the second virtual dataset, the CelebFaces Attributes Dataset (CelebA) [212] and IIT Delhi iris database (version 1.0) [211] are combined to create a multimodal biometric dataset. This dataset is referred as FaceIris-V2 in subsequent portions of the thesis. The remaining two datasets are NIST BSSR1 multimodal dataset (set 1) [193] involving face and fingerprint modalities and OU-ISIR BSS4 multi-algorithm gait dataset [2, 194] involving multiple feature extraction methods of gait biometrics.

Performance of the proposed quality-derived weight estimation approach is also evaluated with two different weight estimation techniques in [49] and [51]. Additionally, the performance of the proposed quality-derived weight estimation approach is also compared with that of the equal weight approach (i.e., each modality is assigned equal weight). Moreover, supremacy of the proposed quality-incorporated particle swarm optimization based rank level and score level fusion approaches with respect to existing fusion schemes at rank and score levels are experimentally exhibited. The above analysis using each of the above four datasets is presented in following subsections.

5.4.1 Fusion of Multimodal Biometrics Involving Face and Iris (Virtual Multimodal Dataset FaceIris-V1)

Description of the Dataset: Performances of the proposed approaches are evaluated on virtually created dataset involving face and iris modalities. The first virtually created dataset (FaceIris-V1) contains face images from the crossage LFW (CALFW) database [210] and iris images from IIT Delhi iris database (version 1.0) [211]. The CALFW dataset contains 3000 positive face pairs and 3000 negative face pairs. Two faces in a positive face pair belong to the same person, but there is an age gap between two such faces. The age gaps in a positive

pair increase intra-class variation in the dataset. This intra-class variation due to cross-age makes the dataset more challenging for the face recognition task. A negative face pair contains faces from two different persons. The CALFW dataset is widely used in face recognition methods [213, 214]. The iris dataset [211] is compiled by the research group at IIT Delhi. It contains left and right iris images from 224 unique subjects. For experiments, left and right iris images are considered from different subjects. As right iris images are missing for 13 subjects, 435 (i.e., $224 \times 2 - 13$) subjects are considered for the experiments. Each subject (treating left iris and right iris images as separate subjects) has 5 iris images. Hence, there are 2175 (i.e., 435×5) images in this dataset. Since only 435subjects are considered from IIT Delhi iris database [211], unique 435 subjects are randomly selected from the CALFW database [210] to create the virtual multimodal biometric dataset (FaceIris-V1). One-to-one correspondence between the subjects in these two databases is assumed for the created virtual dataset. For experiments in this work the 435 face image pairs selected from CALFW dataset [210] are divided into gallery and probe sets. Both the gallery and the probe set contains 435 image corresponding to 435 different classes. For IIT Delhi iris database, one image out of 5 images is selected randomly as probe for a given class. Therefore, 435 images are there in probe set. Remaining 1740 images are part of gallery set.

Generating Score and Rank Lists for Face: State-of-the-art face embedding approach ArcFace [215] is used in this work to compute the embedding for the face biometrics. Detailed description of ArcFace can be found in [215]. The cosine similarity [216] between two embeddings for the probe and the gallery produces a matching score. The cosine similarity is widely used similarity metric in the face recognition paradigm [217, 218, 219]. A score list is generated using the matching scores for all the enrolled users with respect to the probe. Finally, these similarity scores are sorted in descending order to generate a rank list for the face modality.

Generating Score and Rank Lists for Iris: A state-of-the-art iris recognition system in [220] is adopted for generating the matching scores for iris. The work in [220] is based on fully convolutional network (FCN). The FCN helps in generating spatially corresponding iris feature descriptors. Furthermore, an extended triplet loss (ETL) function accurately differentiates between an iris region and a non-iris region to achieve enhanced iris feature descriptors. These iris features are then binarized. Hamming distance [221] generates the matching score between the binarized iris features of the probe and the gallery. The gallery set

contains four images per class. Therefore, the binarized iris feature of a probe is matched with all the four binarized iris features of a gallery class. The binarized iris feature giving minimum distance with the probe is considered as its matching score. Similarly, the matching scores for all the probes in probe set is generated. Detailed description of the adopted iris recognition approach can be found in [220]. A score list is generated using the matching scores for all the enrolled users with respect to the probe. Finally, a rank list is generated using the ascending order of the matching scores for all the enrolled users with respect to the probe.

Performance Analysis of Rank Level and Score Level Fusion: The first virtual multimodal dataset FaceIris-V1 provides two score lists and two rank lists as above. These rank lists are combined using the proposed quality-incorporated particle swarm optimization based rank level fusion approach (Q-PSO Rank) (Section 5.3.1) and other existing rank level fusion approaches as discussed in Section 3.2.2.1. The window size on number of iteration to decide the convergence of the proposed quality-incorporated particle swarm optimization based rank level fusion approach (Q-PSO Rank) is experimentally decided as 800 for virtual multimodal dataset FaceIris-V1.

The two score lists are normalized using min-max normalization (Eq. 2.1). It is to be noted that the generated score for face modality is a similarity score. On the contrary, the generated score for iris modality is a dissimilarity score. Hence, the normalized scores for iris modality are converted to similarity score by subtracting the normalized scores from 1. These normalized similarity score lists are then combined using the proposed quality-incorporated particle swarm optimization based score level fusion approach (Q-PSO Score) (Section 5.3.2) and other existing score level fusion approaches as discussed in Section 3.2.2.1. The window size on number of iteration to decide the convergence of the proposed quality-incorporated particle swarm optimization based score level fusion approach (Q-PSO Score) is experimentally decided as 600 for virtual multimodal dataset FaceIris-V1.

At first, an experiment is performed to observe the impact of the value of h (in Eq. 5.3) for the proposed quality-based weight estimation approach (Section 5.2). For this experiment, the value of the integer h is varied from 1 to 10 to estimate the weights for the two modalities based on their normalized matching scores. These estimated weights are passed to each one of the comparing weighted rank level and score level fusion approaches. Corresponding recognition accuracies are reported in Table 5.1 by considering the top-most ranked subject. It is observed from this table that the highest recognition accuracy is achieved for the value of h

Table 5.1: Performance on FaceIris-V1 dataset: Recognition accuracies (in %) for comparing weighted score and rank level fusion approaches using the proposed quality-derived weight estimation approach with different values of h (in Eq. 5.3)

M	ethods	h = 1	h = 2	h = 3	h = 4	h = 5	h = 6	h = 7	h = 8	h = 9	h = 10
	Weighted Sum [51]	97.70	97.70	97.70	97.70	97.70	96.55	96.09	95.86	95.86	95.86
	WQAM cos [62]	97.70	97.47	97.01	96.55	96.55	96.55	96.32	96.09	95.86	95.86
	WQAM cos^r [62]	98.16	97.70	97.70	97.47	97.47	97.24	97.24	97.01	97.01	96.55
	WQAM tan [62]	98.16	97.70	97.70	97.70	97.47	97.47	97.24	97.01	97.01	96.78
Score Level Fusion	WQAM sin [62]	96.55	95.86	95.63	95.63	95.63	95.40	95.40	95.40	95.40	95.17
Beore Level Fusion	WQAM $r^{1/s}$ [62]	98.16	97.70	97.47	97.47	97.47	97.47	97.01	96.78	96.78	96.55
	WQAM r^s [62]	97.93	97.70	97.47	97.24	96.32	96.32	96.32	96.32	96.09	96.09
	WQAM s^r [62]	97.70	97.70	97.24	96.78	96.55	96.55	96.55	96.09	95.86	95.63
	WQAM log [62]	97.70	97.70	97.24	96.78	96.55	96.55	96.55	96.09	95.86	95.63
	WQAM exp [62]	97.70	97.70	97.70	96.78	96.55	96.55	96.32	96.09	96.09	95.86
	Proposed Q-PSO Score	98.62	98.16	98.16	98.16	97.70	97.47	97.24	97.01	96.55	96.55
	WBorda [34]	95.63	94.94	94.25	94.25	94.48	94.25	94.25	94.02	94.02	94.02
	Exp [33]	94.48	93.79	93.56	93.56	93.56	93.56	93.56	93.33	93.10	93.10
Rank Level Fusion	WExp [33]	91.03	91.03	91.03	91.03	91.03	91.03	91.03	91.03	91.03	90.80
ltank Level Fusion	DivExp [32]	93.33	92.87	92.41	92.18	92.41	92.64	92.64	92.87	92.64	92.41
	Log [32]	96.78	96.78	96.32	96.32	96.32	96.32	96.32	96.32	96.32	96.32
	Proposed Q-PSO Rank	98.16	98.16	97.70	97.47	97.47	97.24	97.01	96.55	96.55	96.55

as 1 in each weighted fusion approach on this dataset. The recognition accuracies monotonically decrease with increase of h for the proposed quality-incorporated PSO based fusion approaches (rank level and score level) and majority of the existing approaches (except for the division exponential approach [32]). It can also be noted that the highest recognition accuracies for few of the approaches are observed for multiple values of h. For example, weighted sum approach [51] achieves the highest recognition accuracy (97.70%) for the values of h in between 1 to 5. Similar observations can be made for few other approaches as well. Finally, the value of h is selected as 1 for weight estimation and further experimental analysis.

The efficacy of the proposed quality-based weight estimation approach (Section 5.2) is presented in Table 5.2 over an equal weight based approach and few other existing weight estimation approaches in [49] and [51]. The estimated weights using the above mentioned approaches are used for state-of-the-art weighted score and rank level fusion approaches along with the proposed quality-incorporated PSO based fusion approaches for rank level (Q-PSO Rank) and score level (Q-PSO Score). It is observed from Table 5.2 that the performances of state-of-the-art weighted score and rank level fusion approaches and the pro-

Table 5.2: Performance comparison of existing weight estimation approaches for weighted score and rank level fusion approaches on FaceIris-V1

Fusias	n Methods		Weight Estimat	ion Approaches	
Fusion	i Methods	Equal Weights	Approach in [49]	Approach in [51]	Quality Based
	Weighted Sum [51]	94.25	94.25	94.25	97.70
	WQAM cos [62]	94.25	94.48	94.48	97.70
	WQAM cos^r [62]	94.71	95.63	95.63	98.16
	WQAM tan [62]	95.40	94.71	88.51	98.16
Score Level Fusion	WQAM sin [62]	94.02	94.02	94.02	96.55
Score Level Fusion	WQAM $r^{1/s}$ [62]	94.25	95.40	94.94	98.16
	WQAM r^s [62]	94.25	94.48	94.48	97.93
	WQAM s^r [62]	94.25	94.48	94.48	97.70
	WQAM log [62]	94.25	94.48	94.48	97.70
	WQAM exp [62]	94.25	94.48	94.48	97.70
	Proposed Q-PSO Score	95.40	95.86	95.63	98.62
	WBorda [34]	92.18	92.18	92.18	95.63
	Exp [33]	90.80	90.80	91.03	94.48
Rank Level Fusion	WExp [33]	90.80	90.80	90.80	91.03
Italik Level Fusion	DivExp [32]	92.87	92.87	92.87	93.33
	Log [32]	94.71	94.71	94.94	96.78
	Proposed Q-PSO Rank	94.94	95.63	95.17	98.16

posed Q-PSO Rank and Q-PSO Score fusion approaches significantly improve by incorporating the proposed quality-based weights (Section 5.2). It can also be observed that the proposed quality-incorporated PSO based fusion approaches achieve superior performances than majority of state-of-the-art weighted fusion approaches even after incorporating the proposed quality-based weights. Only few of the WQAM based approaches [62] perform as equal as the proposed Q-PSO based rank level fusion approach (as underlined in Table 5.2). Moreover, the proposed Q-PSO based score level fusion approach outperforms the proposed Q-PSO based rank level fusion approach.

Furthermore, the recognition accuracy (in %) using the top-most ranked subject in each of the non-weighted rank and score level fusion approaches is compared with that of the proposed Q-PSO based fusion approaches (rank level and score level) in Table 5.3. The reported results establish the superiority of the proposed Q-PSO based fusion approaches over state-of-the-art non-weighted score and rank level fusion approaches.

The changes in recognition accuracies (in %) with the changes in cumulative ranks are presented using cumulative match characteristic (CMC) curves in Fig. 5.3 and Fig. 5.4. The proposed Q-PSO based fusion approaches outperforms existing rank and score level fusion approaches, as it can be observed in the CMC curves in Fig. 5.3 and Fig. 5.4.

Table 5.3: Performance comparison of the existing non-weighted rank and score level fusion approaches with the proposed Q-PSO based fusion approaches on virtual multimodal dataset FaceIris-V1

M	ethods	Recognition Accuracy in %
	Max Rule [1]	91.49
	Min Rule [1]	93.79
	Product [1]	94.02
Score Level Fusion	Sum-OEBA [67]	91.26
Score Level Pusion	Sum-MOEBA [67]	93.79
	Sum-OEVBA [82]	94.48
	Hamacher t-norm [69]	94.02
	Frank t-norm [69]	94.02
	Proposed Q-PSO Score	98.62
	Borda Count [34]	92.18
Rank Level Fusion	Highest Rank [35]	91.49
	Proposed Q-PSO Rank	98.16

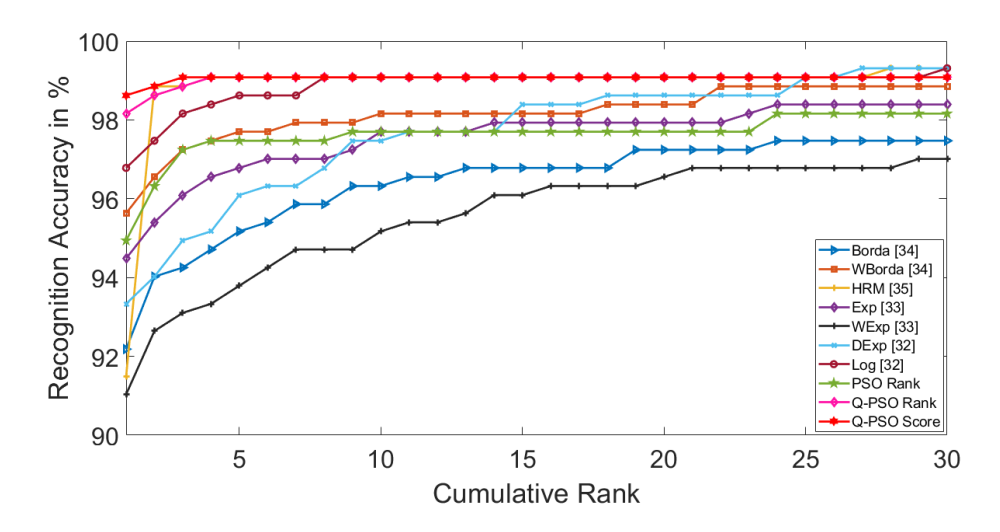


Figure 5.3: CMC plots for existing rank level fusion approaches being compared with that of the proposed Q-PSO based fusion approaches for first virtual multimodal biometric dataset FaceIris-V1

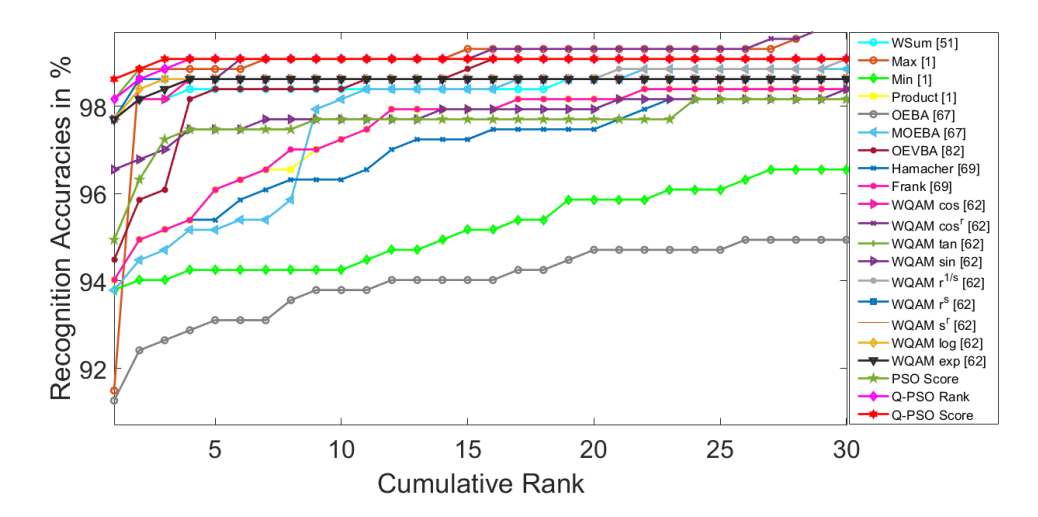


Figure 5.4: CMC plots for existing score level fusion approaches being compared with that of the proposed Q-PSO based fusion approaches for first virtual multimodal biometric dataset FaceIris-V1

5.4.2 Fusion of Multimodal Biometrics Involving Face and Iris (Virtual Multimodal Dataset FaceIris-V2)

Description of the Dataset: The second virtual multimodal biometric dataset (FaceIris-V2) is created by combining the face biometrics from CelebFaces attributes dataset (CelebA) [212] and iris biometrics from IIT Delhi iris database (version 1.0) [211]. The CelebA dataset contains 202599 celebrity images with varying face attributes for 10177 unique subjects. The CelebA dataset is one of the most used dataset for evaluating the performance of face recognition systems [222, 223]. A short description of the IIT Delhi iris database (version 1.0) [211] is presented in Section 5.4.1. Similar to the earlier virtual dataset (FaceIris-V1), face images for only 435 unique subjects are randomly selected from CelebA dataset [212] corresponding to 435 subjects in IIT Delhi iris database [211] (considering left iris and right iris as separate subjects). The selected images from CelebA face dataset [212] containing 435 classes are divided into training (gallery) and test (probe) set. The gallery set contains 9565 face images. The cosine similarity between a probe face embedding and all face embeddings of a class in gallery set is computed. The face embedding in gallery producing maximum cosine similarity is considered as the matching score between the probe and a gallery pair. Similarly, the matching scores for all the probes in probe set is generated. The computation of matching scores for iris modality is same as in Section 5.4.1. The score lists and rank lists for virtual multimodal biometric dataset (FaceIris-V2) are constructed using the same approaches (for face and for iris) as discussed in Section 5.4.1.

Performance Analysis of Rank Level and Score Level Fusion: The second virtual multimodal dataset FaceIris-V2 provides two score lists and two rank lists as above. These rank lists are combined using the proposed quality-incorporated particle swarm optimization based rank level fusion approach (Q-PSO Rank) (Section 5.3.1) and other existing rank level fusion approaches as discussed in Section 3.2.2.1. The window size on number of iteration to decide the convergence of the proposed quality-incorporated particle swarm optimization based rank level fusion approach (Q-PSO Rank) is experimentally decided as 2000 for virtual multimodal dataset FaceIris-V2.

The two score lists are normalized using min-max normalization (Eq. 2.1). Similar to the virtual multimodal dataset FaceIris-V1, the normalized dissimilarity scores for iris modality are converted to similarity score by subtracting the normalized scores from 1. These normalized similarity score lists are then combined using the proposed quality-incorporated particle swarm optimization based score level fusion approach (Q-PSO Score) (Section 5.3.2) and other existing score level fusion approaches as discussed in Section 3.2.2.1. The window size on number of iteration to decide the convergence of the proposed quality-incorporated particle swarm optimization based score level fusion approach (Q-PSO Score) is experimentally decided as 600 for virtual multimodal dataset FaceIris-V2.

Similar to the experiment in Section 5.4.1, an experiment is performed to observe the impact of the value of h (in Eq. 5.3) for the proposed quality-based weight estimation approach (Section 5.2) on virtual multimodal biometric dataset FaceIris-V2. For this experiment, the value of the integer h is also varied from 1 to 10 to estimate the weights for the two modalities based on their normalized matching scores. These estimated weights are used in each one of the comparing weighted rank level and score level fusion approaches. Corresponding recognition accuracies are reported in Table 5.4. It is observed from this table that the highest recognition accuracy is achieved for the value of h as 1 in each weighted fusion approach on this dataset too. The recognition accuracies monotonically decrease with increase of h for the proposed Q-PSO based fusion approaches (rank level and score level) and majority of the existing approaches (except for the weighted exponential [33] and the division exponential [32] approaches). It can also be noted that the highest recognition accuracies for few of these approaches

Table 5.4: Performance on FaceIris-V2 dataset: Recognition accuracies (in %) for comparing weighted score and rank level fusion approaches using the proposed quality-derived weight estimation approach with different values of h

M	ethods	h = 1	h = 2	h = 3	h = 4	h = 5	h = 6	h = 7	h = 8	h = 9	h = 10
	Weighted Sum [51]	98.16	97.70	97.70	97.47	97.47	97.24	97.24	97.24	97.24	97.24
	WQAM cos [62]	98.16	98.16	97.70	97.70	97.70	97.24	97.24	97.24	97.24	97.24
	WQAM cos^r [62]	98.85	98.62	98.39	98.39	98.39	98.39	97.70	97.70	97.70	97.70
	WQAM tan [62]	99.31	99.31	99.08	98.85	98.85	98.85	98.85	98.39	98.39	98.16
Score Level Fusion	WQAM sin [62]	97.24	96.78	96.55	96.32	95.86	95.63	95.63	95.63	95.63	95.63
Score Level Fusion	WQAM $r^{1/s}$ [62]	98.85	98.85	98.62	98.39	98.16	98.16	98.16	97.93	97.93	97.70
	WQAM r^s [62]	98.39	98.16	97.70	97.70	97.70	97.70	97.70	97.24	97.24	97.24
	WQAM s^r [62]	98.16	98.16	97.70	97.70	97.70	97.70	97.47	97.24	97.24	97.24
	WQAM log [62]	98.16	98.16	97.70	97.70	97.70	97.70	97.47	97.24	97.24	97.24
	WQAM exp [62]	98.16	98.16	97.70	97.70	97.70	97.70	97.47	97.47	97.24	97.24
	Proposed Q-PSO Score	99.31	99.31	99.31	99.31	99.08	98.85	98.85	98.85	98.85	98.62
	WBorda [34]	94.94	94.25	94.25	93.79	93.79	93.79	93.79	93.79	93.79	93.79
	Exp [33]	94.48	94.02	93.79	93.79	93.56	93.56	93.33	93.33	93.10	93.10
Rank Level Fusion	WExp [33]	91.03	91.03	91.03	91.03	91.03	91.03	91.03	91.03	91.03	91.03
Leank Devel Fusion	DivExp [32]	94.02	93.56	93.56	93.56	93.33	93.33	93.33	93.56	93.56	93.79
	Log [32]	94.94	94.94	94.94	94.94	94.94	94.94	94.94	94.94	94.71	94.48
	Proposed Q-PSO Rank	99.31	99.08	98.85	98.62	98.62	98.39	98.39	98.39	98.39	98.39

are observed for multiple values of h. For example, WQAM cos approach [62] achieves the highest recognition accuracy (98.16%) for the value of h as 1 and 2. Similar observations can be made for few other approaches as well. Finally, the value of h is selected as 1 for weight estimation and further experimental analysis.

The efficacy of the proposed quality-based weight estimation approach (Section 5.2) is presented in Table 5.5 over an equal weight based approach and few other existing weight estimation approaches in [49] and [51]. The estimated weights using the above mentioned approaches are used for state-of-the-art weighted score and rank level fusion approaches along with the proposed quality-incorporated PSO based fusion approaches for rank level (Q-PSO Rank) and score level (Q-PSO Score). It is observed from Table 5.5 that the performances of state-of-the-art weighted score and rank level fusion approaches and the proposed Q-PSO Rank and Q-PSO Score fusion approaches significantly improve by incorporating the proposed quality-based weights (Section 5.2). It can also be observed that the proposed quality-incorporated PSO based fusion approaches for rank level (Q-PSO Rank) and score level (Q-PSO Score) achieve superior performances than majority of state-of-the-art weighted fusion approaches even after incorporating the proposed quality-based weights. Only the WQAM tan based

Table 5.5: Performance comparison of existing weight estimation approaches for weighted score and rank level fusion approaches on FaceIris-V2

Fusia	n Methods		Weight Estimat	ion Approaches	
Fusion	n Methods	Equal Weights	Approach in [49]	Approach in [51]	Quality Based
	Weighted Sum [51]	94.71	94.71	94.71	98.16
	WQAM cos [62]	95.17	94.71	94.71	98.16
	WQAM cos^r [62]	95.40	94.02	94.94	98.85
	WQAM tan [62]	95.86	93.79	89.20	99.31
Score Level Fusion	WQAM sin [62]	94.94	94.48	94.71	97.24
Score Level Fusion	WQAM $r^{1/s}$ [62]	95.40	93.79	94.94	98.85
	WQAM r^s [62]	95.17	94.48	94.71	98.39
	WQAM s^r [62]	95.17	94.48	94.71	98.16
	WQAM log [62]	95.17	94.48	94.71	98.16
	WQAM exp [62]	95.17	94.71	94.71	98.16
	Proposed Q-PSO Score	96.32	95.17	94.94	99.31
	WBorda [34]	91.49	92.18	91.26	94.94
	Exp [33]	91.03	91.03	91.03	94.48
Rank Level Fusion	WExp [33]	91.03	91.03	91.03	91.03
italik Level Fusion	DivExp [32]	93.56	92.18	93.56	94.02
	Log [32]	94.02	94.25	93.56	94.94
	Proposed Q-PSO Rank	96.09	94.94	94.02	99.31

approach [62] performs as equal as the proposed Q-PSO based fusion approaches (as underlined in Table 5.5).

Furthermore, the recognition accuracy (in %) using the top-most ranked subject in each of the non-weighted rank and score level fusion approaches is compared with that of the proposed Q-PSO based fusion approaches (rank level and score level) in Table 5.6. The reported results establish the superiority of the proposed Q-PSO based fusion approaches over state-of-the-art non-weighted score and rank level fusion approaches.

The changes in recognition accuracies (in %) with the changes in cumulative ranks are presented using cumulative match characteristic (CMC) curves in Fig. 5.5 and Fig. 5.6. The proposed quality-incorporated PSO based fusion approaches for rank level (Q-PSO Rank) and score level (Q-PSO Score) outperform majority of the existing rank and score level fusion approaches, as it can be observed in the CMC curves in Fig. 5.5 and Fig. 5.6.

Table 5.6: Performance comparison of existing non-weighted rank and score level fusion approaches with the proposed Q-PSO based fusion approaches on virtual multimodal biometric dataset FaceIris-V2

M	ethods	Recognition Accuracy in %
	Max Rule [1]	93.10
	Min Rule [1]	94.48
	Product [1]	95.17
Score Level Fusion	Sum-OEBA [67]	93.79
Score Level Fusion	Sum-MOEBA [67]	94.71
	Sum-OEVBA [82]	94.71
	Hamacher t-norm [69]	95.17
	Frank t-norm [69]	95.17
	Proposed Q-PSO Score	99.31
	Borda Count [34]	91.49
Rank Level Fusion	Highest Rank [35]	93.10
	Proposed Q-PSO Rank	99.31

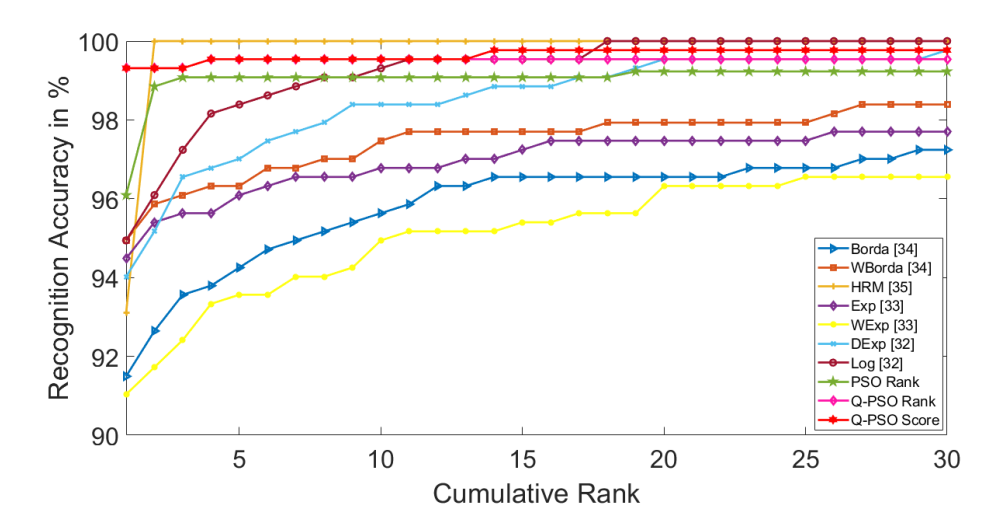


Figure 5.5: CMC plots for existing rank level fusion approaches being compared with that of the proposed Q-PSO based fusion approaches for second virtual multimodal biometric dataset FaceIris-V2

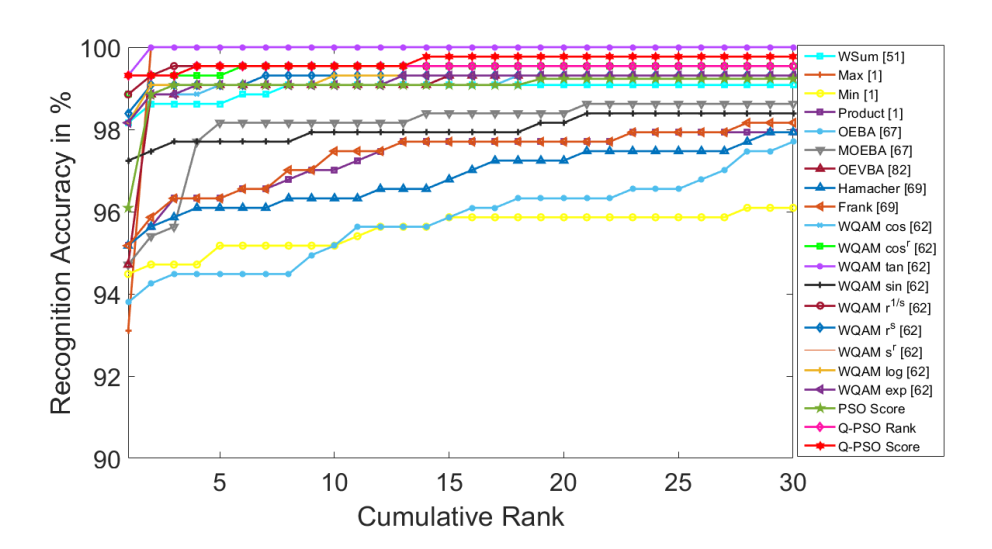


Figure 5.6: CMC plots for existing score level fusion approaches being compared with that of the proposed Q-PSO based fusion approaches for second virtual multimodal biometric dataset FaceIris-V2

5.4.3 Fusion of Multimodal Biometrics Involving Face and Fingerprint (NIST BSSR1 Multimodal Dataset (Set 1))

The performances of the proposed quality-incorporated PSO based fusion approaches for rank level (Q-PSO Rank) and score level (Q-PSO Score) are also evaluated on NIST BSSR1 multimodal dataset (set 1) [193]. This dataset contains four modalities. Hence, four score lists and four rank lists are obtained. A brief description of this dataset can be found in Section 3.2.2.2. The window size on number of iteration to decide the convergence of the proposed qualityincorporated particle swarm optimization based rank (Q-PSO Rank) and score (Q-PSO Score) level fusion approach are experimentally decided as 600 for this dataset. Similar to the experiments on above two virtual datasets, an experiment is performed to observe the impact of the value of h (in Eq. 5.3) for the proposed quality-based weight estimation approach (Section 5.2). For this experiment, the value of the integer h is varied from 1 to 10 to estimate the weights for the four modalities based on their normalized matching scores. Corresponding recognition accuracies based on different weights (by varying h) are reported in Table 5.7 by considering the top-most ranked subject. It is observed from this table that the recognition accuracy remains the same with the values of h in between 1 to 10 in

Table 5.7: Performance on NIST BSSR1 multimodal dataset (set 1): Recognition accuracies (in %) for comparing weighted score and rank level fusion approaches using the proposed quality-derived weight estimation approach with different values of h (in Eq. 5.3)

M	ethods	h = 1	h = 2	h = 3	h = 4	h = 5	h = 6	h = 7	h = 8	h = 9	h = 10
	Weighted Sum [51]	99.23	99.23	99.23	99.23	99.23	99.23	99.23	99.23	99.23	99.23
	WQAM cos [62]	99.42	99.42	99.42	99.42	99.42	99.42	99.42	99.42	99.42	99.42
	WQAM cos^r [62]	99.23	99.23	99.23	99.23	99.23	99.23	99.23	99.23	99.23	99.23
	WQAM tan [62]	99.42	99.42	99.42	99.42	99.42	99.42	99.42	99.42	99.42	99.42
Score Level Fusion	WQAM sin [62]	99.42	99.42	99.42	99.42	99.42	99.42	99.42	99.42	99.42	99.42
Beore Bever rusion	WQAM $r^{1/s}$ [62]	99.42	99.42	99.42	99.42	99.42	99.42	99.42	99.42	99.42	99.42
	WQAM r^s [62]	99.42	99.42	99.42	99.42	99.42	99.42	99.42	99.42	99.42	99.42
	WQAM s^r [62]	99.42	99.42	99.42	99.42	99.42	99.42	99.42	99.42	99.42	99.42
	WQAM log [62]	99.42	99.42	99.42	99.42	99.42	99.42	99.42	99.42	99.42	99.42
	WQAM exp [62]	99.42	99.42	99.42	99.42	99.42	99.42	99.42	99.42	99.42	99.42
	Proposed Q-PSO Score	99.42	99.42	99.42	99.42	99.42	99.42	99.42	99.42	99.42	99.42
	WBorda [34]	92.84	92.84	92.84	92.84	92.84	92.84	92.84	92.84	92.84	92.84
	Exp [33]	89.16	89.16	89.16	89.16	89.16	89.16	89.16	89.16	89.16	89.16
Rank Level Fusion	WExp [33]	88.00	88.00	88.00	88.00	88.00	88.00	88.00	88.00	88.00	88.00
Italik Level Fusioli	DivExp [32]	99.42	99.42	99.42	99.42	99.42	99.42	99.42	99.42	99.42	99.42
	Log [32]	98.06	98.06	98.06	98.06	98.06	98.06	98.06	98.06	98.06	98.06
	Proposed Q-PSO Rank	99.42	99.42	99.42	99.42	99.42	99.42	99.42	99.42	99.42	99.42

each weighted fusion approach. Similar to the reported results for the previous two datasets (Section 5.4.1 and Section 5.4.2), the value of h is selected as 1 for weight estimation and further experimental analysis.

The efficacy of the proposed quality-based weight estimation approach (Section 5.2) is presented in Table 5.8 over an equal weight based approach and few other existing weight estimation approaches in [49] and [51]. The estimated weights using the above mentioned approaches are used for state-of-the-art weighted score and rank level fusion approaches along with the proposed quality-incorporated PSO based fusion approaches for rank level (Q-PSO Rank) and score level (Q-PSO Score). It is observed from Table 5.8 that the performances of the proposed Q-PSO Rank and the Q-PSO Score approaches are equal (99.42%) for all of the comparing weight estimation approaches. It has already been justified in Section 3.3.2.1 and Section 4.3.2.1 that a better recognition accuracy than its reported value (99.42%) can not be achieved for this dataset. Hence, the proposed quality-based weight estimation approach (Section 5.2) can not provide any performance improvement for this dataset. Similarly, performances of only a few state-of-the-art weighted score and rank level fusion approaches improve

Table 5.8: Performance comparison of existing weight estimation approaches for weighted score and rank level fusion approaches on NIST BSSR1 multimodal dataset (set 1)

D	n Methods	Weight Estimation Approaches							
Fusion	n Metnods	Equal Weights	Approach in [49]	Approach in [51]	Quality Based				
	Weighted Sum [51]	99.03	99.03	98.65	99.23				
	WQAM cos [62]	99.42	99.42	99.42	99.42				
	WQAM cos^r [62]	98.84	99.23	99.03	99.23				
	WQAM tan [62]	99.42	99.42	99.42	99.42				
Score Level Fusion	WQAM sin [62]	98.84	98.84	98.84	99.42				
Score Level Fusion	WQAM r^1/s [62]	99.42	99.42	99.42	99.42				
	WQAM r^s [62]	99.42	99.42	99.42	99.42				
	WQAM s^r [62]	99.42	99.42	99.42	99.42				
	WQAM log [62]	99.42	99.42	99.42	99.42				
	WQAM exp [62]	99.42	99.42	99.42	99.42				
	Proposed Q-PSO Score	99.42	99.42	99.42	99.42				
	WBorda [34]	92.26	92.06	92.45	92.84				
	Exp [33]	88.97	88.78	88.97	89.16				
Rank Level Fusion	WExp [33]	87.62	87.62	88.00	88.00				
Tank Level Fusion	DivExp [32]	98.83	99.23	99.23	99.42				
	Log [32]	98.45	98.45	98.06	98.76				
	Proposed Q-PSO Rank	99.42	99.42	99.42	99.42				

by incorporating the proposed quality-based weights (Section 5.2). It can also be observed that the several WQAM based approaches [62] perform as equal as the proposed rank level (Q-PSO Rank) and score level (Q-PSO Score) fusion approaches. The justifications provided in Section 3.3.2.1 regarding the maximum achievable recognition accuracy (i.e., 99.42%) of NIST BSSR1 multimodal dataset (set 1) due to three wrongly identified subjects in this dataset is also applicable in these results.

Furthermore, the recognition accuracy (in %) using the top-most ranked subject in each of the non-weighted rank and score level fusion approaches is compared with that of the proposed quality-incorporated PSO based fusion approaches for rank level (Q-PSO Rank) and score level (Q-PSO Score) in Table 5.9. The reported results establish the superiority of both of the proposed Q-PSO based fusion approaches over state-of-the-art non-weighted score and rank level fusion approaches.

The changes in recognition accuracies (in %) with the changes in cumulative ranks are represented using cumulative match characteristic (CMC) curves in Fig. 5.7 and Fig. 5.8. The proposed quality-incorporated PSO based fusion approaches for rank level (Q-PSO Rank) and score level (Q-PSO Score) outperforms majority of rank and score level fusion approaches, as it can be observed in the CMC curves

Table 5.9: Performance comparison of existing non-weighted rank and score level fusion approaches with the proposed Q-PSO based fusion approaches on NIST BSSR1 multimodal dataset (set 1)

M	ethods	Recognition Accuracy in %
	Max Rule [1]	79.90
	Min Rule [1]	94.80
	Product [1]	97.87
Score Level Fusion	Sum-OEBA [67]	99.03
Score Level Fusion	Sum-MOEBA [67]	98.45
	Sum-OEVBA [82]	98.70
	Hamacher t-norm [69]	97.29
	Frank t-norm [69]	98.07
	Proposed Q-PSO Score	99.42
	Borda Count [34]	92.07
Rank Level Fusion	Highest Rank [35]	79.70
	Proposed Q-PSO Rank	99.42

in Fig. 5.7 and Fig. 5.8. The CMC curves of several WQAM approaches [62] (Fig. 5.8) overlaps with that of the proposed Q-PSO rank and Q-PSO Score fusion approaches.

5.4.4 Fusion of Multimodal Biometrics for Multiple Gait Feature Representations (OU-ISIR BSS4 Multi-Algorithm Gait Dataset)

The OU-ISIR BSS4 multi-algorithm gait dataset [2, 194] provides five score lists for each probe. A brief description about this dataset can be found in Section 3.2.2.3. Rank lists are derived from each of these score lists. These rank lists are combined using the proposed quality-incorporated PSO based fusion approaches for rank level (Q-PSO Rank) and other existing rank level fusion approaches as discussed in Section 3.2.2.1. The window size on number of iteration to decide the convergence of the proposed quality-incorporated particle swarm optimization based rank level fusion approach (Q-PSO Rank) is experimentally decided as 5000 for this dataset. Similarly, the score lists are combined using the proposed quality-incorporated PSO based fusion approaches for score level (Q-PSO Score) and other existing score level fusion approaches as discussed in Section 3.2.2.1. The window size on number of iteration to decide the convergence of the proposed quality-incorporated particle swarm optimization based score level fusion approach (Q-PSO Score) is experimentally decided as 5000 for this dataset

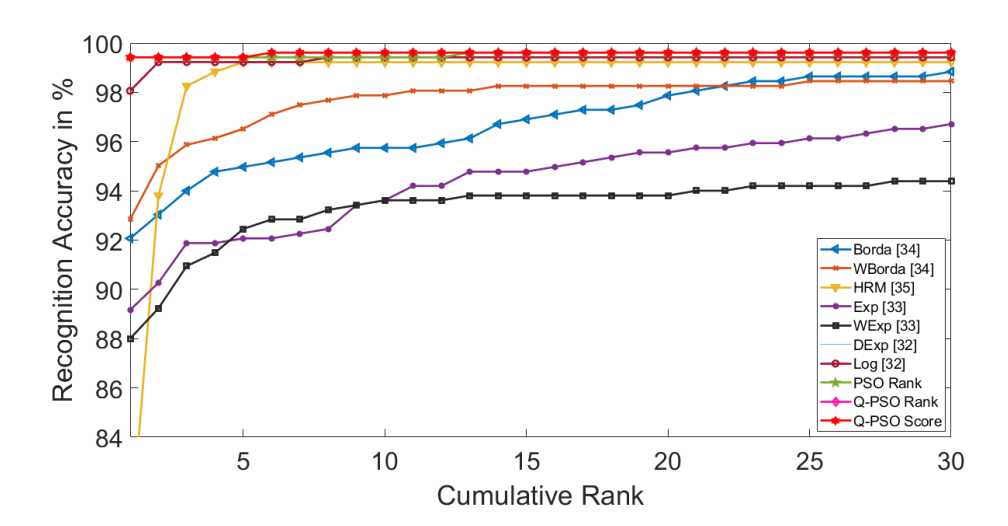


Figure 5.7: CMC plots for existing rank level fusion approaches being compared with that of the proposed Q-PSO based fusion approaches for NIST BSSR1 multimodal dataset (set 1)

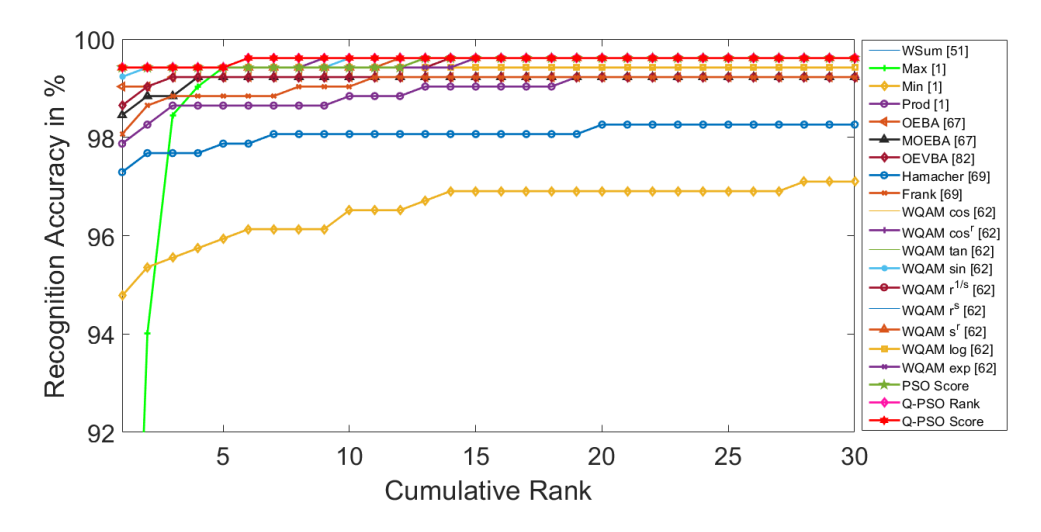


Figure 5.8: CMC plots for existing score level fusion approaches being compared with that of the proposed Q-PSO based fusion approaches for NIST BSSR1 multimodal dataset (set 1)

Table 5.10: Performance on OU-ISIR BSS4 multi-algorithm dataset: Recognition accuracies (in %) for comparing weighted score and rank level fusion approaches using the proposed quality-derived weight estimation approach with different values of h (in Eq. 5.3)

M	ethods	h = 1	h = 2	h = 3	h = 4	h = 5	h = 6	h = 7	h = 8	h = 9	h = 10
	Weighted Sum [51]	86.58	86.64	86.64	86.58	86.67	86.67	86.70	86.61	86.61	86.58
	WQAM cos [62]	86.58	86.64	86.67	86.58	86.67	86.67	86.70	86.61	86.61	86.58
	WQAM cos^r [62]	86.09	86.09	86.00	85.96	86.00	86.00	86.18	85.90	85.90	85.90
	WQAM tan [62]	86.18	86.18	86.24	86.24	86.21	86.21	86.27	86.12	86.09	86.09
Score Level Fusion	WQAM sin [62]	86.24	86.24	86.24	86.24	86.30	86.27	86.33	86.24	86.27	86.27
Beore Bever Fusion	WQAM $r^{1/s}$ [62]	86.61	86.67	86.70	86.61	86.70	86.73	86.73	86.70	86.67	86.64
	WQAM r^s [62]	86.58	86.61	86.70	86.61	86.64	86.70	86.73	86.70	86.64	86.64
	WQAM s^r [62]	86.58	86.61	86.67	86.61	86.67	86.70	86.70	86.67	86.64	86.61
	WQAM log [62]	86.58	86.61	86.67	86.61	86.67	86.70	86.70	86.67	86.64	86.61
	WQAM exp [62]	86.58	86.64	86.67	86.58	86.67	86.67	86.70	86.61	86.61	86.58
	Proposed Q-PSO Score	86.91	86.95	86.95	86.95	86.95	87.16	87.16	87.16	86.95	86.91
	WBorda [34]	83.66	83.69	83.75	83.75	83.75	84.36	84.93	84.93	83.81	83.66
	Exp [33]	82.58	82.58	82.61	82.61	82.98	83.76	83.76	83.76	82.61	82.58
Rank Level Fusion	WExp [33]	81.69	81.69	81.69	81.69	81.69	81.69	81.69	81.69	81.69	81.69
ltank Level Fusion	DivExp [32]	85.66	85.72	85.72	85.72	85.81	86.23	86.84	86.84	85.72	85.66
	Log [32]	84.86	84.95	84.95	84.95	84.95	85.38	85.89	85.89	84.95	84.86
	Proposed Q-PSO Rank	86.73	86.79	86.91	86.95	86.95	87.04	87.10	86.95	86.86	86.82

An experiment is performed to observe the impact of the value of h (in Eq. 5.3) for the proposed quality-derived weight estimation approach (Section 5.2). For this experiment, the value of the integer h is varied from 1 to 10 to estimate the weights for the five modalities based on their normalized matching scores. These estimated weights are used in each one of the comparing weighted rank level and score level fusion approaches. Corresponding recognition accuracies are reported in Table 5.10 by considering the top-most ranked subject. It is observed from this table that the highest recognition accuracy is achieved for the value of h as 7 in each weighted fusion approach on this dataset. It can also be noted that the highest recognition accuracies for few of the approaches are observed for multiple values of h. For example, WQAM $r^{1/s}$ based approach [62] achieves the highest recognition accuracy (86.73%) for the value of h as 6 and 7. Similar observations can be made for few other approaches as well. Finally, the value of h is selected as 7 for weight estimation and further experimental analysis.

The efficacy of the proposed quality-based weight estimation approach (Section 5.2) is presented in Table 5.11 over an equal weight based approach and few other existing weight estimation approaches in [49] and [51]. The esti-

Table 5.11: Performance comparison of existing weight estimation approaches for weighted score and rank level fusion approaches on OU-ISIR BSS4 multi-algorithm dataset

Paris	n Methods	Weight Estimation Approaches							
Fusion	n Methods	Equal Weights	Approach in [49]	Approach in [51]	Proposed Approach				
	Weighted Sum [51]	86.54	86.43	86.61	86.70				
	WQAM cos [62]	86.24	86.61	86.46	86.70				
	WQAM cos^r [62]	85.65	85.81	85.63	86.18				
	WQAM tan [62]	86.24	85.96	85.81	86.27				
Score Level Fusion	WQAM sin [62]	86.24	86.00	85.96	86.33				
Score Level Fusion	WQAM $r^{1/s}$ [62]	85.04	86.61	86.46	86.73				
	WQAM r^s [62]	86.24	86.61	86.46	86.73				
	WQAM s^r [62]	85.1	86.61	86.46	86.70				
	WQAM log [62]	86.24	86.61	86.46	86.70				
	WQAM exp [62]	85.04	86.61	86.46	86.70				
	Proposed Q-PSO Score	86.95	87.01	86.95	87.16				
	WBorda [34]	83.63	83.69	83.58	84.93				
	Exp [33]	82.12	82.54	82.12	83.76				
Rank Level Fusion	WExp [33]	81.42	81.63	81.60	81.69				
italik Level Fusion	DivExp [32]	85.50	85.53	85.44	86.84				
	Log [32]	84.43	84.80	84.86	85.89				
	Proposed Q-PSO Rank	86.73	86.88	86.79	87.10				

mated weights using the above mentioned approaches are used for state-of-the-art weighted score and rank level fusion approaches along with the proposed quality-incorporated PSO based fusion approaches for rank level (Q-PSO Rank) and score level (Q-PSO Score). It is observed from Table 5.11 that the performances of state-of-the-art weighted score and rank level fusion approaches and the proposed rank level (Q-PSO Rank) and score level (Q-PSO Score) fusion approaches improve by incorporating the proposed quality-based weights (Section 5.2). It can also be observed that the proposed quality-incorporated PSO based fusion approaches at rank level (Q-PSO Rank) and at score level (Q-PSO Score) achieve superior performances than state-of-the-art weighted fusion approaches even after incorporating the proposed quality-based weights. The proposed Q-PSO Score approach marginally outperforms the proposed Q-PSO Rank based fusion approach.

Furthermore, the recognition accuracy (in %) using the top-most ranked subject in each of the non-weighted rank and score level fusion approaches is compared with that of the proposed quality-incorporated PSO based fusion approaches for rank level (Q-PSO Rank) and score level (Q-PSO Score) in Table 5.12. The reported results establish the superiority of the proposed Q-PSO Rank

Table 5.12: Performance comparison of existing non-weighted rank and score level fusion approaches with the proposed Q-PSO based fusion approaches on OU-ISIR BSS4 multi-algorithm dataset using cumulative recognition accuracies in %

M	ethods	Recognition Accuracy in %
	Max Rule [1]	85.38
	Min Rule [1]	77.41
	Product [1]	77.41
Score Level Fusion	Sum-OEBA [67]	86.08
Score Level Fusion	Sum-MOEBA [67]	86.45
	Sum-OEVBA [82]	86.40
	Hamacher t-norm [69]	86.37
	Frank t-norm [69]	81.63
	Proposed Q-PSO Score	87.16
	Borda Count [34]	83.63
Rank Level Fusion	Highest Rank [35]	77.41
	Proposed Q-PSO Rank	87.10

and Q-PSO Score based fusion approaches over state-of-the-art non-weighted score and rank level fusion approaches.

The changes in recognition accuracies (in %) with the changes in cumulative ranks are presented using cumulative match characteristic (CMC) curves in Fig. 5.9 and Fig. 5.10. The proposed quality-incorporated PSO based fusion approaches for rank level (Q-PSO Rank) and score level (Q-PSO Score) outperforms existing rank and score level fusion approaches, as it can be observed in the CMC curves in Fig. 5.9 and Fig. 5.10.

5.5 Summary

Particle swarm optimization based fusion approaches at both rank (Section 3.3) and score (Section 4.3) levels of fusion performs better than state-of-the-art rank and score level fusion approaches in terms of recognition accuracy. In this chapter, the performances of these particle swarm optimization based approaches at both rank (Section 3.3) and score (Section 4.3) levels of fusion are further enhanced by incorporating the quality-based weight for each modality. A novel modality-independent biometric quality estimation approach is proposed in this chapter to enhance the performance of PSO based rank and score level fusion approaches. The derived quality is used to estimate weight for each modality. The proposed approach for estimating quality of biometric information in a probe signal uses matching scores between a probe and the gallery. Therefore, the set of estimated

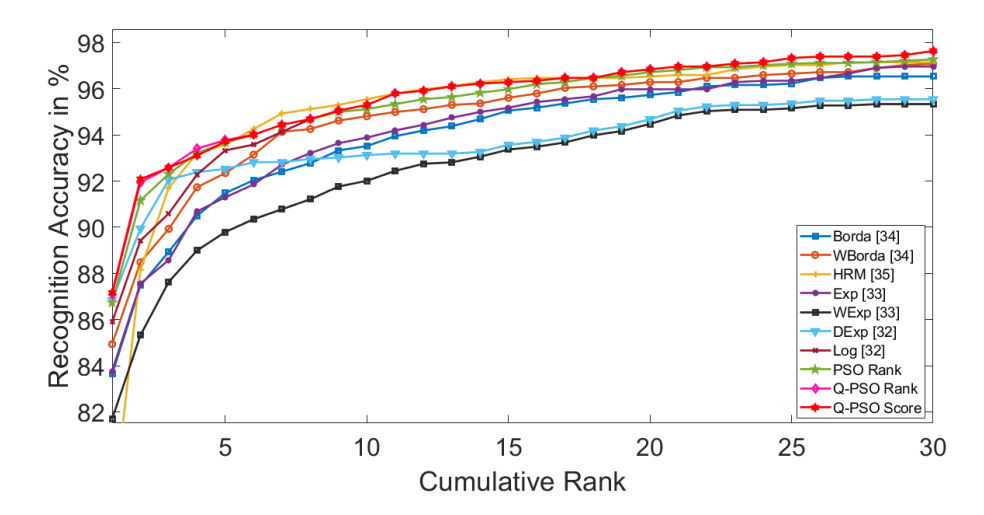


Figure 5.9: CMC plots for existing rank level fusion approaches being compared with that of the proposed Q-PSO based fusion approaches for OU-ISIR BSS4 multi-algorithm dataset

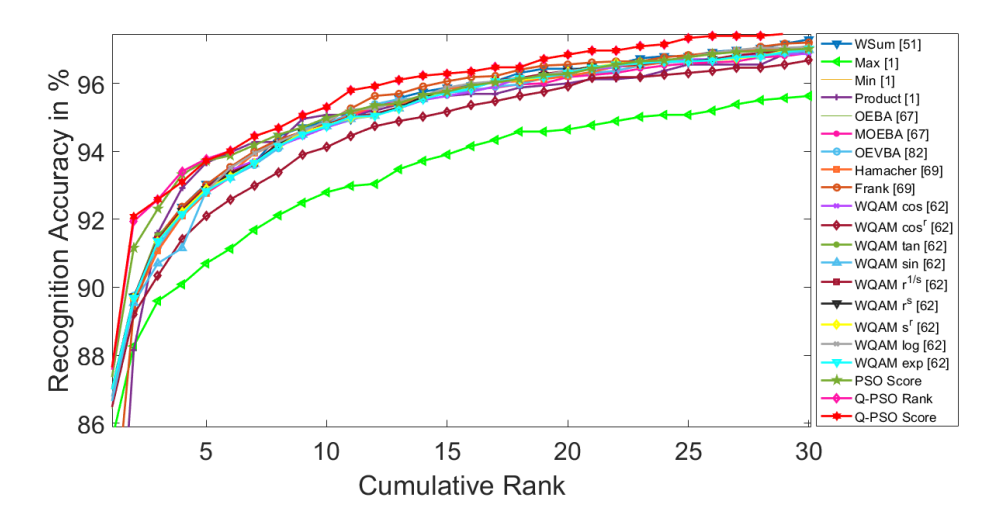


Figure 5.10: CMC plots for existing score level fusion approaches being compared with that of the proposed Q-PSO based fusion approaches for OU-ISIR BSS4 multi-algorithm dataset

weights vary across different probe users. The presented experimental results highlight the efficacy of incorporating quality-derived weight as compared to several weighting strategies (including equal weight for the modalities and weight estimation approaches in [49], [51]). It is to be noted that a suitable value of h for estimating quality in Eq. 5.3 varies across datasets.

Moreover, the proposed quality-incorporated PSO based fusion approaches for rank level (Q-PSO Rank) and score level (Q-PSO Score) perform better than state-of-the-art approaches for rank and score level fusion of multimodal biometrics in terms of recognition accuracies (in %). Moreover, the proposed Q-PSO Score approach performs slightly better than the proposed Q-PSO Rank approach in two out of four datasets.

Chapter 6

Reduction of Search Space Dimension for Optimization Based Fusion Approaches at Rank and Score Levels

Particle swarm optimization (PSO) based rank level and score level fusion of multimodal biometrics have been proposed in Section 3.3 and Section 4.3, respectively. Furthermore, the performances of these PSO based approaches are enhanced by incorporating quality-derived weight for each biometric modality (Chapter 5). The proposed quality-incorporated PSO based rank level (Section 5.3.1) and score level (Section 5.3.2) fusion approaches outperform state-of-the-art rank and score level fusion approaches in terms of recognition accuracies.

It is to be noted that particle swarm optimization (PSO) is an iterative search based optimization algorithm. It searches for the optimum solution by iteratively searching through numerous candidate solutions in a large search space. It takes a substantial number of iterations to converge to the optimum solution (i.e., the aggregated rank list or the aggregated score list). Therefore, a novel approach for search space reduction is proposed in this chapter for attaining faster convergence of the PSO based approaches in the context of above mentioned fusion tasks. It has been shown in Chapter 5 that quality-incorporated PSO (Q-PSO) based rank level and score level fusion approaches achieve better recognition accuracies than the initial PSO based approaches in Section 3.3 and Section 4.3. Hence, the

presented work in this chapter is based on the Q-PSO based approaches for rank level and score level fusion.

The remainder of this chapter is organized as following: The formulation of each of the rank level and the score level fusion of multimodal biometrics as an optimization problem is revisited in Section 6.1. The proposed approach for search space-reduction is presented in Section 6.2. The search space-reduced quality-incorporated particle swarm optimization based rank level and score level fusion approaches are presented in Section 6.3. Performances of the search space-reduced quality-incorporated rank level and score level fusion approaches are discussed in Section 6.4. Finally, the concluding remarks are drawn in Section 6.5.

6.1 Multimodal Fusion as an Optimization Problem

In the earlier works on rank level and score level fusion (Chapter 3 and Chapter 4, respectively), the fusions of multimodal biometrics at rank and at score levels have been conceptualized as optimization problems. The problem formulations for rank level fusion (Chapter 3) and score level fusion (Chapter 4) are briefly revisited in the following subsections.

6.1.1 Rank Level Fusion as an Optimization Problem

Let $L_1, L_2, ..., L_N$ be rank-ordered lists of subjects corresponding to N number of biometric modalities for identifying a person. In Section 3.1, the problem of obtaining an aggregated rank-ordered list of subjects has been formulated as an optimization problem. The objective function for this optimization problem minimizes a weighted summation of distances of the input lists $L_1, L_2, ..., L_N$ from the aggregated list. The objective function (which has been stated earlier in Eq. 3.2) is repeated here for the sake of completeness of this chapter.

$$minimize \ \phi(\delta) = \sum_{i=1}^{N} w_i \times d(\delta, L_i)$$
 (6.1)

Here, a candidate fused list is represented by δ . The distance $d(\delta, L_i)$ is a distance between a candidate fused list δ and an input list L_i . The weighted Spearman footrule distance [180] is used to estimate the distance between these two lists. The estimation of the said distance for two such lists is given in Eq.

3.3. The influence factor as weight in the weighted Spearman footrule distance is estimated using Eq. 3.4. Moreover, a weight w_i is associated with each of the N biometric modalities. Here, the weight represents the significance of the corresponding biometric modality. Similar to the earlier approach of rank level fusion (Section 5.3), the weight of each modality is assigned using the quality of the biometric information in a signal.

6.1.2 Score Level Fusion as an Optimization Problem

Let $\hat{S}_1, \hat{S}_2, \ldots, \hat{S}_N$ be normalized score lists corresponding to N number of biometric modalities for identifying a person. Min-max normalization (Eq. 2.1) is used for score normalization throughout this thesis. Fusion of these normalized score lists has been formulated as an optimization problem in Section 4.1. The objective of this optimization problem is to obtain a fused score list having the minimum weighted summation of distances of the input normalized score lists $\hat{S}_1, \hat{S}_2, \ldots, \hat{S}_N$ from the fused list. As a result, the objective function for generating the aggregated score list is:

minimize
$$\phi(\delta) = \sum_{i=1}^{N} w_i \times d(\delta, \hat{S}_i)$$
 (6.2)

Here, a candidate fused score list is represented by δ . The function $d(\delta, \hat{S}_i)$ denotes distance between a candidate fused score list δ and a normalized input score list \hat{S}_i . Similar to the work on rank level fusion approach (Section 6.1.1), a weighted Spearman footrule distance [180] is used to measure the above said distance. The estimation of the weighted Spearman footrule distance is presented in Eq. 4.4. The influence factor of an enrolled subject as a weight in the estimation of weighted Spearman footrule distance is determined using Eq. 4.5. Moreover, similar to the work on rank level fusion, a weight w_i is associated with each of the N biometric modalities. Here, the weight represents the significance of the corresponding biometric modality. Similar to the earlier approach of score level fusion (Section 5.3.2), the weight of each modality is assigned depending on the quality of the biometric information in a signal.

6.1.3 Challenges in Above Optimization Based Approaches

The above stated optimization problems in the context of rank level fusion and score level fusion have been solved using novel particle swarm optimization (PSO) based approaches in Section 3.3 and Section 4.3, respectively. Genetic algorithm (GA) based approaches have also been proposed in the above contexts (Section 3.2 and Section 4.2). But faster convergence of the PSO based approaches than the GA based approaches have guided the subsequent works to adopt only the PSO based approaches. Quality-incorporated PSO (Q-PSO) based approaches improve the recognition accuracies further in Chapter 5 for rank level and score level fusion approaches. In all of these works, the position of a particle represents a candidate fused list of either ranks or similarity scores of each of the enrolled subjects with respect to a probe subject. Let the number of enrolled subjects be n. Hence, there are n number of ranks or matching scores as part of candidate fused lists. Therefore, position of a particle can be perceived as a point in a n-dimensional space.

The particle swarm optimization (PSO) is a meta-heuristic optimization algorithm. It iteratively searches for the optimal solution in the entire search space. The search space in particle swarm optimization algorithm depends on the dimension of a candidate solution. In context of rank level and score level fusion of multimodal biometrics, this dimension is equal to the total number of enrolled users. If there are n enrolled users, then each candidate solution is of n-dimension. Moreover, the fitness evaluation, velocity updation and position updation involve computations of vectors having n-dimension. Therefore, the particle swarm optimization will converge faster if the dimension of the search space is reduced. Hence, the current work proposes novel approaches for dimensionality reduction of search spaces in the context of optimization based approaches for rank level and score level fusion. This dimensionality reduction is proposed to improve the convergence rate of the Q-PSO based algorithms. The proposed approaches for dimensionality reduction of search spaces are presented in next section.

6.2 Proposed Approaches for Search Space Reduction

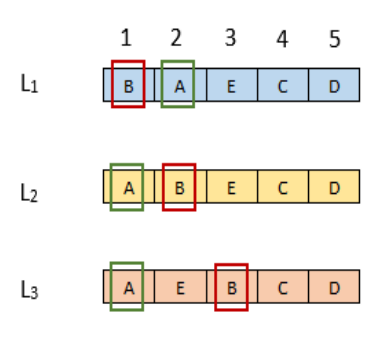
The convergence rate of particle swarm optimization is dependent on the dimension of search space. Therefore, novel approaches for search space reduction are proposed in this work. The detailed descriptions of the proposed approaches for search space reduction are presented in this section in the context of rank level and score level fusion of multimodal biometrics.

6.2.1 Search Space Reduction for Rank Level Fusion

Let $L_1, L_2, ..., L_N$ be rank-ordered lists of subjects corresponding to N number of biometric modalities for identifying a person. Each rank-ordered list is of n-dimension corresponding to n enrolled users. Steps of the proposed approach for dimensionality reduction of search space are narrated here with the help of an example.

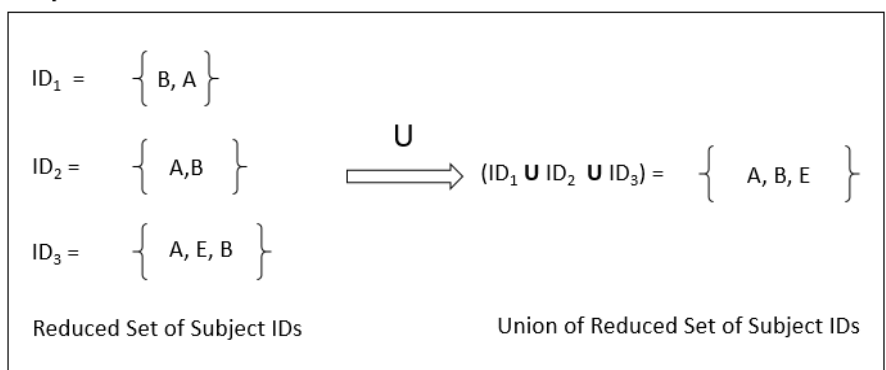
• Step 1: The subjects appearing at the top position in each of the N rankordered lists are identified as $T_1, T_2, ..., T_N$. Due to their appearances in the top positions in the input lists, these subjects are treated as potential matches for the probe subject. Then, the position of the subject T_i (appearing at the top position in L_i list) is identified in every other j^{th} list as P_i^j (for every $j \neq i$). Basically, the position of a potential matching subject is explored in all other rank-ordered lists. Let there be five enrolled subjects A, B, C, D and E. The rank-ordered lists of these subjects are presented as L_1 , L_2 and L_3 in Fig. 6.1 (Step 1) for three different biometric modalities. The subject B appears at the top position in the rank-ordered list L_1 i.e., $T_1 = B$. Similarly, subject A appears at the top positions in rank-ordered lists L_2 and L_3 , i.e., $T_2 = T_3 = A$. Initially, these two subjects have been assessed as the top contenders for the potential match with the probe subject. The subject B (being indicated using red rectangle) is at 2^{nd} position in rank-ordered list L_2 ($P_1^2=2$). The subject B is also at 3^{rd} position in rank-ordered list L_3 ($P_1^3 = 3$). Similarly, the positions of subject A (being indicated using green rectangle) in rank-ordered lists L_1 , L_2 and L_3 are 2^{nd} , 1^{st} and 1^{st} , respectively. Hence, $P_2^1=P_3^1=2$ and $P_2^3=P_3^2=1$.

Step 1:



Rank-Ordered Lists

Step 2:



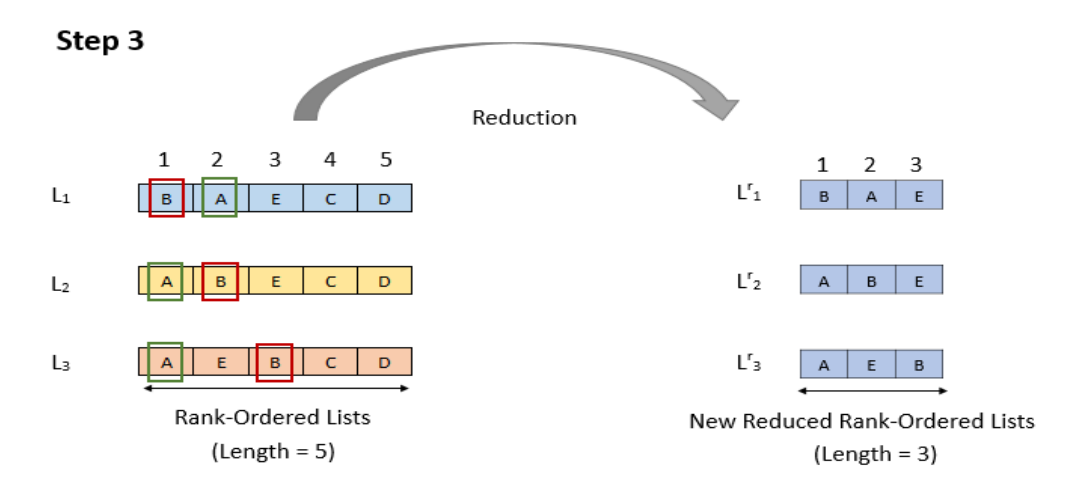


Figure 6.1: An illustration of search space-reduction for rank level fusion

Finally, the maximum position value P^j for each rank-ordered list j is identified as:

$$P^j = \max_{\forall i} P_i^j \tag{6.3}$$

In the above example in Fig. 6.1 (Step 1), the maximum position value P^1 for rank-ordered list L_1 is 2 (as $\max(P_1^1, P_3^1) = 2$). Similarly, the maximum position P^2 in the rank-ordered list L_2 is 2 (as $\max(P_1^2, P_3^2) = \max(2,1) = 2$). The maximum position P^3 in the rank-ordered list L_3 is 3 (as $\max(P_1^3, P_2^3) = \max(3,1) = 3$). This maximum position value P^j in a j^{th} list hosts a potentially matching subject. Hence, all preceding subjects in the list L_j according to rank order have to be considered as potentially matching subjects. These subjects have to be considered in the reduced list. Therefore, according the illustration in Fig. 6.1 (Step 1), subjects B and A (rank-ordered) are potential matches with the probe in rank-ordered list L_1 as the maximum position value P^1 for rank-ordered list L_1 is 2. Similarly, subject identities A and B are potential matches with the probe in rank-ordered list L_2 and subject identities A, E and B are potential matches with the probe in rank-ordered list L_3 .

- Step 2: Therefore, the set of subject identities (ID_j) for each modality j is already obtained in step 1 based on the selected subject identities (potential matches). For example, in Fig. 6.1 (Setp 2), the set of subject identities (ID_1) for list L_1 is $ID_1 = \{B, A\}$. Similarly, the sets of subject identities for lists L_2 and L_3 are $ID_2 = \{A, B\}$ and $ID_3 = \{A, E, B\}$, respectively. In step 2, union of potential matches from these sets of subject identities generates an exhaustive list of potential matches. In the above example, the exhaustive list of potential matches contains subject identities A, B and E as illustrated in Fig. 6.1 (Step 2).
- Step 3: Finally, the selected subjects (subject identities in exhaustive list of potential matches) are only used to construct the reduced rank-ordered list in each modality. The new reduced rank-ordered list L_j^r for j^{th} modality is derived from the initial list L_j . The selected subjects in the reduced rank-ordered list L_j^r maintain their relative ordering as similar to the initial list L_j . As illustrated in Fig. 6.1 (Step 3), the first reduced rank-ordered list L_1^r is B, A, and E. Similarly, the reduced rank-ordered lists L_2^r is A, B and E. The reduced rank-ordered lists L_3^r is A, E and B. Each initial rank-ordered list L_j^r has dimension n. A new reduced rank-ordered list L_j^r is of reduced

dimension n^r . In the above example, dimension of the rank-ordered subject list is reduced from 5 to 3, as it is shown in Fig. 6.1 (Step 3).

6.2.2 Search Space Reduction for Score Level Fusion

Dimensionality reduction of search space is addressed in this subsection for score level fusion of multimodal biometrics. Let \hat{S}_1 , \hat{S}_2 ,..., \hat{S}_N be normalized score lists corresponding to N number of biometric modalities for identifying a person in the context of score level fusion. Each normalized score list is of n-dimension corresponding to n enrolled users. Steps of the proposed approach for dimensionality reduction of search space are narrated here with the help of an example.

• Step 1: The first step is to construct the rank-ordered lists of subjects L_1 , L_2, \ldots, L_N by considering the normalized similarity scores in descending order (for similarity scores). Let there be five enrolled subjects A, B, C, D and E. The normalized score lists \hat{S}_1 , \hat{S}_2 and \hat{S}_2 for three different modalities contain the normalized scores for enrolled subject identities with respect to a probe as shown in Fig. 6.2 (Step 1). The rank-ordered list of subjects corresponding to normalized score list \hat{S}_1 is L_1 . It contains subject identities based on the descending order of their normalized similarity scores in the normalized score list \hat{S}_1 . It is shown in Fig. 6.2 (Step 1). Similarly, the rank-ordered lists L_2 and L_3 are obtained from normalized score lists \hat{S}_2 and \hat{S}_3 , respectively. Then, the step 1 of search space reduction for rank level fusion (Section 6.2.1) is performed to identify the potential matches for each rank-ordered list L_i . This illustration is shown in Fig. 6.2 (Step 1). In the above example, the subject A appears at top positions in L_1 and L_3 lists, i.e., $T_1 = T_3 = A$. Similarly, subject B appears at top position in L_2 , i.e., $T_2 = B'$. Initially, these two subjects have been assessed as the top contenders for the potential match with the probe subject. The subject A (being indicated using red rectangle) is at 3^{rd} position in rank-ordered list L_2 ($P_1^2 = P_3^2 = 3$). The subject A is also at 1^{st} position in rank-ordered list L_3 ($P_1^3 = P_3^1 = 1$). Similarly, the positions of subject B (being indicated using green rectangle) in rank-ordered lists L_1 , L_2 and L_3 are 2^{nd} , 1^{st} and 2^{nd} , respectively. Hence, $P_2^1 = P_2^3 = 2$.

Finally, the maximum position value P^j for each rank-ordered list j is identified using Eq. 6.3. In the above example in Fig. 6.2 (Step 1), the maximum position value P^1 for rank-ordered list L_1 is 2 (as $\max(P_2^1, P_3^1) = \max(2, 1)$

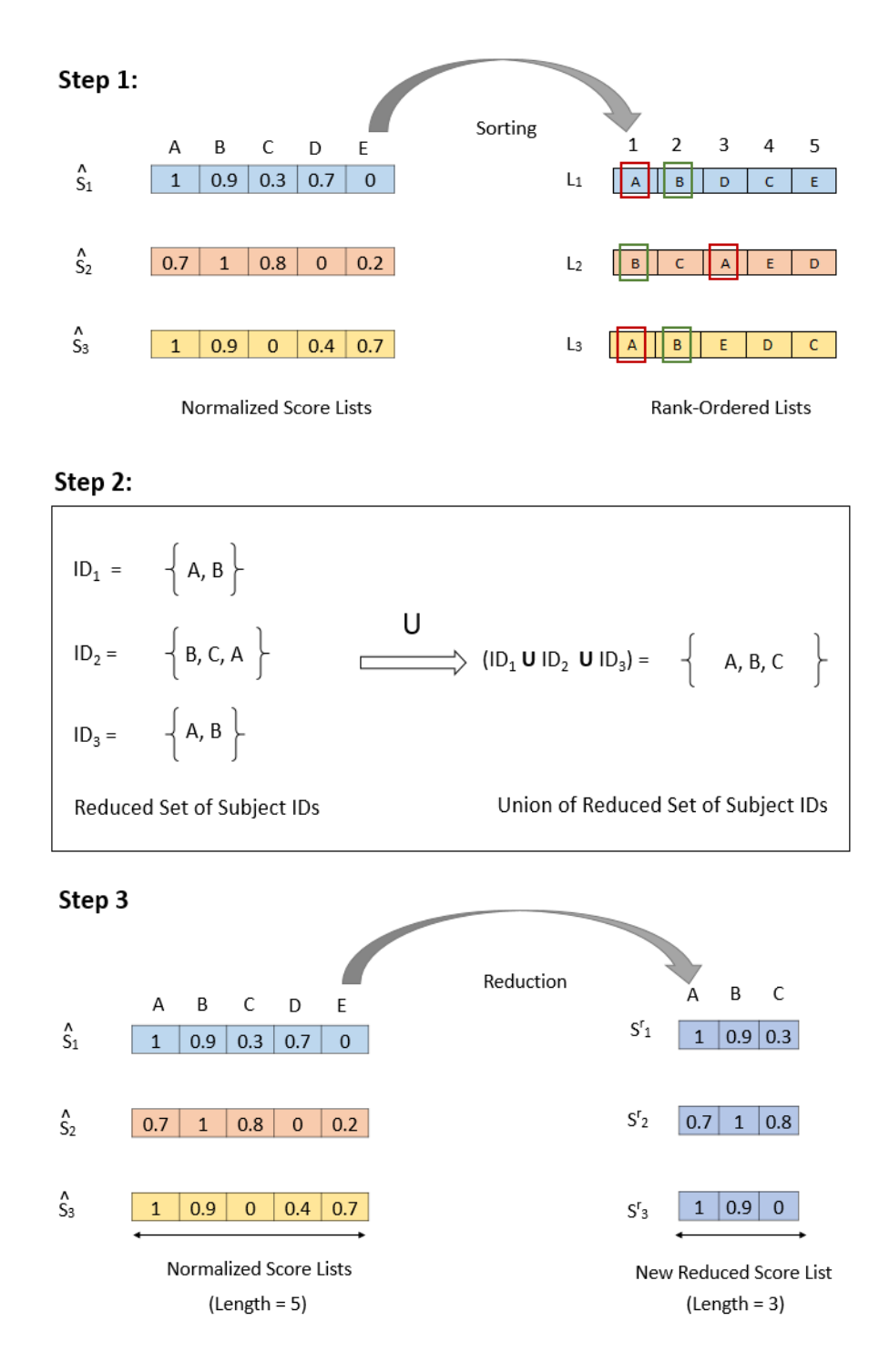


Figure 6.2: An illustration of search space-reduction for score level fusion

- = 2). Similarly, the maximum position P^2 in the rank-ordered list L_2 is 2 (as $\max(P_1^2, P_3^2) = \max(3, 3) = 3$). The maximum position P^3 in the rank-ordered list L_3 is 2 (as $\max(P_1^3, P_2^3) = \max(1, 2) = 2$). This maximum position value P^j in a j^{th} list hosts a potentially matching subject. Hence, all preceding subjects in the list L_j according to rank order have to be considered as potentially matching subjects. These subjects have to be considered in the reduced list. Therefore, according the illustration in Fig. 6.2 (Step 1), subjects A and B (rank-ordered) are potential matches with the probe in rank-ordered list L_1 as the maximum position value P^1 for rank-ordered list L_1 is 2. Similarly, subject identities B, C and A are potential matches with the probe in rank-ordered list L_2 and subject identities A and B are potential matches with the probe in rank-ordered list L_2 and subject identities A and B are potential matches with the probe in rank-ordered list L_2 and subject identities A and B are potential matches with the probe in rank-ordered list L_3 .
- Step 2: A set of subject identities (ID_j) for each list j is obtained in step 1 based on the selected subject identities (potential matches). For example, in Fig. 6.2 (Step 2), the set of subject identities (ID_1) for lists L_1 is $ID_1 = \{A, B\}$. Similarly, the sets of subject identities for list L_2 and L_3 are $ID_2 = \{B, C, A\}$ and $ID_3 = \{A, B\}$, respectively. Similar to the step 2 of search space reduction for rank level fusion (Section 6.2.1), union of these sets of subject identities generates an exhaustive list of potential matches. In the above example, the exhaustive list of potential matches contains subject identities A, B and C as illustrated in Fig. 6.1 (Step 2).
- Step 3: Finally, the normalized scores of the selected subjects (subject identities in the exhaustive list of potential matches) are only used to construct the reduced score list in each modality. The new reduced score list S_j^r for j^{th} modality is derived from the initial list \hat{S}_j . As shown in Fig. 6.2 (Step 3), the first reduced score list S_1^r has normalized scores of subjects A, B and C from the initial normalized score list \hat{S}_1 (i.e., 1, 0.9, and 0.3). Similarly, the reduced score lists S_2^r and S_3^r contain the normalized scores of the selected set of subjects form the original normalized score lists \hat{S}_2 and \hat{S}_3 , respectively. It is shown in Fig. 6.2 (Step 3). Each initial normalized score list S_j^r is of reduced dimension n. The corresponding new reduced score list S_j^r is of reduced dimension n. In the above example, the dimension of the score list is reduced from 5 to 3 as it is shown in Fig. 6.2 (Step 3).

6.3 Proposed Search Space-Reduced Quality-Incorporated Particle Swarm Optimization Based Fusion Approaches

In the previous works on particle swarm optimization based fusion approaches for rank level (Section 3.3 and Section 5.3.1) and score level (Section 4.3 and Section 5.3.2), position of a particle represents a candidate fused list of either rank-ordered subjects or similarity scores. In these approaches, the dimension of each candidate list is same as the number of enrolled users n. Novel approaches for reducing the dimension of search spaces are proposed in Section 6.2.1 and Section 6.2.2 in the context of rank level fusion and score level fusion, respectively. Based on the discussions in Section 6.2, novel search space-reduced quality-incorporated particle swarm optimization based fusion approaches at rank level (RQ-PSO Rank) and at score level (RQ-PSO Score) are presented in this section to achieve faster convergence.

6.3.1 Proposed Search Space-Reduced Quality-Incorporated Particle Swarm Optimization Based Rank Level Fusion Approach

In this work, the approach for weight assignment to each biometric modality (Section 5.2) is combined with the proposed approach for dimensionality reduction of search space (Section 6.2.1). At first, the quality of biometric information is estimated using Eq. 5.3 for each modality. Weight for each modality is derived using the estimated qualities of the input biometric signals (Eq. 5.4). These weights are used in the optimization problem in Eq. 6.1.

Then, the dimensions of the input lists and the search space are reduced using the proposed approach in Section 6.2.1. Subsequently, particle swarm optimization (PSO) is applied to solve the stated optimization problem in a reduced search space. The proposed approach is same as the PSO based rank level fusion approach in Section 3.3 and quality-incorporated PSO based rank level fusion (Q-PSO Rank) approach in Section 5.3.1. Representation of a particle position, initialization of a population, exploration of other candidate solutions and stopping criteria in the proposed search space-reduced quality-incorporated PSO based rank fusion approach (RQ-PSO Rank) are maintained as exactly same as

the previous PSO based rank level fusion approach in Section 3.3 and quality-incorporated PSO based rank level fusion (Q-PSO Rank) approach in Section 5.3.1.

6.3.2 Proposed Search Space-Reduced Quality-Incorporated Particle Swarm Optimization Based Score Level Fusion Approach

Similar to the work in rank level fusion (Section 6.3.1), the proposed approach for weight assignment to each biometric modality (Section 5.2) is combined with the proposed approach for dimensionality reduction of search space (Section 6.2.2). At first, the quality of biometric information is estimated using Eq. 5.3 for each modality. Weight for each modality is derived using the estimated qualities of the input biometric signals (Eq. 5.4). These weights are used in the optimization problem in Eq. 6.2.

The dimensions of the input lists and the search space are reduced using the proposed approach in Section 6.2.2. Subsequently, particle swarm optimization (PSO) is applied to solve the stated optimization problem in a reduced search space. The rest of the proposed approach is same as the PSO based score level fusion approach in Section 4.3 and quality-incorporated PSO based score level fusion (Q-PSO Score) approach in Section 5.3.2. Representation of a particle position, initialization of a population, exploration of other candidate solutions and stopping criteria in the proposed search space-reduced quality-incorporated PSO based score fusion approach (RQ-PSO Score) are maintained as exactly same as the previous PSO based score level fusion approach in Section 4.3 and quality-incorporated PSO based score level fusion (Q-PSO Score) approach in Section 5.3.2.

6.4 Performance Evaluation and Discussion

Detailed performance analysis is carried out for the proposed search space-reduced quality-incorporated PSO based fusion approaches at rank level (RQ-PSO Rank) and at score level (RQ-PSO Score). Experimental study on the performances of the proposed approaches are reported using four multimodal biometric datasets. The first two datasets are virtually created multimodal biometric datasets involving face and iris biometrics, namely virtual multimodal biometric dataset

FaceIris-V1 and virtual multimodal biometric dataset FaceIris-V2. The remaining two datasets are NIST BSSR1 multimodal dataset (set 1) [193] involving face and fingerprint modalities and OU-ISIR BSS4 multi-algorithm gait dataset [2, 194] involving multiple feature extraction methods of gait biometrics.

Performances of the proposed search space-reduced quality-incorporated PSO based fusion approaches at rank level (RQ-PSO Rank) and at score level (RQ-PSO Score) are experimentally exhibited in comparison to existing fusion schemes at score and rank levels. Moreover, supremacies of the proposed approaches are also evaluated with respect to the PSO based rank level fusion approach (Section 3.3) and the PSO based score level fusion approach (Section 4.3) in terms of average number of iterations and the average execution time (in seconds) being taken to achieve convergence. The above analysis is presented in following subsections using each of the above four datasets.

6.4.1 Fusion of Multimodal Biometrics Involving Face and Iris (Virtual Multimodal Biometric Dataset FaceIris-V1)

Performances of the proposed approaches are evaluated on virtually created dataset, namely FaceIris-V1, involving face and iris modalities. This virtually created dataset (FaceIris-V1) contains face images from the cross-age LFW (CALFW) face dataset [210] and iris images from IIT Delhi iris database (version 1.0) [211]. Details of this dataset is presented in Section 5.4.1.

Two score lists are obtained for each probe in the virtual multimodal biometric dataset FaceIris-V1 for two biometric modalities. Two rank lists are derived for each probe from the above two score lists. Initially, these score and rank lists are of size 435, which is equal to number of unique individuals. The size of these rank lists are reduced using the proposed search space-reduction approach (Section 6.2). These reduced rank lists are considered as inputs to the proposed search space-reduced quality-incorporated particle swarm optimization based rank level fusion approach (RQ-PSO Rank) in Section 6.3.1 and other existing rank level fusion approaches in Section 3.2.2.1. The window size on number of iteration to decide the convergence of the proposed RQ-PSO Rank based fusion approach is experimentally decided as 60 for this dataset.

Moreover, the two score lists are normalized using min-max normalization (Eq. 2.1). It is to be noted that the generated score for face modality is a similarity

Table 6.1: Recognition accuracies (in %) of the proposed search space-reduced quality-incorporated PSO based fusion approaches with respect to those of unimodal matchers on virtual multimodal biometric dataset FaceIris-V1

	Method	Top-1 Rank	Top-2 Ranks	Top-3 Ranks
Unimodal		91.26	92.41	92.41
Ullimodai		89.66	90.80	91.49
Proposed	l RQ-PSO Rank Fusion	98.16	98.62	98.62
Proposed RQ-PSO Score Fusion		98.62	98.85	99.08

score. On the contrary, the generated score for iris modality is a dissimilarity score. Hence, the normalized scores for iris modality are converted to similarity scores by subtracting the normalized scores from 1. Similar to the rank level fusion, in score level fusion, the sizes of these normalized score lists are reduced using the proposed search space-reduction approach (Section 6.2). These reduced normalized similarity score lists are then used as inputs to the proposed search space-reduced quality-incorporated particle swarm optimization based score level fusion approach (RQ-PSO Score) (Section 6.3.2) and other existing score level fusion approaches in Section 3.2.2.1. The window size on number of iteration to decide the convergence of the proposed RQ-PSO Score based fusion approach is experimentally decided as 100 for this dataset.

The recognition accuracies (in %) for the proposed search space-reduced quality-incorporated PSO based fusion approaches at rank level (RQ-PSO Rank) and at score level (RQ-PSO Score) as well as each unimodal matcher are presented in Table 6.1 for virtual multimodal biometric dataset FaceIris-V1. The recognition accuracies are estimated using Eq. 3.7. These recognition accuracies are reported for the probe being found within top-1, top-2 and top-3 ranks (cumulative) in the aggregated rank lists and score lists. The usefulness of the proposed fusion approaches over each of the unimodal matchers is obvious from the reported results in Table 6.1.

Furthermore, the recognition accuracies of the comparing approaches within top-1, top-2 and top-3 positions along with those for the proposed approaches are presented in Table 6.2. It can be seen from the reported recognition accuracies that the proposed search space-reduced quality-incorporated PSO based fusion approaches at rank level (RQ-PSO Rank) and at score level (RQ-PSO Score) perform better than existing state-of-the-art rank and score level fusion approaches.

Table 6.2: Performance comparison of the existing rank and score level fusion approaches with the proposed RQ-PSO based fusion approaches on virtual multimodal dataset FaceIris-V1 using cumulative recognition accuracies in %

	Methods	Top-1 Rank	Top-2 Ranks	Top-3 Ranks
	Weighted Sum [51]	97.70	98.16	98.16
	Max [1]	91.49	98.85	98.85
	Min [1]	93.79	94.02	94.02
	Product [1]	94.02	94.94	95.17
	Sum-OEBA [67]	91.26	92.41	92.64
	Sum-MOEBA [67]	93.79	94.48	94.71
	Sum-OEVBA [82]	94.48	95.86	96.09
	Hamacher t-norm [69]	94.02	94.94	95.17
	Frank t-norm [69]	94.02	94.94	95.17
Score Level	WQAM cos [62]	97.70	98.16	98.16
Score Level	$WQAM cos^r [62]$	98.16	98.62	98.62
	WQAM tan [62]	98.16	98.85	99.08
	WQAM sin [62]	96.55	96.78	97.01
	$\overline{\text{WQAM } r^{1/s} \text{ [62]}}$	98.16	98.62	98.62
	WQAM r^s [62]	97.93	98.62	98.62
	$WQAM s^r [62]$	97.70	98.39	98.62
	WQAM log [62]	97.70	98.39	98.62
	WQAM exp [62]	97.70	98.16	98.39
	PSO Score (Section 4.3)	95.40	97.70	98.16
	Q-PSO Score (Section 5.3.2)	98.62	98.85	99.08
	Proposed RQ-PSO Score	98.62	98.85	99.08
	Borda Count [34]	92.18	94.02	94.25
	WBorda [34]	95.63	96.55	97.24
	Highest Rank [35]	91.49	98.85	98.85
	Exp [33]	94.48	95.4	96.09
Rank Level	WExp [33]	91.03	92.64	93.1
	DivExp [32]	93.33	94.02	94.94
	Log [32]	96.78	97.47	98.16
	PSO Rank (Section 3.3)	94.94	96.32	97.24
	Q-PSO Rank (Section 5.3.1)	98.16	98.62	98.62
	Proposed RQ-PSO Rank	98.16	98.62	98.62

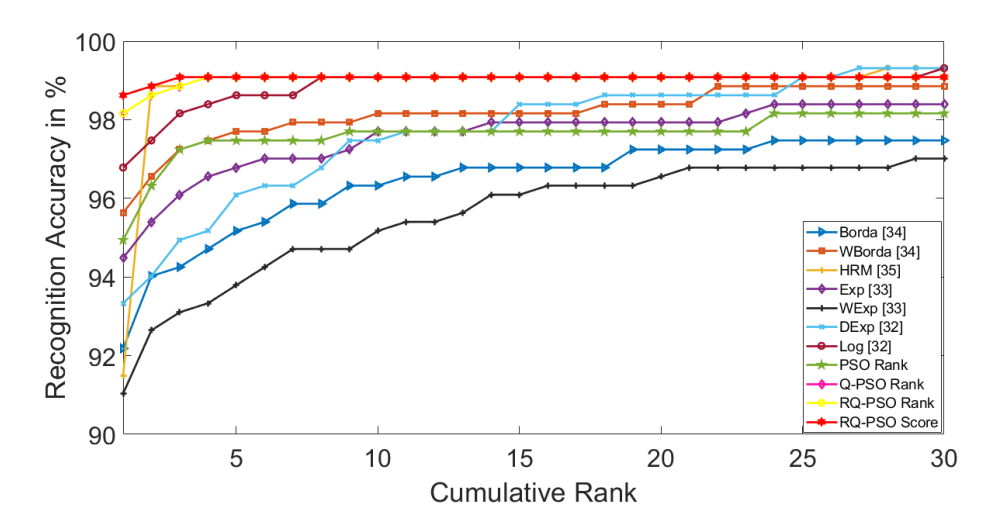


Figure 6.3: CMC plots for existing rank level fusion approaches being compared with that of the proposed RQ-PSO based fusion approaches for first virtual multimodal biometric dataset FaceIris-V1

Moreover, it can also be observed from the Table 6.2 that the recognition accuracies of the proposed RQ-PSO Rank (Section 6.3.1) and RQ-PSO Score (Section 6.3.2) based approaches after reducing the dimension of the search space remain as same as that of quality-incorporated PSO based fusion approaches at rank level (Q-PSO Rank) (Section 5.3.1) and at score level (Q-PSO Score) (Section 5.3.2).

The changes in recognition accuracies (in %) with the changes in cumulative ranks are presented using cumulative match characteristic (CMC) curves in Fig. 6.3 and Fig. 6.4. The proposed RQ-PSO based fusion approaches outperform existing rank and score level fusion approaches, as it can be observed in the CMC curves in Fig. 6.3 and Fig. 6.4.

Moreover, the main idea behind the proposed work in this chapter is to speed up the execution of the PSO based approaches for multimodal biometrics while maintaining the same level of recognition accuracies. The effectiveness of the proposed search space-reduction approach (Section 6.2) is presented in Table 6.3. It can be observed from the table that average number of iterations to converge for each of the proposed RQ-PSO based rank and score level fusion approaches significantly decreases by using the proposed search space-reduction approach (Section 6.2). The PSO based rank level fusion approach (Section 3.3) takes 1280 iterations (rounded off to the nearest integer) on an average to reach at

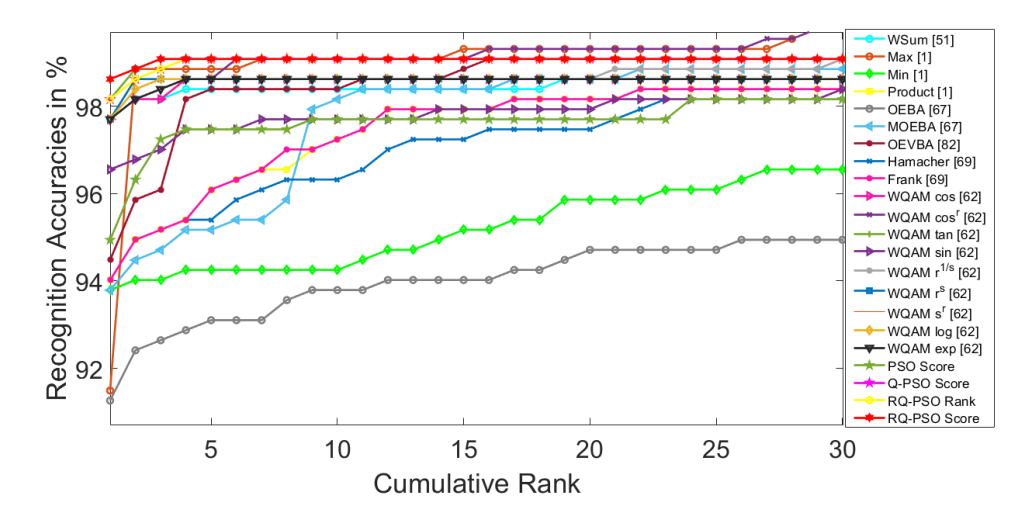


Figure 6.4: CMC plots for existing score level fusion approaches being compared with that of the proposed RQ-PSO based fusion approaches for first virtual multimodal biometric dataset FaceIris-V1

the optimal solution in 2.72 seconds. Here, the average dimension of the search space is 435, as there are 435 enrolled users in this dataset. After applying the proposed search space-reduction approach (Section 6.2.1), the average dimension of the search space is reduced to 45 (rounded off to the nearest integer). Due to the achieved reduction in average dimension of search space, the proposed RQ-PSO based rank level fusion approach takes only 103 number of iterations on an average (rounded off to the nearest integer) to find the optimal solution. Furthermore, the significant improvement in the average execution time due to reduced dimension is also seen from Table 6.3. The proposed RQ-PSO based rank level fusion approach takes 0.10 seconds on an average to find the optimal solution.

Similar observations are reported in Table 6.3 for PSO based score level fusion approach (Section 4.3) and the proposed RQ-PSO based score level fusion approach. The PSO based score level fusion approach (Section 4.3) takes 1027 iterations (rounded off to the nearest integer) on an average to reach at the optimal solution in 0.35 seconds. Here, the average dimension of the search space is 435, as there are 435 enrolled users in this dataset. After applying the proposed search space-reduction approach (Section 6.2.2), the average dimension of the search space is reduced to 45 (rounded off to the nearest integer). Due to the achieved reduction in average dimension of search space, the proposed RQ-

Table 6.3: Performance comparison of PSO based rank (Section 3.3) and PSO based score (Section 4.3) level fusion approaches with the proposed RQ-PSO based fusion approaches on virtual multimodal dataset FaceIris-V1 using average number of iterations, average execution time and average dimension of search space

Methods	Average number of iterations to converge (rounded off	Average execution time	Average dimension of search space (rounded off to
	to the nearest integer)	(seconds)	the nearest integer)
PSO Rank (Section 3.3)	1280	2.72	435
Proposed RQ-PSO Rank	103	0.10	45
PSO Score (Section 4.3)	1027	0.35	435
Proposed RQ-PSO Score	243	0.06	45

PSO based score level fusion approach takes only 243 number of iterations on an average (rounded off to the nearest integer) to find the optimal solution. Furthermore, the significant improvement in the average execution time due to reduced dimension is also seen in Table 6.3. The proposed RQ-PSO based score level fusion approach takes 0.06 seconds on an average to find the optimal solution. It is also noted that the proposed RQ-PSO Score based approach executes faster (average execution time 0.06 seconds) than the proposed RQ-PSO Rank based approach (average execution time 0.10 seconds). Moreover, the reduced dimension of search space for both the approaches (RQ-PSO Rank and RQ-PSO Score) is same. This is because the search space-reduction approach for score level fusion (Section 6.2.2) converts the score lists into rank-ordered lists and then use the steps as similar as the search space-reduction approach for rank level fusion (Section 6.2.1) to reduce the dimension of the search space.

6.4.2 Fusion of Multimodal Biometrics Involving Face and Iris (Virtual Multimodal Dataset FaceIris-V2)

The second virtual multimodal biometric dataset (FaceIris-V2) is created by combining the face biometrics from CelebFaces attributes dataset (CelebA) [212] and iris biometrics from IIT Delhi iris database (version 1.0) [211]. Details of this dataset is presented in Section 5.4.2.

Two score lists are obtained for each probe in the virtual multimodal biometric dataset FaceIris-V2 for two biometric modalities. Two rank lists are derived for each probe from the above two score lists. Initially, these score and rank lists are of size 435, which is the number of unique individuals in this dataset. The

sizes of these rank lists are reduced using the proposed search space-reduction approach (Section 6.2). These reduced rank lists are considered as inputs to the proposed search space-reduced quality-incorporated particle swarm optimization based rank level fusion approach (RQ-PSO Rank) in Section 6.3.1 and other existing rank level fusion approaches in Section 3.2.2.1. The window size on number of iteration to decide the convergence of the proposed RQ-PSO Rank based fusion approach is experimentally decided as 600 for this dataset.

Moreover, the two score lists are normalized using min-max normalization (Eq. 2.1). Similar to the virtual multimodal dataset FaceIris-V1, the normalized dissimilarity scores for iris modality are converted to similarity score by subtracting the normalized scores from 1. The sizes of these normalized score lists are reduced using the proposed search space-reduction approach (Section 6.2). These reduced normalized similarity score lists are then used as inputs to the proposed search space-reduced quality-incorporated particle swarm optimization based score level fusion approach (RQ-PSO Score) (Section 6.3.2) and other existing score level fusion approaches in Section 3.2.2.1. The window size on number of iteration to decide the convergence of the proposed RQ-PSO Score based fusion approach is experimentally decided as 100 for this dataset.

The recognition accuracies (in %) for the proposed search space-reduced quality-incorporated PSO based fusion approaches at rank level (RQ-PSO Rank) and at score level (RQ-PSO Score) as well as each unimodal matcher are presented in Table 6.4 for virtual multimodal biometric dataset FaceIris-V2. The recognition accuracies are estimated using Eq. 3.7. These recognition accuracies are reported for the probe being found within top-1, top-2 and top-3 ranks (cumulative) in the aggregated rank lists and score lists. The usefulness of the proposed fusion approaches over each of the unimodal matchers is obvious from the reported results in Table 6.4.

Furthermore, the recognition accuracies of the comparing approaches within top-1, top-2 and top-3 positions along with those for the proposed approaches are presented in Table 6.5. It can be seen from the reported recognition accuracies that the proposed search space-reduced quality-incorporated PSO based fusion approaches at rank level (RQ-PSO Rank) and at score level (RQ-PSO Score) perform better than the majority of existing state-of-the-art rank and score level fusion approaches. Only the WQAM tan approach [62] performs as equal as the proposed approaches for the top most position. Moreover, it can also be observed from the Table 6.5 that the recognition accuracies of the proposed RQ-PSO Rank (Section 6.3.1) and RQ-PSO Score (Section 6.3.2) based approaches after reducing

Table 6.4: Recognition accuracies (in %) of the proposed search space-reduced quality-incorporated PSO based fusion approaches with respect to those of unimodal matchers on virtual multimodal biometric dataset FaceIris-V2

	Method	Top-1 Rank	Top-2 Ranks	Top-3 Ranks
Unimodal		93.79	94.25	94.48
Unimodai		89.66	90.80	91.49
Proposed	l RQ-PSO Rank Fusion	99.31	99.31	99.31
Proposed	l RQ-PSO Score Fusion	99.31	99.31	99.31

the dimension of the search space remain as same as that of quality-incorporated PSO based fusion approaches at rank level (Q-PSO Rank) (Section 5.3.1) and at score level (Q-PSO Score) (Section 5.3.2).

The changes in recognition accuracies (in %) with the changes in cumulative ranks are presented using cumulative match characteristic (CMC) curves in Fig. 6.5 and Fig. 6.6. The proposed RQ-PSO based fusion approaches outperform existing rank and score level fusion approaches, as it can be observed in the CMC curves in Fig. 6.5 and Fig. 6.6.

Moreover, the main idea behind the proposed work in this chapter is to speed up the execution of the PSO based approaches for multimodal biometrics while maintaining the same level of recognition accuracies. The effectiveness of the proposed search space-reduction approach (Section 6.2) is presented in Table 6.6. It can be observed from the table that average number of iterations to converge for each of the proposed RQ-PSO based rank and score level fusion approaches significantly improves by using the proposed search space-reduction approach (Section 6.2). The PSO based rank level fusion approach (Section 3.3) takes 3054 iterations (rounded off to the nearest integer) on an average to reach at the optimal solution in 6.95 seconds. Here, the average dimension of the search space is 435, as there are 435 enrolled users in this dataset. After applying the proposed search space-reduction approach (Section 6.2.1), the average dimension of the search space is reduced to 46 (rounded off to the nearest integer). Due to the achieved reduction in average dimension of the search space, the proposed RQ-PSO based rank level fusion approach takes only 1088 number of iterations on an average (rounded off to the nearest integer) to find the optimal solution. Furthermore, the significant improvement in the average execution time due to

Table 6.5: Performance comparison of the existing rank and score level fusion approaches with the proposed RQ-PSO based fusion approaches on virtual multimodal biometric dataset FaceIris-V2 using cumulative recognition accuracies in %

	Methods	Top-1 Rank	Top-2 Ranks	Top-3 Ranks
	Weighted Sum [51]	98.16	98.62	98.62
	Max [1]	93.1	100	100
	Min [1]	94.48	94.71	94.71
	Product [1]	95.17	95.63	96.32
	Sum-OEBA [67]	93.79	94.25	94.48
	Sum-MOEBA [67]	94.71	95.4	95.63
	Sum-OEVBA [82]	94.71	95.4	95.63
	Hamacher t-norm [69]	95.17	95.86	96.32
	Frank t-norm [69]	95.17	95.63	95.86
	WQAM cos [62]	98.16	98.85	98.85
Score Level	$WQAM \ cos^r \ [62]$	98.85	99.31	99.31
	WQAM tan [62]	99.31	100	100
	WQAM sin [62]	97.24	97.47	97.7
	WQAM $r^{1/s}$ [62]	98.85	99.31	99.31
	$\overline{\text{WQAM } r^s \text{ [62]}}$	98.39	99.08	99.08
	WQAM s^r [62]	98.16	99.08	99.08
	WQAM log [62]	98.16	99.08	99.08
	$WQAM \exp [62]$	98.16	98.85	98.85
	PSO Score (Section 4.3)	96.32	98.85	99.08
	Q-PSO Score (Section 5.3.2)	99.31	99.31	99.31
	Proposed RQ-PSO Score	99.31	99.31	99.31
	Borda Count [34]	91.49	92.64	93.56
	WBorda [34]	94.94	95.86	96.09
	Highest Rank [35]	93.10	100	100
	Exp [33]	94.48	95.40	95.63
Rank Level	WExp [33]	91.03	91.72	92.41
nank Level	DivExp [32]	94.02	95.17	96.55
	Log [32]	94.94	96.09	97.24
	PSO Rank (Section 3.3)	96.09	98.85	99.08
	Q-PSO Rank (Section 5.3.1)	99.31	99.31	99.31
	Proposed RQ-PSO Rank	99.31	99.31	99.31

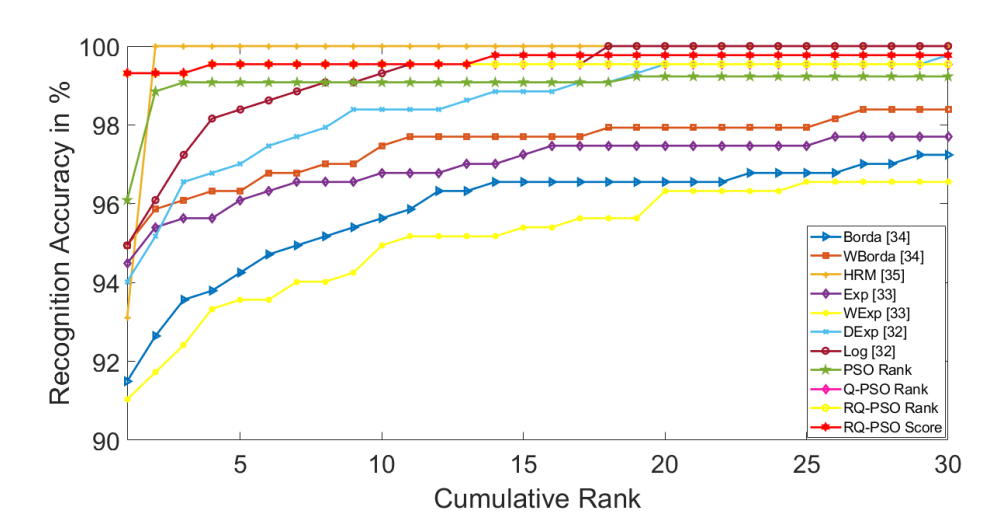


Figure 6.5: CMC plots for existing rank level fusion approaches being compared with that of the proposed RQ-PSO based fusion approaches for second virtual multimodal biometric dataset FaceIris-V2

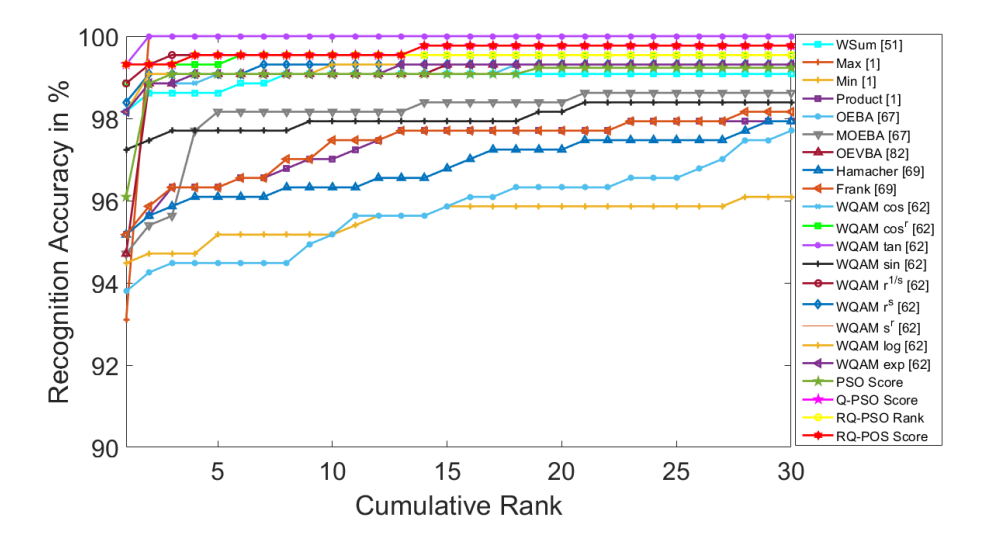


Figure 6.6: CMC plots for existing score level fusion approaches being compared with that of the proposed RQ-PSO based fusion approaches for second virtual multimodal biometric dataset FaceIris-V2

Table 6.6: Performance comparison of PSO based rank (Section 3.3) and PSO based score (Section 4.3) level fusion approaches with the proposed RQ-PSO based fusion approaches on virtual multimodal dataset FaceIris-V2 using average number of iterations, average execution time and average dimension of search space

Methods	Average number of iterations to converge (rounded off	Average execution time	Average dimension of search space (rounded off to
	to the nearest integer)	(seconds)	the nearest integer)
PSO Rank (Section 3.3)	3054	6.95	435
Proposed RQ-PSO Rank	1088	0.65	46
PSO Score (Section 3.3)	984	0.35	435
Proposed RQ-PSO Score	259	0.07	46

reduced dimension is also seen in Table 6.6. The proposed RQ-PSO based rank level fusion approach takes 0.65 seconds on an average to find the optimal solution.

Similar observations are reported in Table 6.6 for PSO based score level fusion approach (Section 4.3) and the proposed RQ-PSO based score level fusion approach. The PSO based score level fusion approach (Section 4.3) takes 984 iterations (rounded off to the nearest integer) on an average to reach at an optimal solution in 0.35 seconds. Here, the average dimension of the search space is 435, as there are 435 enrolled users in this dataset. After applying the proposed search space-reduction approach (Section 6.2.2), the average dimension of the search space is reduced to 46 (rounded off to the nearest integer). Due to the achieved reduction in average dimension of search space, the proposed RQ-PSO based score level fusion approach takes only 259 number of iterations on an average (rounded off to the nearest integer) to find the optimal solution. Furthermore, the significant improvement in the average execution time due to reduced dimension is also seen in Table 6.6. The proposed RQ-PSO based score level fusion approach takes 0.07 seconds on an average to find the optimal solution. It is also noted that the proposed RQ-PSO Score based approach executes faster (average execution time 0.07 seconds) than the proposed RQ-PSO Rank based approach (average execution time 0.65 seconds). Moreover, the reduced dimension of search space for both the approaches (RQ-PSO Rank and RQ-PSO Score) is same. This is because the search space-reduction approach for score level fusion (Section 6.2.2) converts the score lists into rank-ordered lists and then use the steps as similar to the search space-reduction approach for rank level fusion (Section 6.2.1) to reduce the dimension of the search space.

Table 6.7: Recognition accuracies (in %) of the proposed search space-reduced quality-incorporated PSO based fusion approaches with respect to those of unimodal matchers on NIST BSSR1 multimodal dataset (set 1)

	Method	Top-1 Rank	Top-2 Ranks	Top-3 Ranks
	Face Matcher G	83.37	86.28	88.40
Unimodal	Face Matcher C	88.78	90.52	91.50
Ullillodai	Left Fingerprint	85.70	87.04	87.81
	Right Fingerprint	92.07	93.23	93.62
Proposed PSO Rank Fusion		99.42	99.42	99.42
Proposed PSO Score Fusion		99.42	99.42	99.42

6.4.3 Fusion of Multimodal Biometrics Involving Face and Fingerprint (NIST BSSR1 Multimodal Dataset (Set 1))

The performances of the proposed search space-reduced quality-incorporated PSO based fusion approaches for rank level (RQ-PSO Rank) and score level (RQ-PSO Score) are also evaluated on NIST BSSR1 multimodal dataset (set 1) [193]. This dataset contains four modalities. Hence, four score lists are provided in this dataset for each probe. Four rank lists are constructed for each probe from the above score lists. A brief description of this dataset can be found in Section 3.2.2.2. Similar to above two virtual datasets, the sizes of these score and rank lists are reduced using the proposed search space-reduced approach (Section 6.2). These reduced rank lists are considered as inputs to the proposed search spacereduced quality-incorporated PSO based rank level fusion approach (RQ-PSO Rank) in Section 6.3.1 and other existing rank level fusion approaches as discussed in Section 3.2.2.1. The window size on number of iteration to decide the convergence of the RQ-PSO Rank based fusion approach is experimentally decided as 200 for this dataset. Similarly, these reduced score lists are combined using the proposed search space-reduced quality-incorporated PSO based score level fusion approach (RQ-PSO Score) in Section 6.3.2 and other existing rank level fusion approaches in Section 3.2.2.1. The window size on number of iteration to decide the convergence of the proposed RQ-PSO Score based fusion approach is experimentally decided as 200 for this dataset.

Table 6.8: Performance comparison of the existing rank and score level fusion approaches with the proposed RQ-PSO based fusion approaches on NIST BSSR1 multimodal dataset (set 1) using cumulative recognition accuracies in %

	Methods	Top-1 Rank	Top-2 Ranks	Top-3 Ranks
	Weighted Sum [62]	99.23	99.23	99.23
	Max [1]	79.90	94.00	98.85
	Min [1]	94.80	95.40	95.60
	Product [1]	97.87	98.26	98.67
	Sum-OEBA [67]	99.03	99.03	99.26
	Sum-MOEBA [67]	98.45	98.84	98.84
	Sum-OEVBA [82]	98.70	99.03	99.26
	Hamacher t-norm [69]	97.29	97.68	97.68
	Frank t-norm [69]	98.07	98.65	98.84
Score Level	WQAM cos [62]	99.42	99.42	99.42
Score Level	$WQAM cos^r [62]$	99.23	99.42	99.42
	WQAM tan [62]	99.42	99.42	99.42
	WQAM sin [62]	99.42	99.42	99.42
	WQAM $r^{1/s}$ [62]	99.42	99.42	99.42
	$\overline{\text{WQAM } r^s \text{ [62]}}$	99.42	99.42	99.42
	$WQAM s^r [62]$	99.42	99.42	99.42
	WQAM log [62]	99.42	99.42	99.42
	WQAM exp [62]	99.42	99.42	99.42
	PSO Score (Section 4.3)	99.42	99.42	99.42
	Q-PSO Score (Section 5.3.2)	99.42	99.42	99.42
	Proposed RQ-PSO Score	99.42	99.42	99.42
	Borda Count [34]	92.07	93.04	94.00
	WBorda [34]	92.84	95.02	95.87
	Highest Rank [35]	79.70	94.81	98.26
	Exp [33]	89.16	90.27	91.88
Rank Level	WExp [33]	88.00	89.23	90.95
	DivExp [32]	99.42	99.42	99.42
	Log [32]	98.76	99.23	99.23
	PSO Rank (Section 3.3)	99.42	99.42	99.42
	Q-PSO Rank (Section 5.3.1)	99.42	99.42	99.42
	Proposed RQ-PSO Rank	99.42	99.42	99.42

The recognition accuracies (in %) for the proposed search space-reduced quality-incorporated PSO based fusion approaches at rank level (RQ-PSO Rank) and at score level (RQ-PSO Score) as well as each unimodal matcher are presented in Table 6.7 for NIST BSSR1 multimodal dataset (set 1) [193]. These recognition accuracies are reported for the probe being found within top-1, top-2 and top-3 ranks (cumulative) in the aggregated rank lists and score lists. The usefulness of the proposed fusion approaches over each of the unimodal matchers is obvious from the reported results in Table 6.7.

Furthermore, the recognition accuracies of the comparing approaches within top-1, top-2 and top-3 positions along with the proposed approaches are presented in Table 6.8. It can be seen from the reported recognition accuracies that the proposed search space-reduced quality-incorporated PSO based fusion approaches at rank level (RQ-PSO Rank) and at score level (RQ-PSO Score) perform better than majority of state-of-the-art rank and score level fusion approaches except several WQAM based score level fusion approaches [62]. Moreover, it can also be observed from the Table 6.8 that the recognition accuracies of the proposed RQ-PSO Rank (Section 6.3.1) and RQ-PSO Score (Section 6.3.2) based approaches after reducing the dimension of the search space remain as same as those of quality-incorporated PSO based fusion approaches at rank level (Q-PSO Rank) (Section 5.3.1) and at score level (Q-PSO Score) (Section 5.3.2).

The changes in recognition accuracies (in %) with the changes in cumulative ranks are represented using cumulative match characteristic (CMC) curves in Fig. 6.7 and Fig. 6.8. The proposed search space-reduce quality-incorporated PSO based fusion approaches for rank level (RQ-PSO Rank) and score level (RQ-PSO Score) outperform majority of rank and score level fusion approaches, as it can be observed in the CMC curves in Fig. 6.7 and Fig. 6.8. The CMC curves of several WQAM approaches [62] (Fig. 6.8) overlap with those of the proposed RQ-PSO rank and RQ-PSO Score fusion approaches as well as with those of the Q-PSO Rank (Section 5.3.1) and Q-PSO Score (Section 5.3.2) based fusion approaches.

The effectiveness of the proposed search space-reduction approaches (Section 6.2) in achieving speed up of execution is presented in Table 6.9. It can be observed from the table that average number of iterations to converge for each of the proposed RQ-PSO based rank and score level fusion approaches significantly improves by using the proposed space-reduction approach (Section 6.2). The PSO based rank level fusion approach (Section 3.3) takes 1240 iterations (rounded off to the nearest integer) on an average to reach at an optimal solution in 5.10 seconds. Here, the dimension of search space is 517, as there are 517 enrolled users in this

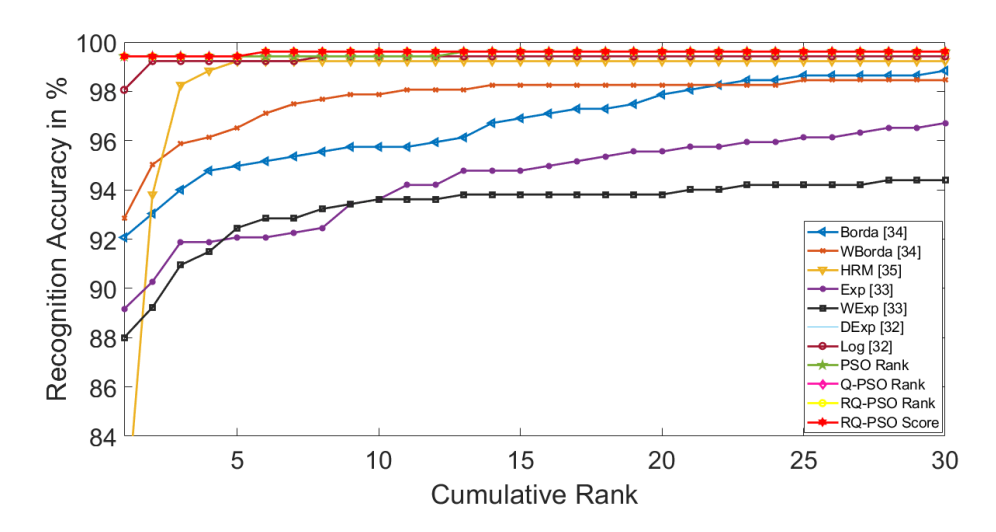


Figure 6.7: CMC plots for existing rank level fusion approaches being compared with that of the proposed RQ-PSO based fusion approaches for NIST BSSR1 multimodal dataset (set 1)

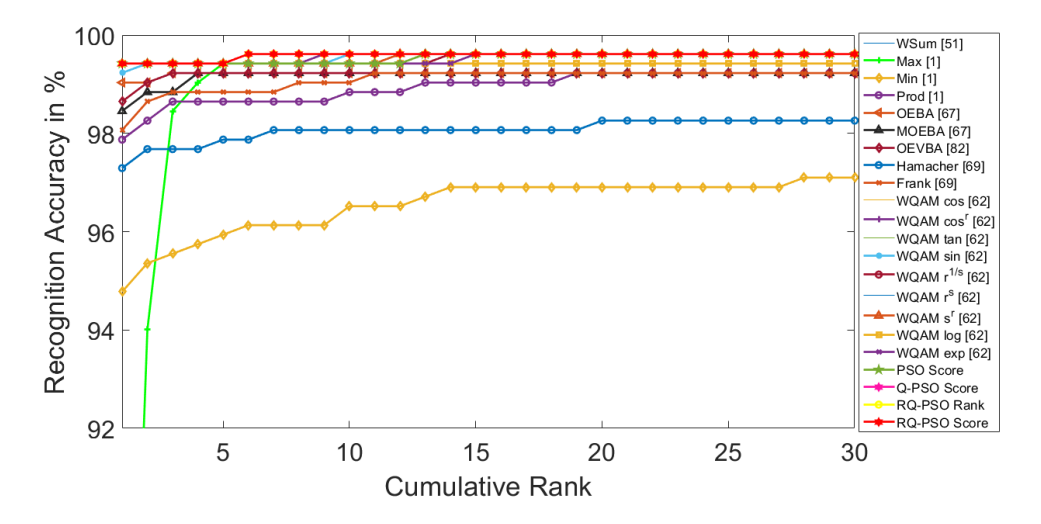


Figure 6.8: CMC plots for existing score level fusion approaches being compared with that of the proposed RQ-PSO based fusion approaches for NIST BSSR1 multimodal dataset (set 1)

Table 6.9: Performance comparison of PSO based rank (Section 3.3) and PSO based score (Section 4.3) level fusion approaches with the proposed RQ-PSO based fusion approaches on NIST BSSR1 multimodal dataset (set 1) using average number of iterations, average execution time and average dimension of search space

Methods	Average number of iterations to converge (rounded off	Average execution time	Average dimension of search space (rounded off to
	to the nearest integer)	(seconds)	the nearest integer)
PSO Rank (Section 3.3)	1240	5.10	517
Proposed RQ-PSO Rank	831	1.71	142
PSO Score (Section 4.3)	1874	1.45	517
Proposed RQ-PSO Score	1328	0.69	142

dataset. After applying the proposed search space-reduction approach (Section 6.2.1), the average particle dimension is reduced to 142 (rounded off to the nearest integer), as it is reported in Table 6.9. Due to reduction in average dimension of the search space, the proposed RQ-PSO based rank level fusion approach takes only 831 number of iterations (rounded off to the nearest integer) on an average to find the optimal solution. Furthermore, the significant improvement in the average execution time due to reduced dimension is also seen in Table 6.9. The proposed RQ-PSO based rank level fusion approach takes on an average 1.71 seconds to find the optimal solution.

Similar observations are reported in Table 6.9 for PSO based score level fusion approach (Section 4.3) and the proposed RQ-PSO based score level fusion approach. The PSO based score level fusion approach (Section 4.3) takes 1874 iterations (rounded off to the nearest integer) on an average to reach at the optimal solution in 1.45 seconds. Here, the dimension of search space is 517, as there are 517 enrolled users in this dataset. After applying the proposed search spacereduction approach (Section 6.2.2), the average particle dimension is reduced to 142 (rounded off to the nearest integer), as it is reported in Table 6.9. Due to reduction in average dimension of the search space, the proposed RQ-PSO based score level fusion approach takes only 1328 number of iterations (rounded off to the nearest integer) on an average to find the optimal solution. Furthermore, the significant improvement in the average execution time due to reduced dimension is also seen in Table 6.9. The proposed RQ-PSO based score level fusion approach takes on an average 0.69 seconds to find the optimal solution. It is also noted that the proposed RQ-PSO Score based approach executes faster (average execution time 0.69 seconds) than the proposed RQ-PSO Rank based approach (average execution time 1.71 seconds). Moreover, the reduced dimension of search space for both the approaches (RQ-PSO Rank and RQ-PSO Score) is same. This is because the search space-reduction approach for score level fusion (Section 6.2.2) converts the score lists into rank-ordered lists and then use the steps as similar to the search space-reduction approach for rank level fusion (Section 6.2.1) to reduce the dimension of the search space.

6.4.4 Fusion of Multimodal Biometrics for Multiple Gait Feature Representations (OU-ISIR BSS4 Multi-Algorithm Gait Dataset)

The OU-ISIR BSS4 multi-algorithm gait dataset [2, 194]) provides five score lists for each probe. Five rank lists are constructed from the above score lists. for each probe. The sizes of these rank lists are reduced using proposed search spacereduction approach (Section 6.2.1). These reduced rank lists are considered as inputs to the proposed search space-reduced quality-incorporated PSO based rank level fusion approach (RQ-PSO Rank) in Section 6.3.1 and other existing rank level fusion approaches as discussed in Section 3.2.2.1. The window size on number of iteration to decide the convergence of the proposed RQ-PSO Rank based fusion approach is experimentally decided as 1500 for this dataset. Similarly, the sizes of score lists are reduced using proposed search space-reduction approach (Section 6.2.2). These reduced score lists are considered as inputs to the proposed search space-reduced quality-incorporated PSO based score level fusion approach (RQ-PSO Score) in Section 6.3.2 and other existing rank level fusion approaches in Section 3.2.2.1. The window size on number of iteration to decide the convergence of the proposed RQ-PSO Score based fusion approach is experimentally decided as 2000 for this dataset.

The recognition accuracies (in %) for the proposed space-reduced quality-incorporated PSO based fusion approaches at rank level (RQ-PSO Rank) and at score level (RQ-PSO Score) as well as each unimodal matcher are presented in Table 6.10 for OU-ISIR BSS4 multi-algorithm dataset [2, 194]. These recognition accuracies are reported for the probe being found within top-1, top-2 and top-3 ranks (cumulative) in the aggregated rank lists and score lists. The usefulness of the proposed fusion approaches over each of the unimodal matchers is obvious from the reported results in Table 6.10.

Table 6.10: Recognition accuracies (in %) of the proposed search space-reduced quality-incorporated PSO based fusion approaches with respect to those of unimodal matchers on OU-ISIR BSS4 multi-algorithm dataset

	Method	Top-1 Rank	Top-2 Ranks	Top-3 Ranks
	CEnI	80.95	85.50	87.50
	CGI	83.35	87.44	89.04
Unimodal	FDF	85.90	89.87	91.23
	GEI	85.72	89.54	91.20
	GFI	74.92	79.93	82.12
Proposed	d RQ-PSO Rank Fusion	87.10	91.94	92.58
Proposed	d RQ-PSO Score Fusion	87.16	92.08	92.58

Furthermore, the recognition accuracies of the comparing approaches within top-1, top-2 and top-3 positions along with the proposed approaches are presented in Table 6.11. It can be seen from the reported recognition accuracies that the proposed search space-reduced quality-incorporated PSO based fusion approaches at rank level (RQ-PSO Rank) and at score level (RQ-PSO Score) perform better than majority of state-of-the-art rank and score level fusion approaches. Moreover, it can also be observed from the Table 6.11 that the recognition accuracies of the proposed RQ-PSO Rank (Section 6.3.1) and RQ-PSO Score (Section 6.3.2) based approaches after reducing the dimension of the search space remain as same as those of quality-incorporated PSO based fusion approaches at rank level (Q-PSO Rank) (Section 5.3.1) and at score level (Q-PSO Score) (Section 5.3.2).

The changes in recognition accuracies (in %) with the changes in cumulative ranks are represented using cumulative match characteristic (CMC) curves in Fig. 6.9 and Fig. 6.10. The proposed search space-reduced quality-incorporated PSO based fusion approaches for rank level (RQ-PSO Rank) and score level (RQ-PSO Score) outperform existing rank and score level fusion approaches, as it can be observed in the CMC curves in Fig. 6.9 and Fig. 6.10. Moreover, the CMC curves of the proposed RQ-PSO Rank and RQ-PSO Score fusion approaches overlap with those of the Q-PSO Rank (Section 5.3.1) and Q-PSO Score (Section 5.3.2) based fusion approaches.

The effectiveness of the proposed search space-reduction approaches (Section 6.2) in achieving speed up of execution is presented in Table 6.12. It can be

Table 6.11: Performance comparison of the existing rank and score level fusion approaches with the proposed RQ-PSO based fusion approaches on OU-ISIR BSS4 multi-algorithm dataset using cumulative recognition accuracies in %

	Methods	Top-1 Rank	Top-2 Ranks	Top-3 Ranks
	Weighted Sum [51]	86.70	89.69	91.38
	Max [1]	85.38	88.27	89.60
	Min [1]	77.41	88.15	91.60
	Product [1]	77.41	88.21	91.60
	Sum-OEBA [67]	86.08	89.60	91.07
	Sum-MOEBA [82]	86.45	89.75	91.17
	Sum-OEVBA [82]	86.40	89.75	91.19
	Hamacher t-norm [69]	86.37	89.57	91.07
	Frank t-norm [69]	81.63	89.32	91.47
Score Level	WQAM cos [62]	86.70	89.69	91.35
Score Level	$WQAM cos^r [62]$	86.18	89.21	90.34
	WQAM tan [62]	86.27	89.69	91.54
	WQAM sin [62]	86.33	89.54	90.7
	WQAM $r^{1/s}$ [62]	86.73	89.72	91.41
	WQAM r^s [62]	86.73	89.72	91.35
	WQAM s^r [62]	86.70	89.69	91.35
	WQAM log [62]	86.70	89.69	91.35
	$WQAM \exp [62]$	86.70	89.69	91.35
	PSO Score (Section 4.3)	86.95	91.16	92.31
	Q-PSO Score (Section 5.3.2)	87.16	92.08	92.58
	Proposed RQ-PSO Score	87.16	92.08	92.58
	Borda Count [34]	83.63	87.47	88.77
	WBorda [34]	84.93	88.48	89.76
	Highest Rank [35]	77.41	88.15	91.54
	Exp [33]	83.76	87.56	88.41
Rank Level	WExp [33]	81.69	85.32	87.43
	DivExp [32]	86.84	89.94	91.65
	Log [32]	85.89	89.42	90.43
	PSO Rank (Section 3.3)	86.73	91.16	92.31
	Q-PSO Rank (Section 5.3.1)	87.10	91.94	92.58
	Proposed RQ-PSO Rank	87.10	91.94	92.58

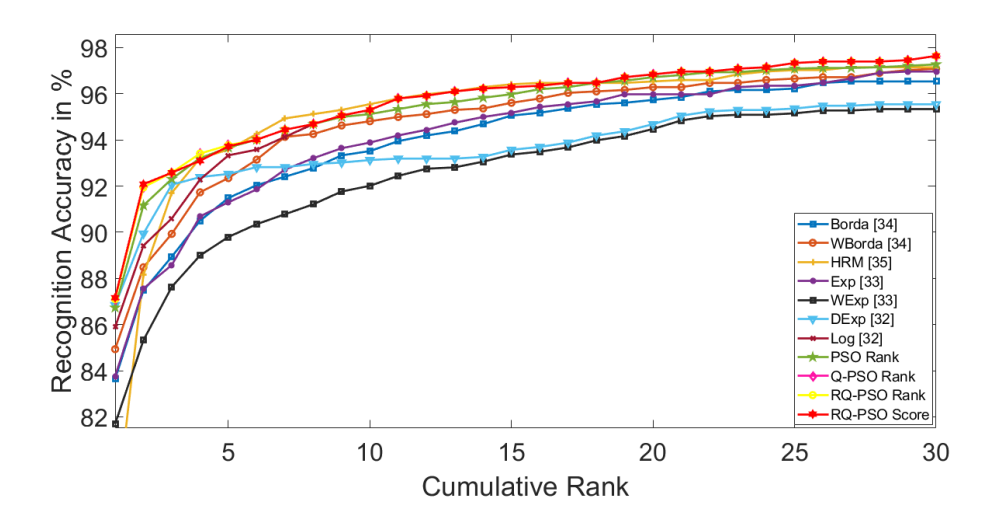


Figure 6.9: CMC plots for existing rank level fusion approaches being compared with that of the proposed RQ-PSO based fusion approaches for OU-ISIR BSS4 multi-algorithm dataset

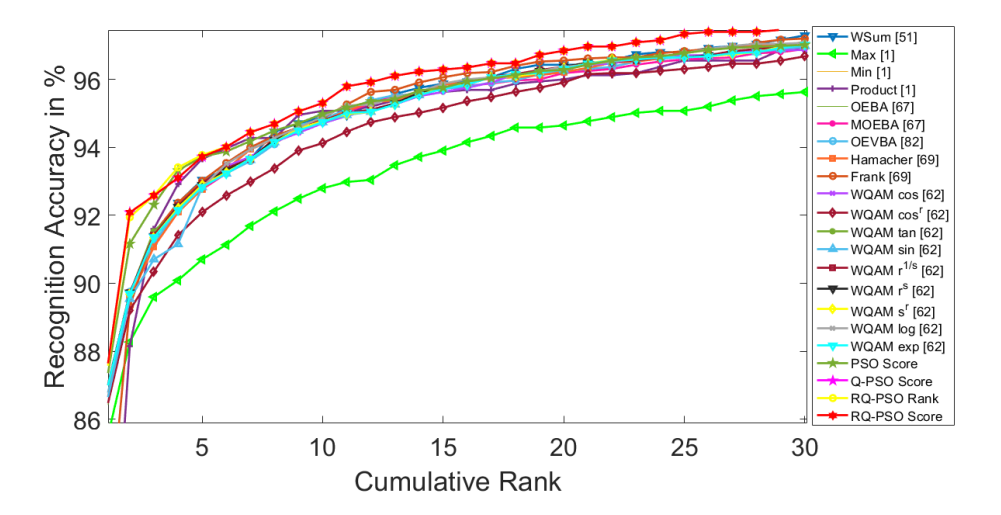


Figure 6.10: CMC plots for existing score level fusion approaches being compared with that of the proposed RQ-PSO based fusion approaches for OU-ISIR BSS4 multi-algorithm dataset

Table 6.12: Performance comparison of PSO based rank (Section 3.3) and PSO based score (Section 4.3) level fusion approaches with the proposed RQ-PSO based fusion approaches on OU-ISIR BSS4 multi-algorithm gait dataset using average number of iterations, average execution time and average dimension of search space

Methods	Average number of iterations to converge (rounded off	Average execution time	Average dimension of search space (rounded off to
	to the nearest integer)	(seconds)	the nearest integer)
PSO Rank (Section 3.3)	7728	106.23	3249
Proposed RQ-PSO Rank	2155	3.79	79
PSO Score (Section 4.3)	7585	16.03	3249
Proposed RQ-PSO Score	3495	2.52	79

observed from the table that average number of iterations to converge for each of the proposed RQ-PSO based rank and score level fusion approaches significantly improves by using the proposed search space-reduction approach (Section 6.2). The PSO based rank level fusion approach (Section 3.3) takes 7728 iterations (rounded off to the nearest integer) on an average to reach at an optimal solution in 106.23 seconds. Here, the dimension of search space is 3249, as there are 3249 enrolled users in this dataset. After applying the proposed search space-reduction approach (Section 6.2.1), the average dimension of search space is reduced to 79 (rounded off to the nearest integer), as it is reported in Table 6.12. Due to reduction in average dimension of the search space, the proposed RQ-PSO based rank level fusion approach takes only 2155 number of iterations (rounded off to the nearest integer) on an average to find the optimal solution. Furthermore, the significant improvement in the average execution time due to reduced dimension is also seen in Table 6.12. The proposed RQ-PSO based rank level fusion approach takes on an average 3.79 seconds to find the optimal solution.

Similar observations are reported in Table 6.12 for PSO based score level fusion approach (Section 4.3) and the proposed RQ-PSO based score level fusion approach. The PSO based score level fusion approach (Section 4.3) takes 7585 iterations (rounded off to the nearest integer) on an average to reach at an optimal solution in 16.03 seconds. Here, the dimension of search space is 3249, as there are 3249 enrolled users in this dataset. After applying the proposed search space-reduction approach (Section 6.2.2) the average dimension of search space is reduced to 79 (rounded off to the nearest integer), as it is reported in Table 6.12. Due to reduction in average dimension of the search space, the proposed RQ-PSO based score level fusion approach takes only 3495 number of iterations

(rounded off to the nearest integer) on an average to find the optimal solution. Furthermore, the significant improvement in the average execution time due to reduced dimension is also seen in Table 6.12. The proposed RQ-PSO based score level fusion approach takes on an average 2.52 seconds to find the optimal solution. It is also noted that the proposed RQ-PSO Score based approach executes faster (average execution time 2.52 seconds) than the proposed RQ-PSO Rank based approach (average execution time 3.79 seconds). Moreover, the reduced dimension of search space for both the approaches (RQ-PSO Rank and RQ-PSO Score) is same. This is because the search space-reduction approach for score level fusion (Section 6.2.2) converts the score lists into rank-ordered lists and then use the steps as similar to the search space-reduction approach for rank level fusion (Section 6.2.1) to reduce the dimension of the search space.

6.5 Summary

Meta-heuristic optimization based approaches search for the optimum solution by iteratively exploring numerous candidate solutions in a large search space. Particle swarm optimization based approaches are not an exception too. It takes a substantial number of iterations for these approaches to converge to the optimum solution (i.e., the aggregated rank list or the aggregated score list). Therefore, novel approaches for search space reduction are proposed in this chapter for attaining faster convergence of the PSO based approaches in the context of rank level and score level fusion in multimodal biometrics. Experimental analysis of the proposed search space-reduced quality-incorporated PSO based rank level and score level fusion approaches shows the effect of reducing the dimension of the search space of PSO based approaches. This reduction in dimension of search space helps in achieving faster convergence (in terms of number of iterations and execution time) than the initial particle swarm optimization based rank level (Section 3.3) and score level (Section 4.3) fusion approaches without any compromise in the recognition accuracies. Additionally, it is also observed that the proposed search space-reduced quality-incorporated score level fusion approach (RQ-PSO Score) requires smaller execution time than the proposed search space-reduced quality-incorporated rank level fusion approach (RQ-PSO Rank) across all four datasets.

Chapter 7

Identifying a Person in Mask: Fusion of Masked Face and Iris for Person Identification in Post-Covid19 Era

In previous chapters, the effectiveness of a search space-reduced quality-incorporated particle swarm optimization (RQ-PSO) based approach for fusion of multimodal biometrics is established in a step-by-step fashion. Moreover, it is also experimentally observed in Section 6.4 that the search space-reduced quality-incorporated particle swarm optimization based score level fusion (RQ-PSO Score) approach (Section 6.3.2) executes faster than the search space-reduced quality-incorporated particle swarm optimization based rank level fusion (RQ-PSO Rank) approach (Section 6.3.1). Therefore, the RQ-PSO Score approach is picked up in this work as a solution to a contemporary challenge in biometric based identification. In the context of Covid19 or any other pandemic where the virus transmits through breathing, people tend to protect themselves and others by wearing face masks. Face mask poses a challenge for face-based identification. Therefore, fusion of masked face and iris modalities is taken up in this chapter as a very relevant use case for fusion of multimodal biometrics using RQ-PSO based score level fusion.

This chapter is organized as following: The relevance of such a fusion in the context of face and iris biometrics is discussed in Section 7.1. An overview of proposed approach for identifying a person wearing a mask is presented in Section 7.2. The approach to generate matching scores for masked face image is presented in Section 7.3. In Section 7.4, approach to generate the matching scores for iris modality is presented. In Section 7.5, the detailed formulation of the score level fusion as an optimization problem is presented. Moreover, the search space-reduced quality-incorporated particle swarm optimization based score level fusion approach is revisited in this section. Experimental results are discussed in Section 7.6. Finally, concluding remarks are drawn in Section 7.7.

7.1 Relevance of the Proposed Fusion Task

Traditionally, a biometric system uses either contact-based (e.g., fingerprint, palm-print, etc.) or contactless (e.g., iris, face etc.) system to establish a person's identity. The ongoing covid19 pandemic [224] has imposed several challenges on the biometric recognition system [225]. The study in [225] shows that the face, fingerprint and voice are the most affected biometric modalities due to covid19. The study also highlights that the contact-based biometric systems have become irrelevant at the time of covid19 outbreak.

Covid19 [224] can easily spread using contact-based biometric systems. Therefore, the ongoing covid19 pandemic has forced the biometric systems to go contactless. Another major covid19 induced change in our day-to-day lifestyle is the use of face and nose protective gears (such as personal protective equipment (PPE), face mask, face shields etc.) to stop the spread of covid19. A face recognition system is generally trained on unmasked face images. Therefore, the changed scenario due to use of face mask significantly reduces the performance of face recognition system. A recent study by National Institute of Standards and Technology (NIST) shows that the pre-covid19 state-of-the-art face recognition systems perform significantly poor with the masked face [226]. Similar studies are also presented in [227, 228].

Recently a masked face recognition challenge has been organized within the international joint conference on biometrics (IJCB 2021) [229]. This challenge has highlighted the major shortcoming of face recognition system due to covid19 outbreak. Several solutions have been presented in this challenge. These solutions have used the ArcFace [215] architecture to identify a person in mask. These models have been trained on synthetically created masked face dataset to improve the recognition accuracy. A convolutional neural network (CNN) based mask aware network (MAN) for masked face recognition has been proposed in [230].

This method puts a mask in a face image. Here, the training data set is augmented with masked faces to improve the performance of a face recognition system. This type of data augmentation have also been used in [231, 232]. A paired differential siamese network (PDSN) based masked face recognition system has been proposed in [231]. Here, the PDSN is used to remove the occluded portion of the image and to highlight only the key features for recognition. In [232], the ArcFace loss has been combined with specially designed mask-usage classification loss to boost the performance of the masked face recognition system.

In a completely different approach, a CNN based template unmasking method is presented in [233]. A self-restrained triplet (SRT) loss function minimizes the intra-class variation between the positive and anchor image pair to enhance the recognition accuracy of face recognition model. Similarly, a generative adversarial network (GAN) based approach is presented in [234] to unmask the masked face image. In contrast, occluded region removal based masked face recognition systems can be found in [235, 236]. Here, the masked or occluded area is cropped. The image containing the remaining face region is then passed to the CNN based model for training and recognition. In [237], a deep-learning based dynamic ensemble model is presented. It dynamically switches to the ocular region for recognition in the presence of face mask.

In post-covid19 era, the iris recognition [5, 7] can emerge as an alternative means for biometric recognition. The iris based biometric recognition systems are unaffected as the iris region is clearly visible in a masked face image. Though the iris based recognition systems have shown improved performance, but this biometric modality faces several challenges. Segmentation of iris region [238, 239] and iris recognition at distance [240] are the major challenges for iris recognition. Therefore, it is important to use a combination of biometric modalities to improve recognition accuracy. Multimodal biometric systems are frequently used for authentication at various establishments [4, 64]. Fusion of face and iris is extensively studied in literature [241, 242] and the results are astonishing. The fusion in multimodal biometrics can be performed at various levels: sensor level, feature level, score level, rank level and decision level (Section 1.2.1). Score level fusion is one of the widely used level of fusion [51, 62, 67, 69, 82]. Therefore, in this work, fusion of masked face and iris is performed at score level to achieve better recognition accuracy as compared to using only a single biometric modality (face or iris) in post-covid19 era.

The current work presents a novel approach involving fusion of masked face and iris to improve recognition performance of the biometric system in post-covid19 era. Here, the generative adversarial network (GAN) based approach [234] is used for mask removal and reconstruction of the face image (unmasking of the face). This unmasked face image is passed to an ArcFace based face recognition system [215] to compute the matching scores for face modality. Similarly, the iris image is passed to the iris recognition system [220] to generate the matching scores for iris modality. For each one of these two modalities, score list is constructed from the matching scores of a probe with every enrolled subject (gallery) in an identification setup. Fusion of these two score lists for unmasked face and iris is performed at score level. Here, the fusion is performed using the search space-reduced quality-incorporated particle swarm optimization based score level fusion (RQ-PSO Score) approach (Section 6.3.2).

7.2 Overview of Person Identification in Masked Face

The use of face mask due to ongoing covid19 pandemic [224] has posed a big challenge to existing face recognition systems. State-of-the-art face recognition systems are not able to correctly identify an enrolled person due to the occlusion created by the masked face images [226, 227, 228]. The complete face information is not present in a masked face image to correctly identify a person. The presented probe with missing biometric information can be complemented by removing the occluded region [235, 236] and by training the face recognition system on these new images. Another approach is the use of other available biometric modalities, such as iris and ocular region [237].

In this work, a multimodal biometric fusion based approach is proposed to solve the problem of person identification in masked faces. Figure 7.1 presents an overview of the proposed approach. This approach contains following three stages: (i) matching score generation for masked face modality, (ii) matching score generation for iris modality and (iii) score level fusion of these two modalities. In the face biometrics stage, a masked face image of probe user is unmasked using a generative adversarial network (GAN) based approach [234]. This generated unmasked face image is passed to the ArcFace based face recognition system [215] to generate the matching scores. The matching scores for all the enrolled users with the probe user construct the matching score list for face modality. In

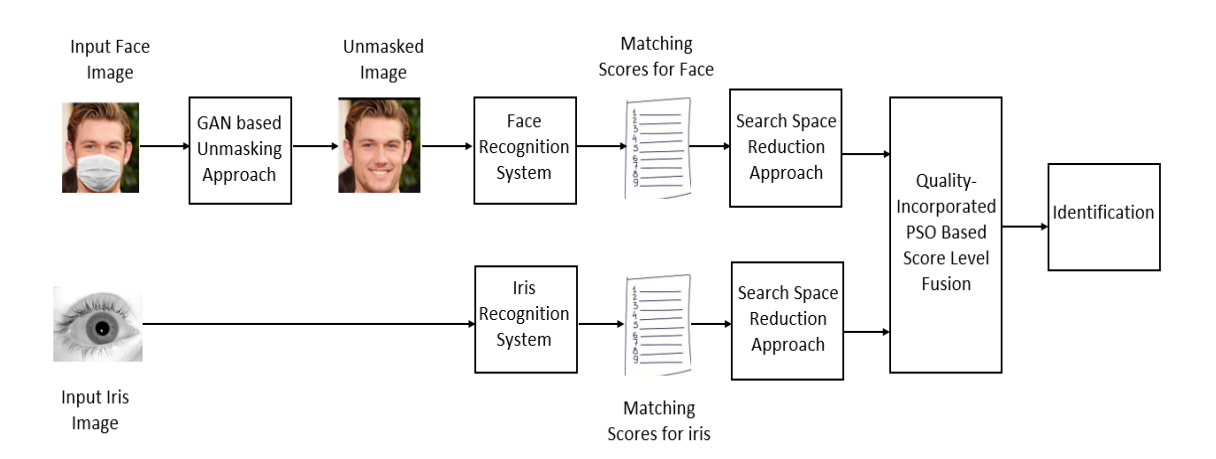


Figure 7.1: Stages of proposed masked face and iris fusion approach

the iris biometrics stage, an iris image of probe user is passed as an input to the iris recognition system [220] and matching scores are generated. The matching scores for all the enrolled users with the probe user construct the matching score list for iris modality. Finally, the matching score lists of both the modalities are fused using search space-reduced quality-incorporated particle swarm optimization based score level fusion (RQ-PSO Score) approach (Section 6.3.2) to identify a person. Details of these stages are presented in subsequent sections.

7.3 Matching Score Generation for Face Modality

A face image of a person wearing mask is captured for person identification. This section narrates the steps of matching score generation of masked face modality.

7.3.1 GAN based Unmasking Approach

At first, the face mask is removed and the complete face is reconstructed using a generative adversarial network (GAN) based approach [234]. This GAN-based unmasking approach is briefly described in this section. This approach takes a masked face as input and works in two steps. The first step finds the masked region in the face image using U-Net model [243]. In the second step, GAN generates the unmasked face image using the mask region and the input masked face

image. This GAN-based approach uses two discriminators. The first discriminator is used for learning global structure of the face. The feedback from the first discriminator helps the generator to generate the unmasked face image. Moreover, the learning of missing region of the masked face due to the mask is carried out using the second discriminator. The second discriminator aids the generator to generate the unmasked image more precisely by incorporating the leaning about the missing region. Detailed description of this adopted GAN-based unmasking approach can be found in [234].

7.3.2 Generating Matching Scores

The proposed approach uses state-of-the-art face embedding approach ArcFace [215] to compute the embedding for the GAN generated unmasked face image. Detailed description of ArcFace can be found in [215]. The cosine similarity [216] between two embeddings for the probe and the gallery produces a matching score. The cosine similarity is widely used similarity metric in the face recognition paradigm [217, 218, 219]. A score list is generated using the matching scores for all the enrolled users with the probe.

7.4 Matching Score Generation for Iris Modality

The iris is visible in spite of wearing a mask. Therefore, the proposed method for person identification in post-covid19 era suggests to consider iris biometrics along with the masked face biometrics. In this work, a state-of-the-art iris recognition system in [220] is adopted for generating the matching scores for iris. The work in [220] is based on fully convolutional network (FCN). The FCN helps in generating spatially corresponding iris feature descriptors. Furthermore, an extended triplet loss (ETL) function accurately differentiates between the iris region and the non-iris region to achieve enhanced iris feature descriptors. These iris features are then binarized. Hamming distance [221] generates the matching score between the binarized iris features of the probe and the gallery. Detailed description of the adopted iris recognition approach can be found in [220]. A score list is generated using the matching scores for all the enrolled users with the probe.

7.5 Score Level Fusion

The last stage of the proposed method is score level fusion. The works in previous chapters have conceptualized the fusion of multimodal biometrics at the score level as an optimization problem. Furthermore, the incorporation of quality-based weight (Section 5.2) and search space-reduction approach (Section 6.2) are the key highlights of the earlier work in Section 6.3.2. The current work formulates the score level fusion of face and iris biometrics as an optimization problem and adopts the approach in Section 6.3.2.

Let S_f and S_i be the generated score lists for face and iris modalities, respectively. The ranges of these matching scores vary due to different similarity measures in these modalities. Therefore, these matching scores are normalized to bring them into a common range. One of the widely used score normalization approach is the min-max normalization [49, 62, 63]. Hence, the min-max normalization approach is adopted in this work to bring these scores in the range between [0,1]. Though other score normalization approaches such as tanh [63], z-score [63] could have also been applied.

It is to be noted that the generated score for face modality (Section 7.3) is a similarity score. On the contrary, the generated score for iris modality (Section 7.4) is a dissimilarity score. Hence, the normalized scores for iris modality are converted to similarity score by subtracting the normalized scores from 1. Let \hat{S}_f and \hat{S}_i be the normalized score lists for face and iris modalities, respectively. A combination of these two normalized score lists generates an aggregated score list. Generation of the aggregated score list is treated as an optimization problem in this work. The objective of this optimization problem is to minimize a weighted summation of distances of the aggregated list from the input normalized score lists \hat{S}_f and \hat{S}_i . The objective function for generating the aggregated score list is stated below:

$$minimize \ \Phi(\delta) = w_f \times d(\delta, \hat{S}_f) + w_i \times d(\delta, \hat{S}_i)$$
(7.1)

A candidate fused score list is represented by δ . Here, weights w_f and w_i are associated with face and iris biometric modalities, respectively. The weight represents the significance of the corresponding biometric modality. The function d() in Eq. 7.1 denotes the distance between an aggregated and the normalized input score lists. In the current work, weighted Spearman footrule [180] metric is used for the distance measure between a pair of score lists. The stated distance

metric estimates the weighted summation of absolute differences between normalized scores of each subject in the concerned pair of lists. The influence factor of a subject in weighted Spearman footrule distance is also calculated using Eq. 4.5.

Finally, a search space-reduced quality-incorporated particle swarm optimization (RQ-PSO) based score level fusion approach (Section 6.3.2) is adopted in this work for solving the stated optimization problem (Eq. 7.1). The superiority of the RQ-PSO based score level fusion approach over existing score and rank level fusion approaches as well as the earlier proposed rank (Chapter 3) and score (Chapter 4) level fusion approaches is experimentally proved in Section 6.4. A particle position in the proposed RQ-PSO based score level fusion approach represents a reduced candidate score list δ . It indicates the similarity scores of the probe with the subjects in reduced score lists. Moreover, the objective function (in Eq. 7.1) of the proposed RQ-PSO Score based approach uses the qualitybased weight to indicate significance of face and iris modalities for a particular probe. In RQ-PSO Score approach, the particle's velocity and position in the solution space are updated iteratively until a stopping criteria is met. The window size on number of iteration to decide the convergence of the adopted RQ-PSO Score based fusion approach is experimentally decided as 100 for this dataset. When the personal best positions of all the particles do not change over a certain period of iterations, the proposed search space-reduced quality-incorporated particle swarm optimization based score level fusion approach is considered to have converged.

7.6 Performance Evaluation and Discussion

Performance of the proposed approach is experimentally presented in this section. A virtually created multimodal biometric dataset FaceIris-V2 is used for this purpose. The virtual dataset contains CelebFaces Attributes face dataset (CelebA) [212] and IIT Delhi iris dataset [211]. Description of this virtual data set is provided in Section 5.4.2.

7.6.1 Experimental Setup

The experimental setup of the proposed work is presented in this sections.

			9.6	
00	0.02	-0.01	-0.03	0.09
	0.07	-0.01	0.02	0.07
96	0.01	0.01	-0.03	-0.06
	0.04	0.01	0.05	0.03

Figure 7.2: Similarity scores between masked face images (probe) and corresponding gallery images

7.6.1.1 Generating Masked Face Dataset

The major challenge faced by masked face recognition system is lack of large scale masked face dataset. Therefore, several researches [232, 233, 235] have used synthetically applied mask face dataset for training the model. To carry out the experiments in this work, a similar approach is used. The mask is applied on all the selected images of CelebA face dataset [212] using synthetic mask generation approach [244]. The synthetic mask generation approach is widely used by researchers [229, 232] to generate synthetic masked face dataset.

7.6.1.2 Division of Dataset

The selected images from CelebA face dataset [212] containing 435 classes are divided into training (gallery) and test (probe) set. The training set contains 9565 masked face images and corresponding ground truth face images (without mask). The test set contains 435 masked face images corresponding to 435 classes. The training dataset is used to train the GAN based model [234]. The evaluation of trained model is performed on the test (probe) dataset.

7.6.2 Experimental Results

In this work, at first, the effect of mask on the face recognition system is studied. For the person identification task, the masked face (probe) is compared with the gallery face images (without mask). The similarity scores for few such probe images with their ground truth are illustrated in Fig. 7.2. It can be observed form

			96	
E	0.65	0.18	0.08	-0.01
	0.02	0.63	0.15	0.10
96	0.07	0.14	0.55	0.15
	0.04	0.10	-0.04	0.67

Figure 7.3: Similarity scores between unmasked faces images and corresponding gallery images

the presented similarity scores in Fig. 7.2 that the ArcFace based face recognition system [215] is not able to correctly identify the genuine subject from the gallery.

Therefore, the proposed method involves an unmasking stage using a GAN based approach [234]. Figure 7.3 illustrates the similarity scores of unmasked face images as probe against the gallery images (without mask). It is to be noted that these unmasked face images in Fig. 7.3 correspond to the masked face images of Fig. 7.2. It is observed from the Fig. 7.3 that the unmasked face images are close to the actual images (gallery). Therefore, persons are correctly identified based on the similarity scores in Fig. 7.3. Thus, the results establish the effectiveness of GAN based approach [234] to generate the unmasked face images from the masked images.

Furthermore, the fusion of unmasked face and iris modalities is performed using the search space-reduced quality-incorporated particle swarm optimization (RQ-PSO) based score level fusion (Section 6.3.2). The subject having the highest score in the fused list is identified as a match for the probe. Performance of the proposed approach is compared against the performances of state-of-the-art score and rank level fusion approaches as discussed in Section 3.2.2.1. The effect of combining unmasked face and iris modalities using the proposed as well as state-of-the-art score and rank level fusion approach is presented in Table 7.1. The performance of each approach is represented as its ability to recognize a probe correctly. Recognition accuracy (in %) is used as the metric for performance comparison. It is observed from Table 7.1 that fusion of face and iris modalities achieves better recognition accuracy than using only the face modality. Additionally, experiments are performed without removing the mask. The recognition

Table 7.1: Performance comparison (recognition accuracies in %) of the adopted RQ-PSO based score level fusion approach and state-of-the-art score and rank level fusion approaches in the context of masked face and unmasked face and iris

Method		Masked Face and Iris	Unmasked Face and Iris
		Fusion	Fusion
Unimodal	Face	0.92	88.05
	Iris	89.66	89.66
Score Level	Weighted Sum [51]	59.77	96.32
	Max Rule [1]	89.66	90.35
	Min Rule [1]	4.37	91.72
	Product Rule [1]	8.28	92.41
	Sum-OEBA [67]	7.36	89.89
	Sum-MOEBA [67]	54.02	92.41
	Sum-OEVBA [82]	78.62	92.18
	Hamacher t-norm [69]	7.57	92.18
	Frank t-norm [69]	8.28	92.41
	WQAM cos [62]	63.22	96.32
	WQAM cos^r [62]	57.24	97.01
	WQAM tan [62]	63.22	97.24
	WQAM sin [62]	36.55	94.02
	WQAM r^(1/s) [62]	69.89	97.01
	WQAM r^s [62]	66.44	96.55
	WQAM s^r [62]	56.09	96.55
	WQAM log [62]	51.49	96.09
	WQAM exp(-r/s) [62]	64.37	96.55
Rank Level	Borda Count [34]	5.29	91.26
	Weighted Borda [34]	14.02	93.10
	Highest Rank [35]	89.66	90.35
	Exponential [33]	3.91	92.41
	Weighted Exponential [33]	4.14	88.74
	Division Exponential [32]	39.54	94.02
	Logarithm [32]	10.58	92.87
RQ-PSO	Score (Section 6.3.2)	78.62	97.93

accuracies for masked face and iris fusion are also presented in Table 7.1 for the RQ-PSO based score level fusion approach (Section 6.3.2) and state-of-the-art score and rank level fusion approaches.

There are a few interesting observations in Table 7.1. (i) The recognition accuracy of only masked face modality is very less (0.92%). It establishes the known fact that a masked face can not be used for person identification. (ii) Recognition accuracy using iris modality is 89.66%. The adopted RQ-PSO score level fusion approach as well as state-of-the-art fusion approaches perform worse than the individual iris modality. This is because the masked face modality brings down the performances of the fusion based approaches. Though the fusion based approaches perform much better than only masked face modality, iris modality is the best method for person identification in the presence of face mask. (iii) The recognition accuracy of the face modality after unmasking the face image has significantly increased from 0.92% to 88.05% (Table 7.1). It justifies the usefulness of the GAN based unmasking of the masked faces. (iv) Fusion based approaches of unmasked face and iris modalities perform even better than individual unmasked face or iris modalities. This justifies the usefulness of multimodal biometrics over unimodal biometrics. (v) The adopted RQ-PSO based score level fusion approach achieves better performance than state-of-the-art score and rank level fusion approaches. At the end, the experimental results establish the superiority of the adopted GAN based unmasking of face and RQ-PSO based score level fusion of unmasked and iris biometrics.

7.7 Summary

The major contributions of this chapter are summarized in this section. In this work, a novel approach involving fusion of masked face and iris is presented to improve recognition performance of the biometric system in post-covid19 era. A GAN based approach [234] is suggested to generate the unmasked face images. The score level fusion is conceptualized as an optimization problem. Furthermore, a search space-reduced quality-incorporated particle swarm optimization (RQ-PSO) based score level fusion approach (Section 6.3.2) is adopted to solve the stated optimization problem. The reported experimental results highlight that the fusion of masked face (through GAN based unmasking) and iris achieves better recognition accuracy in post-covid19 era. The adopted RQ-PSO based score level fusion approach also exhibits superior performance than the existing score and

rank level fusion approaches. This justifies the adaptation of a novel RQ-PSO based score level fusion approach in this work. Therefore, the proposed fusion of masked face (through GAN based unmasking) and iris using RQ-PSO based score level fusion can be utilized to identify a person wearing mask in post-covid19 era.

Chapter 8

Conclusion and Future Work

In this chapter, concluding remarks are presented on the research works being presented in the thesis. This chapter is organized in following two sections: A summary of the contributions of the works in this thesis is presented in Section 8.1. Finally, a few glimpses on future research directions are placed in Section 8.2.

8.1 Summary of Contributions

In a multimodal biometric system, fusion of biometric information from various modalities can be performed at five different levels: sensor, feature, score, rank and decision level. These levels of fusion are stated in Section 1.2.1. The score level and rank level fusion are widely used levels of fusion for multimodal biometrics. Therefore, the scope of the research work in this thesis is also centred around the score and rank level fusion.

At first, the rank level fusion in multimodal biometrics is formulated as an optimization problem. The formulation of this optimization problem considers minimization of a weighted summation of distances between the aggregated rank list and the input rank lists. This problem formulation adds novelty to the proposed works in Chapter 3. The weighted Spearman footrule distance metric [180] is used to compute the distance between two rank lists. The weight in the weighted Spearman footrule distance is incorporated to ensure more influence of a better ranked subject than other subjects. A novel way to decide the weight of a subject is conceptualized in this context. To solve the stated optimization problem in the context of rank level fusion of multimodal biometrics,

two novel approaches are proposed using genetic algorithm (GA) and particle swarm optimization (PSO). Context-specific representation of a candidate solution and custom-designed operators are the highlights of the proposed GA and PSO based approaches. The proposed approaches are tested using two different multi-biometric datasets, namely (i) NIST BSSR1 multimodal dataset (set 1) [193] involving fingerprint and face modalities and (ii) OU-ISIR BSS4 multi-algorithm gait dataset [2, 194] involving several gait feature extraction methods. These approaches exhibit better performance in identifying the subjects than majority of the existing approaches of fusion at rank and at score levels for multimodal biometrics. Moreover, it is experimentally observed that the proposed particle swarm optimization based approach achieves faster convergence than the proposed genetic algorithm based approach. This superiority of the proposed PSO based approach over the proposed GA based approach in terms of execution time is established using two-sample Kolmogorov-Smirnov (K-S) test.

Similar to the work in Chapter 3, the score level fusion for multimodal biometrics is formulated as an optimization problem in Chapter 4. The formulation of this optimization problem considers minimization of a weighted summation of distances between the aggregated score list and the normalized input score lists. This problem formulation adds novelty to the proposed works in this chapter. The weighted Spearman footrule distance metric [180] is used to compute the distance between two score lists. The weight in the weighted Spearman footrule distance is incorporated to ensure more influence of a high scoring subject than other subjects. A novel way to decide the weight of a subject is conceptualized in this context. To solve the stated optimization problem, two novel score level fusion approaches based on (i) genetic algorithm (GA) and (ii) particle swarm optimization (PSO) are proposed in Chapter 4. Context-specific representation of a candidate solution and custom-designed operators are the highlights of the proposed GA and PSO based score level fusion approaches. The work in Chapter 4 is also experimentally evaluated on two different multimodal biometric datasets, namely (i) NIST BSSR1 multimodal dataset (set 1) [193] and (ii) OU-ISIR BSS4 multi-algorithm gait dataset [2, 194]. The proposed approaches exhibit better performance in identifying the subjects than majority of the existing approaches of fusion at rank and score levels for multimodal biometrics. The reported experimental results in Section 4.3.2 also show that the particle swarm based fusion approaches at both rank (Section 3.3) and score (Section 4.3) levels of fusion perform better than the proposed genetic algorithm based fusion approaches (rank and score level) in terms of recognition accuracy. Therefore, particle swarm optimization based score and rank level fusion approaches are adopted in all the subsequent chapters. It is additionally to be noted that particle swarm optimization based score level fusion approach (Section 4.3) converges faster than particle swarm optimization based rank level fusion approach (Section 3.3).

Particle swarm optimization based fusion approaches at both rank (Section 3.3) and score (Section 4.3) levels of fusion perform better than state-of-the-art rank and score level fusion approaches in terms of recognition accuracy. The reported results also show significant improvement in performances of the proposed optimization based fusion approaches (score and rank level) in spite of considering same weight to each input list. In Chapter 5, the performances of these particle swarm optimization based approaches at both rank (Section 3.3) and score (Section 4.3) levels of fusion are further enhanced by incorporating the quality-based weight for each modality. A novel modality-independent biometric quality estimation approach is proposed in this chapter to enhance the performance of PSO based rank and score level fusion approaches. The derived quality is used to estimate weight for each modality. The proposed approach for estimating quality of biometric information in a probe signal uses matching scores between a probe and the gallery. Therefore, the set of estimated weights vary across different probe users. The presented experimental results highlight the efficacy of incorporating quality-derived weight as compared to several weighting strategies.

It is to be noted that particle swarm optimization (PSO) is an iterative search based optimization algorithm. It searches for the optimum solution by iteratively searching through numerous candidate solutions in a large search space. It takes a substantial number of iterations to converge to the optimum solution (i.e., the aggregated rank list or the aggregated score list). Therefore, a novel approach for search space reduction is proposed in Chapter 6 for attaining faster convergence of the PSO based approaches in the context of above mentioned fusion tasks. It has been shown in Chapter 5 that quality-incorporated PSO (Q-PSO) based rank level and score level fusion approaches achieve better recognition accuracies than the initial PSO based approaches in Section 3.3 and Section 4.3. Hence, the presented work in this chapter is based on the Q-PSO based approaches for rank level and score level fusion. Experimental analysis of the proposed search space-reduced quality-incorporated particle swarm optimization (RQ-PSO) based rank level and score level fusion approaches shows the effect of reducing search space of PSO based approaches. The RQ-PSO based approaches achieve faster convergence than the quality-incorporated particle swarm optimization based rank level and

score level fusion approaches without any decrease in the recognition accuracies. Moreover, the proposed RQ-PSO Score approach performs slightly better than the proposed RQ-PSO Rank approach in two out of four datasets.

Finally, the proposed concepts on fusion of multimodal biometrics are applied to the task of person identification in the era of covid-19 pandemic or similar situations where persons are using face masks. A novel approach involving fusion of masked face and iris is presented to improve recognition performance of the biometric system in post-covid19 era. A generative adversarial network (GAN) based approach [234] is used to generate the unmasked face images. Then, two score lists are generated for the face and the iris modalities. Hereafter, a search space-reduced quality-incorporated particle swarm optimization (RQ-PSO) based score level fusion approach (Section 6.3.2) is adopted to fuse the normalized score lists of face and iris modalities. The adopted RQ-PSO based score level fusion approach exhibits superior performance than the existing score and rank level fusion approaches. This justifies the adaptation of a novel RQ-PSO based score level fusion approach in this work. Therefore, the proposed fusion of masked face (through GAN based unmasking) and iris using RQ-PSO based score level fusion can be utilized to identify a person wearing mask in post-covid19 era.

At the end, it is to be noted that the proposed works in this thesis relate to an identification task. In an identification task, a probe is compared with all the enrolled subjects in the gallery. On the contrary, in a verification task, a probe is compared with one enrolled subject whose identity is being claimed. Therefore, verification task does not generate any score or rank list for the probe. Hence, the proposed works are not applicable for a verification task. It is to be additionally noted that the proposed works are related with a closed-set identification problem, where the probe subject is definitely present in the gallery.

8.2 Future Research Directions

In this section, a few points are stated as a continuation of this research work in future. These research directions are listed here:

• The proposed works in this thesis formulate the tasks of score level and rank level fusion of multimodal biometrics as a single objective optimization problem. Here, a weighted summation of distances between an aggregated list and the input lists is minimized. Alternatively, the score and rank level fusion of multimodal biometrics can be conceptualized as multi-objective

optimization problems. In a multi-objective optimization setting, all the distances between an aggregated list and the input lists are minimized individually.

- Parallel implementations of the evolutionary-computing based approaches [205, 206, 207] can be adopted to speed up the proposed approaches for fusion of multimodal biometrics at rank level and at score level.
- Quality of biometric signal significantly influences the performance of a biometric system. There have been works on estimating the quality of biometric signal [158, 159, 160, 176]. Moreover, one matching score based (hence modality-independent) approach to estimate the quality of biometric signal is proposed in Chapter 5. This area requires further attention of the researchers. Specifically, deep learning based approaches may be explored. Few deep learning based approaches for quality estimation exist in literature [165, 178, 179]. But these approaches of quality estimation are modality dependent. Usage of deep learning for modality-independent quality estimation may be explored in future.
- The covid19 has changed the way of using biometric system. Face modality is one of the most affected biometric modality due to the presence of face mask [226, 227, 228]. Other biometric modalities can replace or can be combined with face modality for better performance. Thus, further research can be made in the direction of combining various biometric modalities (iris, gait, soft biometrics) to identify a person in current era [235, 236, 245, 246].
- Accurately identifying a person in wild scenarios (on street, parking area, public places) [247, 248] can be studied. Furthermore, the real world applications of biometrics (such as emigration, border control, welfare schemes, banking and other financial operations) [4, 7, 247] can be better understood and better solutions can be presented.

List of Publications

Journals

- 1. Shadab Ahmad, Rajarshi Pal, and Avatharam Ganivada, Rank Level Fusion of Multimodal Biometrics using Genetic Algorithm, Multimedia Tools and Applications, Springer, pages:1-28, 2022. Indexed in: SCIE, Scopus, DBLP. Status: Accepted and Published
- 2. Shadab Ahmad, Rajarshi Pal, and Avatharam Ganivada, Score Level Fusion of Multimodal Biometrics using Particle Swarm Optimization, Pattern Recognition, Elsevier, 2022. Indexed in: SCI, Scopus. Status: Under Review

Conference Proceedings

- 1. Shadab Ahmad, Rajarshi Pal, and Avatharam Ganivada, Rank Level Fusion of Multimodal Biometrics Based on Cross-Entropy Monte Carlo Method, Proceedings of Signal Processing and Intelligent Recognition Systems, Springer, pages: 64-74, 2019. Indexed in: DBLP, Scopus. Status: Accepted and Published
- 2. Shadab Ahmad, Rajarshi Pal, and Avatharam Ganivada, Score Level Fusion of Multimodal Biometrics Using Genetic Algorithm, Proceedings of IEEE Congress on Evolutionary Computation, IEEE, pages: 2242-2250, 2021. Indexed in: DBLP, Scopus. Status: Accepted and Published
- 3. Shadab Ahmad, Rajarshi Pal, and Avatharam Ganivada, Rank Level Fusion of Multimodal Biometrics using Particle Swarm Optimization, Proceedings of 9th International Conference on Pattern Recognition

- and Machine Intelligence, Springer, 2021. Indexed in: DBLP. Status: Accepted and In press
- 4. Shadab Ahmad, Kunal Burgul, Rajarshi Pal, and Avatharam Ganivada; Identifying a Person in Mask: Fusion of Masked Face and Iris for Person Identification in Post-Covid19 Era, Proceedings of 16th Asian Conference on Computer Vision, Springer, 2022. Indexed in: DBLP. Status: Communicated

References

- [1] ARUN A ROSS, KARTHIK NANDAKUMAR, AND ANIL K JAIN. *Handbook of multibiometrics*. Springer, 2006.
- [2] HARUYUKI IWAMA, MAYU OKUMURA, YASUSHI MAKIHARA, AND YASUSHI YAGI. The OU-ISIR gait database comprising the large population dataset and performance evaluation of gait recognition. *IEEE Transactions on Information Forensics and Security*, **7**(5):1511–1521, 2012.
- [3] UNIQUE IDENTIFICATION AUTHORITY OF INDIA, GOVERNMENT OF INDIA. About UIDAI. https://uidai.gov.in/about-uidai.html. Online; accessed 10 April 2022.
- [4] NATIONAL ECONOMIC AND DEVELOPMENT AUTHORITY, REPUBLIC OF THE PHILIPPINES. Philippine identification system act (PhilSys). https://neda.gov.ph/philsys/. Online; accessed 31 July 2022.
- [5] UK BORDER AGENCY. Iris recognition immigration system (IRIS). https://webarchive.nationalarchives.gov.uk/ukgwa/20100408130108/http://www.ukba.homeoffice.gov.uk/managingborders/technology/iris/. Online; accessed 31 July 2022.
- [6] HOMELAND SECURITY DEPARTMENT. United States visitor and immigrant status indicator technology program ("US-VISIT"). https://www.dhs.gov/sites/default/files/publications/pia_nppd_001_h_04152008.pdf. Online; accessed 31 July 2022.
- [7] JOHN DAUGMAN. Iris recognition border-crossing system in the UAE. International Airport Review, 8(2), 2004.

- [8] AXIS BANK. A biometric authentication solution for net banking transactions. https://www.axisbank.com/about-us/press-releases/axis-bank-partners-with-minkasupay-for-a-seamless-net-banking-experience-for-its-customers/. Online; accessed 06 May 2022.
- [9] BIOID. **KYC** with biometrics know your customer. https://www.bioid.com/kyc-with-biometrics/. Online; accessed 06 May 2022.
- [10] ICICI BANK. Rekyc updation through eKyc authentication. https://www.icicibank.com/terms-condition/ekyc-rekyc-updation.page. Online; accessed 06 May 2022.
- [11] AXIS BANK. Instant savings account (biometric KYC). https://apiportal.axisbank.com/portal/node/3271. Online; accessed 06 May 2022.
- [12] NATIONAL PAYMENTS CORPORATION OF INDIA. AePS product overview. https://www.npci.org.in/what-we-do/aeps/product-overview. Online; accessed 06 May 2022.
- [13] NATIONAL PAYMENTS CORPORATION OF INDIA. BHIM Aadhaar. https://www.npci.org.in/what-we-do/bhim-aadhaar/product-overview. Online; accessed 06 May 2022.
- [14] INTERNATIONAL CRIMINAL POLICE ORGANIZATION (INTER-POL). Project first- biometric based law enforcement. https://www.interpol.int/en/News-and-Events/News/2017/Biometric-data-plays-key-role-in-fighting-crime-and-terrorism. Online; accessed 06 May 2022.
- [15] NATIONAL INSTITUTE OF STANDARDS AND TECHNOLOGY (NIST). Biometric standards for law enforcement. https://www.nist.gov/industry-impacts/biometric-standards-law-enforcement. Online; accessed 06 May 2022.
- [16] KEVIN W BOWYER AND PATRICK J FLYNN. Biometric identification of identical twins: A survey. Proceedings of IEEE International Conference on Biometrics Theory, Applications and Systems, pages 1–8, 2016.

- [17] MICHAEL FAIRHURST, MERYEM ERBILEK, AND MARJORY DA COSTA-ABREU. Selective review and analysis of aging effects in biometric system implementation. *IEEE Transactions on Human-Machine Systems*, **45**(3):294–303, 2015.
- [18] STEFANO MARRONE AND CARLO SANSONE. On the transferability of adversarial perturbation attacks against fingerprint based authentication systems. Pattern Recognition Letters, Elsevier, 152:253–259, 2021.
- [19] TARANG CHUGH AND ANIL K JAIN. Fingerprint spoof detector generalization. *IEEE Transactions on Information Forensics and Security*, 16:42–55, 2020.
- [20] YAOJIE LIU, JOEL STEHOUWER, AND XIAOMING LIU. On disentangling spoof trace for generic face anti-spoofing. Proceedings of European Conference on Computer Vision, Springer, pages 406–422, 2020.
- [21] Meiling Fang, Naser Damer, Florian Kirchbuchner, and Arjan Kuijper. Real masks and spoof faces: On the masked face presentation attack detection. *Pattern Recognition*, *Elsevier*, **123**:108398, 2022.
- [22] NORMAN POH AND JERZY KORCZAK. **Hybrid biometric person authentication using face and voice features**. Proceedings of International Conference on Audio-and Video-Based Biometric Person Authentication, Springer, pages 348–353, 2001.
- [23] ARUN ROSS, ANIL JAIN, AND JAIN-ZHONG QIAN. Information fusion in biometrics. Proceedings of International Conference on Audioand Video-Based Biometric Person Authentication, Springer, pages 354–359, 2001.
- [24] ANIL K JAIN AND ARUN ROSS. **Multibiometric systems**. Communications of the ACM, **47**(1):34–40, 2004.
- [25] STAN Z LI. Encyclopedia of Biometrics: I-Z., 2. Springer Science, 2009.

- [26] Mohammad Imran, Ashok Rao, and G Hemantha Kumar. Multi-biometric systems: A comparative study of multi-algorithmic and multimodal approaches. *Procedia Computer Science*, Elsevier, 2:207–212, 2010.
- [27] RISEUL RYU, SOONJA YEOM, SOO-HYUNG KIM, AND DAVID HERBERT. Continuous multimodal biometric authentication schemes: a systematic review. *IEEE Access*, 9:34541–34557, 2021.
- [28] Mohamed Abdul-Al, George Kumi Kyeremeh, Naser Ojaroudi Parchin, Raed A Abd-Alhameed, Rami Qahwaji, and Jonathan Rodriguez. Performance of multimodal biometric systems using face and fingerprints (short survey). Proceedings of IEEE International Workshop on Computer Aided Modeling and Design of Communication Links and Networks, pages 1–6, 2021.
- [29] MING JIE LEE, ANDREW BENG JIN TEOH, ANDREAS UHL, SHIUAN-NI LIANG, AND ZHE JIN. A tokenless cancellable scheme for multimodal biometric systems. Computers & Security, Elsevier, page 102350, 2021.
- [30] Sahar A El_Rahman. Multimodal biometric systems based on different fusion levels of ECG and fingerprint using different classifiers. Soft Computing, Springer, 24(16):12599–12632, 2020.
- [31] NORMAN POH, SAMY BENGIO, AND JERZY KORCZAK. A multi-sample multi-source model for biometric authentication. Proceedings of IEEE Workshop on Neural Networks for Signal Processing, pages 375–384, 2002.
- [32] Salma Ben Jemaa, Mohamed Hammami, and Hanene Ben-Abdallah. Finger surfaces recognition using rank level fusion. *The Computer Journal, Oxford*, **60**(7):969–985, 2017.
- [33] AJAY KUMAR AND SUMIT SHEKHAR. Personal identification using multibiometrics rank-level fusion. *IEEE Transactions on Systems, Man, and Cybernetics Part C (Applications and Reviews)*, **41**(5):743–752, 2011.

- [34] MD WASIUR RAHMAN, FATEMA TUZ ZOHRA, AND MARINA L GAVRILOVA. Rank level fusion for kinect gait and face biometrie identification. Proceedings of IEEE Symposium Series on Computational Intelligence, pages 1–7, 2017.
- [35] DV RAJESHWARI DEVI AND K NARASIMHA RAO. A multimodal biometric system using partition based dwt and rank level fusion. Proceedings of IEEE International Conference on Computational Intelligence and Computing Research, pages 1–5, 2016.
- [36] Nadia Othman and Bernadette Dorizzi. Impact of quality-based fusion techniques for video-based iris recognition at a distance. *IEEE Transactions on Information Forensics and Security*, **10**(8):1590–1602, 2015.
- [37] LIUKUI CHEN, HSING-CHUNG CHEN, ZUOJIN LI, AND YING WU. A fusion approach based on infrared finger vein transmitting model by using multi-light-intensity imaging. Human-Centric Computing and Information Sciences, Springer, 7(1):35, 2017.
- [38] Dexing Zhong, Huikai Shao, and Xuefeng Du. A hand-based multi-biometrics via deep hashing network and biometric graph matching. *IEEE Transactions on Information Forensics and Security*, 14(12):3140–3150, 2019.
- [39] NABIL HEZIL AND ABDELHANI BOUKROUCHE. Multimodal biometric recognition using human ear and palmprint. *IET Biometrics*, **6**(5):351–359, 2017.
- [40] Pedro H Silva, Eduardo Luz, Luiz A Zanlorensi, David Menotti, and Gladston Moreira. Multimodal feature level fusion based on particle swarm optimization with deep transfer learning. Proceedings of IEEE Congress on Evolutionary Computation, pages 1–8, 2018.
- [41] HIMANSHU PUROHIT AND PAWAN K AJMERA. Optimal feature level fusion for secured human authentication in multimodal biometric system. *Machine Vision and Applications, Springer*, **32**(1):1–12, 2021.

- [42] TEENA JOSEPH, SA KALAISELVAN, SU ASWATHY, R RADHAKRISH-NAN, AND AR SHAMNA. A multimodal biometric authentication scheme based on feature fusion for improving security in cloud environment. Journal of Ambient Intelligence and Humanized Computing, Springer, 12(6):6141–6149, 2021.
- [43] PARTHA PRATIM SARANGI, DEEPAK RANJAN NAYAK, MADHUMITA PANDA, AND BANSHIDHAR MAJHI. A feature-level fusion based improved multimodal biometric recognition system using ear and profile face. Journal of Ambient Intelligence and Humanized Computing, Springer, pages 1–32, 2022.
- [44] Haider Mehraj and Ajaz Hussain Mir. Robust multimodal biometric system based on feature level fusion of Optimiseddeepnet Features. Wireless Personal Communications, Springer, pages 1–22, 2021.
- [45] BASMA ABD EL-RAHIEM, FATHI E ABD EL-SAMIE, AND MOHAMED AMIN. Multimodal biometric authentication based on deep fusion of electrocardiogram (ECG) and finger vein. Multimedia Systems, Springer, pages 1–13, 2022.
- [46] NEETI POKHRIYAL AND VENU GOVINDARAJU. Learning discriminative factorized subspaces with application to touchscreen biometrics. *IEEE Access*, 8:152500–152511, 2020.
- [47] LI WANG, HAIGANG ZHANG, AND JINGFENG YANG. Finger multi-modal features fusion and recognition based on CNN. Proceedings of IEEE Symposium Series on Computational Intelligence, pages 3183–3188, 2019.
- [48] Zahid Akhtar, Attaullah Buriro, Bruno Crispo, and Tiago H Falk. Multimodal smartphone user authentication using touchstroke, phone-movement and face patterns. *Proceedings of IEEE* Global Conference on Signal and Information Processing, pages 1368–1372, 2017.
- [49] HELALA ALSHEHRI, MUHAMMAD HUSSAIN, HATIM A ABOALSAMH, AND MANSOUR A AL ZUAIR. Cross-sensor fingerprint matching method based on orientation, gradient, and Gabor-HoG descriptors with score level fusion. *IEEE Access*, **6**:28951–28968, 2018.

- [50] RENU SHARMA, SUKHENDU DAS, AND PADMAJA JOSHI. Score-level fusion using generalized extreme value distribution and DSmT, for multi-biometric systems. *IET Biometrics*, **7**(5):474–481, 2018.
- [51] SIMA SOLTANPOUR AND QINGMING JONATHAN WU. Multimodal 2D—3D face recognition using local descriptors: pyramidal shape map and structural context. *IET Biometrics*, **6**(1):27–35, 2017.
- [52] Pankaj Wasnik, R Raghavendra, Kiran Raja, and Christoph Busch. Subjective logic based score level fusion: combining faces and fingerprints. Proceedings of IEEE International Conference on Information Fusion, pages 515–520, 2018.
- [53] Gurjit Singh Walia, Shivam Rishi, Rajesh Asthana, Aarohi Kumar, and Anjana Gupta. Secure multimodal biometric system based on diffused graphs and optimal score fusion. *IET Biometrics*, 8(4):231–242, 2019.
- [54] KESHAV GUPTA, GURJIT SINGH WALIA, AND KAPIL SHARMA. Quality based adaptive score fusion approach for multimodal biometric system. Applied Intelligence, Springer, **50**(4):1086–1099, 2020.
- [55] JIALIANG PENG, AHMED A ABD EL-LATIF, QIONG LI, AND XIAMU NIU. Multimodal biometric authentication based on score level fusion of finger biometrics. *Optik*, *Elsevier*, **125**(23):6891–6897, 2014.
- [56] ZAHRA S SHARIATMADAR AND KARIM FAEZ. Finger-knuckle-print recognition performance improvement via multi-instance fusion at the score level. *Optik, Elsevier*, **125**(3):908–910, 2014.
- [57] MAURO BARNI, GIULIA DROANDI, RICCARDO LAZZERETTI, AND TOM-MASO PIGNATA. **SEMBA: secure multi-biometric authentication**. *IET Biometrics*, **8**(6):411–421, 2019.
- [58] MD. MARUF MONW AND MARINA GAVRILOVA. Markov chain model for multimodal biometric rank fusion. Signal, Image and Video Processing, Springer, 7:137–149, 2013.

- [59] YAPENG YE, HE ZHENG, LIAO NI, SHILEI LIU, AND WENXIN LI. A study on the individuality of finger vein based on statistical analysis. Proceedings of IEEE International Conference on Biometrics, pages 1–5, 2016.
- [60] Padma Polash Paul, Marina L Gavrilova, and Reda Alhajj. Decision fusion for multimodal biometrics using social network analysis. *IEEE Transactions on Systems, Man, and Cybernetics: Systems*, 44(11):1522–1533, 2014.
- [61] CAI LI, JIANKUN HU, JOSEF PIEPRZYK, AND WILLY SUSILO. A new biocryptosystem-oriented security analysis framework and implementation of multibiometric cryptosystems based on decision level fusion. *IEEE Transactions on Information Forensics and Security*, 10(6):1193–1206, 2015.
- [62] HERBADJI ABDERRAHMANE, GUERMAT NOUBEIL, ZIET LAHCENE, ZA-HID AKHTAR, AND DIPANKAR DASGUPTA. Weighted quasi-arithmetic mean based score level fusion for multi-biometric systems. *IET Biometrics*, **9**(3):91–99, 2020.
- [63] ANIL JAIN, KARTHIK NANDAKUMAR, AND ARUN ROSS. Score normalization in multimodal biometric systems. Pattern Recognition, Elsevier, 38(12):2270–2285, 2005.
- [64] EMIRATES MEDIA-CENTRE. Emirates launches integrated biometric path at the airport for added convenience. https://www.emirates.com/media-centre/emirates-launches-integrated-biometric/. Online; accessed 23 October 2020.
- [65] IMMIGRATION AND CHECKPOINTS AUTHORITY (SINGAPORE). Immigration clearance with multi-modal biometrics. https://www.ica.gov.sg/enter-depart/at-our-checkpoints/for-travellers/MMBS. Online; accessed 22 May 2022.
- [66] ACCENTURE. The future of identity in banking. https://deepsense.ai/wp-content/uploads/2020/08/. Online; 2020.

- [67] WAZIHA KABIR, M OMAIR AHMAD, AND M N S SWAMY. Normalization and weighting techniques based on genuine-impostor score fusion in multi-biometric systems. *IEEE Transactions on Information Forensics and Security*, **13**(8):1989–2000, 2018.
- [68] Kyoung Jun Noh, Jiho Choi, Jin Seong Hong, and Kang Ryoung Park. Finger-vein recognition based on densely connected convolutional network using score-Level fusion with shape and texture images. *IEEE Access*, 8:96748–96766, 2020.
- [69] Madasu Hanmandlu, Jyotsana Grover, Ankit Gureja, and Hari Mohan Gupta. Score level fusion of multimodal biometrics using triangular norms. Pattern Recognition Letters, Elsevier, 32(14):1843–1850, 2011.
- [70] MOURAD CHAA, NACEUR-EDDINE BOUKEZZOULA, AND ABDELOUA-HAB ATTIA. Score-level fusion of two-dimensional and threedimensional palmprint for personal recognition systems. *Journal* of Electronic Imaging, 26(1):013018, 2017.
- [71] LIBERATO IANNITELLI AND STEFANO RICCIARDI. Ubiquitous face-ear recognition based on frames sequence capture and analysis. Proceedings of IEEE International Conference on Signal-Image Technology & Internet-Based Systems, pages 706–712, 2019.
- [72] SANJIDA NASREEN TUMPA AND MARINA L GAVRILOVA. Score and rank level fusion algorithms for social behavioral biometrics. *IEEE Access*, 8:157663–157675, 2020.
- [73] KARTHIK NANDAKUMAR, YI CHEN, SARAT C DASS, AND ANIL K JAIN. Likelihood ratio-based biometric score fusion. *IEEE Transactions on Pattern Analysis and Machine Intelligence*, **30**(2):342–347, 2008.
- [74] KARTHIK NANDAKUMAR, ARUN ROSS, AND ANIL K JAIN. Biometric fusion: does modeling correlation really matter? Proceedings of IEEE International Conference on Biometrics: Theory, Applications, and Systems, pages 1–6, 2009.

- [75] F WANG AND J HAN. Multimodal biometric authentication based on score level fusion using support vector machine. Opto-Electronics Review, Springer, 17(1):59–64, 2009.
- [76] JULIAN FIERREZ-AGUILAR, JAVIER ORTEGA-GARCIA, JOAQUIN GONZALEZ-RODRIGUEZ, AND JOSEF BIGUN. Discriminative multimodal biometric authentication based on quality measures. *Pattern Recognition*, *Elsevier*, **38**(5):777–779, 2005.
- [77] JAY BHATNAGAR, AJAY KUMAR, AND NIPUN SAGGAR. A novel approach to improve biometric recognition using rank level fusion. Proceedings of IEEE Conference on Computer Vision and Pattern Recognition, pages 1–6, 2007.
- [78] Renu Sharma, Sukhendu Das, and Padmaja Joshi. Rank level fusion in multibiometric systems. Proceedings of National Conference on Computer Vision, Pattern Recognition, Image Processing and Graphics, Springer, pages 1–4, 2015.
- [79] AJAY KUMAR AND SUMIT SHEKHAR. Palmprint recognition using rank level fusion. Proceedings of IEEE International Conference on Image Processing, pages 3121–3124, 2010.
- [80] Sushma Niket Borade, Ratnadeep R Deshmukh, and Sivakumar Ramu. Face recognition using fusion of PCA and LDA: Borda count approach. Proceedings of Mediterranean Conference on Control and Automation, IEEE, pages 1164–1167, 2016.
- [81] NANANG SUSYANTO. Pool adjacent violators based biometric rank level fusion. Proceedings of IEEE International Conference of the Biometrics Special Interest Group, pages 1–3, 2017.
- [82] WAZIHA KABIR, M OMAIR AHMAD, AND M N S SWAMY. **A multi-biometric system based on feature and score level fusions**. *IEEE Access*, **7**:59437–59450, 2019.
- [83] Zhixin Shi, Frederick Kiefer, John Schneider, and Venu Govindaraju. Modeling biometric systems using the general pareto distribution (gpd). Biometric Technology for Human Identification, SPIE, 6944:203–213, 2008.

- [84] RITESH VYAS, TIRUPATHIRAJU KANUMURI, GYANENDRA SHEORAN, AND PAWAN DUBEY. Iris recognition through score-level fusion. Proceedings of International Conference on Computer Vision and Image Processing, Springer, pages 25–35, 2018.
- [85] S MALATHI AND C MEENA. Improved partial fingerprint matching based on score level fusion using pore and sift features. Proceedings of International Conference on Process Automation, Control and Computing, pages 1–4, 2011.
- [86] PARUL ARORA, SANDEEP BHARGAVA, SMRITI SRIVASTAVA, AND MADASU HANMANDLU. Multimodal biometric system based on information set theory and refined scores. Soft Computing, Springer, 21(17):5133–5144, 2017.
- [87] THOMAS TRUONG, JONATHAN GRAF, AND SVETLANA YANUSHKEVICH. Hybrid score-and rank-level fusion for person identification using face and ECG data. Proceedings of IEEE International Conference on Emerging Security Technologies, pages 1–6, 2019.
- [88] MD ZAHIDUR RAHMAN, MD HASAN HAFIZUR RAHMAN, AND MD MU-JIBUR RAHMAN MAJUMDAR. **Distinguishing a person by face and iris using fusion approach**. Proceedings of IEEE International Conference on Sustainable Technologies for Industry, pages 1–5, 2019.
- [89] BINGCHEN H GUO, MARK S NIXON, AND JOHN N CARTER. Soft biometric fusion for subject recognition at a distance. *IEEE Transactions on Biometrics, Behavior, and Identity Science*, 1(4):292–301, 2019.
- [90] CHANDNY RAMACHANDRAN AND DEEPA SANKAR. Score Level based fusion method for multimodal biometric recognition using palmprint and iris. Proceedings of Advanced Computing and Communication Technologies for High Performance Applications, IEEE, pages 281–286, 2020.
- [91] Zulaida Rahmi, Muhammad Imran Ahmad, Mohd Nazrin Md Isa, and Zahereel Ishwar Abdul Khalib. Matching score level fusion for face and palmprint recognition system on spatial domain. Proceedings of IEEE International Conference on System Engineering and Technology, pages 45–49, 2019.

- [92] FADI BOUTROS, NASER DAMER, KIRAN RAJA, RAGHAVENDRA RA-MACHANDRA, FLORIAN KIRCHBUCHNER, AND ARJAN KUIJPER. Fusing iris and periocular region for user verification in head mounted displays. Proceedings of IEEE International Conference on Information Fusion, pages 1–8, 2020.
- [93] L LATHA AND S THANGASAMY. A robust person authentication system based on score level fusion of left and right irises and retinal features. *Procedia Computer Science*, **2**:111–120, 2010.
- [94] MEENAKSHI CHOUDHARY, VIVEK TIWARI, AND U VENKANNA. Iris anti-spoofing through score-level fusion of handcrafted and data-driven features. Applied Soft Computing, 91:106206, 2020.
- [95] NICOLAS MORIZET AND JÉRÔME GILLES. A new adaptive combination approach to score level fusion for face and iris biometrics combining wavelets and statistical moments. *Proceedings of International Symposium on Visual Computing, Springer*, pages 661–671, 2008.
- [96] Nefissa Khiari-Hili, Christophe Montagne, Sylvie Lelandais, and Kamel Hamrouni. Quality dependent multimodal fusion of face and iris biometrics. Proceedings of International Conference on Image Processing Theory, Tools and Applications, IEEE, pages 1–6, 2016.
- [97] SYED MS ISLAM, MOHAMMED BENNAMOUN, AJMAL S MIAN, AND ROWAN DAVIES. Score level fusion of ear and face local 3D features for fast and expression-invariant human recognition. Proceedings of International conference image analysis and recognition, Springer, pages 387–396, 2009.
- [98] HIEW MOI SIM, HISHAMMUDDIN ASMUNI, ROHAYANTI HASSAN, AND RAZIB M OTHMAN. Multimodal biometrics: Weighted score level fusion based on non-ideal iris and face images. Expert Systems with Applications, Elsevier, 41(11):5390–5404, 2014.
- [99] Guangwei Gao, Lei Zhang, Jian Yang, Lin Zhang, and David Zhang. Reconstruction based finger-knuckle-print verification with score level adaptive binary fusion. *IEEE Transactions on Image Processing*, **22**(12):5050–5062, 2013.

- [100] KE XIAO, YUTONG TIAN, YUANYAO LU, YUPING LAI, AND XUNCHANG WANG. Quality assessment-based iris and face fusion recognition with dynamic weight. The Visual Computer, Springer, 38(5):1631–1643, 2022.
- [101] JAVAD KHODADOUST, MIGUEL ANGEL MEDINA-PÉREZ, RAÚL MON-ROY, ALI MOHAMMAD KHODADOUST, AND SEYED SAEID MIRKAMALI. A multibiometric system based on the fusion of fingerprint, fingervein, and finger-knuckle-print. Expert Systems with Applications, Elsevier, 176:114687, 2021.
- [102] GIANNI FENU, MIRKO MARRAS, AND LUDOVICO BORATTO. A multibiometric system for continuous student authentication in elearning platforms. Pattern Recognition Letters, Elsevier, 113:83–92, 2018.
- [103] NASER DAMER, ALEXANDER OPEL, AND ALEXANDER NOUAK. CMC curve properties and biometric source weighting in multi-biometric score-level fusion. Proceedings of International Conference on Information Fusion, IEEE, pages 1–6, 2014.
- [104] Mustafa Berkay Yilmaz and Berrin Yanikoğlu. Score level fusion of classifiers in off-line signature verification. *Information Fusion*, *Elsevier*, **32**:109–119, 2016.
- [105] NISHA SRINIVAS, KALYAN VEERAMACHANENI, AND LISA ANN OSAD-CIW. Fusing correlated data from multiple classifiers for improved biometric verification. Proceedings of International Conference on Information Fusion, IEEE, pages 1504–1511, 2009.
- [106] HIMANSHU VAJARIA, TANMOY ISLAM, P MOHANTY, SUDEEP SARKAR, RAVI SANKAR, AND RANGACHAR KASTURI. **Evaluation and analysis of a face and voice outdoor multi-biometric system**. *Pattern Recognition Letters, Elsevier*, **28**(12):1572–1580, 2007.
- [107] Madasu Hanmandlu, Jyotsana Grover, Vamsi Krishna Madasu, and Shantaram Vasirkala. Score level fusion of hand based biometrics using t-norms. Proceedings of IEEE International Conference on Technologies for Homeland Security, pages 70–76, 2010.

- [108] MOHAMED CHENITI, NACEUR-EDDINE BOUKEZZOULA, AND ZAHID AKHTAR. Symmetric sum-based biometric score fusion. *IET Biometrics*, **7**(5):391–395, 2018.
- [109] SARAT C DASS, KARTHIK NANDAKUMAR, AND ANIL K JAIN. A principled approach to score level fusion in multimodal biometric systems. Proceedings of International Conference on Audio-and Video-Based Biometric Person Authentication, Springer, pages 1049–1058, 2005.
- [110] KARTHIK NANDAKUMAR, YI CHEN, ANIL K JAIN, AND SARAT C DASS. Quality-based score level fusion in multibiometric systems. Proceedings of International Conference on Pattern Recognition, IEEE, 4:473–476, 2006.
- [111] EMANUELA MARASCO AND CARLO SANSONE. Improving the accuracy of a score fusion approach based on likelihood ratio in multimodal biometric systems. Proceedings of International Conference on Image Analysis and Processing, Springer, pages 509–518, 2009.
- [112] QIAN TAO AND RAYMOND VELDHUIS. Robust biometric score fusion by naive likelihood ratio via receiver operating characteristics. *IEEE Transactions on Information Forensics and Security*, **8**(2):305–313, 2013.
- [113] HYUN-AE PARK AND KANG RYOUNG PARK. Iris recognition based on score level fusion by using SVM. Pattern Recognition Letters, Elsevier, 28(15):2019–2028, 2007.
- [114] A MUTHUKUMAR AND A KAVIPRIYA. A biometric system based on Gabor feature extraction with SVM classifier for finger-knuckle-print. Pattern Recognition Letters, Elsevier, 125:150–156, 2019.
- [115] MINGXING HE, SHI-JINN HORNG, PINGZHI FAN, RAY-SHINE RUN, RONG-JIAN CHEN, JUI-LIN LAI, MUHAMMAD KHURRAM KHAN, AND KEVIN OCTAVIUS SENTOSA. Performance evaluation of score level fusion in multimodal biometric systems. Pattern Recognition, Elsevier, 43(5):1789–1800, 2010.

- [116] YACINE BOUZOUINA AND LATIFA HAMAMI. Multimodal biometric: iris and face recognition based on feature selection of iris with GA and scores level fusion with SVM. Proceedings of International Conference on Bio-engineering for Smart Technologies, IEEE), pages 1–7, 2017.
- [117] DAKSHINA RANJAN KISKU, JAMUNA KANTA SING, AND PHALGUNI GUPTA. Multibiometrics belief fusion. Proceedings of IEEE International Conference on Machine Vision, pages 37–40, 2009.
- [118] Lamia Mezai, Fella Hachouf, and Messaoud Bengherabi. Score fusion of face and voice using Dempster-Shafer theory for person authentication. Proceedings of International Conference on Intelligent Systems Design and Applications, IEEE, pages 894–899, 2011.
- [119] KIEN NGUYEN, SIMON DENMAN, SRIDHA SRIDHARAN, AND CLINTON FOOKES. Score-level multibiometric fusion based on Dempster-Shafer theory incorporating uncertainty factors. *IEEE Transactions on Human-Machine Systems*, 45(1):132–140, 2015.
- [120] RICHA SINGH, MAYANK VATSA, AND AFZEL NOORE. Integrated multilevel image fusion and match score fusion of visible and infrared face images for robust face recognition. *Pattern Recognition, Elsevier*, 41(3):880–893, 2008.
- [121] MAYANK VATSA, RICHA SINGH, AFZEL NOORE, AND ARUN ROSS. On the dynamic selection of biometric fusion algorithms. *IEEE Transactions on Information Forensics and Security*, **5**(3):470–479, 2010.
- [122] Bong-Nam Kang, Yonghyun Kim, and Daijin Kim. Deep convolutional neural network using triplets of faces, deep ensemble, and score-level fusion for face recognition. *Proceedings of IEEE Conference on Computer Vision and Pattern Recognition Workshops*, pages 109–116, 2017.
- [123] Satrajit Mukherjee, Kunal Pal, Bodhisattwa Prasad Majumder, Chiranjib Saha, Bijaya K Panigrahi, and Sanjoy Das. Differential evolution based score level fusion for multi-modal biometric systems. Proceedings of IEEE Symposium on Computational Intelligence in Biometrics and Identity Management, pages 38–44, 2014.

- [124] KESHAV GUPTA, GURJIT SINGH WALIA, AND KAPIL SHARMA. Multimodal biometric system using grasshopper optimization. Proceedings of International Conference on Computing, Communication, and Intelligent Systems, IEEE, pages 387–391, 2019.
- [125] SHAHRZAD SAREMI, SEYEDALI MIRJALILI, AND ANDREW LEWIS. Grasshopper optimisation algorithm: theory and application. Advances in Engineering Software, Elsevier, 105:30–47, 2017.
- [126] LAMIA MEZAI AND FELLA HACHOUF. Score-level fusion of face and voice using particle swarm optimization and belief functions. *IEEE Transactions on Human-Machine Systems*, **45**(6):761–772, 2015.
- [127] GURJIT SINGH WALIA, TARANDEEP SINGH, KULDEEP SINGH, AND NEE-LAM VERMA. Robust multimodal biometric system based on optimal score level fusion model. Expert Systems with Applications, Elsevier, 116:364–376, 2019.
- [128] AJAY KUMAR, VIVEK KANHANGAD, AND DAVID ZHANG. A new framework for adaptive multimodal biometrics management. *IEEE Transactions on Information Forensics and Security*, **5**(1):92–102, 2010.
- [129] LAMIA MEZAI AND FELLA HACHOUF. Adaptive multimodal biometric fusion algorithm using particle swarm optimization and belief functions. Proceedings of IEEE International Conference on Biometrics and Forensics, pages 1–6, 2016.
- [130] Padma Polash Paul and Marina Gavrilova. Rank level fusion of multimodal cancelable biometrics. Proceedings of IEEE International Conference on Cognitive Informatics and Cognitive Computing, pages 80–87, 2014.
- [131] Zhiyong Liu and Guan Yang. Use wavelet transform to gait recognition. Proceedings of IEEE International Congress on Image and Signal Processing, pages 1635–1639, 2015.
- [132] AYMAN ABAZA AND ARUN ROSS. Quality based rank-level fusion in multibiometric systems. Proceedings of International Conference on Biometrics: Theory, Applications, and Systems, IEEE, pages 1–6, 2009.

- [133] MD MARUF MONWAR AND MARINA GAVRILOVA. **FES: A system for combining face, ear and signature biometrics using rank level fusion**. Proceedings of International Conference on Information Technology: New Generations, IEEE, pages 922–927, 2008.
- [134] MD MARUF MONWAR AND MARINA L GAVRILOVA. Multimodal biometric system using rank-level fusion approach. *IEEE Transactions on Systems, Man, and Cybernetics, Part B (Cybernetics)*, **39**(4):867–878, 2009.
- [135] MD MARUF MONWAR AND MARINA L GAVRILOVA. Integrating monomodal biometric matchers through logistic regression rank aggregation approach. Proceedings of IEEE Applied Imagery Pattern Recognition Workshop, pages 1–7, 2008.
- [136] A Jameer Basha, V Palanisamy, and T Purusothaman. Fast multimodal biometric approach using dynamic fingerprint authentication and enhanced iris features. Proceedings of International Conference on Computational Intelligence and Computing Research, IEEE, pages 1–8, 2010.
- [137] FAISAL AHMED, PADMA POLASH PAUL, AND MARINA L GAVRILOVA. DTW-based kernel and rank-level fusion for 3D gait recognition using kinect. The Visual Computer, Springer, 31(6-8):915–924, 2015.
- [138] Alaa S Al-Waisy, Rami Qahwaji, Stanley Ipson, Shumoos Al-Fahdawi, and Tarek AM Nagem. **A multi-biometric iris recognition system based on a deep learning approach**. *Pattern Analysis and Applications, Springer*, **21**(3):783–802, 2018.
- [139] MD MARUF MONWAR, BVK VIJAYAKUMAR, VISHNU NARESH BODDETI, AND JONATHON M SMEREKA. Rank information fusion for challenging ocular image recognition. Proceedings of IEEE International Conference on Cognitive Informatics and Cognitive Computing, pages 175–181, 2013.
- [140] Amioy Kumar, Madasu Hanmandlu, and Shantaram Vasikarla. Rank level integration of face based biometrics. Proceedings of International Conference on Information Technology-New Generations, IEEE, pages 36–41, 2012.

- [141] Ava Tahmasebi, Hossein Pourghasem, and Homayoun Mahdavi-Nasab. A novel rank-level fusion for multispectral palmprint identification system. Proceedings of International Conference on Intelligent Computation and Bio-Medical Instrumentation, IEEE, pages 208–211, 2011.
- [142] JUHA YLIOINAS, ABDENOUR HADID, JUHO KANNALA, AND MATTI PIETIKÄINEN. An in-depth examination of local binary descriptors in unconstrained face recognition. *Proceedings of IEEE International Conference on Pattern Recognition*, pages 4471–4476, 2014.
- [143] HOSSEIN TALEBI AND MARINA L GAVRILOVA. Prior resemblance probability of users for multimodal biometrics rank fusion. Proceedings of IEEE International Conference on Identity, Security and Behavior Analysis, pages 1–7, 2015.
- [144] OGECHUKWU N ILOANUSI. Fusion of finger types for fingerprint indexing using minutiae quadruplets. Pattern Recognition Letters, Elsevier, 38:8–14, 2014.
- [145] HIMANSHU S BHATT, RICHA SINGH, AND MAYANK VATSA. On rank aggregation for face recognition from videos. *Proceedings of International Conference on Image Processing*, *IEEE*, pages 2993–2997, 2013.
- [146] CYNTHIA DWORK, RAVI KUMAR, MONI NAOR, AND DANDAPANI SIVAKUMAR. Rank aggregation methods for the web. Proceedings of International Conference on World Wide Web, ACM, pages 613–622, 2001.
- [147] Jamuna Kanta Sing, Aniruddha Dey, and Manas Ghosh. Confidence factor weighted Gaussian function induced parallel fuzzy rank-level fusion for inference and its application to face recognition. *Information Fusion*, *Elsevier*, 47:60–71, 2019.
- [148] ROBERT SNELICK, UMUT ULUDAG, ALAN MINK, MIKE INDOVINA, AND ANIL JAIN. Large-scale evaluation of multimodal biometric authentication using state-of-the-art systems. *IEEE Transactions on Pattern Analysis and Machine Intelligence*, 27(3):450–455, 2005.

- [149] MARYAM ESKANDARI AND ONSEN TOYGAR. Selection of optimized features and weights on face-iris fusion using distance images. Computer Vision and Image Understanding, 137:63–75, 2015.
- [150] TAN DAT TRINH, JIN YOUNG KIM, AND SEUNG YOU NA. Enhanced face recognition by fusion of global and local features under varying illumination. Proceedings of IEEE International Conference on IT Convergence and Security, pages 1–4, 2014.
- [151] ANIESHA ALFORD, CARESSE HANSEN, GERRY DOZIER, KELVIN BRYANT, JOHN KELLY, TAMIRAT ABEGAZ, KARL RICANEK, AND DAMON L WOODARD. **GEC-based multi-biometric fusion**. Proceedings of IEEE Congress of Evolutionary Computation, pages 2071–2074, 2011.
- [152] FERNANDO ALONSO-FERNANDEZ, JULIAN FIERREZ, AND JAVIER ORTEGA-GARCIA. Quality measures in biometric systems. *IEEE Security & Privacy, IEEE*, **10**(6):52–62, 2011.
- [153] SAMARTH BHARADWAJ, MAYANK VATSA, AND RICHA SINGH. Biometric quality: a review of fingerprint, iris, and face. EURASIP journal on Image and Video Processing, Springer, 2014(1):1–28, 2014.
- [154] Krzysztof Kryszczuk, Jonas Richiardi, and Andrzej Drygajlo. Impact of combining quality measures on biometric sample matching. Proceedings of International Conference on Biometrics: Theory, Applications, and Systems, IEEE, pages 1–6, 2009.
- [155] NORMAN POH AND JOSEF KITTLER. A unified framework for biometric expert fusion incorporating quality measures. *IEEE Transactions on Pattern Analysis and Machine Intelligence*, **34**(1):3–18, 2011.
- [156] NORMAN POH, THIRIMACHOS BOURLAI, JOSEF KITTLER, LORENE ALLANO, FERNANDO ALONSO-FERNANDEZ, ONKAR AMBEKAR, JOHN BAKER, BERNADETTE DORIZZI, OMOLARA FATUKASI, JULIAN FIERREZ, ET AL. Benchmarking quality-dependent and cost-sensitive score-level multimodal biometric fusion algorithms. *IEEE Transactions on Information Forensics and Security*, 4(4):849–866, 2009.

- [157] Krzysztof Kryszczuk and Andrzej Drygajlo. Credence estimation and error prediction in biometric identity verification. Signal processing, Elsevier, 88(4):916–925, 2008.
- [158] Zhou Wang and Alan C Bovik. A universal image quality index. *IEEE Signal Processing Letters*, **9**(3):81–84, 2002.
- [159] HARIN SELLAHEWA AND SABAH A JASSIM. Image-quality-based adaptive face recognition. *IEEE Transactions on Instrumentation and Measurement*, *IEEE*, **59**(4):805–813, 2010.
- [160] Kamal Nasrollahi and Thomas B Moeslund. Face quality assessment system in video sequences. *Proceedings of European Workshop on Biometrics and Identity Management, Springer*, pages 10–18, 2008.
- [161] Maneet Singh, Richa Singh, and Arun Ross. A comprehensive overview of biometric fusion. *Information Fusion, Elsevier*, **52**:187–205, 2019.
- [162] JINYU ZUO AND NATALIA A SCHMID. Global and local quality measures for NIR iris video. Proceedings of IEEE Computer Society Conference on Computer Vision and Pattern Recognition Workshops, pages 120–125, 2009.
- [163] JUNYAN WANG, YAN SHANG, GUANGDA SU, AND XINGGANG LIN. Age simulation for face recognition. Proceedings of International Conference on Pattern Recognition, IEEE, 3:913–916, 2006.
- [164] PINA MARZILIANO, FREDERIC DUFAUX, STEFAN WINKLER, AND TOURADJ EBRAHIMI. A no-reference perceptual blur metric. Proceedings of International Conference on Image Processing, IEEE, 3:III–III, 2002.
- [165] Jun Yu, Kejia Sun, Fei Gao, and Suguo Zhu. Face biometric quality assessment via light CNN. Pattern Recognition Letters, Elsevier, 107:25–32, 2018.
- [166] EMNA FOURATI, WAEL ELLOUMI, AND ALADINE CHETOUANI. Anti-spoofing in face recognition-based biometric authentication using image quality assessment. Multimedia Tools and Applications, Springer, 79(1):865–889, 2020.

- [167] YI CHEN, SARAT C DASS, AND ANIL K JAIN. Localized iris image quality using 2-D wavelets. Proceedings of International Conference on Biometrics, Springer, pages 373–381, 2006.
- [168] MAYANK VATSA, RICHA SINGH, AND AFZEL NOORE. Integrating image quality in 2 ν -SVM biometric match score fusion. International Journal of Neural Systems, World Scientific, 17(05):343–351, 2007.
- [169] MAYANK VATSA, RICHA SINGH, ARUN ROSS, AND AFZEL NOORE. Quality-based fusion for multichannel iris recognition. Proceedings of International Conference on Pattern Recognition, IEEE, pages 1314–1317, 2010.
- [170] MAYANK VATSA, RICHA SINGH, AFZEL NOORE, AND MAX M HOUCK. Quality-augmented fusion of level-2 and level-3 fingerprint information using DSm theory. International Journal of Approximate Reasoning, Elsevier, 50(1):51–61, 2009.
- [171] ZEHIRA HADDAD, AZEDDINE BEGHDADI, AMINA SERIR, AND ANISSA MOKRAOUI. Wave atoms based compression method for fingerprint images. Pattern Recognition, Elsevier, 46(9):2450–2464, 2013.
- [172] JULIAN FIERREZ-AGUILAR, YI CHEN, JAVIER ORTEGA-GARCIA, AND ANIL K JAIN. Incorporating image quality in multi-algorithm fingerprint verification. *Proceedings of International Conference on Biometrics, Springer*, pages 213–220, 2006.
- [173] ELHAM TABASSI, CHARLES WILSON, AND CRAIG I WATSON. Finger-print image quality. NIST Interagency/Internal Report (NISTIR), 2004.
- [174] ELHAM TABASSI, TIMO RUHLAND, OLIVER BAUSINGER, OLAF HENNIGER, MARTIN OLSEN, AND JOHANNES MERKLE. **NIST fingerprint** image quality: NFIQ 2. https://nvlpubs.nist.gov/nistpubs/ir/2021/NIST.IR.8382.pdf. NIST; 2021.
- [175] RAM PRAKASH SHARMA AND SOMNATH DEY. Two-stage quality adaptive fingerprint image enhancement using fuzzy c-means clustering based fingerprint quality analysis. *Image and Vision Computing, Elsevier*, 83:1–16, 2019.

- [176] Zhi Zhou, Eliza Yingzi Du, Craig Belcher, N Luke Thomas, and Edward J Delp. Quality fusion based multimodal eye recognition. *Proceedings of IEEE International Conference on Systems, Man, and Cybernetics, IEEE*), pages 1297–1302, 2012.
- [177] Andrea F Abate, Silvio Barra, Andrea Casanova, Gianni Fenu, and Mirko Marras. Iris quality assessment: a statistical approach for biometric security applications. *Proceedings of International Symposium on Cyberspace Safety and Security, Springer*, pages 270–278, 2018.
- [178] JAVIER HERNANDEZ-ORTEGA, JAVIER GALBALLY, JULIAN FIERREZ, RUDOLF HARAKSIM, AND LAURENT BESLAY. Faceqnet: Quality assessment for face recognition based on deep learning. *Proceedings of International Conference on Biometrics, IEEE*, pages 1–8, 2019.
- [179] PHILIPP TERHORST, JAN NIKLAS KOLF, NASER DAMER, FLORIAN KIRCHBUCHNER, AND ARJAN KUIJPER. **SER-FIQ:** Unsupervised estimation of face image quality based on stochastic embedding robustness. Proceedings of the IEEE/CVF Conference on Computer Vision and Pattern Recognition, pages 5651–5660, 2020.
- [180] VASYL PIHUR, SOMNATH DATTA, AND SUSMITA DATTA. RankAggreg, an R package for Weighted Rank Aggregation. *BMC Bioinformatics*, **10**(1):62, 2009.
- [181] RONG ZHANG, YAXING CHEN, BO DONG, FENG TIAN, AND QINGHUA ZHENG. A genetic algorithm-based energy-efficient container placement strategy in CaaS. *IEEE Access*, 7:121360–121373, 2019.
- [182] Zhipeng Sun, Jian Chen, Yu Han, Rui Huang, Qi Zhang, and Shanshan Guo. An optimized water distribution model of irrigation district based on the genetic backtracking search algorithm. *IEEE Access*, 7:145692–145704, 2019.
- [183] YING ZHANG, PEISONG LI, AND XINHENG WANG. Intrusion detection for IoT based on improved genetic algorithm and deep belief network. *IEEE Access*, **7**:31711–31722, 2019.

- [184] Wenke Zang, Weining Zhang, Zehua Wang, Dong Jiang, Xiyu Liu, and Minghe Sun. A novel double-strand DNA genetic algorithm for multi-objective optimization. *IEEE Access*, 7:18821–18839, 2019.
- [185] Arash Mohammadi, Houshyar Asadi, Shady Mohamed, Kyle Nelson, and Saeid Nahavandi. Multiobjective and interactive genetic algorithms for weight tuning of a model predictive control-based motion cueing algorithm. *IEEE Transactions on Cybernetics*, 49(9):3471–3481, 2019.
- [186] XUEFEI YIN, YANMING ZHU, AND JIANKUN HU. Contactless finger-print recognition based on global minutia topology and loose genetic algorithm. *IEEE Transactions on Information Forensics and Security*, 2019.
- [187] NANCY BANSAL, AMIT VERMA, IQBALDEEP KAUR, AND DOLLY SHARMA. Multimodal biometrics by fusion for security using genetic algorithm. Proceedings of IEEE International Conference on Signal Processing, Computing and Control, pages 159–162, 2017.
- [188] G Rudolph. Evolutionary search under partially ordered sets. Dept. Comput. Sci./LS11, Univ. Dortmund, Dortmund, Germany, Tech. Rep. CI-67/99, 1999.
- [189] ECKART ZITZLER, KALYANMOY DEB, AND LOTHAR THIELE. Comparison of multiobjective evolutionary algorithms: Empirical results. *Evolutionary Computation, MIT Press*, 8(2):173–195, 2000.
- [190] ANUJ PRAKASH, FELIX TS CHAN, AND SG DESHMUKH. FMS scheduling with knowledge based genetic algorithm approach. Expert Systems with Applications, Elsevier, 38(4):3161–3171, 2011.
- [191] J MARK WARE, IAN D WILSON, AND J ANDREW WARE. A knowledge based genetic algorithm approach to automating cartographic generalisation. Proceedings of Applications and Innovations in Intelligent Systems X, Springer, pages 33–49, 2003.

- [192] YANRONG HU AND SIMON X YANG. A knowledge based genetic algorithm for path planning of a mobile robot. Proceedings of IEEE International Conference on Robotics and Automation, 5:4350–4355, 2004.
- [193] NIST Biometric Scores Set (BSSR1). https://www.nist.gov/itl/iad/image-group/nist-biometric-scores-set-bssr1.
- [194] OU. The OU-ISIR Biometric Score Database (BSS4). http://www.am.sanken.osaka-u.ac.jp/BiometricDB/BioScore.html, 2013.
- [195] Chaw Chia, Nasser Sherkat, and Lars Nolle. Towards a best linear combination for multimodal biometric fusion. *Proceedings of IEEE International Conference on Pattern Recognition*, pages 1176–1179, 2010.
- [196] Yasushi Makihara, Daigo Muramatsu, Haruyuki Iwama, and Yasushi Yagi. On combining gait features. Proceedings of IEEE International Conference and Workshops on Automatic Face and Gesture Recognition, pages 1–8, 2013.
- [197] HOANG NGUYEN, HOSSEIN MOAYEDI, LOKE KOK FOONG, HUSAM ABDULRASOOL H AL NAJJAR, WAN AMIZAH WAN JUSOH, AHMAD SAFUAN A RASHID, AND JAMALODDIN JAMALI. Optimizing ANN models with PSO for predicting short building seismic response. Engineering with Computers, Springer, 36:823–837, 2020.
- [198] OMAR LLERENA-PIZARRO, NESTOR PROENZA-PEREZ, CELSO ED-UARDO TUNA, AND JOSE LUZ SILVEIRA. A PSO-BPSO technique for hybrid power generation system sizing. *IEEE Latin America Transactions*, 18(08):1362–1370, 2020.
- [199] Hui Jiang, Zheng He, Gang Ye, and Huyin Zhang. Network intrusion detection based on PSO-XGBoost model. *IEEE Access*, 8:58392–58401, 2020.
- [200] YANCHUN ZUO, LIXIN GUO, WEI LIU, AND JIANYANG DING. Mixing ratio optimization of chaff elements for wideband jamming using PSO. *IEEE Antennas and Wireless Propagation Letters, IEEE*, 19(12):2408–2412, 2020.

- [201] Chao Ou and Weixing Lin. Comparison between PSO and GA for parameters optimization of PID controller. Proceedings of IEEE International Conference on Mechatronics and Automation, pages 2471–2475, 2006.
- [202] PAOLO CAZZANIGA, MARCO S NOBILE, AND DANIELA BESOZZI. The impact of particles initialization in PSO: parameter estimation as a case in point. Proceedings of IEEE Conference on Computational Intelligence in Bioinformatics and Computational Biology, pages 1–8, 2015.
- [203] Hajira Jabeen, Zunera Jalil, and Abdul Rauf Baig. Opposition based initialization in particle swarm optimization (O-PSO).

 Proceedings of Annual Conference Companion on Genetic and Evolutionary Computation Conference: Late Breaking Papers, ACM, pages 2047–2052, 2009.
- [204] Andries Engelbrecht. Particle swarm optimization: velocity initialization. Proceedings of IEEE Congress on Evolutionary Computation, pages 1–8, 2012.
- [205] TOMOHIRO HARADA AND ENRIQUE ALBA. Parallel genetic algorithms: a useful survey. ACM Computing Surveys, 53(4):1–39, 2021.
- [206] SEYED POURYA HOSEINI ALINODEHI, SAJJAD MOSHFE, MA-SOUMEH SABER ZAEIMIAN, ABDOLLAH KHOEI, AND KHAIROLLAH HA-DIDI. **High-speed general purpose genetic algorithm processor**. *IEEE Transactions on Cybernetics*, **46**(7):1551–1565, 2016.
- [207] Soniya Lalwani, Harish Sharma, Suresh Chandra Satapathy, Kusum Deep, and Jagdish Chand Bansal. A survey on parallel particle swarm optimization algorithms. Arabian Journal for Science and Engineering, Springer, 44(4):2899–2923, 2019.
- [208] Chun-Wei Tan and Ajay Kumar. Efficient and accurate at-a-distance iris recognition using geometric key-based iris encoding. *IEEE Transactions on Information Forensics and Security*, **9**(9):1518–1526, 2014.

- [209] HYUNJU MAENG, SHENGCAI LIAO, DONGOH KANG, SEONG-WHAN LEE, AND ANIL K JAIN. Nighttime face recognition at long distance: Cross-distance and cross-spectral matching. Asian Conference on Computer Vision, Springer, pages 708–721, 2012.
- [210] TIANYUE ZHENG, WEIHONG DENG, AND JIANI HU. Cross-age lfw: A database for studying cross-age face recognition in unconstrained environments. arXiv preprint arXiv:1708.08197, 2017.
- [211] AJAY KUMAR AND ARUN PASSI. Comparison and combination of iris matchers for reliable personal authentication. *Pattern Recognition*, *Elsevier*, **43**(3):1016–1026, 2010.
- [212] ZIWEI LIU, PING LUO, XIAOGANG WANG, AND XIAOOU TANG. **Deep learning face attributes in the wild**. *Proceedings of International Conference on Computer Vision*, *IEEE*, pages 3730–3738, 2015.
- [213] Bong-Nam Kang, Yonghyun Kim, Bongjin Jun, and Daijin Kim. Attentional feature-pair relation networks for accurate face recognition. Proceedings of the IEEE/CVF International Conference on Computer Vision, pages 5472–5481, 2019.
- [214] HE ZHAO, YONGJIE SHI, XIN TONG, XIANGHUA YING, AND HONG-BIN ZHA. QAMFace: Quadratic additive angular margin loss for face recognition. Proceedings of IEEE International Conference on Image Processing, pages 1901–1905, 2020.
- [215] JIANKANG DENG, JIA GUO, NIANNAN XUE, AND STEFANOS ZAFEIRIOU. Arcface: Additive angular margin loss for deep face recognition. Proceedings of the IEEE/CVF Conference on Computer Vision and Pattern Recognition, pages 4690–4699, 2019.
- [216] HIEU V NGUYEN AND LI BAI. Cosine similarity metric learning for face verification. Asian Conference on Computer Vision, Springer, pages 709–720, 2010.
- [217] YUGE HUANG, YUHAN WANG, YING TAI, XIAOMING LIU, PENGCHENG SHEN, SHAOXIN LI, JILIN LI, AND FEIYUE HUANG. Curricularface: adaptive curriculum learning loss for deep face recognition. Proceedings of the IEEE/CVF Conference on Computer Vision and Pattern Recognition, pages 5901–5910, 2020.

- [218] STEPAN KOMKOV AND ALEKSANDR PETIUSHKO. Advhat: Real-world adversarial attack on arcface face id system. Proceedings of International Conference on Pattern Recognition, IEEE), pages 819–826, 2021.
- [219] ALI ELMAHMUDI AND HASSAN UGAIL. Experiments on deep face recognition using partial faces. *Proceedings of International Conference on Cyberworlds*, *IEEE*, pages 357–362, 2018.
- [220] ZIJING ZHAO AND AJAY KUMAR. Towards more accurate iris recognition using deeply learned spatially corresponding features. Proceedings of the IEEE International Conference on Computer Vision, pages 3809–3818, 2017.
- [221] LIBOR MASEK. Ph.D. thesis: Recognition of human iris patterns for biometric identification. The University of Western Australia.
- [222] Philipp Terhörst, Daniel Fährmann, Jan Niklas Kolf, Naser Damer, Florian Kirchbuchner, and Arjan Kuijper. MAAD-Face: A massively annotated attribute dataset for face images. *IEEE Transactions on Information Forensics and Security*, **16**:3942–3957, 2021.
- [223] Hanrui Wang, Shuo Wang, Zhe Jin, Yandan Wang, Cunjian Chen, and Massimo Tistarelli. Similarity-based gray-box adversarial attack against deep face recognition. *Proceedings of IEEE International Conference on Automatic Face and Gesture Recognition*, pages 1–8, 2021.
- [224] WORLD HEALTH ORGANIZATION. Coronavirus disease (COVID-19) pandemic. https://www.who.int/emergencies/diseases/novel-coronavirus-2019. Online; April 2022.
- [225] Marta Gomez-Barrero, Pawel Drozdowski, Christian Rathgeb, Jose Patino, Massimmiliano Todisco, Andras Nautsch, Naser Damer, Jannis Priesnitz, Nicholas Evans, and Christoph Busch. Biometrics in the era of COVID-19: challenges and opportunities. arXiv preprint arXiv:2102.09258, 2021.

- [226] MEI L NGAN, PATRICK J GROTHER, KAYEE K HANAOKA, ET AL. Ongoing face recognition vendor test (frvt) part 6b: Face recognition accuracy with face masks using post-covid-19 algorithms. NIST Interagency/Internal Report, Accessed July 5, 2022.
- [227] NASER DAMER, JONAS HENRY GREBE, CONG CHEN, FADI BOUTROS, FLORIAN KIRCHBUCHNER, AND ARJAN KUIJPER. The effect of wearing a mask on face recognition performance: an exploratory study. Proceedings of International Conference of the Biometrics Special Interest Group, IEEE, pages 1–6, 2020.
- [228] ARUN VEMURY, AKE HASSELGREN, JOHN HOWARD, AND YEVGENIY SIROTIN. Biometric rally results face masks face recognition performance. https://mdtf.org/Rally2020/Results2020. Online; April 2022.
- [229] Fadi Boutros, Naser Damer, Jan Niklas Kolf, Kiran Raja, Flo-Rian Kirchbuchner, Raghavendra Ramachandra, Arjan Kui-Jper, Pengcheng Fang, Chao Zhang, Fei Wang, et al. **MFR 2021:** Masked face recognition competition. Proceedings of IEEE International Joint Conference on Biometrics, pages 1–10, 2021.
- [230] KAI WANG, SHUO WANG, JIANFEI YANG, XIAOBO WANG, BAIGUI SUN, HAO LI, AND YANG YOU. Mask aware network for masked face recognition in the wild. Proceedings of the IEEE/CVF International Conference on Computer Vision, pages 1456–1461, 2021.
- [231] Lingxue Song, Dihong Gong, Zhifeng Li, Changsong Liu, and Wei Liu. Occlusion robust face recognition based on mask learning with pairwise differential siamese network. *Proceedings of the IEEE/CVF International Conference on Computer Vision*, pages 773–782, 2019.
- [232] DAVID MONTERO, MARCOS NIETO, PETER LESKOVSKY, AND NAIARA AGINAKO. Boosting masked face recognition with multi-task arcface. arXiv preprint arXiv:2104.09874, 2021.
- [233] FADI BOUTROS, NASER DAMER, FLORIAN KIRCHBUCHNER, AND ARJAN KUIJPER. Self-restrained triplet loss for accurate masked face recognition. Pattern Recognition, Elsevier, 124:108473, 2022.

- [234] NIZAM UD DIN, KAMRAN JAVED, SEHO BAE, AND JUNEHO YI. A novel GAN-based network for unmasking of masked face. *IEEE Access*, 8:44276–44287, 2020.
- [235] WALID HARIRI. Efficient masked face recognition method during the covid-19 pandemic. Signal, Image and Video Processing, Springer, 16(3):605–612, 2022.
- [236] YANDE LI, KUN GUO, YONGGANG LU, AND LI LIU. Cropping and attention based approach for masked face recognition. *Applied Intelligence*, Springer, **51**(5):3012–3025, 2021.
- [237] Shreyas Dharanesh and Ajita Rattani. **Post-COVID-19 mask-aware face recognition system**. Proceedings of IEEE International Symposium on Technologies for Homeland Security, pages 1–7, 2021.
- [238] HALA FATHEE AND SHAABAN SAHMOUD. Iris segmentation in uncooperative and unconstrained environments: state-of-the-art, datasets and future research directions. Digital Signal Processing, Elsevier, 118:103244, 2021.
- [239] FARMANULLAH JAN, SALEH ALRASHED, AND NASRO MIN-ALLAH. Iris segmentation for non-ideal Iris biometric systems. Multimedia Tools and Applications, Springer, pages 1–29, 2021.
- [240] KIEN NGUYEN, CLINTON FOOKES, RAGHAVENDER JILLELA, SRIDHA SRIDHARAN, AND ARUN ROSS. Long range iris recognition: A survey. Pattern Recognition, Elsevier, 72:123–143, 2017.
- [241] Zhengding Luo, Qinghua Gu, Guoxiong Su, Yuesheng Zhu, and Zhiqiang Bai. An adaptive face-Iris multimodal identification system based on quality assessment network. *Proceedings of International Conference on Multimedia Modeling, Springer*, pages 87–98, 2021.
- [242] Dane Brown. Deep face-iris recognition using robust image segmentation and hyperparameter tuning. Proceedings of Computer Networks and Inventive Communication Technologies, Springer, pages 259–275, 2022.

- [243] OLAF RONNEBERGER, PHILIPP FISCHER, AND THOMAS BROX. U-net: Convolutional networks for biomedical image segmentation. Proceedings of International Conference on Medical Image Computing and Computer-Assisted Intervention, Springer, pages 234–241, 2015.
- [244] AQEEL ANWAR AND ARIJIT RAYCHOWDHURY. Masked face recognition for secure authentication. arXiv preprint arXiv:2008.11104, 2020.
- [245] Punam Kumari and KR Seeja. A novel periocular biometrics solution for authentication during Covid-19 pandemic situation.

 Journal of Ambient Intelligence and Humanized Computing, Springer, 12(11):10321–10337, 2021.
- [246] VEERU TALREJA, NASSER M NASRABADI, AND MATTHEW C VALENTI. Attribute-based deep periocular recognition: Leveraging soft biometrics to improve periocular recognition. Proceedings of the IEEE/CVF Winter Conference on Applications of Computer Vision, pages 4041–4050, 2022.
- [247] DAVID SEMEDO, DAVID CARMO, RUSLAN PADNEVYCH, AND JOAO MAGALHAES. Contact-free airport borders with biometrics-on-the-Move. Proceedings of IEEE International Workshop on Biometrics and Forensics, pages 1–2, 2021.
- [248] ZHENG ZHU, XIANDA GUO, TIAN YANG, JUNJIE HUANG, JIANKANG DENG, GUAN HUANG, DALONG DU, JIWEN LU, AND JIE ZHOU. Gait recognition in the wild: A benchmark. Proceedings of the IEEE/CVF International Conference on Computer Vision, pages 14789–14799, 2021.

Optimization Based Approaches for Score and Rank Level Fusion of Multimodal Biometrics

by Shadab Ahmad

Indira Gandhi Memorial Library

UNIVERSITY OF HYDERABAD

Central University P.O. HYDERABAD-500 046.

Submission date: 04-Aug-2022 11:40AM (UTC+0530)

Submission ID: 1878689031

File name: Shadab_thesis_plag_check.pdf (8.21M)

Word count: 62460 Character count: 314466

Optimization Based Approaches for Score and Rank Level Fusion of Multimodal Biometrics

ORIGINALITY REPORT

25_%

3%

INTERNET SOURCES

24%

PUBLICATIONS

2%

STUDENT PAPERS

PRIMARY SOURCES

Shadab Ahmad, Rajarshi Pal, Avatharam Ganivada. "Rank level fusion of multimodal biometrics using genetic algorithm",
Multimedia Tools and Applications, 2022
Publication

11%

FAVETROSO

Rajaoshi Pel

Shadab Ahmad, Rajarshi Pal, Avatharam
Ganivada. "Score Level Fusion of Multimodal
Biometrics Using Genetic Algorithm", 2021
IEEE Congress on Evolutionary Computation
(CEC), 2021
Publication

7%

- Gajasohi Pal

Rajasohi Pal

"Advances in Signal Processing and Intelligent Recognition Systems", Springer Science and Business Media LLC, 2020

1 %

Bayardhi Pil

Submitted to University of Hyderabad,
Hyderabad
Student Paper

1% ×

Kalyan Veeramachaneni, Weizhong Yan, Kai Goebel, Lisa Osadciw. "Improving Classifier

<1%

The above sources (wherever signed) belong to Shadat Ahmad.

g. Arethorard 5/8/22

Rajarshi Pal 5/8/2022

Fusion Using Particle Swarm Optimization", 2007 IEEE Symposium on Computational Intelligence in Multi-Criteria Decision-Making, 2007

Publication

www.researchgate.net <1% Internet Source "Advances in Biometrics", Springer Science and Business Media LLC, 2009 Publication Jayanta Basak, Kiran Kate, Vivek Tyagi, Nalini <1% Ratha. "A Gradient Descent Approach for Multi-modal Biometric Identification", 2010 20th International Conference on Pattern Recognition, 2010 **Publication** Encyclopedia of Biometrics, 2015. Publication <1% Shadab Ahmad, Rajarshi Pal, Avatharam 10 Ganivada. "Chapter 6 Rank Level Fusion of Multimodal Biometrics Based on Cross-Entropy Monte Carlo Method", Springer Science and Business Media LLC, 2020 Publication kar.kent.ac.uk

Internet Source

Biometrics, 2011.

Publication

19	Submitted to University of Technology, Sydney Student Paper	<1%
20	www.science.gov Internet Source	<1%
21	Sanjida Nasreen Tumpa, Marina L. Gavrilova. "Score and Rank Level Fusion Algorithms for Social Behavioral Biometrics", IEEE Access, 2020 Publication	<1%
22	Ferdous Ahmed, Brandon Sieu, Marina L. Gavrilova. "Score and Rank-Level Fusion for Emotion Recognition Using Genetic Algorithm", 2018 IEEE 17th International Conference on Cognitive Informatics & Cognitive Computing (ICCI*CC), 2018 Publication	<1%
23	dyuthi.cusat.ac.in Internet Source	<1%
24	www.mdpi.com Internet Source	<1%
25	Peng, Jialiang, Ahmed A. Abd El-Latif, Qiong Li, and Xiamu Niu. "Multimodal biometric authentication based on score level fusion of finger biometrics", Optik - International Journal for Light and Electron Optics, 2014. Publication	<1%

26	Yasushi Makihara, Daigo Muramatsu, Yasushi Yagi, Md. Altab Hossain. "Score-level fusion based on the direct estimation of the Bayes error gradient distribution", 2011 International Joint Conference on Biometrics (IJCB), 2011 Publication	<1%
27	Salma Ben Jemaa, Mohamed Hammami, Hanene Ben-Abdallah. "Finger Surfaces Recognition Using Rank Level Fusion", The Computer Journal, 2016 Publication	<1%
28	Wang, L "Stochastic economic emission load dispatch through a modified particle swarm optimization algorithm", Electric Power Systems Research, 200808 Publication	<1%
29	ir.library.osaka-u.ac.jp Internet Source	<1%
30	"Pattern Recognition and Machine Intelligence", Springer Science and Business Media LLC, 2015 Publication	<1%
31	archive.org Internet Source	<1%
32	library.isical.ac.in:8080 Internet Source	<1%

33	K. S. Arun, V. K. Govindan, S. D. Madhu Kumar. "On integrating re-ranking and rank list fusion techniques for image retrieval", International Journal of Data Science and Analytics, 2017	<1%
34	Md. Maruf Monwar, Marina Gavrilova, Yingxu Wang. "A novel fuzzy multimodal information fusion technology for human biometric traits identification", IEEE 10th International Conference on Cognitive Informatics and Cognitive Computing (ICCI-CC'11), 2011 Publication	<1%
35	livrepository.liverpool.ac.uk Internet Source	<1%
36	www.sciencepublication.org Internet Source	<1%
37	Mandar Gogate, Ahsan Adeel, Amir Hussain. "A novel brain-inspired compression-based optimised multimodal fusion for emotion recognition", 2017 IEEE Symposium Series on Computational Intelligence (SSCI), 2017 Publication	<1%
38	www.docstoc.com Internet Source	<1%
39	J.G. Vlachogiannis, K.Y. Lee. "A Comparative Study on Particle Swarm Optimization for	<1%

Optimal Steady-State Performance of Power Systems", IEEE Transactions on Power Systems, 2006

Publication

40	Lecture Notes in Computer Science, 2011. Publication	<1%
41	Mohamed Cheniti, Naceur - Eddine Boukezzoula, Zahid Akhtar. "Symmetric sum - based biometric score fusion", IET Biometrics, 2017 Publication	<1%
42	Karthik Nandakumar. "Fusion in Multibiometric Identification Systems: What about the Missing Data?", Lecture Notes in Computer Science, 2009	<1%
43	Handbook of Iris Recognition, 2013. Publication	<1%
44	ethesis.nitrkl.ac.in Internet Source	<1%
45		<1 _%

PSO", International Journal of Advanced Computer Science and Applications, 2013

Publication

47	Submitted to University of New South Wales Student Paper	<1%
48	digitalcommons.njit.edu Internet Source	<1%
49	dr.ntu.edu.sg Internet Source	<1%
50	"Computational Intelligence in Pattern Recognition", Springer Science and Business Media LLC, 2020 Publication	<1%
51	Submitted to The Hong Kong Polytechnic University Student Paper	<1%
52	Law Kumar Singh, Munish Khanna, Hitendra Garg. "Multimodal Biometric Based on Fusion of Ridge Features with Minutiae Features and Face Features", International Journal of Information System Modeling and Design, 2020 Publication	<1%
53	J. Grover, M. Hanmandlu. "Personal identification using the rank level fusion of finger-knuckle-prints", Pattern Recognition and Image Analysis, 2017	<1%

54	Divya, R., and V. Vijayalakshmi. "Secure and efficient multibiometric fusion-based cryptosystem using blind separation encryption algorithm", International Journal of Biometrics, 2016. Publication	<1%
55	Submitted to Jawaharlal Nehru Technological University Student Paper	<1%
56	www.ijircst.org Internet Source	<1%
57	Leila Boussaad, Aldjia Boucetta. "An effective component-based age-invariant face recognition using Discriminant Correlation Analysis", Journal of King Saud University - Computer and Information Sciences, 2020 Publication	<1%
58	Submitted to Eastern Mediterranean University Student Paper	<1%
59	www.preprints.org Internet Source	<1%
60	Ayman Abaza, Arun Ross. "Quality based rank-level fusion in multibiometric systems", 2009 IEEE 3rd International Conference on	<1%

Biometrics: Theory, Applications, and Systems, 2009 Publication

61	Chao-Tang Tseng, Ching-Jong Liao. "A particle swarm optimization algorithm for hybrid flow-shop scheduling with multiprocessor tasks", International Journal of Production Research, 2008 Publication	<1%
62	Submitted to Panjab University Student Paper	<1%
63	Submitted to Universitaet Dortmund Hochschulrechenzentrul Student Paper	<1%
64	"Computer Analysis of Images and Patterns", Springer Nature, 2015 Publication	<1%
65	Anastasio, Thomas J "Tutorial on Neural Systems Modeling", Oxford University Press	<1%
66	Ikenna Odinaka, Joseph A. O'Sullivan, Erik J. Sirevaag, John W. Rohrbaugh. "Cardiovascular Biometrics: Combining Mechanical and Electrical Signals", IEEE Transactions on Information Forensics and Security, 2015 Publication	<1%

67	Mina Farmanbar, Önsen Toygar. "A Hybrid Approach for Person Identification Using Palmprint and Face Biometrics", International Journal of Pattern Recognition and Artificial Intelligence, 2015 Publication	<1%
68	Peng, Jialiang, Qiong Li, Ahmed A. Abd El Latif, and Xiamu Niu. "Finger multibiometric cryptosystem based on score-level fusion", International Journal of Computer Applications in Technology, 2015. Publication	<1%
69	journals.plos.org Internet Source	<1%
70	vdoc.pub Internet Source	<1%
71	www.ncjrs.gov Internet Source	<1%
72	"Computer Analysis of Images and Patterns", Springer Science and Business Media LLC, 2015 Publication	<1%
73	Ajay Kumar, Sumit Shekhar. "Palmprint recognition using rank level fusion", 2010 IEEE International Conference on Image Processing, 2010 Publication	<1%

74	Gayathri Mahalingam, Karl Ricanek. "LBP-based periocular recognition on challenging face datasets", EURASIP Journal on Image and Video Processing, 2013 Publication	<1%
75	Lecture Notes in Computer Science, 2013. Publication	<1%
76	Pellechia, Matthew F., Kannappan Palaniappan, Shiloh L. Dockstader, Peter J. Doucette, Donnie Self, Ankit Agarwal, Usashi Chaudhuri, Subhasis Chaudhuri, and Guna Seetharaman. "Detection of potential mosquito breeding sites based on community sourced geotagged images", Geospatial InfoFusion and Video Analytics IV and Motion Imagery for ISR and Situational Awareness II, 2014. Publication	<1%
77	scholarworks.bridgeport.edu Internet Source	<1%
78	www.ncbi.nlm.nih.gov Internet Source	<1%
79	Jinxing Li, Bob Zhang, David Zhang. "Information Fusion", Springer Science and Business Media LLC, 2022 Publication	<1%

80	Saiyed Umer, Bibhas Chandra Dhara, Bhabatosh Chanda. "Face recognition using fusion of feature learning techniques", Measurement, 2019	<1%
8	hexad.org Internet Source	<1%
82	www.computingonline.net Internet Source	<1%
83	Submitted to City University of Hong Kong Student Paper	<1%
84	Hanmandlu, M "Score level fusion of multimodal biometrics using triangular norms", Pattern Recognition Letters, 20111015 Publication	<1%
85	J.S. Heo, K.Y. Lee, R. Garduno-Ramirez. "Multiobjective Control of Power Plants Using Particle Swarm Optimization Techniques", IEEE Transactions on Energy Conversion, 2006 Publication	<1%
86	Md Wasiur Rahman, Fatema Tuz Zohra, Marina L. Gavrilova. "Score Level and Rank Level Fusion for Kinect-Based Multi-Modal Biometric System", Journal of Artificial Intelligence and Soft Computing Research, 2019	<1%

87	Submitted to Universiti Malaysia Sarawak Student Paper	<1%
88	researchrepository.wvu.edu Internet Source	<1%
89	tel.archives-ouvertes.fr Internet Source	<1%

Exclude quotes On Exclude matches < 14 words

Exclude bibliography On